**The Hong Kong Polytechnic University**
**Department of Health Technology and Informatics**

# Normal tissue clinical radiosensitivity in patients with nasopharyngeal carcinoma: Potential prediction using genetic and cellular approaches

**CHEUK Wai Yin**

A Thesis Submitted in Partial Fulfilment
of the Requirements for the Degree of
Doctor of Philosophy

September 2013

# Certificate of Originality

I hereby declare that this thesis is my own work and that, to the best of my knowledge and belief, it reproduces no material previously published or written, nor material that has been accepted for the award of any other degree or diploma, except where due acknowledge has been made in the text.

Signature: _____

Name of student: CHEUK Wai Yin

# Abstract

Nasopharyngeal carcinoma (NPC) is one of the common cancers in Hong Kong. Radiation therapy (RT) is the primary treatment of NPC. Radiation-induced toxicities are the major obstacles affecting treatment effectiveness and quality of life in post-radiotherapy patients. The aims of this study were to investigate the potentials of genetic variants and direct cellular response in predicting radiosensitivity in Chinese NPC patients.

Acute skin reactions, acute mucositis, and chronic neck fibrosis were the three phenotypes of radiation-induced toxicities evaluated in the first part of this study. Associations between each phenotype and six candidate genes (*ATM*, *SOD2*, *TGFβ1*, *TP53*, *XRCC1* and *XRCC3*) were investigated. Besides tagging single nucleotide polymorphisms (SNPs), previously reported functional SNPs were also included to investigate their role as universal biomarkers to predict risk of each phenotype. One hundred and twenty eight Chinese NPC patients were recruited and they were classified into controls or cases according to toxicity grading criteria established by Radiation Therapy Oncology Group (RTOG). Genotyping was performed by restriction fragment length polymorphism or unlabelled probe melting curve analysis. Single-marker and haplotype analyses were performed by PLINK. Multiple testing was corrected by 10,000 permutations. None of the investigated SNPs and constructed haplotypes showed association with the risk of any phenotype after

permutation ($P_{emp}$>0.05).

A meta-analysis was conducted to overcome the sample size limitation. A comprehensive literature search was performed to identify all existing literature. *XRCC1* and *XRCC3* were selected to investigate their potential roles in radiation-induced mucositis in head and neck cancer patients. Three functional SNPs and 332 head and neck cancer patients were included in this meta-analysis. Meta-analysis was performed with RevMan version 5.2. However, none of the SNPs showed any association with the risk of radiation-induced mucositis in dominant model, recessive model and allelic model ($P$>0.05).

Quantification of radiation-induced apoptosis as direct cellular response was the third part of this study. Thirty NPC patients were recruited. Peripheral blood mononuclear cells (PBMCs) were isolated from patients blood samples. Patients were classified as normal or sensitive according to the highest grade of acute skin reactions and mucositis observed during RT. Flow cytometry was used to measure the percentage of radiation-induced apoptosis in PBMCs at two time points (2hr and 18 hr) after irradiation (0 Gy, 2 Gy, and 8 Gy). Two-way ANOVA was used to compare difference of percent of radiation-induced apoptosis between radiation dose and time points. Percentage of radiation-induced apoptosis between normal and sensitive groups was not significantly different at all time points at all doses ($P$>0.05).

To conclude, our findings suggested that individual genetic variant and measurement of direct cellular response alone are insufficient to predict radiosensitivity in Chinese NPC patients. Meta-analysis is a useful tool to investigate the effect of reported biomarkers in different ethnic origins with a higher statistical power.

Further studies are needed to explore the cumulative effect of genetic variants, in addition to individual direct cellular response, to understand the underlying complex mechanism of radiation-induced toxicities.

# Publications

**Papers**

1. Cheuk I, Yip SP, Kwong D, Wu V. A study on the association of *XRCC1* and *XRCC3* haplotypes and the development of radiation-induced chronic neck fibrosis in nasopharyngeal carcinoma patients. Molecular and Clinical Oncology (Accepted).

2. Cheuk I and Wu V. Genetic association on radiation induced mucosal and skin toxicity in patients with nasopharyngeal carcinoma. Journal of Nasopharyngeal Carcinoma (Accepted).

**Conference Abstracts**

1. Cheuk I, Yip SP, Kwong D, Wu V. Association of single nucleotide polymorphism in *TGFβ1* and acute radiation-induced mucositis in patients with nasopharyngeal carcinoma. European Human Genetics Conference, 2012, Nuremberg, Germany (Poster Presentation)

2. Cheuk I, Yip SP, Kwong D, Wu V. Role of genetic factors in post-radiotherapy complications in nasopharyngeal carcinoma patients. Postgraduate Symposium 2011, Department of Health Technology and Informatics, The Hong Kong Polytechnic University, 2011, Hunghom, Hong Kong (Oral Presentation)

# Acknowledgements

I would like to express my sincere gratitude to my supervisor, Dr. Vincent Wu for giving this opportunity to purse my postgraduate study in the Hong Kong Polytechnic University. Thank you for his encouragement, guidance and supervision throughout this study. I am deeply grateful to Professor SP Yip, my co-supervisor, for his advice and guidance in this research study. I sincerely thank Professor Dora Kwong, my co-supervisor from the Department of Clinical Oncology, the University of Hong Kong, for her support in this research work.

I am grateful to Dr. Helen Law, for her invaluable advice and technical support in the predictive assay study.

I would like to thank Miss Nerys Chu and Miss Nerissa Lee from the Department of Clinical Oncology, the University of Hong Kong, for their kind support in patient recruitment and data collection in Queen Mary Hospital and Princess Margaret Hospital. I would also like to thank Dr. KT Yuen, Miss Annie Yung, Mr. WK Hung, and Miss YW Liu from Princess Margaret Hospital for their technical support and arrangement.

I would like to thank Dr. Edith Cheung, Dr. SW Choi, Mr. Henry Hung, Dr. Blanka Lee, Dr. George Leung, Miss Michelle Ng, Dr. Emily Tsang and Dr. Christy Yiu for teaching me all the lab techniques and their sincere help. Special thanks goes to my good friend Miss Susu Koh, who started her postgraduate study at the same time as me. It would have been a lonely journey without her. I would like to thank my friends and colleagues from the department for their support.

I am grateful to my parents, my brothers and my boyfriend, Dick Chow, for their love, support, and understanding.

This project is supported by grant from the Hong Kong Polytechnic University (RPFG). I would like to thank all the patients who participated in this study.

# Contents

# List of Figures

# List of Tables

# List of Abbreviations

| | |
|---|---|
| 3DCRT | Three-dimensional conformal radiation therapy |
| 5-FU | Fluorouracil |
| A | Adenine |
| AJCC | The American Joint Committee on Cancer |
| APS | Ammonium persulphate |
| AT | Ataxia telangiectasia |
| ATM | Ataxia telangiectasia mutated |
| ATP | Adenosine triphosphate |
| AUC | Area under receiver-operating characteristic curve |
| Bcl-2 | B-cell lymphoma 2 |
| C | Cytosine |
| CDKN2A | Cyclin-dependent kinase inhibitors 2A |
| CDKN2B | Cyclin-dependent kinase inhibitors 2B |
| CHO | Chinese hamster ovary |
| CI | Confidence interval |
| Cisplatin | Cis-diamminedichloroplatinum(II) |
| CNKI | China National Knowledge Infrastructure |
| CNV | Copy number variants |
| Conventional RT | Conventional radiation therapy |
| COX-2 | Cyclooxygenase-2 |
| CRT | Chemoradiation therapy |
| CT | Computer tomography |

| | |
|---|---|
| CTCAE | Common Terminology Criteria for Adverse Events |
| ddNTP | Dideoxynucleoside triphosphate |
| df | Degree of freedom |
| DMSO | Dimethyl sulfoxide |
| DNA | Deoxyribonucleic acid |
| DNase | Deoxyribonuclease |
| dNTP | Deoxynucleoside triphosphate |
| DSB | DNA double strand break |
| EA | Early antigen |
| EBNA-1 | Latent viral nuclear antigen 1 |
| EBNA-2 | Latent viral nuclear antigen 2 |
| EBV | EpsteinBarr virus |
| ECM | Extracellular matrix |
| EORTC | European Organisation for Research and Treatment of Cancer |
| eQTL | Quantitative levels of expression |
| ExoI | Exonuclease I |
| FBS | Fetal bovine serum |
| FITC | Fluorescein Isothiocyanate |
| FSHR | Follicle-stimulating hormone receptor |
| G | Guanine |
| GTV | Gross tumour volume |
| GWAS | Genome wide association study |
| Gy | Gray |
| H2AX | H2A histone family, member X |
| HLA | Human leucocyte antigen |
| HR | Homologous recombination |

| | |
|---|---|
| HRMA | High resolution melting analysis |
| HWE | Hardy-Weinberg equilibrium |
| IARC | International Agency for Research on Cancer |
| IMRT | Intensity-modulated radiation therapy |
| ITGA9 | Integrin, alpha 9 |
| KGF | Keratinocyte growth factor |
| LCL | Lymphoblastoid cell lines |
| LD | Linkage disequilibrium |
| M-H | Mantel-Haenszel |
| MAF | Minor allele frequency |
| MnSOD | Manganese superoxide dismutase |
| MPT | Mitochondrial permeability transition |
| MRI | Magnetic resonance imaging |
| NCBI | National Centre of Biotechnology Information |
| NF-$\kappa$B | Nuclear factor kappa-B |
| NHEJ | Non-homologous end joining |
| NPC | Nasopharyngeal carcinoma |
| OAR | Organ at risk |
| OR | Odd ratio |
| OS | Overall survival |
| $P_{asym}$ | Asymptomatic P value |
| $P_{emp}$ | Empirical P value |
| PAGE | Polyacrylamide gel |
| PARP | Poly (ADP-ribose) polymerase |
| PBMC | Peripheral blood mononuclear cell |
| PBS | Phosphate buffered solution |
| PCR | Polymerase chain reaction |

| | |
|---|---|
| PFGE | Pulsed-field gel electrophoresis |
| PI | Propidium iodide |
| PRISMA | Preferred reporting items for systematic reviews and meta-analyses |
| PS | Phosphatidylserine |
| Q | Chi-square statistics |
| QUANTEC | Quantitative Analyses of Normal Tissue Effects in the Clinic |
| RFLP | Restriction fragment length polymorphism |
| RNS | Reactive nitrogen species |
| ROC | Receiver-operating characteristic |
| ROS | Reactive oxygen species |
| rs number | Reference SNP ID number |
| RT | Radiation therapy |
| RTOG | Radiation Therapy Oncology Group |
| SAP | Shrimp alkaline phosphatase |
| Silane | $\gamma$-methacryloxypropyltrimethoxysilane |
| SNP | Single nucleotide polymorphism |
| SOD2 | Superoxide dismutase 2 |
| SSB | DNA single strand break |
| SSLD | Soild spine of linkage disequilibrium |
| STREGA | Strengthening the Reporting of Genetic Association studies |
| T | Thymine |
| $T_m$ | Melting temperature |
| TBE | Tris Borate Ethylenediaminetetraacetic acid buffer |
| TE | Tris ethylenediaminetetraacetic acid |
| TEMED | Tetramethylethylenediamine |

| | |
|---|---|
| TGF$\beta$ | Transforming growth factor beta |
| TNF$\alpha$ | Tumour necrosis factor alpha |
| TNFRSF19 | Tumor necrosis factor receptor superfamily, member 19 |
| TNM | tumour-node-metastasis |
| TUNEL | Terminal dUTP Nick End-Labeling |
| UICC | The Union for International Cancer Control |
| VNTR | Variable-number tandem repeats |
| WHO | World health organisation |
| XRCC1 | X-ray repair cross complementing group 1 |
| XRCC3 | X-ray repair cross complementing group 3 |

# Chapter 1

# Literature review

Radiation therapy (RT) is the primary treatment for nasopharyngeal carcinoma (NPC). Major RT-induced acute and late toxicities such as erythema, dermatitis, chronic fibrosis, mucositis, xerostomia, or temporal necrosis, not only affect treatment outcome during cancer treatment, but also the quality of life after treatment. Although many drugs have been developed and preliminary results from clinical trials seem promising, current management of RT-induced toxicities is mainly palliative. Many factors are considered to be the main contributors to the variations of normal tissue radiosensitivity in NPC patients.

Clinical factors such as age, body mass, cancer staging, gender, genetic factors, and lifestyles play a part in individual variations in radiation susceptibility. Among these clinical factors, genetic factors may be the major contributors to the development of RT-induced toxicities with various degrees of severity (Andreassen et al., 2012b; Barnett et al., 2009). The association of radiosensitivity with genes involved in deoxyribonucleic acid (DNA) repair, removal of reactive oxygen species (ROS), and apoptosis signalling pathway, have been investigated mainly in breast

and prostate cancers. Since most genetic association studies were performed in Caucasian populations, information related to genetic factors and radiosensitivity is limited in Asian populations. Another approach focuses on predicting the likelihood of severe toxicities based on quantifying radiation-induced damage in cells derived from cancer patients. This project investigates the potential of predicting normal tissue clinical radiosensitivity in Chinese NPC patients by means of genetic and cellular approaches. This chapter begins with background information of NPC and the basis of cellular killing during RT. Previous research and research approaches are also discussed to provide the rationale of this study.

## 1.1 Epidemiology of Nasopharyngeal Carcinoma

### 1.1.1 Aetiology of NPC

NPC is an endemic cancer in Southest Asia. According to the International Agency for Research on Cancer (IARC), 80% of new NPC cases came from Asia while only 5% came from Europe in 2008 (Lee et al., 2012). In 2010, NPC is the seventh most common cancer with an incidence of 12.2 per 100,000 in Hong Kong (*Hong Kong Cancer Stat 2010*, 2012). The median age of patients at the time of diagnosis is around 50-52 years old. The incidence is three times higher in males than in females (*Hong Kong Cancer Stat 2010*, 2012). Age-specific incidence and mortality rates for NPC in 2010, and incidence and mortality trends for NPC from 1996 to 2010 in Hong Kong are shown in Figure 1.1.

NPC is a multifactorial disease and many risk factors contribute to its development. Risk factors of NPC include Epstein-Barr virus (EBV) infection, genetic predisposition, and environmental factors (Lee et al., 2012). EBV infects over 90% of the world's population and over 80% of children were infected by the age of 6 in Hong Kong (Chang and Adami, 2006). EBV infection is associated with non-keratinising NPC regardless of the ethnic origin (Nicholls et al., 1997), although detection of EBV in keratinising carcinoma is non-consistent (Chang and Adami, 2006). NPC patients have elevated level of IgA, IgG, and neutralising antibodies against EBV-associated antigens. EBV-specific deoxyribonuclease (DNase) is targeted by neutralising antibodies (Chang and Adami, 2006). Changes in IgA and IgG antibody levels are associated with the tumour burden and recurrence. Detection of antigen against EBV viral capsid antigens is used for screening in high-risk populations (Chang and Adami, 2006). Circulating EBV DNA is used for NPC diagnosis and also for monitoring treatment response and disease progression.

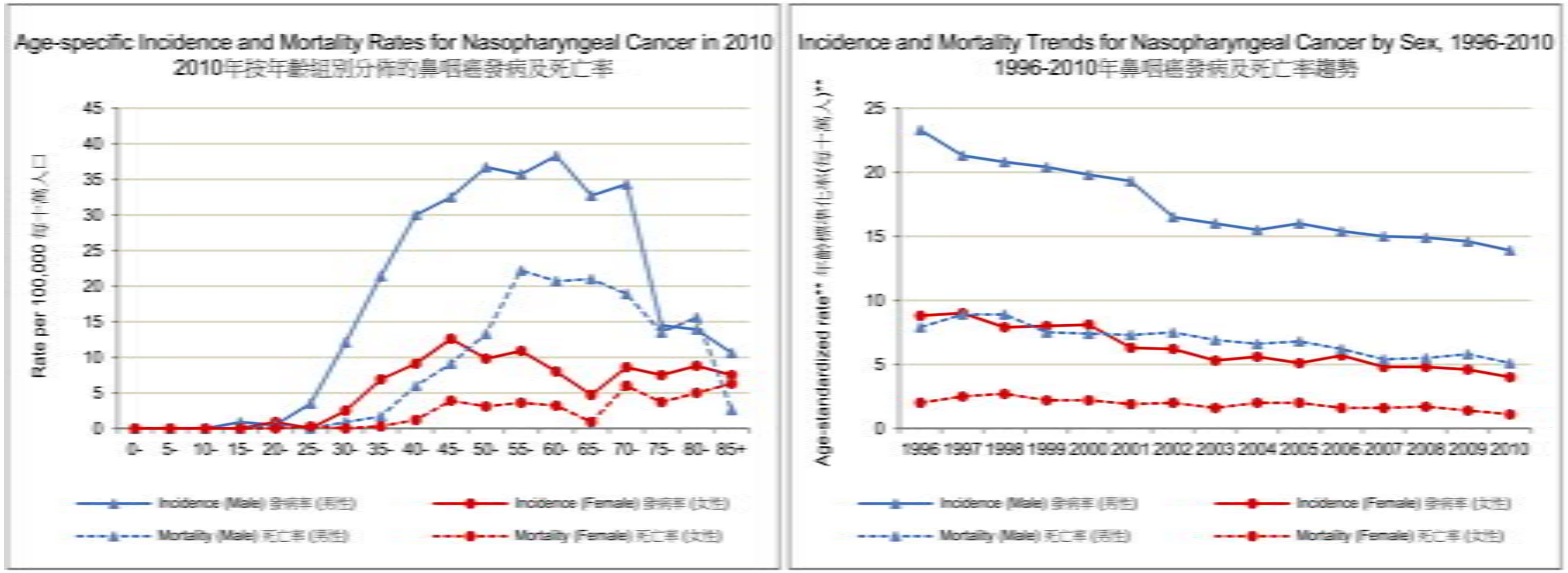


Figure 1.1: Age-specific incidence and mortality rates for NPC in 2010 (left) and incidence and mortality trends for NPC from 1996 to 2010 (right) in Hong Kong. (*Hong Kong Cancer Stat 2010*, 2012)

NPC is a complex disease that is the results of combined genetic factors and environmental factors, rather than caused by particular susceptibility genes (Chang and Adami, 2006). Incidence of NPC in Hong Kong has decreased more than 50% over the past 30 years (Lee et al., 2012). Decreasing incidence of NPC is illustrated in Figure 1.2. Salted fish is a traditional Chinese food in NPC-endemic areas. High consumption of salted fish is strongly associated with high risk of NPC (Chang and Adami, 2006). Changing lifestyles and consumption patterns of southern Chinese, such as decreased consumption of salted fish and increased consumption of fruits and vegetables, are reasons of the decreasing trend (Chang and Adami, 2006; Lee et al., 2012).

Individuals with family history of NPC in first degree relatives have 4- to 10-fold higher risk than individuals with no family history (Chang and Adami, 2006). A familial screening program was conducted in Hong Kong from 1994 to 2005 in 1,199 asymptomatic family members (Ng et al., 2010). Eighteen out of 1,199 participants developed NPC during this screening program. Sixteen participants among the 18 cases were detected by this screening program. Thus, early detection of NPC can be achieved by familial screening program to increase survival rate (Ng et al., 2010).

Genetic variants in different subtypes of human leukocyte antigen (*HLA*) have been extensively studied since 1975 (Bei et al., 2010). *HLA* genes are located on chromosome 6 and encode proteins that present specific antigens to T lymphocytes. Foreign antigens will be eliminated by the immune system via targeted lysis (Chang and Adami, 2006). As a result, genetic variants of *HLA* that reduce function of encoded proteins may have increased risk of NPC development (Chang and Adami, 2006). The association of subtype *HLA-A* and NPC has been reported in genetic association studies and linkage studies (Bei et al., 2010). In

addition to *HLA*, genome-wide association studies (GWAS) of NPC identified many new susceptibility loci, such as genes belonging to tumour necrosis factor receptor superfamily, member 19,(*TNFRSF19*), cyclin-dependent kinase inhibitors (*CDKN2A-CDKN2B*) and integrin, alpha 9 (*ITGA9*). Genetic variants of these new susceptibility loci may be involved in NPC pathogenesis (Bei et al., 2010; Ng et al., 2009).

### 1.1.2 Pathology of NPC

NPC is classified into three histological types according to the World Health Organisation (WHO). Type I is keratinising squamous carcinoma. Type II and type III are both non-keratinising carcinoma, in which type II is differentiated and type III is poorly differentiated or undifferentiated (Chang and Adami, 2006). The incidence of histological subtypes is different in endemic and non-endemic regions. Type III is the most common type diagnosed in 95% of southern Chinese NPC patients and 63% of patients from North America. In contrast, histological distributions of type I and type II are, respectively, 2% and 3% in southern Chinese, and 25% and 12% for patients in North America (Wei and Sham, 2005). Local tumour control rate and distant metastasis rate are higher for undifferentiated carcinomas than differentiated carcinomas (Wei and Sham, 2005).

NPC is classified into different stages according to the tumour-node-metastasis (TNM) cancer staging system established by the American Joint Committee on Cancer (AJCC) and the Union for International Cancer Control (UICC). Before AJCC/UICC adopted the TNM staging customised for NPC to the 5th edition AJCC/UICC staging system in 1997, Ho's staging system was the preferred system in Asia while AJCC/UICC staging system was preferred in America and Europe (Wei and Sham, 2005). AJCC/UICC staging system and Ho's staging system are

shown in Table 1.1. The current AJCC/UICC effective classification is the 7th edition released in 2010.

### 1.1.3 Diagnosis of NPC

Most symptoms presented in patients with NPC are non-specific, such as headache, facial pain, nasal obstruction and excessive nasal discharges (Wei and Sham, 2005). Presentation of uncommon symptoms such as anorexia and weight loss indicates the possibility of distant spread of NPC (Wei and Sham, 2005). Due to non-specific nature of NPC symptoms, most NPC patients are only diagnosed at advanced-stage of NPC (Wei and Sham, 2005). Once NPC is suspected, detection of circulating EBV DNA and endoscopy examination will be conducted. Imaging of the skull down to the neck will be carried out by computed tomography (CT) and magnetic resonance imaging (MRI). Biopsy will be taken for definitive diagnosis of NPC (Chan et al., 2002; Wei and Sham, 2005).

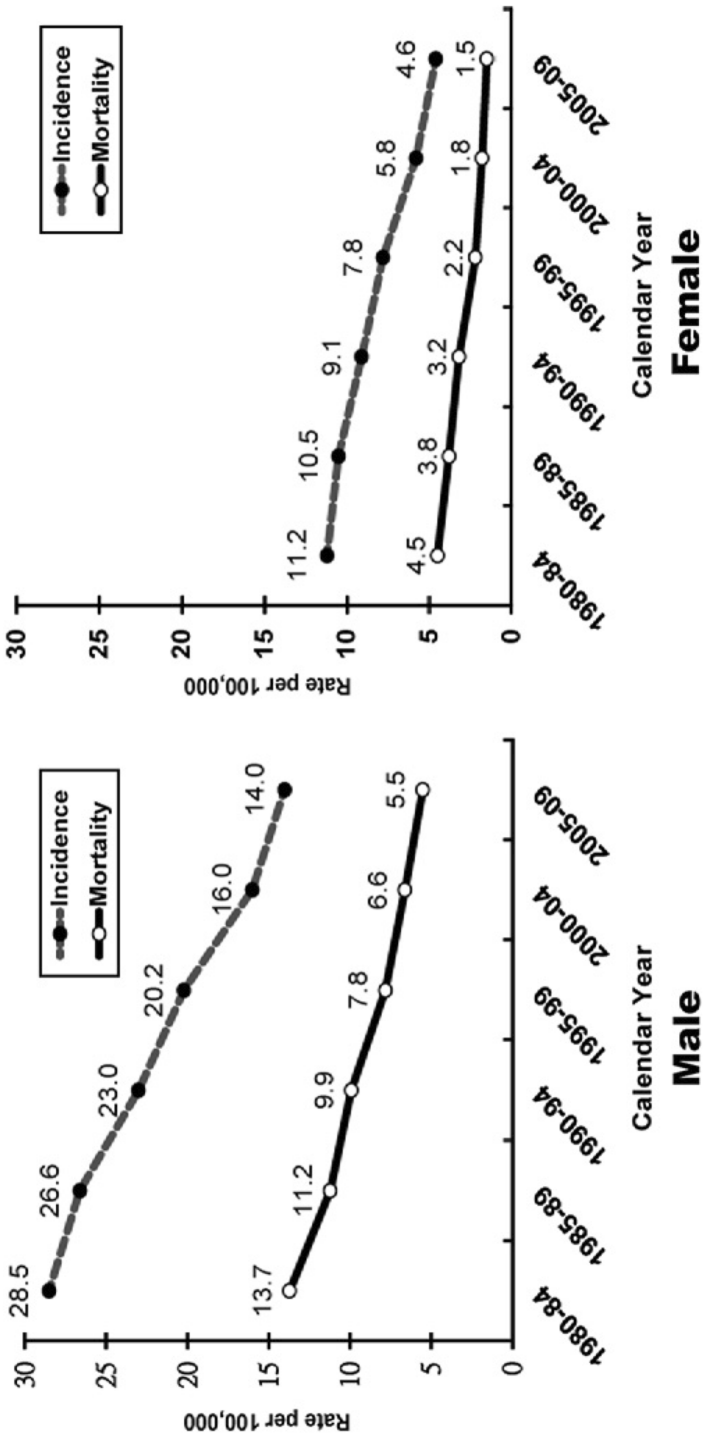


Figure 1.2: Incidence of NPC over the past 30 years in Hong Kong (Lee et al., 2012).

Table 1.1: AJCC and Ho's staging systems (Wei and Sham, 2005)

| The American Joint Committee on Cancer Staging[53] | | | | Ho Staging[49] | | |
|---|---|---|---|---|---|---|
| **Tumour in nasopharynx (T)** | | | | **Primary tumour (T)** | | |
| T1 | Tumour confined to the nasopharynx | | | T1 | Tumour confined to nasopharynx (space behind choanal orifices and nasal septum and above posterior margin of soft palate in resting position) | |
| T2 | Tumour extends to soft tissues of oropharynx and/or nasal fossa | | | T2 | Tumour extended to nasal fossa, oropharynx, or adjacent muscles or nerves below base of skull | |
| T2a | without parapharyngeal extension | | | | | |
| T2b | with parapharyngeal extension | | | | | |
| T3 | Tumour invades bony structures and/or paranasal sinuses | | | T3 | Tumour extended beyond T2 limits and subclassified as follows: | |
| | | | | T3a | Bone involvement below base of skull (floor of sphenoid sinus is included in this category) | |
| | | | | T3b | Involvement of base of skull | |
| | | | | T3c | Involvement of cranial nerve(s) | |
| | | | | T3d | Involvement of orbits, laryngopharynx (hypopharynx), or infratemporal fossa | |
| T4 | Tumour with intracranial extension and/or involvement of cranial nerves, infratemporal fossa, hypopharynx, or orbit | | | | | |
| **Regional lymph nodes (N)** | | | | **Regional lymph nodes (N)** | | |
| The distribution and the prognostic effect of regional lymph node spread from nasopharynx cancer, especially of the undifferentiated type, is different from that of other head and neck mucosal cancers and justifies use of a different N classification scheme. | | | | | | |
| NX | Regional lymph nodes cannot be assessed | | | | | |
| N0 | No regional lymph node metastasis | | | N0 | Node palpable or thought to be benign | |
| N1 | Unilateral metastasis in lymph node(s), 6 cm or less in greatest dimension, above the supraclavicular fossa | | | N1 | Node(s) wholly in upper cervical level, bounded below by the skin crease extending laterally and backward from or just below thyroid notch (laryngeal eminence) | |
| N2 | Bilateral metastasis in lymph node(s), 6 cm or less in greatest dimension, above the supraclavicular fossa | | | N2 | Node(s) palpable between crease and supraclavicular fossa, the upper limit being a line joining the upper margin of the sternal end of the clavicle and the angle formed by the lateral surface of the neck and the superior margin of the trapezius | |
| N3 | Metastasis in a lymph node(s) | | | N3 | Node(s) palpable in the supraclavicular fossa and/or skin involvement in the form of carcinoma en cuirasse or satellite nodules above the clavicles | |
| N3a | greater than 6 cm in dimension | | | | | |
| N3b | extension to the supraclavicular fossa | | | | | |
| **Distant metastasis (M)** | | | | **Metastases (M)** | | |
| MX | Distant metastasis cannot be assessed | | | | | |
| M0 | No distant metastasis | | | M0 | No haematogenous metastases | |
| M1 | Distant metastasis | | | M1 | Haematogenous metastases present, and/or lymph nodal metastases below the clavicle | |
| **Stage grouping** | | | | **Stage grouping** | | |
| Stage 0 | T1s | N0 | M0 | | | |
| Stage I | T1 | N0 | M0 | Stage I | T1, | N0 |
| Stage IIA | T2a | N0 | M0 | Stage II | T2 and/or N1 | |
| Stage IIB | T1 | N1 | M0 | | | |
| | T2 | N1 | M0 | | | |
| | T2a | N1 | M0 | | | |
| | T2b | N0 | M0 | | | |
| | T2b | N1 | M0 | | | |
| Stage III | T1 | N2 | M0 | Stage III | T3 and/or N2 | |
| | T2a | N2 | M0 | | | |
| | T2b | N2 | M0 | | | |
| | T3 | N0 | M0 | | | |
| | T3 | N1 | M0 | | | |
| | T3 | N2 | M0 | | | |
| Stage IVA | T4 | N0 | M0 | Stage IV | N3 (any T) | |
| | T4 | N1 | M0 | | | |
| | T4 | N2 | M0 | | | |
| Stage IVB | Any T | N3 | M0 | | | |
| Stage IVC | Any T | Any N | M1 | | | |
| | | | | Stage V | M1 | |

## 1.2 Management of NPC

Undifferentiated NPC is highly sensitive to RT. As a result, RT is the primary treatment for all stages of NPC. It is also because of the deep-seated anatomical site of NP, which is not readily accessible by surgical treatment. High 5-year overall and disease-free survival rates have been achieved by RT in early-stage diseases (Wei and Sham, 2005). For more advanced-stage diseases, chemotherapy is used concurrently and adjuvantly to improve regional control rate (Lee et al., 2005).

### 1.2.1 Radiation Therapy

#### 1.2.1.1 Two-dimensional conventional radiation therapy

Conventional radiation therapy (Conventional RT) is a two-dimensional RT technique. It was the most commonly used technique until early 1990s (Teo et al., 2004). During treatment planning, all parameters, such as the number of beams and beam direction, are optimised manually by treatment planners (Hunt and Burman, 2003). For NPC, conventional RT delivers a total radiation dose of 60-70 grays (Gy) to target in 2-2.5 Gy per fraction per day over 6 to 7 weeks (Chan et al., 2002; Teo et al., 2004). Conventional RT consists of two phases. In phase I, 40 Gy is delivered by using two lateral opposing fields to facio-cervical region to the primary tumour and upper cervical lymphatics (Kwong et al., 2004b). A separate anterior photon field is used to deliver dose to lower cervical lymphatics with shielded mid-line structures (Chau et al., 2001). In phase I, patient's head is immobilised in the "flexed-neck position" using cobex cast (Chau et al., 2001) (Figure 1.3a). In phase II, one anterior and two lateral opposing facial fields are used to cover the primary tumour at the nasopharynx and to avoid irradiation to spinal cord (Kwong et al., 2004b). The patient is re-positioned to the "extended-neck" position in phase II (Chau et al., 2001)(Figure 1.3b). Critical organs such

as the brainstem, eyeballs and spinal cord are shielded using pre-determined distances from bony anatomical landmarks (Chau et al., 2001). Overall loco-regional control rate of NPC, taking all T-stages and treated by conventional RT, is 80% (Chan et al., 2002). The advantage of conventional RT is that this technique is relatively simple and easy to apply, since it uses simple beam arrangement and the target region is defined two-dimensionally by certain anatomical landmarks instead of tumour volume (Chau et al., 2001). However, even with the use of carefully designed beam direction and shielding, many normal tissues are unavoidably irradiated and this leads to significant toxicities in different aspects.

#### 1.2.1.2 Three-dimensional conformal radiation therapy

Three-dimensional conformal radiation therapy (3DCRT) allows non-coplanar beam arrangement and therefore opens up more options in beam orientation and treatment parameters. It is planned with the patients CT data, with or without MRI that allows a more detail delineation of tumour target than conventional RT (Teo et al., 2004). Compared with conventional RT, 3DCRT is able to deliver higher dose to the tumour volume with less compromise to the organ at risk (OAR) (Teo et al., 2004). In 3DCRT, the numbers of coplanar and non-coplanar beams are customised in relation to the extent of tumour for individual treatment planning (Figure 1.4a,b)(Fang et al., 2001). Three-year loco-regional control rate and three-year metastasis-free survival rate for all stages are around 85% and 77% respectively (Fang et al., 2008).

#### 1.2.1.3 Intensity-modulated radiation therapy

Intensity-modulated radiation therapy (IMRT) is an advanced form of 3DCRT (Hunt et al., 2001). IMRT uses intensity-modulated radiation beams and an inverse treatment planning approach, in contrast to the forward planning approach in

conventional RT and 3DCRT (Hunt et al., 2001). IMRT uses multiple fields with static or dynamic multi-leaf collimator during dose delivery. IMRT increases dose conformity to the targeted tumours and provides better protection to OARs (Ng et al., 2011). Dose uniformity of the target is also improved with 36% reduction of dose heterogeneity when compared with conventional RT (Hunt et al., 2001). Thus, higher dose can be delivered and it is possible to escalate the gross tumour volume (GTV) dose up to 80 Gy without compromising the normal tissue (Kam et al., 2003). One hundred percent of overall survival rate was reported in NPC patients treated by IMRT with early-stage diseases (Kwong et al., 2004a). Since IMRT has a better loco-regional disease control with reduced normal tissue toxicities, it is now used as the standard RT technique for treating NPC in Hong Kong (Teo et al., 2004). An example of IMRT treatment plan with seven coplanar beams is shown in Figure 1.4c.

### 1.2.2 Chemotherapy

Due to high rates of local and distant failures for loco-regional advanced NPC, combined-modality treatment such as concurrent and/or adjuvant chemotherapy with RT (CRT) is used to improve local and distant control of the disease. The use of the chemotherapeutic agent cis-diamminedichloroplatinum(II) (Cisplatin) concurrently with RT is the standard CRT treatment for loco-regional advanced NPC (Chan, 2010). Cisplatin is a platinum-based complex that inhibits DNA synthesis by disrupting DNA cross-linking (Wagner and Karnitz, 2009). Adjuvant chemotherapy with chemotherapeutic agents such as fluorouracil (5-FU) is considered optional (Chan, 2010). Chemotherapy is also the first line treatment for recurrent and metastatic disease. Cisplatin is used in combination with 5-FU or other modern chemotherapeutic agents such as gemcitabine or paclitaxel.

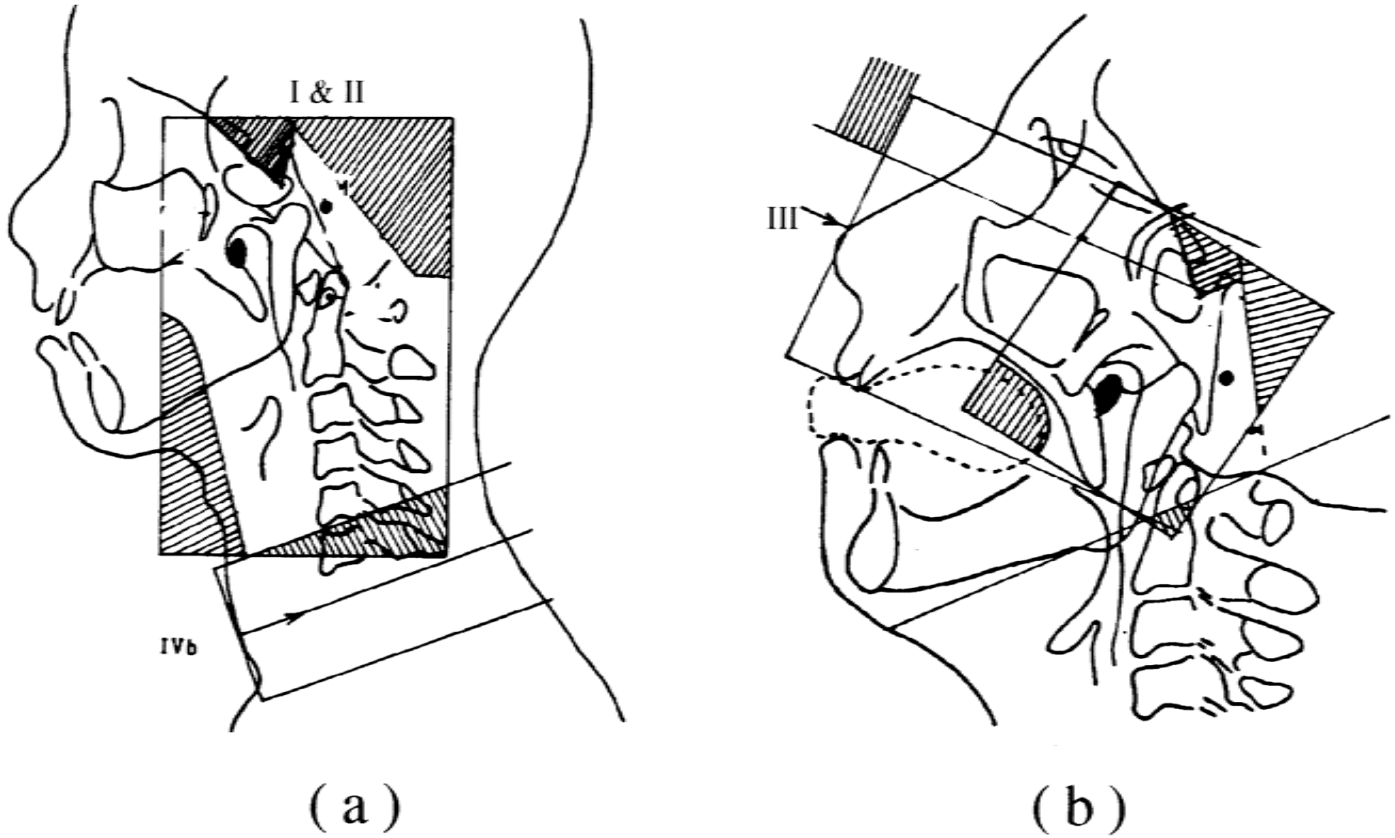


Figure 1.3: Treatment plannings for 2DRT (a) Lateral opposing fields in Phase I of 2DRT. (b) Three fields in Phase II of 2DRT. (Chau et al., 2001)

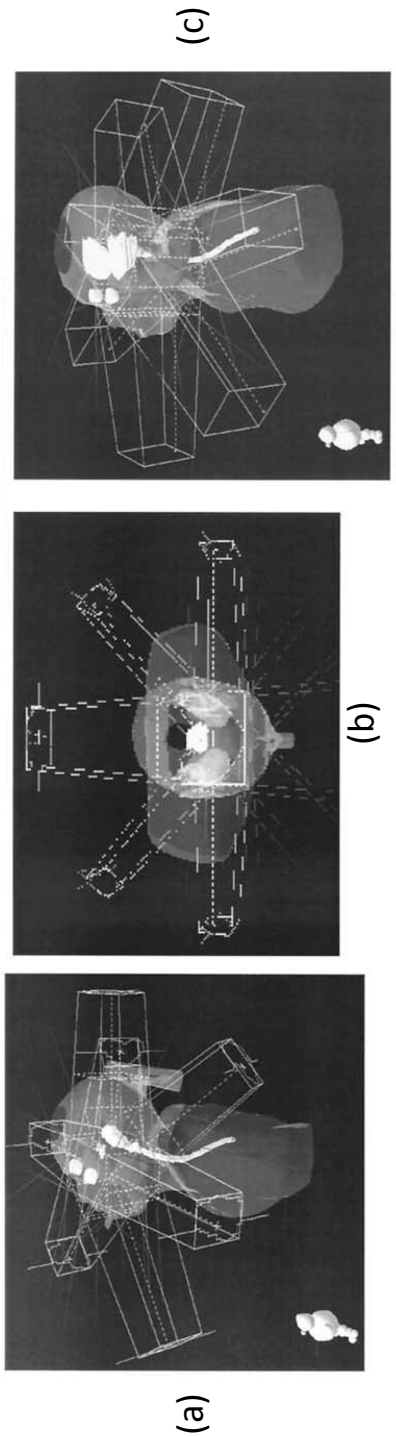


Figure 1.4: Treatment plannings for 3DCRT and IMRT. (a) Seven coplanar fields in Phase I of 3DCRT. (b) Six non-coplanar fields in Phase II of 3DCRT. (c) Seven-field arrangement of IMRT. (Kam et al., 2003)

## 1.3 Radiation-induced complications in NPC

Skin reactions, mucositis and chronic neck fibrosis are the most commonly seen radiation-induced complications in NPC patients regardless of RT methods. According to a retrospective analysis performed on 4,527 NPC patients from 1976 to 1985, 31% of NPC patients developed one or more late sequelae after conventional RT (Lee et al., 1992). Ten percent of patients developed neurological complications, such as temporal lobe necrosis, that resulted in serious disabilities, and 1% of patients died from severe post-RT sequelae (Lee et al., 1992). Xerostomia is also one of the common post-RT sequelae developing in NPC patients treated by conventional RT alone (Tuan et al., 2012). With the advancement of RT technique, RT is more specific to the target region of tumour and achieves higher overall survival rate. In addition, critical organs, such as spinal cord, are preserved and irradiation to OARs is minimised. IMRT has been shown with better parotid sparing than conventional RT in early-stage NPC patients (Kam et al., 2007; Kwong et al., 2004a). Incidence of neurological complications was also reduced with the use of IMRT to improve critical organ dose sparing and target dose delivery (Hunt et al., 2001; Kam et al., 2003). Thus, better overall quality of life can be achieved (Fang et al., 2010). Nevertheless, many radiation-induced complications in NPC still affect quality of life after cancer treatment. Three commonly used grading systems to assess severity of RT-induced sequelae include WHO classification, acute radiation morbidity scoring criteria and late radiation morbidity scoring schema established by Radiation Therapy Oncology Group (RTOG)/European Organisation for Research and Treatment of Cancer (EORTC), and Common Terminology Criteria for Adverse Events (CTCAE). Details of acute skin reactions, acute mucositis and late skin reactions as established by RTOG are shown in Tables 1.2 and 1.3 (Cox et al., 1995).

Table 1.2: RTOG/EORTC acute radiation scoring criteria of skin and mucous membrane

| Grade | 0 | 1 | 2 | 3 | 4 |
|---|---|---|---|---|---|
| Skin | | | | | |
| | No change over baseline | Follicular, faint or dull erythema; epilation; dry desquamation; decreased sweating | Tender or bright erythema, patchy moist desquamation; moderate oedema | Confluent, moist desquamation other than skinfolds, pitting oedema | Ulceration, haemorrhage, necrosis |
| Mucous membrane | | | | | |
| | No change over baseline | Injection/may experience mild pain not requiring analgesic | Patchy mucositis which may produce an inflammatory serosanguinitis discharge/may experience moderate pain requiring analgesia | Confluent fibrinous mucositis/may include severe pain requiring narcotic | Ulceration, haemorrhage or necrosis |

Table 1.3: RTOG/EORTC late radiation scoring criteria of skin, subcutaneous tissue, and mucous membrane

| Grade | 0 | 1 | 2 | 3 | 4 | 5 |
|---|---|---|---|---|---|---|
| Skin | | | | | | |
| | None | Slight atrophy; Pigmentation change; Some hair loss | Patch atrophy; Moderate telangiectasia; Total hair loss | Marked atrophy; Gross telangiectasia | Ulceration | Death directly related to radiation late effect |
| Subcutaneous tissue | | | | | | |
| | None | Slight induration (fibrosia) and loss of subcutaneous fat | Moderate fibrosis but asymptomatic; Slight field contracture <10% linear reduction | Severe induration and loss of subcutaneous tissue; Field contracture>10% linear measurement | Necrosis | Death directly related to radiation late effect |
| Mucous membrane | | | | | | |
| | None | Slight atrophy and dryness | Moderate atrophy and telangiectasia; Little mucous | Marked atrophy with complete dryness; Severe telangiectasia | Ulceration | Death directly related to radiation late effect |

### 1.3.1 Basis of cell killing during radiation therapy

During RT, ionising radiation induces damages by generating reactive free radicals that randomly interacts with DNA, RNA, proteins and plasma membrane. DNA is the principal target of RT-induced cell killing (Jioner and van der Kogel, 2009). Free radicals introduce damage such as induction of DNA single-strand breaks (SSBs), DNA double-strand breaks (DSBs), DNA-DNA cross-linkings, membrane lipid peroxidation, and leakage of cytochrome c from mitochondria (Faulhaber and Bristow, 2005; Kiang et al., 2010). The primary lethal damage induced by ionising radiation is DSBs (Kiang et al., 2010). Many signal transduction pathways are activated to repair DNA damage. For example, DSBs are repaired by two pathways: homologous recombination (HR) and non-homologous end joining (NHEJ). The protein ataxia telangiectasia mutated (ATM) detects complexes formed by DNA repair proteins and DSBs (Kiang et al., 2010). Activity of ATM activates p53 and Chk2 and induces cell cycle arrest. Depending on the level of DNA damage, cells with adequate repair re-enter the cell cycle while lethal damage leads to cell death (Kiang et al., 2010). A simplified diagram of radiation-induced signal transduction pathways is shown in Figure 1.5.

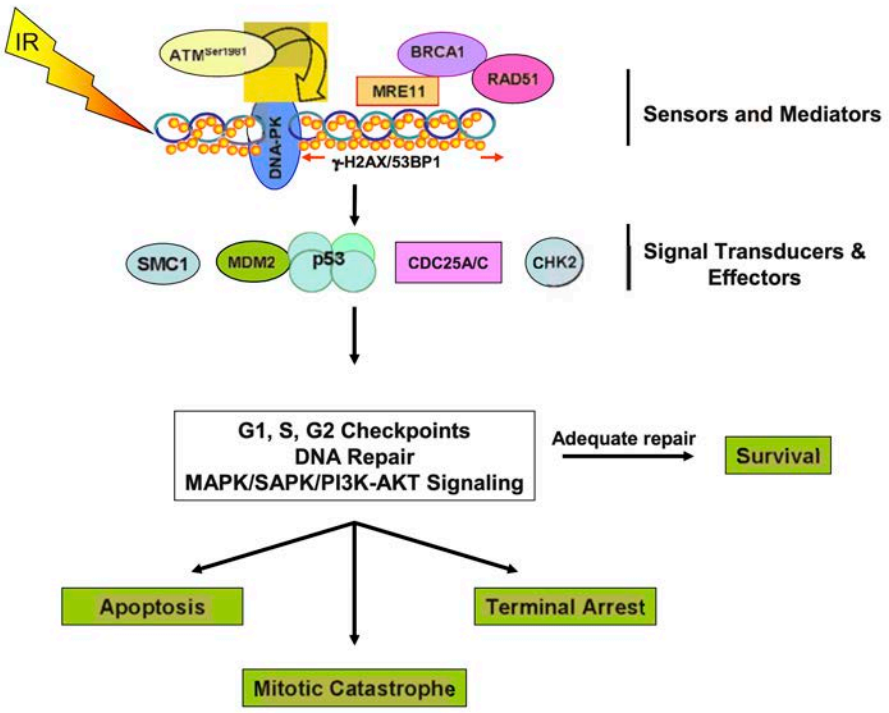


Figure 1.5: Simplified diagram of cellular events during irradiation. Ionising radiation (IR) introduces damage to DNA, plasma membrane and cell organelles. ATM and other protein complexes are activated by DNA damage and this leads to histone phosphorylation. Proteins involved in DNA repair are recruited to the site of DNA damage. Damage signals induce checkpoint proteins to arrest cell cycle. Repaired cells re-enter cell cycles while cell death occurs in cells with lethal DNA damage (Faulhaber and Bristow, 2005).

### 1.3.2 Acute and late reactions

According to the acute radiation morbidity scoring criteria established by RTOG, RT-induced reactions developing within 90 days after the commencement of RT are considered acute complications. EORTC/RTOG late radiation morbidity scoring schema is used if RT-induced complications appears after the period specified in the acute radiation morbidity scoring criteria (Cox et al., 1995).

#### 1.3.2.1 Acute mucositis

Radiation-induced oral mucositis is one of the major sequelae developing during RT treatment. One hundred percent of NPC patients treated with RT developed radiation-induced mucositis and 48% of patients treated with RT alone developed Grade 3 oral mucositis (Kam et al., 2004; Lee et al., 2010). The use of CRT also increased the incidence of radiation-induced mucositis (Kwong et al., 2004b; Lee et al., 2005, 2010). Development of radiation-induced mucositis is a consequence of multiple biological events within a complex network rather than a direct clonogenic cell death induced by radiation (Sonis, 2009).

Radiation-induced mucositis is characterised by 5 phases: Initiation, primary damage response, signal amplification, ulceration and healing (Sonis, 2007). During initiation, clonogenic cell death and injuries of basal epithelial cells are caused by lethal DNA damage, such as SSBs and DSBs induced during RT. In addition to direct damage, ROS are generated during the initiation phase and cause further damage in lipids, connective tissues and other biomolecules (Sonis, 2007). These primary damage responses stimulate transduction signalling pathways involved in damage response, such as activation of transcription factors p53 and nuclear factor kappa-B (NF-$\kappa$B). Transcription factors regulate the expression of many genes, increase production of pro-inflammatory cytokines and other proteins, and this

leads to stimulation of additional injuries through positive feedback loops during signal amplification (Sonis, 2007). Accumulated damage increases and prolongs tissue damage, in addition to fractionated RT, lead to tissue ulceration (Sonis, 2009). Ulceration is the most significant event associated with mucositis (Sonis, 2007). Owing to the loss of mucosal integrity, mucositis ulcers are deep, broad and painful (Sonis, 2007, 2004). Mucositis ulcers are colonised by oral bacteria that may stimulate inflammatory responses and lead to bacteraemia and sepsis in neutropenic patients (Sonis, 2007, 2004). Ulceration may last up to 3 or 4 weeks after completion of RT (Sonis, 2009). Angiogenesis is potentiated by cyclooxygenase-2 (COX-2) during the end of the ulcerative phase (Sonis, 2007). At the end, the submucosal extracellular matrix (ECM) releases signals to direct differentiation, migration and proliferation of epithelial cells at the ulcerative sites to replenish epithelium during the healing phase (Sonis, 2007). The pathogenesis of mucositis is shown in Figure 1.6. Current management of radiation-induced mucositis is mainly palliative. Palifermin is a recombinant truncated human keratinocyte growth factor (KGF) protein that has shown in clinical trials reduced incidence of radiation-induced mucositis in patients with head and neck cancers (Han et al., 2013).

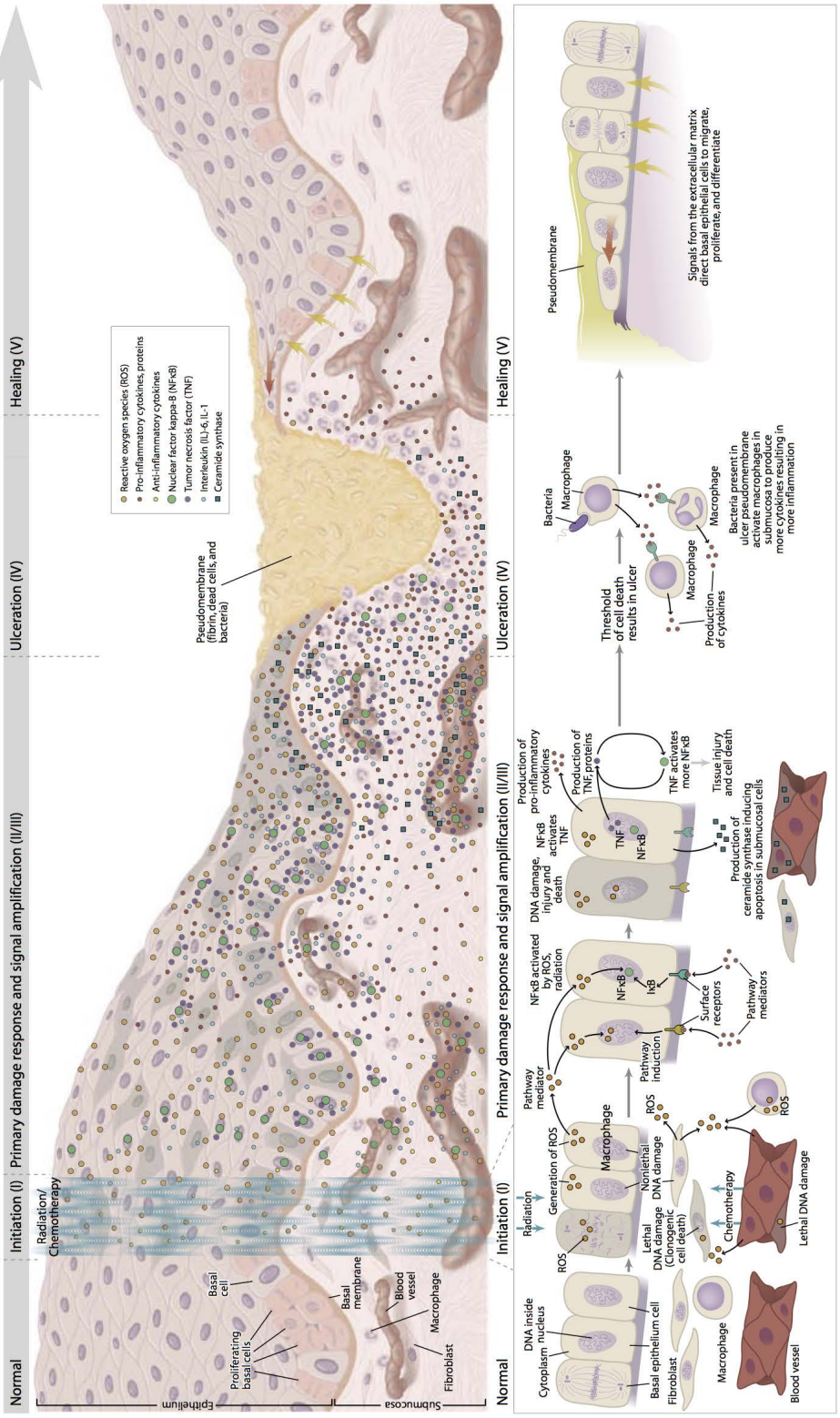


Figure 1.6: Pathogenesis of mucositis (Sonis, 2007).

#### 1.3.2.2 Acute and late skin reactions

Radiation-induced skin reactions are considered inevitable, since tumour volumes are surrounded by normal tissues. Although the severity of skin reactions has been reduced by the use of skin sparing techniques, radiation-induced skin reactions remain a significant issue affecting cancer treatment and quality of life of patients.

Similar to RT-induced mucositis, one hundred percent of NPC patients developed grade 1 or above RT-induced skin reactions (Kam et al., 2004). Over 50% of patients experienced grade 1 or above RT-induced neck fibrosis (Kam et al., 2004). Skin erythema and dry or moist desquamation of the skin are common RT-induced acute side effects while chronic neck fibrosis is a common RT-induced late complication in NPC patients. The structure of skin is shown in Figure 1.7 (Wells and MacBride, 2003). During normal skin homoeostasis, the basal layer of the epidermis proliferates rapidly to replace superficial cells lost through normal desquamation (Wells and MacBride, 2003). Approximately 4 weeks are needed for the repopulation of epidermis. Mitotic ability of clonogenic cells within the basal layer is damaged during RT. Cell repopulation is delayed and this weakens the skin integrity (Wells and MacBride, 2003). Fractionated RT repeatedly disrupts the proliferation of basal cells in epidermis and results in broken epidermis (Wells and MacBride, 2003). Necrosis is the most severe form of radiation-induced acute reaction although it is rarely seen (Wells and MacBride, 2003). Acute skin reactions start to appear approximately in the second or third week after RT commencement, and it is possible to have erythema, dry and moist desquamation at the same time within the radiation field (Wells and MacBride, 2003). Symptoms of skin reactions include uncomfortable sensations, such as itchiness and pain (Wells and MacBride, 2003). Moisturising creams and symptom-relieving agents such as hydrocortisone cream are commonly used in managing acute skin reactions (Wells and MacBride,

2003).

Acute skin reactions are transient and the healing process will be completed within a few weeks after completion of RT (Bentzen, 2006; Wells and MacBride, 2003). Inflammation, proliferation and remodelling are three distinct and overlapping phases involved in normal wound healing (Westbury and Yarnold, 2012). Early phases of fibrogenesis undergo the common inflammation and proliferative phases as normal wound healing (Westbury and Yarnold, 2012). The major difference between fibrogensis and normal wound healing is during the remodelling phase, in which injured cells are not replaced by normal parenchymal tissues or the same cell types, but permanent scar tissues (Wynn, 2008).

During inflammatory phase, many pro-inflammatory cytokines such as tumour-necrosis factor-$\alpha$ (TNF$\alpha$) and growth factors are upregulated by radiation. Release of chemokines initiate the recruitment of circulating inflammatory cells into irradiated tissue. Proliferation and recruitment of leukocytes are also stimulated. Macrophages and neutrophils recruited across the ECM eliminate tissue debris and dead cells, and produce mitogenic cytokines and chemokines for endothelial cells. Profibrotic cytokines such as transforming growth factor-$\beta$ (TGF$\beta$) released by lymphocytes or other cells during wound healing process activate the transformation of fibroblasts to myofibroblasts, which promote wound contraction. At the end of the wound healing process, damaged tissues are regenerated from divided and migrated epithelial and/or endothelial cells (Wynn, 2008). Besides the pathways involved in normal wound healing, ionising radiation also activates a series of processes directly or indirectly, such as radiation-induced apoptosis, ROS or reactive nitrogen species (RNS) imbalance, and tissue hypoxia (Bentzen, 2006). These processes perpetuate the injury response by disturbing the normal tissue remodelling. Simplified overview of radiation fibrogenesis is shown in Figure 1.8.

Similar to radiation-induced mucositis, there is currently no effective treatment to prevent radiation-induced fibrosis (Westbury and Yarnold, 2012). Treatment strategy of radiation-induced fibrosis is palliative. Anti-inflammatory treatment such as corticosteroids, vascular therapy using hyperbaric oxygen or pentoxifylline, and antioxidant treatment such as vitamin E are commonly used for symptomatic relief (Westbury and Yarnold, 2012).

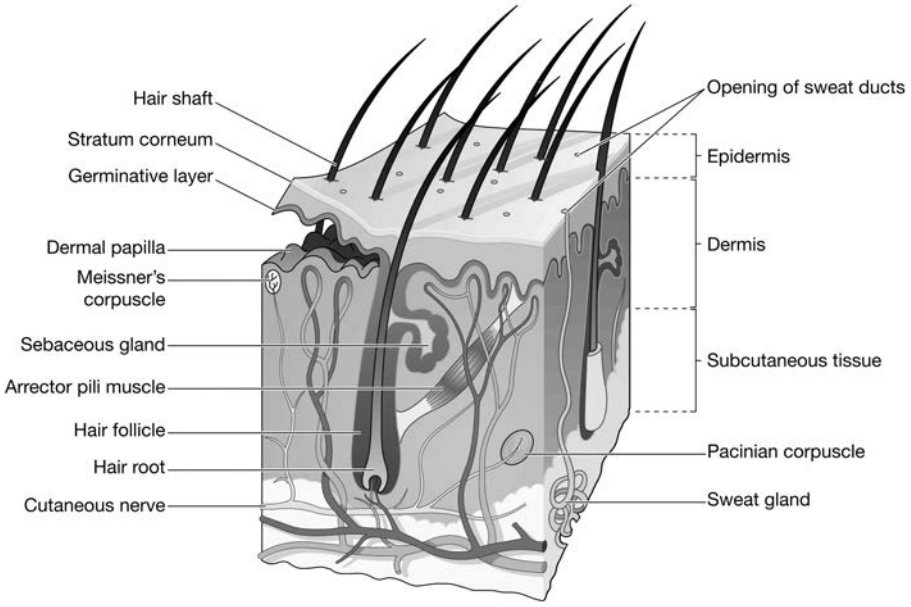


Figure 1.7: Structure of skin (Wells and MacBride, 2003).

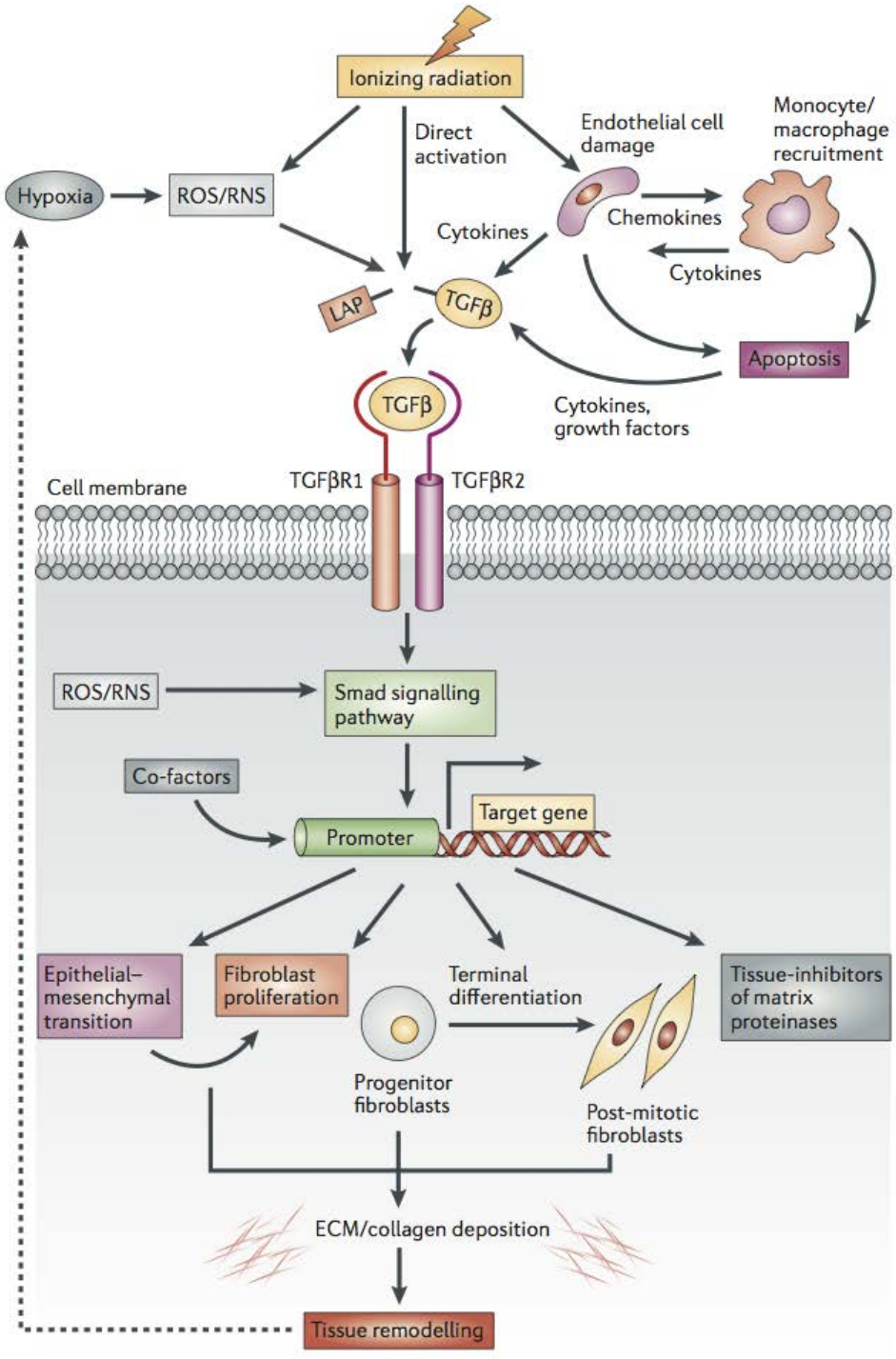


Figure 1.8: Simplified version of radiation-induced fibrogenesis (Bentzen, 2006).

## 1.4 Risk factors increasing susceptibility to normal tissue complications

Variations in the degree of normal tissue complications in patients receiving similar treatment trigger the investigation of underlying risk factors, particularly factors involved in the development of late complications, since late complications are irreversible and symptoms may worsen overtime. Risk factors contributing to these variations are mainly related to treatment regimen, such as total dose and irradiated volume, and patients' characteristics including predisposing factors and genetic variations (Azria et al., 2012; Barnett et al., 2009).

### 1.4.1 Factors related to treatment regimen

Total prescribed radiation dose is one of the treatment-related, confounding factors in the development of radiation-induced complications (Barnett et al., 2009). Steep radiation dose response curves of normal tissues suggested that small change in dose resulted in large variation in toxicity severity (Barnett et al., 2009). The prescribed dose is delivered to maximise treatment outcome with minimal toxicities. Dose response curves for tumour control and normal tissue damage are shown in Figure1.9a. Cumulative frequency dose response curves of skin telangiectasia and spinal cord necrosis development are shown in Figure1.9b (Barnett et al., 2009). Use of concurrent chemotherapy also increased radiation-induced mucositis in NPC patients (Kwong et al., 2004b; Lee et al., 2010).

Correlation of irradiated volume and the risk of late complications have been investigated in many cancers, such as breast, liver and lung cancers (Azria et al., 2012; Wells and MacBride, 2003). Breast cancer patients with larger breast volumes have higher risk in developing skin reactions (Wells and MacBride, 2003). Severity

of radiation-induced pneumonitis and radiation-induced liver diseases has been correlated with irradiated lung and liver volumes (Azria et al., 2012).

### 1.4.2 Factors related to patients' characteristics

Age, sex and medical complications such as hypertension and diabetes are patient-related predisposing factors that influence the risk of normal tissue complications (Azria et al., 2012; Barnett et al., 2009; Wells and MacBride, 2003). Age and menopause status have been shown to increase risk of erythema in breast cancer patients (Turesson et al., 1996). Smoking reduces the ability of cell reoxygenation during RT, thus indirectly increases the risk of normal tissue complications (Wells and MacBride, 2003).

Genetic variations are thought to be the most important factors contributing to varying degrees of normal tissue complications since up to 80% of the severity of radiation toxicity cannot be explained by known factors such as treatment-related factors and patient-related factors (Barnett et al., 2009). As a result, recording and analysing clinical data of cancer patients carefully may help to explain part of the individual variations in radiation-induced toxicities. Identifying genetic variations and cellular radiosensitivity in cancer patients may help to customise cancer treatment, maximise treatment results without compromising normal tissues, and provide better care to patients with high risk of developing severe normal tissue complications.

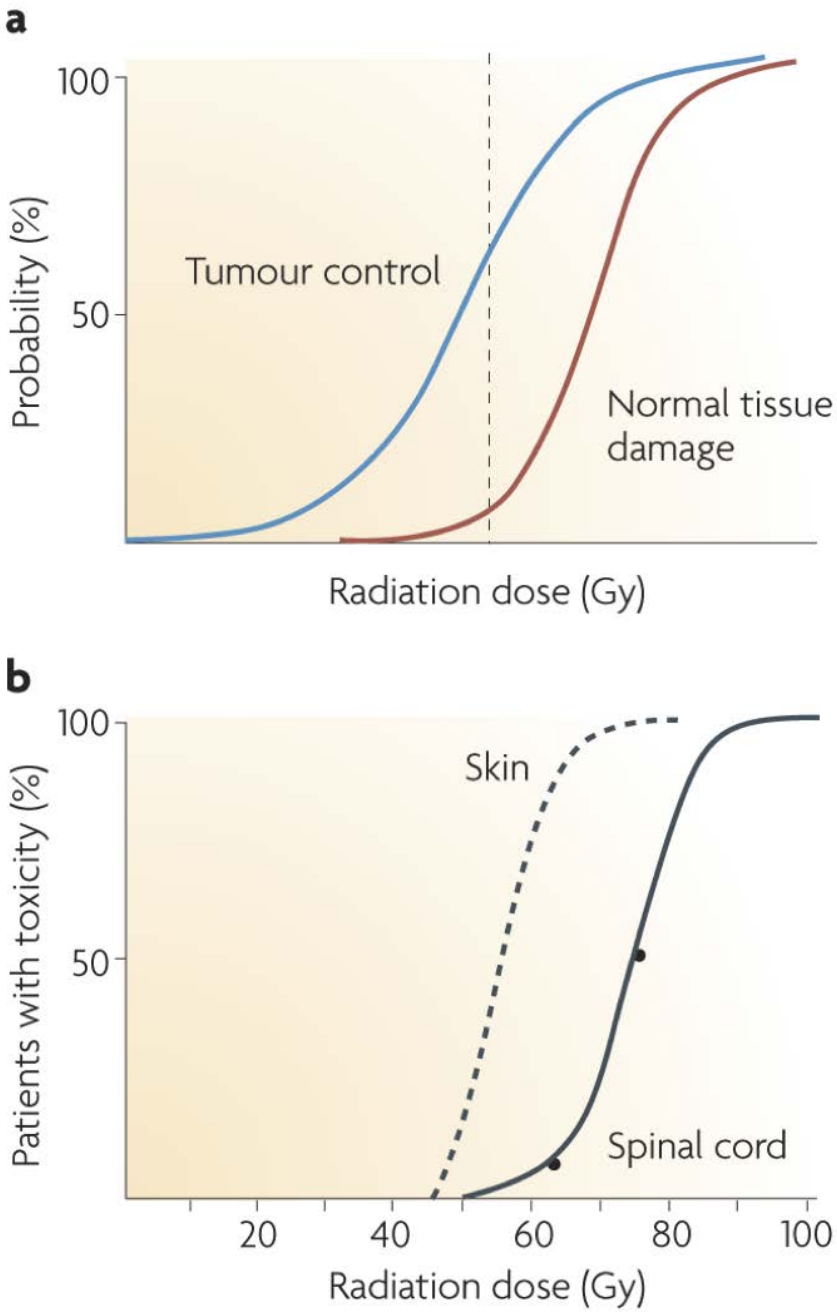


Figure 1.9: Dose response curve of radiation therapy. (a) Radiation therapy aims to maximise the probability of tumour control with minimal normal tissue toxicities. The dotted line represents approximately 60% of tumour control and 5% of severe late toxicities. (b) Cumulative frequency dose-response curves for skin telangiectasia (left) and spinal cord necrosis (right) (Barnett et al., 2009).

## 1.5 Research approaches in studying radiation damage

Two main research approaches have been used in predicting patients' likelihood of developing severe radiation-induced normal tissue complications. One approach focuses on investigating individual genetic variations and the association of radiation-induced complications while the another approach focuses on the end result of radiation-induced damage by using primary cells or cell lines derived from patients. These two approaches have identified patients with genetic disorders related to extreme radiation sensitivity, such as ataxia telangiectasia (Gatti, 2001). Isolated fibroblasts from patients with ataxia telangiectasia were shown to be three times more sensitive to radiation than healthy individuals (Barnett et al., 2009).

### 1.5.1 Genetic association studies

Adenine (A), guanine (G), cytosine (C), and thymine (T) are the bases of DNA. DNA bases bond to the sugar-phosphate backbone of DNA to form a DNA strand. Double stranded DNA consists of two complementary DNA strands, according to the base pairing rules; complement of A is T and complement of G is C. Double-stranded DNA forms a double helix. A sequence of hundreds or thousands of DNA bases forms a gene. Amino acids are the building blocks of proteins and each amino acid is coded by a set of three consecutive DNA bases, called codon. There are over 20,000 protein-encoding genes in humans and DNA base sequence variations in protein-encoding genes between individuals. These DNA base sequence variations are called alleles (Lewis, 2009).

Single nucleotide polymorphism (SNP) is defined as polymorphic genetic variant that occurs in at least 1% of a population. It is also the most widely tested genetic

marker in genetic association studies when compared with microsatellite markers, insertions, deletions, variable-number tandem repeats (VNTRs), and copy number variants (CNVs) (Lewis and Knight, 2012). Most of the SNPs are biallelic with one major allele and one minor allele. An individual who carries two major alleles or two minor alleles of a SNP is homozygous whereas an individual is heterozygous if he or she carries both major and minor alleles. The specific combination of these alleles are known as genotype. Haplotype refers to a combination of consecutive SNPs on a single chromosome (Pettersson et al., 2009b).

Most genetic association studies of complex diseases are population-based case control studies (Zondervan and Cardon, 2007). The controls are either unaffected individuals or selected randomly from a population while cases are those with a diagnosed disease or phenotype of interest (Lewis, 2002). Since it is neither feasible nor cost effective to genotype all SNPs from the genome in a large number of samples, tagging SNPs are chosen to predict allelic status of nearby SNPs. This non-random association of alleles in a population is known as linkage disequilibrium (LD) (Wang et al., 2005b). In addition, individual SNP may not be sufficient to result in a disease phenotype (Page et al., 2003). As a result, haplotype blocks are constructed from selected tag SNPs on the same chromosome to screen for possible association (Wall and Pritchard, 2003).

Hypersensitivity to radiation is due to genetic mutations or protein deficiencies that interfere with normal cell-cycle checkpoint, weaken the ability of DNA repair, or involve accumulated effects of one or more cell repair pathways (Gatti, 2001). Since a large number of genes are involved in cell-cycle checkpoint, DNA repair, and apoptosis, SNPs in these genes may be the major contributors in the variations in individual radiosensitivity. Over 100 genetic association studies addressing the association of SNPs and normal tissue radiosensitivity have been published since

2001 (Andreassen et al., 2012a).

Since a large number of genes may be involved in the development of normal tissue complications, a candidate-gene approach has been used in most of the genetic association studies focusing on normal tissue complications (Alsner et al., 2008). With the advancement of high-throughput SNP genotyping technologies, the number of GWAS is also increasing. The first GWAS investigating the association of normal tissue radiosensitivity in prostate cancer patients was published in 2010 (Kerns et al., 2010). A summary of the advantages and disadvantages of candidate-gene approach and GWAS approach is shown in Table 1.4.

Table 1.4: Comparison of candidate-gene approach and GWAS approach

| | Approach | Advantages | Disadvantages |
|---|---|---|---|
| Candidate-gene approach | Hypothesis-driven | • Useful in studying genetic variants with low allele frequency<br>• Able to detect genetic variants with small to moderate effect<br>• Inexpensive and useful to explore genes in potential pathways | • Unable to study all possible genes and genetic variants<br>• Require prior knowledge of candidate genes and their possible roles in disease development |
| GWAS | Hypothesis-free | • No prior knowledge is required<br>• Comprehensive and unbiased<br>• Able to detect population stratification | • Unable to identify rare variants<br>• Expensive<br>• Lack of functional information about identified variants |

#### 1.5.1.1 Candidate-gene approach

Candidate-gene approach is a hypothesis-driven study approach. It is commonly used in studying small to moderate genetic influences of complex diseases (Tabor et al., 2002). Studies using candidate-gene approach select genes of interest based on their mechanistic understanding and their possible roles in disease aetiology (Tabor et al., 2002). Candidate-gene approach is an useful and inexpensive approach in exploring the association between casual variants and complex diseases (Hirschhorn and Daly, 2005; Tabor et al., 2002). Further replication studies in other independent populations can be performed once a statistically significant association of a gene is detected (Tabor et al., 2002).

#### 1.5.1.2 Genome-wide association study

GWAS is a study approach in which a dense set of SNPs is captured to investigate the role of common genetic variations and the susceptibility to complex diseases and quantitative traits (McCarthy et al., 2008). GWAS have successfully identified many novel loci involved in the predisposition to complex diseases, such as breast cancer, prostate cancer, type I and II diabetes, and inflammatory bowel disease (McCarthy et al., 2008). In contrast to candidate-gene approach, no presumption of casual genes or genetic variants is made in performing GWAS (Hirschhorn and Daly, 2005). As a result, GWAS approach is a comprehensive and unbiased approach to perform in the absence of convincing evidence (Hirschhorn and Daly, 2005). GWAS is able to detect population stratification (McCarthy et al., 2008). In order to perform GWAS, advanced knowledge of common variants is required. With the availability of large SNPs databases such as dbSNP database, International HapMap Project, and 1000 Genome Projects, and the advancement in high-throughput genotyping technologies, large-scale GWAS with thousands of genotypes can be performed in a relatively more cost-effective manner (Hirschhorn

and Daly, 2005).

### 1.5.2 Meta-analysis

Meta-analysis is a statistical tool to combine existing literature to investigate the gene-disease relationship and to resolve discrepancies between studies (Berman and Parker, 2002; Munafò and Flint, 2004). Meta-analysis overcomes the limitation of small sample size and increases statistical power by summarising and integrating results from studies with similar research protocols. Discrepancies between studies can be analysed by meta-analysis to investigate the source of heterogeneity, such as publication bias, population stratification or misclassification of clinical outcome. Investigation of effects of interest through meta-analysis also increases precision in estimating effects, thereby generating new hypothesis or determining if future studies are needed (Walker et al., 2008). Meta-analysis is commonly used in some fields of research, such as clinical trials in cancer research, when it is impossible to recruit a large number of patients in a single centre. Meta-analysis of a number of clinical trials may provide sufficient information on the treatment outcome of new treatment regimens, hence avoiding the delay of delivering new treatments and reducing the cost of performing large randomised clinical trials (Berman and Parker, 2002).

The preferred reporting items for systematic reviews and meta-analyses (PRISMA) statement consists of guidelines and a checklist of 27 items to improve reporting meta-analyses and systematic reviews (Moher et al., 2009). In performing meta-analysis of genetic association studies, it is essential to check the Hardy-Weinberg equilibrium (HWE) and to determine heterogeneity (Nakaoka and Inoue, 2009). Flow chart of performing literature-based meta-analysis is shown in Figure 1.10.

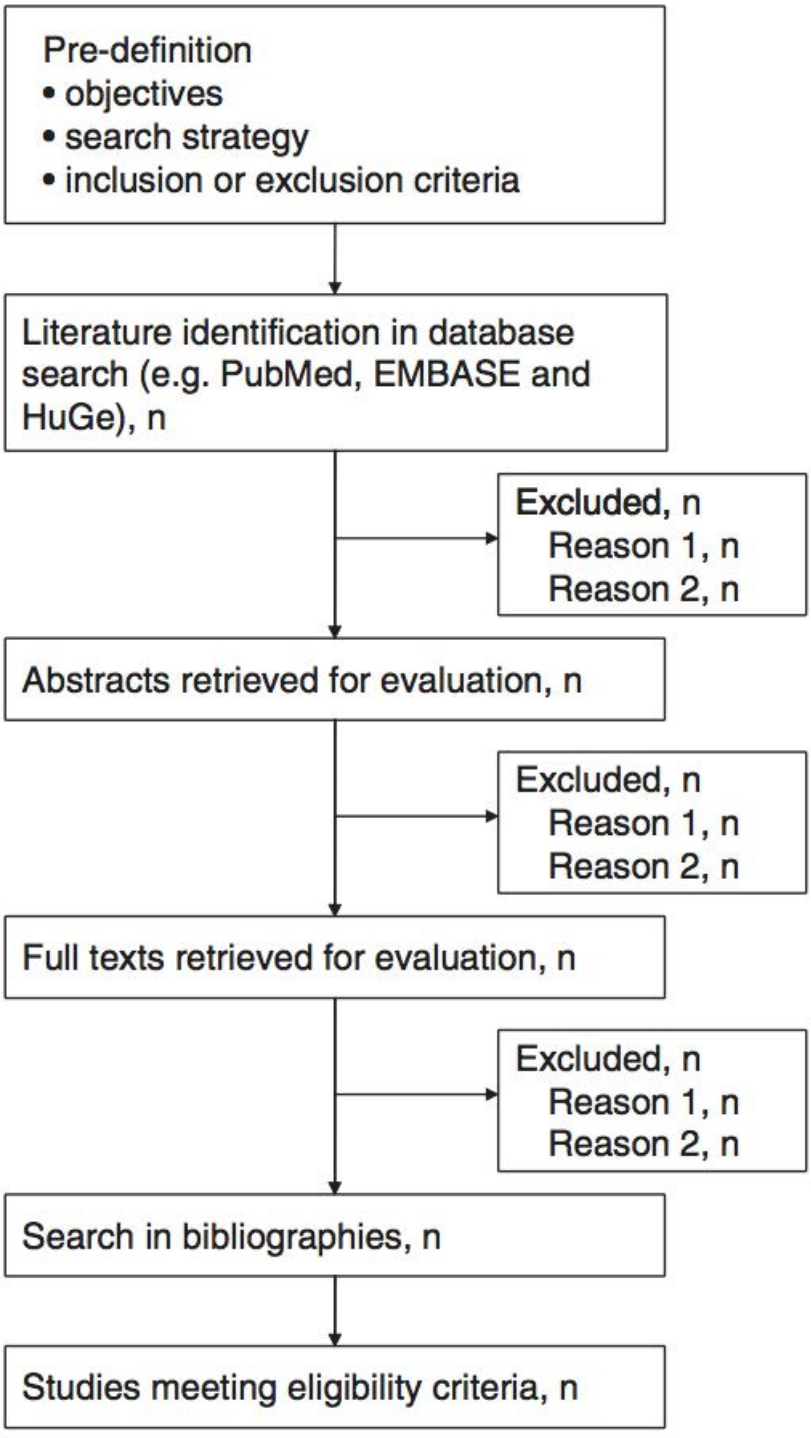


Figure 1.10: Example work flow of literature-based meta-analysis. The number of study included or excluded in each step is represented by n (Nakaoka and Inoue, 2009).

### 1.5.3 Predictive assays

Besides investigation of causal variants through genetic association studies, establishing correlation between the level of cellular damage during radiation and normal tissue clinical radiosensitivity is another approach to investigate individual variations in normal tissue toxicities. Individual or combination of pathways that interfere with DNA repair, DNA stability, DNA synthesis and control of cell-cycle checkpoint may lead to hypersensitivity to radiation. Cell blebbing, cell shrinkage, DNA laddering and formation of nuclear apoptotic bodies are examples of classical apoptotic response induced by radiation (Faulhaber and Bristow, 2005). Association of radiation-induced complications in cancer patients and radiation-induced damages, such as radiation-induced apoptosis, initial DNA damages, and DNA capacity in fibroblasts or peripheral blood mononuclear cells (PBMCs) derived from clinically radiosensitive cancer patients have been investigated using various assays (Henríquez-Hernández et al., 2012). For example, Annexin V assay, comet assay and caspase activity assay are commonly used methods to detect and to quantify apoptosis based on target of interest. Some apoptosis assays can also be performed in a flow cytometer to provide quantitative and rapid information. The advantages and disadvantages of selected assays are compared in Table 1.5.

#### 1.5.3.1 Cell types

Fibroblasts and PBMCs are two commonly used cell types in assays quantifying and measuring apoptosis. Fibroblasts cultured from human skin fibroblasts were first used to determine normal tissue clinical radiosensitivity in 1980s (Henríquez-Hernández et al., 2012). Although significant correlation between cultured fibroblasts and late normal tissue complications have been observed, results could not be replicated in large confirmatory studies (Henríquez-Hernández et al., 2012). Owing to practical difficulty in obtaining and culturing fibroblasts, PBMCs are the

alternative cell type used in apoptosis assays with several advantages (Borgmann et al., 2002; Henríquez-Hernández et al., 2012). A linear correlation of DSBs between PBMCs and epidermal skin cells derived from the same patient has been reported (Núñez et al., 1998). PBMCs can be isolated easily from peripheral blood by density gradient centrifugation. Compared to fibroblasts, PBMCs can be used and obtained more quickly in large quantities (Henríquez-Hernández et al., 2012). Cryopreservation of viable cells is commonly used when apoptosis assays cannot be performed immediately in clinical setting.

#### 1.5.3.2 Comet assay

Comet assay is a DNA gel electrophoresis technique to measure DNA damage in individual cells. There are different versions of comet assays to detect specific DNA lesions. For example, neutral comet assay detects SSBs and DSBs while enzyme-assisted comet assay detects specific types of damage with higher sensitivity (Wong et al., 2004). Individual cells with DNA damage are embedded in agarose gel. A DNA distribution is generated after gel electrophoresis and this DNA distribution resembles the shape of a comet (Huang et al., 2005). Undamaged DNA, represented by a comet head, prevents migration during gel electrophoresis. Comet tails represent migrating fragments of broken or relaxed DNA supercoils (Olive and Banáth, 2006). Relative amount of DNA damage is determined by measuring the extent and length of comet tail visualised under fluorescence microscopy. Since only a small number of cells is required to perform comet assay, comet assay has practical advantage over other techniques especially when samples are limited (Olive and Banáth, 2006). However, accuracy of information obtained by comet assay, such as base damage or strand breaks, may be affected by the predominance of apoptotic cells or necrotic cells in cell suspension (Olive and Banáth, 2006). In addition, there is practical difficulty in handling a large number of samples, since

only 50 slides, with a recommended 50 comets per sample, can be scored per day even with the use of an automated machine (Olive and Banáth, 2006). Figure 1.11a-b illustrates DNA distribution observed using comet assay.

#### 1.5.3.3 Terminal dUTP nick end-labelling (TUNEL) assay

Terminal dUTP nick end-labelling (TUNEL) assay is a DNA fragmentation-based detection method and is able to detect cells undergoing active DNA repair, apoptosis and necrosis (Loo, 2002). Samples are first pretreated with proteinase K or microwaves to improve sensitivity (Watanabe et al., 2002). Labelled nucleotides are added to the 3' end of DNA fragments of pretreated samples by terminal deoxynucleotidyl transferase. Compared to comet assay, no viable cell is needed to perform TUNEL assay. Since DNA fragmentation only occurs at late stage of apoptosis, TUNEL assay is unable to detect cells undergoing early apoptosis (Martinez et al., 2010). Terminal deoxynucleotidyl transferase is an expensive enzyme and hence TUNEL assay may not be the method of choice in large-scale analyses (Watanabe et al., 2002).

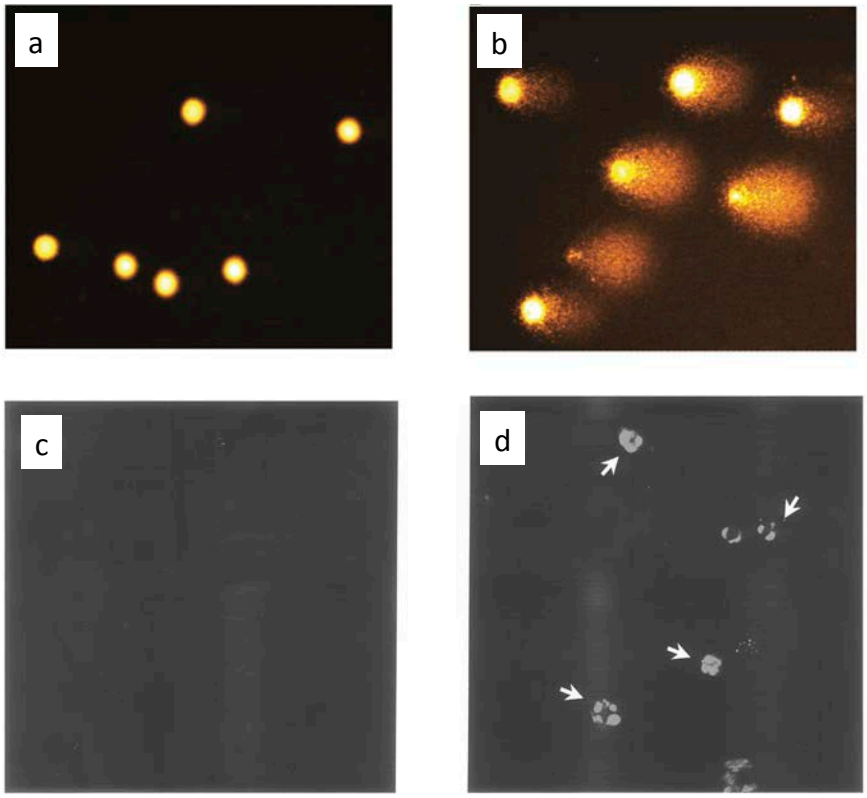


Figure 1.11: Images of comet assay (a-b) and confocal micrographs of TUNEL assay (c-d). (a) Undamaged DNA (comet score 0). (b) Minor (comet score 1) to severe DNA damage (comet score 4). (c) Untreated culture and (d) treated cells undergoing apoptosis. Cells undergoing apoptosis with condensed TUNEL-positive chromatin are indicated by arrows (Loo, 2002; Wong et al., 2004)

#### 1.5.3.4 Annexin V

Phosphatidylserine (PS) is a phospholipid containing serine. PS in plasma membrane of healthy cells are facing internally by adenosine triphosphate (ATP)-dependent enzymes (Watanabe et al., 2002). During apoptosis, PS residues are flipped to external plasma membrane due to loss of ATP dependent enzyme activity (Watanabe et al., 2002). In the presence of calcium ions ($Ca^{2+}$), fluorescence-labelled Annexin V is able to bind to exposed PS residues (Watanabe et al., 2002). Compared to TUNEL assay, Annexin V assay is able to detect cells undergoing early apoptosis. Cells in suspension or tissue samples are applied with high concentration of Annexin V for at least 15-30 minutes in advance before washing or fixation. However, false positive signals may be obtained with certain cell types such as blood platelets and healthy B-lymphocytes (Watanabe et al., 2002).

#### 1.5.3.5 Caspase activity assay and mitochondrial assays

Caspases are proteases that are activated during apoptosis. In order to monitor different stages of apoptosis, various versions of caspase-specific assays are developed based on caspase-specific fluorescence probes or cleaved substances (Watanabe et al., 2002). On the other hand, mitochondrial assays can be used to monitor apoptosis and early changes of intrinsic pathways. Mitochondrial parameters such as increase of mitochondrial permeability transition (MPT), release of ROS and $Ca^{2+}$, are characteristics of cells undergoing apoptosis (Watanabe et al., 2002). Caspase activity assays are rapid and results are quantitative. However, cell membrane integrity is unable to maintain. Mitochondrial assays are unable to differentiate apoptotic cells and necrotic cells.

#### 1.5.3.6 Flow cytometry

Apoptosis assays are commonly used in conjunction with flow cytometry to provide quantitative information such as cell types, cell morphological changes, changes in cellular constituents, cell viability and ratio of apoptotic cells (Cram, 2002; Martinez et al., 2010; Wlodkowic et al., 2011). A flow cytometer is a fluidics system consisting of two parts: a sheath reservoir and a flow cell (Figure 1.12a) (Hawley and Hawley, 2004). Both cell suspension from sample tube and sheath fluid from sheath reservoir are pushed into the flow cell by air pressure. When cell suspension is injected to the centre of the flow cell, which is a wide and rapidly flowing stream, cells are hydrodynamically focused at the centre of the flow cell so that cells are confined and aligned at the centre (Figure 1.12b). Cells are separated and then pass through the narrow sheath stream with no blockage (Hawley and Hawley, 2004). As a result, cell suspension passes through the laser beam one cell at a time and light scattered of each cell is collected by photodetectors (Figure 1.12c) (Hawley and Hawley, 2004). One forward-scatter photodetector is located in front of the light beam. Several side scatter photodetectors are located to the side of the light beam (Hawley and Hawley, 2004). Forward-scatter photodetector provide information about the size of cells while side-scatter photodetectors provide information about the granularity of the cells (Hawley and Hawley, 2004). Fluorescence signal from stained cells are detected by optical detectors (Cram, 2002). With the use of specific probes and dyes, autophagic or necrotic cell death can be differentiated by flow cytometry (Wlodkowic et al., 2011). Cell sorting can also be performed by flow cytometry with the use of specific antibodies (Cram, 2002). The major limitation of flow cytometry is the requirement of single cell suspension and prior cell disaggregation is required (Martinez et al., 2010).

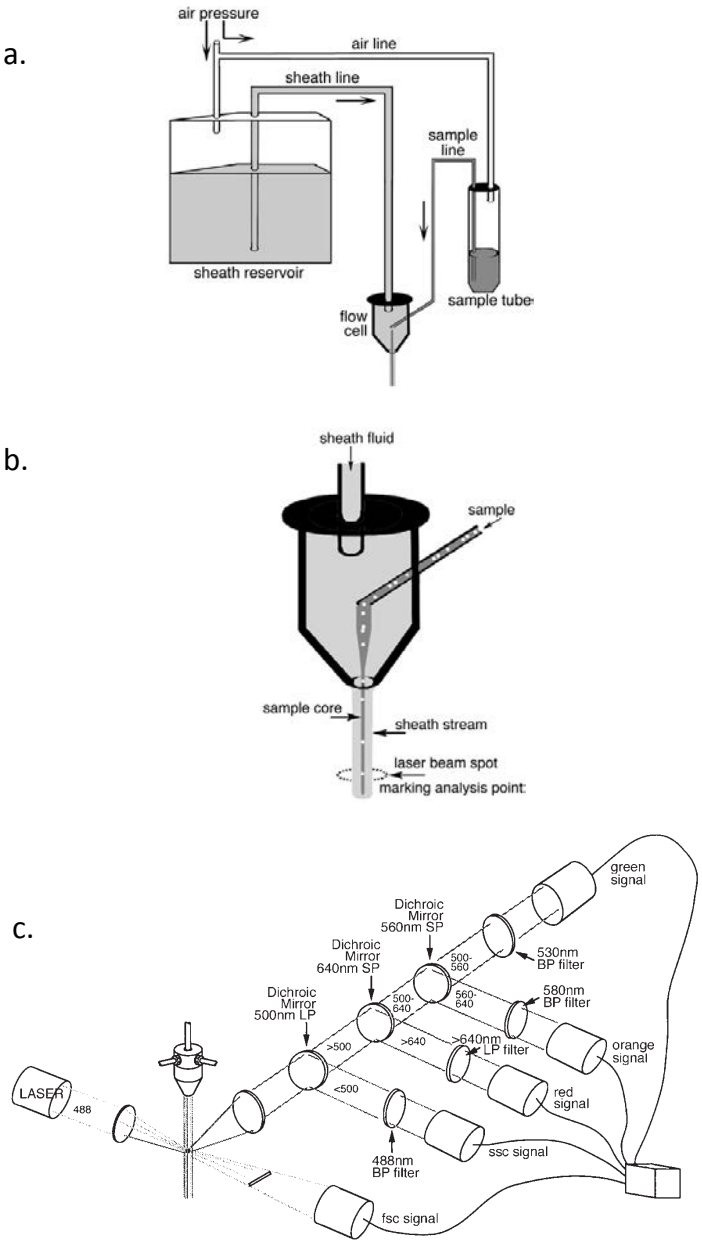


Figure 1.12: Introduction to flow cytometry. (a) The fluidics system. (b) A flow cell. (c) Light sources and optical systems (Hawley and Hawley, 2004).

Table 1.5: Summary of commonly used apoptosis assays for detecting radiation-induced damage

| Assay | Approach | Pros | Cons |
|---|---|---|---|
| Annexin V | Phosphatidylserine exposure and membrane imbalance | - Rapid<br>- Able to identify cell types<br>- Able to detect early and late apoptotic events | - Unable to differentiate necrotic cells and apoptotic cells<br>- False positive results may obtain for adherent cells after trypsinisation |
| Caspase activity assays | Caspase activity | - Quantitative and rapid | - Cell death-unrelated caspase activation may occur |
| Comet Assay | DNA fragmentation | - Small number of cells per sample is required<br>- Able to visualize DNA damage | - Viable cell suspension is required<br>- Unable to determine length of DNA fragments<br>- Time-consuming |
| Flow cytometry | Laser light scatter characteristics | - Convenient and rapid<br>- May use in conjunction with other assays<br>High cell count<br>- Able to perform cell sorting | - Single cell suspension is required |
| Mitochondrial assay | Mitochondrial events | - Able to monitor early phase of intrinsic pathway | - Unable to differentiate apoptosis and necrosis |
| TUNEL assay | DNA fragmentation | - Well accepted histological assay | - Time consuming<br>- Unable to differentiate necrotic cells and apoptotic cells<br>- Cell pretreatment is required |

## 1.6 Candidate genes

Over 3,000 thousand SNPs from approximately 1,500 candidate genes have been studied and published in the field of normal tissue radiogenomics (West et al., 2012). A number of candidate genes have been extensively studied and these genes are involved in cell cycle check point and DNA repair pathways.

### 1.6.1 Ataxia telangiectasia mutated (*ATM*)

*ATM* is located on chromosome 11 (11q22-q23) of the human genome. As mentioned previously, the *ATM* gene was discovered in 1970s from ataxia telangiectasia, a rare autosomal recessive disease with a wide range of characteristics such as increased cancer risk, hypogonadism, immunodeficiency, progressive cerebellar ataxia, telangiectasia and hypersensitivity to ionising radiation (Becker-Catania et al., 2000; Jeggo and Lavin, 2009). *ATM* heterozygosity was found to be more common in breast cancer than the general population (Iannuzzi et al., 2002). During ionising radiation, the ATM protein is rapidly activated by autophosphorylation of serine residue at position 1981 on the ATM protein (Lavin et al., 2004). Activated ATM protein phospharylates a variety of protein substrates involved in the DNA repair pathway (Lavin et al., 2004). Association of functional variant rs1801516 (Asp1853Asn) from *ATM* and late radiation-induced reactions has been reported by previous studies (Andreassen and Alsner, 2009). Due to the low minor allele frequency (MAF) of this functional SNP (MAF $< 0.1$), only common variations of *ATM* and radiation-induced complications were investigated.

### 1.6.2 Superoxide dismutase 2 (*SOD2*)

*SOD2* is located at chromosome 6 (6q25.3). The major antioxidant enzyme within the mitochondria, manganese superoxide dismutase (MnSOD), is encoded by su-

peroxide dismutase 2 (*SOD2*) (Green et al., 2002). MnSOD plays an important role in cellular defence by removing ROS generated or induced by cytotoxic reagents. As a result, *SOD2* is a potential candidate gene associated with individual variation in radiosensitivity. Significant association between functional variant rs4880 (Val16Ala) and higher risk of subcutaneous fibrosis have been reported (Andreassen et al., 2003). However, this result could not be replicated by the same research group (Andreassen et al., 2006a). In this study, association of common and functional variants of *SOD2* and radiation-induced complications were investigated.

### 1.6.3 Transforming growth factor beta 1 (*TGFβ1*)

The *TGFβ1* gene is located at chromosome 19 (19q13.1) and the protein is a multifunctional cytokine involved in the pathogenesis of fibrosis. SNPs in *TGFβ1* are associated with many human diseases since the protein of *TGFβ1* is a key regulator in cell growth regulation, immunosuppressive activities and regulation of deposition of extracellular matrix components (Martin et al., 2000). Because of its functional role, *TGFβ1* is one of the most extensively studied genes in the field of normal tissue radiogenomics. Variant rs1800469, located in the promoter region, and functional variant rs1800470 (Leu10Pro) are in strong LD that association of these two SNPs and increased risk of radiation-induced complications have been reported in most studies focusing on breast cancer and prostate cancer patients (Andreassen and Alsner, 2009; Zschenker et al., 2010). In order to investigate the role of this gene involved in radiation-induced complications in NPC patients, common variants, in addition these two reported SNPs, were included in this study.

### 1.6.4 Tumor protein p53 (*TP53*)

*TP53* is located at chromosome 17 (17p13.1) and it encodes the tumour suppressor protein p53. p53 is involved in cell cycle regulation, such as induction of apoptosis or cell cycle arrest. The *ATM* protein and other DNA damage-induced kinases are responsible for p53 activation during cellular stress (Tan et al., 2005). During RT, phosphorylated p53 protein is activated to induce transcription of downstream genes involved in apoptosis, cell-cycle regulation and DNA repair (Tan et al., 2005). Lymphocytes from patients with genetic disorders related to hypersensitivity to radiation, such as ataxia telangiectasia, Bloom syndrome and Fanconi anaemia, have shown absence of p53 induction (Bordon et al., 2009). Therefore, individual variation of radiation response is likely to be associated with genetic variants of *TP53*. Functional variants, rs1042522 (Arg72Pro) and rs17878362 (PIN3), are the two most studied genetic variants in *TP53* (Tan et al., 2005). Common variants and rs1042522 of *TP53* and the association of radiation-induced complications were examined. Since rs17878362 is 16bp duplication polymorphism but not SNP, this variant was not included in this study.

### 1.6.5 X-ray repair cross complementing group 1 and group 3 (*XRCC1* and *XRCC3*)

*XRCC1* is located at chromosome 19 (19q13.213.3) and codes for the XRCC1 protein, a scaffold protein that is involved in base excision repair pathway (Zhou et al., 2010). During radiation-induced DNA damage, XRCC1 forms a DNA-protein complex at the DNA damage sites with DNA ligase III, DNA polymerase $\beta$, and poly(ADP-ribose) polymerase (PARP) to repair DNA damage (Zhou et al., 2010). *XRCC3*, which belongs to the same family of *XRCC1*, is located at chromosome 14 (14q32.3). *XRCC3* is one of the components of the homologous re-

combination pathway that is involved in DSB repair (Bartsch et al., 2007; Falvo et al., 2011). Radiosensitivity of the Chinese hamster ovary (CHO) DNA repair mutant cells (EM9) has been shown to be fully corrected by cloning *XRCC1* into the cell (Thompson et al., 1990). Partially corrected chromosome instability, mutagen sensitivity and radiation sensitivity in another CHO mutant irslSF by cloning *XRCC3* have also been reported (Price et al., 1997). Previous studies have shown correlation between functional variants rs1799782 (Arg194Trp) and rs25487 (Arg399Gln) from *XRCC1*, and rs861539 (Thr241Met) from *XRCC3* and increased risk of radiation-induced complications Andreassen and Alsner (2009). In order to obtain more information, common SNPs and reported functional SNPs of *XRCC1* and *XRCC3* were investigated for their roles in contributing individual variations in radiation sensitivity.

## 1.7 Genotyping methods

Polymerase chain reaction (PCR) is a fast and efficient method for replicating DNA in closed tube environment. A pair of primers complementary to the DNA sequence of interest is designed and is annealed to denatured single-stranded DNA. DNA polymerase extends the primer by incorporating the deoxynucleotides (dNTP) complementary to DNA strand according to base pairing rules (Section 1.5.1). PCR consists of three phases in each cycle, denaturation, annealing, and extension. During denaturation, the double-stranded DNA is denatured by heating up to 95 °C. Following denaturation is annealing in which the reaction is cooled to an optimal annealing temperature of specific primers for primer-template hybridisation. Temperature is heated to 72 °C for efficient primer extension catalysed by thermostable DNA polymerase. PCR products are produced exponentially during each cycle. PCR has many applications such as PCR-based diagnosis, DNA sequencing, and mutation screening (McPherson and Møller, 2007). Many methods can be used for SNP genotyping and three of them used in this study are discussed.

### 1.7.1 Restriction fragment length polymorphism (RFLP)

Restriction fragment length polymorphism (RFLP) analysis is a simple and inexpensive method to detect sequence variation in a large number of individuals. Restriction endonucleases are bacterial enzymes that digest DNA at specific recognition sequence. Since restriction endonucleases are extremely sequence-specific, sequence variation at the recognition site alters DNA cleavage and produces different fragment sizes. Sequence of interest is first amplified using PCR. PCR products are digested by specific restriction endonucleases under optimal conditions. After digestion, products are separated by gel electrophoresis to separate digested fragments. Figure 1.13 shows an example results of RFLP analysis.

Since restriction enzymes only work optimally under specific conditions, internal digestion control is recommended to determine if the condition is optimal and to detect any incomplete digestion. There are several limitations of using RFLP analysis. Recognition sites may be altered by other nearby sequence variations that affect cleavage by restriction endonucleases. Manual sequence alteration is needed to introduce recognition site if there is no natural recognition site or another recognition site found near the SNP of interest. Some restriction enzymes are expensive. In addition, incubation time of restriction endonucleases and PCR products may take up to 16 hours for complete digestion. Thus, it is not suitable for high-throughput analysis (Jenkins, 2008; Rasmussen, 2012).

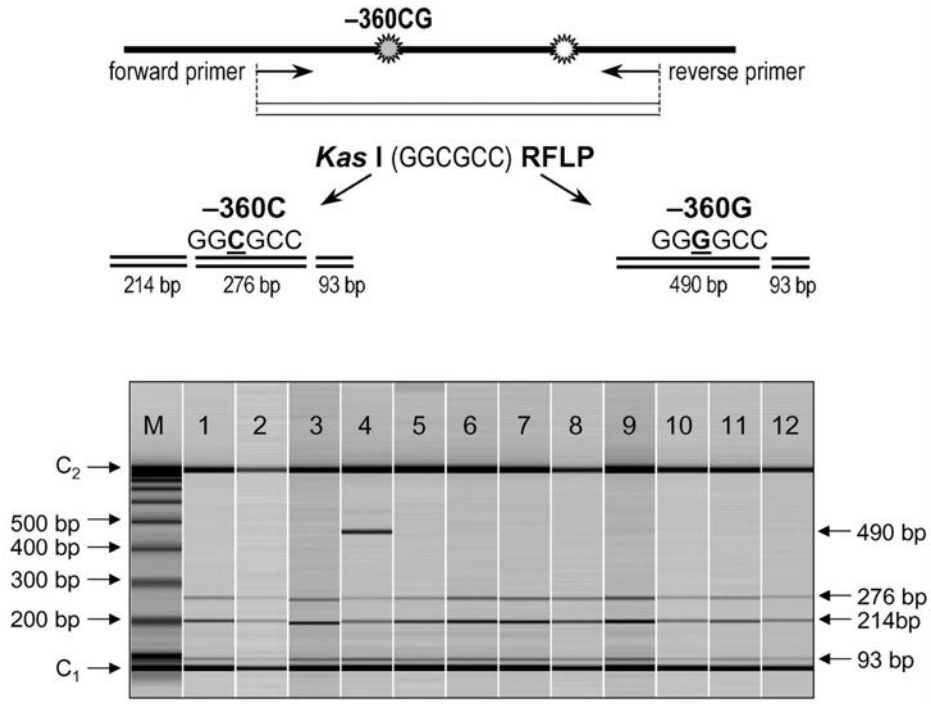


Figure 1.13: Genotyping by restriction fragment length polymorphism. Amplified region is digested with restriction enzyme Kas I with recognition site GGCGCC. Three restriction fragments are produced for CC homozygotes (left) and two restriction fragments are produced for GG homozygotes (right). An internal control cutting site is introduced and produced a 93bp fragment for complete digested products (Rasmussen, 2012)

### 1.7.2 High-resolution melting curve analysis using unlabelled probe

High-resolution melting analysis (HRMA) using unlabelled probe is an effective and inexpensive genotyping and mutation detection method for known sequence variants with high sensitivity (Montgomery et al., 2007). Besides a pair of primers, an oligonucleotide probe containing 18-30 bases and complementary to a specific sequence of interest is designed for hybridisation (de Muro, 2008). Probe is added with a non-radioactive 3' blocker, such as the most commonly used 3' phosphorylation, to prevent extension during PCR (Montgomery et al., 2007). Since thermal stability of PCR product is determined by base sequence, sequence variation alters duplex stability and leads to different melting behaviour (Montgomery et al., 2007). Asymmetric PCR is performed to overproduce the strand complementary to the designed probe to allow probe hybridisation. Wild-type sequence that is perfectly matched with the probe produces the highest melting temperature ($T_m$) while other sequence variations destabilise the probe-amplicon duplex and produce a lower $T_m$ (Montgomery et al., 2007). As a result, both homozygous and heterozygous states can be easily differentiated by identifying the $T_m$, in which a single peak is produced by homozygous state and two peaks are produced by heterozygous state (Montgomery et al., 2007). The stability of probe-amplicon duplex is monitored by fluorescence dyes such as Syto 9 and LCGreen Plus (Montgomery et al., 2007). The mechanism of unlabelled probe melting analysis is shown in Figure 1.14.

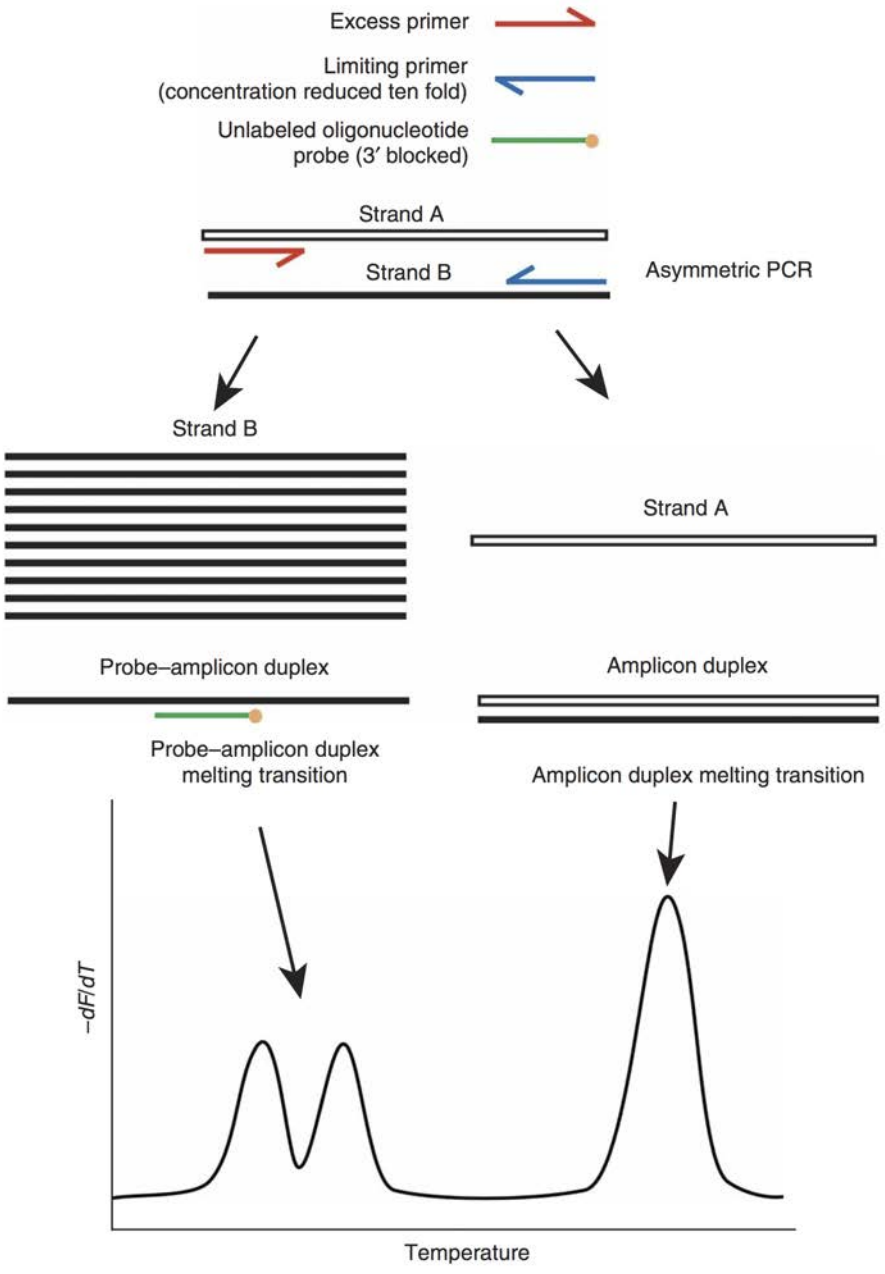


Figure 1.14: High resolution melting curve analysis with unlabelled probe. Excess primer (red) is complementary to strand A and limiting primer (blue) is complementary to strand B. Asymmetric polymerase chain reaction produces excess copies of strand B. Unlabelled probe (green) is designed complementary to either wild type or mutant sequence. Melting transition of probe-amplicon duplex is visualised by plotting negative derivative of the normalised fluorescence (-dF/dT) versus temperature (Montgomery et al., 2007).

### 1.7.3 Sequencing

Sanger sequencing is a chain-termination sequencing method developed since 1970s (Sanger et al., 1977). Fluorescently labelled dideoxynucleotides (ddNTPs) are used as terminating bases in cycle sequencing reactions (Pettersson et al., 2009a). Non-terminating dNTPs and terminating ddNTPs are incorporated during primer extension after primer denaturing and primer annealing. As a result, single-stranded, labelled fragments of all length are generated during cycle sequencing and can be separated by capillary or gel electrophoresis (Shendure and Ji, 2008). Base-specific colours of fragments emitted by laser excitation are traced and analysed by DNA sequencing analysis programs. With the advancement of technology, the read length can be up to 700 to 1000 bases with approximately $0.5 per kilobase (Pettersson et al., 2009a; Shendure and Ji, 2008). Novel variations, such as SNPs, insertions and deletions can be identified by DNA sequencing. Figure 1.15 illustrates the biochemistry of Sanger sequencing.

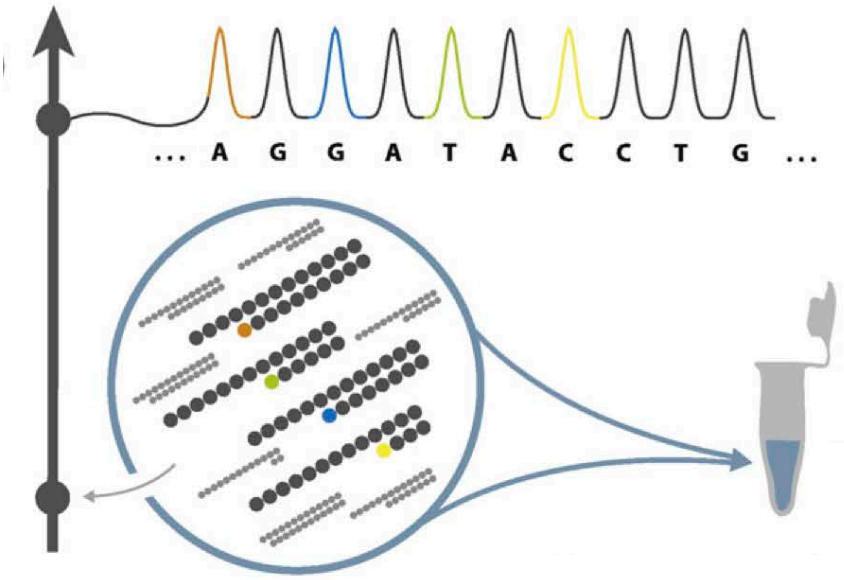


Figure 1.15: DNA sequencing by chain termination. Fluorescently labelled dideoxynucleotides are used as terminating bases in cycle sequencing reactions. Non-terminating dNTPs and terminating ddNTPs are incorporated during primer extension after primer denaturing and primer annealing. Labelled fragments of all length are separated by capillary or gel electrophoresis. Base-specific colours of fragments emitted by laser excitation are traced and analysed by DNA sequencing analysis programs (Pettersson et al., 2009a).

## 1.8 Quantification of radiation-induced apoptosis

Quantification of DNA damage and radiation-induced apoptosis by the use of specific assays (Section 1.5.3) appear to be clinically useful in identifying individuals with a higher risk of normal tissue complications (Henríquez-Hernández et al., 2012). Significant correlation of risk of radiation-induced acute skin reactions and the level of cellular damages, such as the level of DNA damages, DNA repair capacity, chromosome sensitivity, and radiation-induced apoptosis, have been reported (Crompton et al., 1999; Huber et al., 2011; Mariano Ruiz de Almodóvar et al., 2002; Núñez et al., 1998; Popanda et al., 2003; Wang et al., 2005a). In order to be practically useful in normal clinical practice, a rapid, replicative and robust predictive assay must be developed. For instance, comet assay is useful in measuring DNA damage in individual cells. Although only a small number of cells are required, comet assay is a time-consuming detection method that it is not suitable in clinical setting when a large number of patients have to be screened. In contrast, Annexin V and TUNEL assays can be used as flow cytometry-based assays so that rapid and quantitative results can be obtained. In addition, individual cell-based mode of analysis can be performed using flow cytometry-based apoptosis assays (Hawley and Hawley, 2004).

Compared to TUNEL assay, no pretreatment such as proteinase K or microwave is required for Annexin V assay to increase sensitivity. Since Annexin V is only able to identify cells undergoing early apoptosis, propidium iodide (PI) usually is used in combination with Annexin V to identify cells undergoing late apoptosis and to discriminate necrotic cells (Wilkins et al., 2002a). PI is a viability stain and is used as plasma membrane permeability indicator (Hawley and Hawley, 2004). Dead cells are stained by PI when cell membrane is permeable.

Besides the choice of prediction method, selection of cell types is another major concern in developing practically useful assay. As mentioned previously (Section 1.5.3.1), fibroblasts and PBMCs are the two commonly used cell types in studying radiosensitivity. Mechanistically, fibroblasts has several advantages over PBMCs as the cell model used in studying radiosensitivity (Section 1.3.2.2). However, PBMCs are easier to obtain and can be used readily without culturing when compared to fibroblasts.

Under all the circumstances, fluorescein Isothiocyanate (FITC)-conjugated Annexin V and PI are used in combination with flow cytometry to quantify radiation-induced apoptosis in PBMCs from blood donors and Chinese NPC patients in this study.

## 1.9 Research gap and project significance

RT is one of the standard treatment for many cancers. Technological advancement of RT techniques improves the local regional control rate and survival rate of cancer patients. Acute and progressive adverse reactions induced by RT are the major obstacles affecting the treatment experience and quality of life in cancer patients. Individual susceptibility to RT varies because of many risk factors such as age, gender, medical history and treatment regimen. Previous findings suggested that 80-90% of the variability was contributed by deterministic events related to individual genetic variations (Ho et al., 2006).

Radiation-induced complications are the results of complex biological interactions that involving numerous genes. Two approaches have been used to investigate the underlying cause of this common clinical phenomenon. The first approach focuses on the investigation of SNPs in genes involved in cell cycle regulation, DNA repair, inflammatory response and cytokine activity (Popanda et al., 2009). The second approach uses cells extracted from cancer patients to develop predictive assays based on the level of DNA damage and/or cellular apoptosis related to phenotypic information such as radiation-induced acute skin reactions and mucositis. As a result of methodological variations, such as selected cancer types, candidate-gene selection, apoptosis-assay selection and treatment methods, conflicting results have been reported. Allele frequencies vary in different ethnic origins. In addition, most studies were performed in breast cancer and prostate cancer patients. Few studies focus NPC cancer patients, who also suffer from a range of radiation-induced complications such as fibrosis, mucositis, and necrosis. Therefore, NPC patients with a higher risk of suffering severe radiation-induced complications has to be identified before RT. Treatment experience and quality of life of high-risk patients can be improved by customised treatment protocols.

## 1.10 Aims of this study

This study included three parts. A genetic approach and a cellular approach were adopted in this study. The first part aimed to investigate the association of acute and late radiation-induced complications with genetic variants in Chinese NPC patients by means of candidate-gene approach. A meta-analysis was performed to investigate the association between radiation-induced mucositis and genetic variants in head and neck cancer patients in the second part of this study. Finally, the correlation between acute radiation-induced complications and radiation-induced apoptosis in PBMCs was investigated in the last part of this study.

### 1.10.1 Genetic association using a candidate-gene approach

Six candidate genes, *ATM*, *SOD2*, *TGFβ1*, *TP53*, *XRCC1* and *XRCC3*, were selected based on existing literature. The objectives of this part were:

1. To investigate the association of tag SNPs and functional SNPs in six candidate genes and Chinese NPC patients with and without radiation-induced complications

2. To investigate the reliability of reported functional SNPs as universal biomarkers in Chinese NPC patients

### 1.10.2 Meta-analysis of radiation-induced mucositis in head and neck cancer patients

Radiation-induced mucositis is one of the complications specific to head and neck cancers and information from existing literature is limited. A meta-analysis was performed to pool genotype information of *XRCC1* and *XRCC3* in studies including only head and neck cancer patients. The objectives of this part were:

1. To investigate the association between genetic variants in *XRCC1* and *XRCC3* and radiation-induced mucositis in head and neck cancer patients
2. To overcome the sample size limitation and to increase the power of the study findings

### 1.10.3 Radiation-induced PBMC apoptosis and the correlation to acute radiation-induced complications

In this part of study, cell-based assay was used to investigate the correlation of acute radiation-induced complications by quantification of radiation-induced apoptosis in PBMCs. The objective of this part was:

1. To establish a correlation between radiation-induced PBMCs apoptosis and acute radiation-induced complications in Chinese NPC patients

## 1.11 Chapter summary

The following chapters are divided into three parts. Part I consists of two chapters, part II one chapters, and part III two chapters. Overall discussion and conclusion form the last two chapters and summarise the findings from Part I to Part III.

**Part I**

Chapter 2 lists all the chemicals and reagents used in the first part of this study. Work flow of this part, patient recruitment criteria and experimental protocols are also described in this chapter.

Chapter 3 summarises the study design and major findings of single-marker and haplotype analyses of six candidate genes.

**Part II**

Chapter 4 reports the result of meta-analysis.

**Part III**

Chapter 5 lists all the chemicals and reagents used in the third part of this study. Work flow of this part, patient recruitment criteria and experimental protocols are also described in this chapter.

Chapter 6 presents the results of predictive assay.

Chapter 7 discusses the results from genetic association analysis, meta-analysis, and predictive assay. Potential future studies are suggested based on overall findings.

Chapter 8 summarises and concludes the overall findings.

# Part I

# Genetic association using candidate gene approach

# Chapter 2

# Materials and Methods

## 2.1 Chemicals and reagents

All buffers and solutions used in subsequent experiments were prepared using purified water by reverse osmosis (Millipore, Bedford, USA). Autoclaved water purified by reverse osmosis (Millipore, Bedford, USA) or UltraPure$^{TM}$DNase/RNase-Free Distilled Water (Life Technologies, Rockville, USA) were used for PCR. Tris ethylenediaminetetraacetic acid (TE) buffer was prepared using purified water by reverse osmosis (Millipore, Bedford, USA) and was autoclaved 121 °C for 15 minutes before use.

### 2.1.1 DNA extraction

DNA extraction was performed using FlexiGene DNA kit (Qiagen, Hilden, Germany). Lysis buffer (FG1), denaturation buffer (FG2), rehydration buffer (FG3), and protease were included in this kit. AnalaR grade absolute ethanol was obtained from Sigma (Sigma, St. Louis, USA). AnalaR grade isopropanol was obtained from Riedel-de Han (Riedel-de Han, Seelze, Germany).

### 2.1.2 Adjustment of DNA concentration

The concentration of DNA samples was adjusted using 1× TE buffer containing 1 mM $Na_2EDTA$ (BDH, Poole, UK) and 10 mM Tris-hydrochloric acid (Tris-HCl) (Sigma, St. Louis, USA).

### 2.1.3 Polymerase chain reaction (PCR)

All PCRs were performed using HotStarTaq Plus DNA polymerase, 10× PCR buffer containing Tris-Cl, KCl, $(NH_4)_2SO_4$ and 15 mM $MgCl_2$ with pH 8.7, and 25 mM $MgCl_2$ obtained from Qiagen (Qiagen, Hilden, Germany). Deoxyribonucleoside triphosphates (dATP, dCTP, dGTP and dTTP) were obtained from GE Healthcare (GE Healthcare, Piscataway, USA). All primers used were ordered from either Integrated DNA Technologies (Coralville, IA, USA) or Invitrogen (Carlsbad, CA, USA).

### 2.1.4 Electrophoresis

Loading dye (6×) was prepared using 0.05% bromophenol blue (Sigma, St. Louis, USA), 30% glycerol (AJAX Chemicals, Auburn, Australia), and 1× TE buffer. The 10× tris borate ethylenediaminetetraacetic acid (TBE) buffer contained 890 mM boric acid (Riedel-de Han, Seelze, Germany), 1 mM $Na_2EDTA$ (BDH, Poole, UK), and 890 mM Tris (Sigma, St. Louis, USA).

#### 2.1.4.1 Agarose gel

Agarose gel was prepared using either SeaKem LE agarose (Cambrex BioScience Rockland, ME, USA) or Biowest regular agraose G-10 (Biowest, Spain). Agarose gel was stained by ethidium bromide (Sigma, St. Louis, USA). DNA ladder was obtained from Invitrogen (1kb Plus DNA Ladder; Carlsbad, CA, USA).

#### 2.1.4.2 Polyacrylamide gel (PAGE)

PAGE was prepared with 40% acrylamide-bis (19:1) solution, 25% ammonium persulphate (APS) (Sigma, St. Louis, USA), 10× TBE buffer, and tetramethylethylenediamine (TEMED) (Bio-Rad laboratories, Hercules, CA, USA). Acrylamide (Acros Organic, Geel, Belgium) and bis-acrylamide (Acros Organic, Geel, Belgium) were used to prepare 40% acrylamide-bis (19:1) solution. SYBR®Green I Nucleic Acid Gel Stain (Invitrogen, Carlsbad, CA, US) was used to visualise digested PCR products. Pre-coated glass plates were prepared with $\gamma$-methacryloxypropyltrimethoxysilane (Silane), 10% acetic acid, and absolute ethanol.

### 2.1.5 Restriction fragment length polymorphism (RFLP)

PCR products were digested with restriction enzymes obtained either from MBI Fermentas (Vilnius, Lithuania) or New England Biolabs (Beverly, MA, USA).

### 2.1.6 High resolution melting analysis using unlabelled probe

All 3' phosphorylated probes used were ordered from Integrated DNA Technologies (Coralville, IA, USA). SYTO 9 green fluorescent nucleic acid stain was ordered from Invitrogen (Carlsbad, CA, USA) and was used as a saturated dye.

### 2.1.7 DNA Sequencing

Exonuclease I (ExoI) (New England Biolabs, Beverly, MA, USA) and shrimp alkaline phosphatase (SAP) (GE Healthcare, Piscataway, USA) were used for purification of PCR products before cycle sequencing. BigDye®terminator cycle sequencing kit v1.1 (Applied Biosystems, Foster City, CA, USA) was used for all cy-

cle sequencing reactions. PCR products were precipitated with 3 M sodium acetate (Sigma-Aldrick, St. Louis, USA), 70% and 95% AnalaR grade absolute ethanol (Sigma, St. Louis, USA). PCR products were resuspened in Hi-Di$^{TM}$Formamide (Applied Biosystems, Foster City, CA, USA).

## 2.2 Methods

Study work flow is summarised in Figure 2.1.

### 2.2.1 Subject recruitment

This study followed the Declaration of Helsinki and ethics approval was obtained from the Human Subjects Ethics Sub-Committee, the Hong Kong Polytechnic University prior to any subject recruitment (Project ID: HSEARS20100224001). All subjects were recruited during their follow-up sessions at the Department of Clinical Oncology, Queen Mary Hospital from May 2010 to September 2011. Recruited subjects were Chinese NPC patients, aged 18 or above with no distant metastasis at the time of recruitment, previously treated with Conventional RT or IMRT. Detailed patient recruitment criteria was shown in Table 2.1. Recruited subjects were explained with study-related information. A written consent form was signed by each subject before joining the study. The following patient-related clinical information was provided by a research assistant working in the clinic: date of birth, age, sex, admission date, stage of disease, RT method, treatment start and end dates, total dose received, treatment regimen, highest grade of all acute and chronic RT induced complications, last date that a patient attended the clinic, and any cancer-related medical history. One hundred and twenty eight subjects were recruited. Subjects with inadequate clinical information were excluded from analysis for each phenotype.

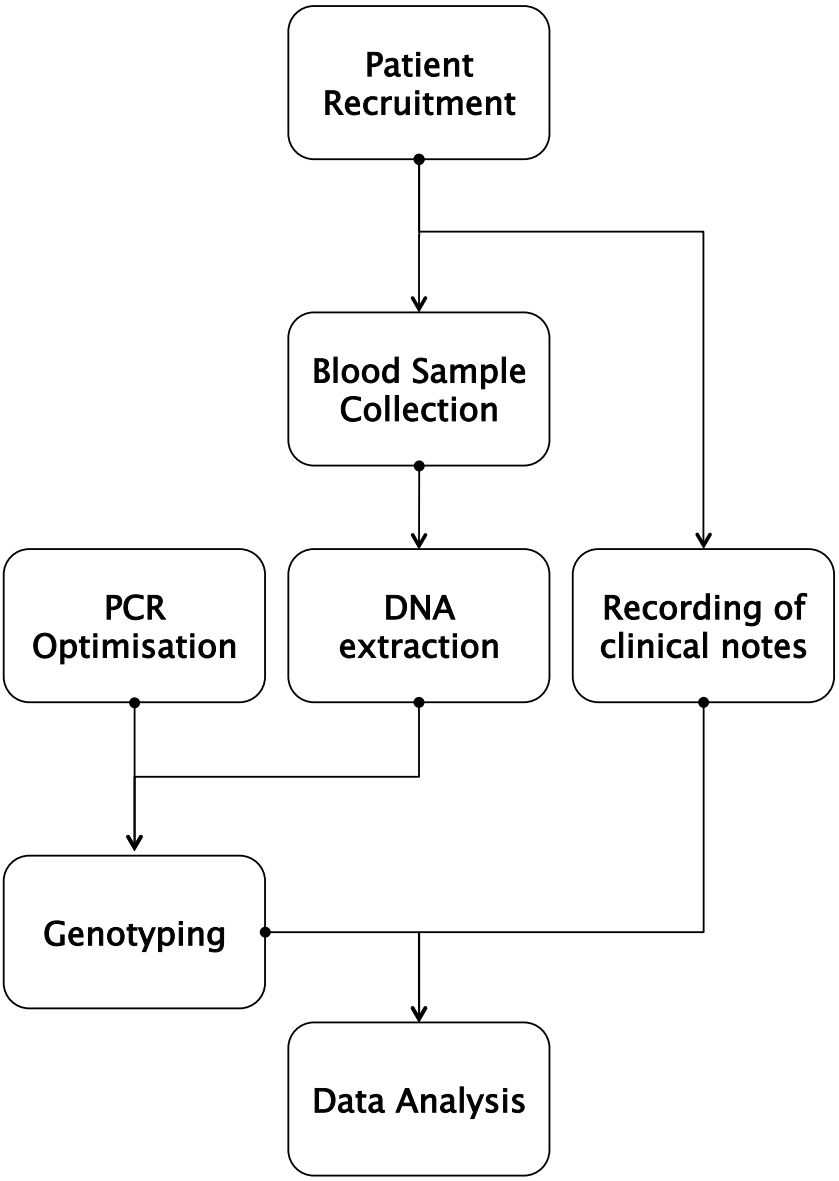


Figure 2.1: Work flow of genetic association study.

Table 2.1: Detailed inclusion/exclusion criteria of patient recruitment

| | Inclusions | Exclusions |
|---|---|---|
| Participants | NPC patients with no distant metastasis | Diseases other than NPC or NPC patients with multiple cancers or distant metastasis |
| Ethnicity | Chinese | Non-Chinese |
| Age | 18 or above | Below 18 |
| Treatment method | Radiation therapy with or without chemotherapy | Treated with two times or above with radiation therapy or with previous surgery |

### 2.2.2 Classification of control and case

#### 2.2.2.1 Acute skin reactions and mucositis

One hundred and seventeen subjects were divided into controls (grade 0-1) and cases (grade 2 or above) based on acute radiation morbidity scoring criteria published by RTOG.

#### 2.2.2.2 Chronic neck fibrosis

One hundred and twenty subjects were divided into controls and cases based on RTOG/EORTC Late Radiation Morbidity Scoring Schema. Subjects were classified as controls with no remarkable change (grade 0) for at least two years after RT.

### 2.2.3 DNA extraction

DNA extraction was performed using FlexiGene DNA kit (Qiagen, Hilden, USA). Three millilitres of blood were centrifuged at 2000 $g$ for 10 minutes. Leucocytes were transferred to a 2-ml microcentrifuge tube with 1.25 ml of FG1. Microcentrifuge tube was inverted a few times until no visible cell pellet remained, followed by centrifugation at 10000 $g$ for 20 seconds. The supernatant was carefully discarded by pipetting. A freshly prepared 500-$\mu$l mixture containing FG2 and protease was added to the cell pellet and was vortexed immediately until the cell pellet was homogenised. Homogenised solution was incubated overnight at 65 °C. DNA was precipitated by inversion after adding 500 $\mu$l isopropanol, followed by centrifugation at 10000 $g$ for 3 minutes. The supernatant was discarded by pipetting and washed by 500 $\mu$l 70% ethanol, and followed by centrifugation at 10000 $g$ for 3 minutes. The supernatant was discarded by pipetting, and the cell pellet was air-dried for 10 minutes. Two hundred microlitres of FG3 was added

to resuspend cell pellet and was incubated overnight at 65 °C or until DNA was completely dissolved. DNA concentration was measured by NanoDrop$^{TM}$ND1000 Spectrophotometer (Thermo Fisher Scientific, Wilmington, USA) at 260nm. DNA concentration of all working stocks was adjusted to 2 ng/$\mu$l with TE buffer for subsequent PCR reactions.

### 2.2.4 Selection of tag SNPs

Tag SNPs of each candidate genes were selected based on information obtained from International HapMap Project data for Han Chinese subjects (release 27, phase II+III, Feb09). Tag SNPs were selected based on the following criteria: pairwise tagging algorithm, $r^2 \geq 0.8$, and MAF>0.2. In order to capture any potential regulatory elements of each candidate gene, tag SNPs were selected from 3kb upstream and downstream of the candidate region together with the candidate gene.

### 2.2.5 Sample size estimation

Sample size estimation was performed with Genetic power calculator (`http://pngu.mgh.harvard.edu/~purcell/gpc/`). Minimum 268 and 134 patients were required for controls and cases to achieve 90% power. Parameters used in sample size estimation is listed in Table 2.2.

Table 2.2: Parameters used for sample size estimation

| Parameters | Values |
|---|---|
| High risk allele frequency (A) | 0.2 |
| Prevalence of any post-RT complications | 0.31 |
| Genotype relative risk (Aa) | 2 |
| Genotype relative risk (AA) | 3 |
| Number of tag SNPs for this study | 29 |
| Ratio of cases to controls | 1:2 |
| Type 1 error | 0.05/29 = 0.00172 |
| User-defined Power | 90% |
| Minimum sample size estimated for experimental: control | 134:268 |

### 2.2.6 Design and primers and probes

Flanking sequences of selected tag SNPs were obtained from GeneWindow (`http://genewindow.nci.nih.gov/`) and Ensembl genome browser (`http://www.ensembl.org/index.html`). All tag SNPs were genotyped by RFLP or unlabelled probe melting curve analysis. RFLP was used as the standard genotyping method, and restriction enzyme for each tag SNP was selected from WatCut (`http://watcut.uwaterloo.ca/watcut/watcut/template.php`). If no suitable restriction enzyme was available or RFLP analysis failed to be optimised, SNPs would be genotyped by unlabelled probe melting curve analysis.

All primers and probes were designed using Oligo version 6.57 (Molecular Biology Insights, Cascade, USA) to amplify region containing SNP of interest. Mismatches were introduced to some primers to generate internal control recognition site and SNP of interest recognition site for genotyping by RFLP. An in-house equation was used to estimate all $T_m$ of primers:

$$T_m = 69.3\,^{\circ}\text{C} + (0.41 \times \text{GC\%}) - (650 \div \text{primer length in bp})$$

The difference of $T_m$ between forward and reverse primers must be smaller than 2 °C. $T_m$ of probes were estimated by Tm Utility (Idaho technology, Utah, USA). The difference of $T_m$ between perfectly matched and mismatched probes must be greater than 4 °C. Estimated $T_m$ was used as a reference annealing temperature during PCR optimisation for RFLP and unlabelled probe melting curve analysis. Specificity of all primers and probes was checked based on reference sequence of the human genome on National Centre of Biotechnology Information (NCBI) by Primer-BLAST (`http://www.ncbi.nlm.nih.gov/tools/primer-blast/`).

### 2.2.7 Polymerase chain reaction

Three types of PCR were performed in this study. Target regions of tag SNPs genotyped by RFLP were amplified using conventional PCR or touchdown PCR. Target regions of tag SNPs genotyped by unlabelled probe melting curve analysis were amplified using asymmetric PCR.

#### 2.2.7.1 Conventional PCR for RFLP

Target regions of tag SNPs genotyped by RFLP were amplified by conventional PCR in a reaction volume of 10 $\mu$l containing 10 ng of genomic DNA, 0.2 mM of each dNTP, 0.2 unit of HotStarTaq Plus DNA polymerase, 1× PCR buffer, 0.1 or 0.3 $\mu$M of each primer, and 1.5 or 2.5 mM $MgCl_2$. Amplification was performed in GeneAmp 9700 96-Well PCR system (Applied Biosystems, Foster City, USA) or Veriti®96-Well thermal cycler (Applied Biosystems, Foster City, USA). PCR was generally performed with an initial cycle of denaturation at 95 °C for 5 minutes, followed by 30-35 cycles of three steps: denaturation at 95 °C for 30 seconds, 55-65 °C for 20-30 seconds annealing time, and 72 °C for 30-60 seconds for primer elongation. An additional cycle of 72 °C for 5 minutes was added to allow final extension of primers.

#### 2.2.7.2 Touchdown PCR for RFLP

Target regions of tag SNPs genotyped by RFLP were amplified by touchdown PCR in a reaction volume of 10 $\mu$l containing 10 ng of genomic DNA, 0.2 mM of each dNTP, 0.2 unit of HotStarTaq Plus DNA polymerase, 1× PCR buffer, 0.1 or 0.3 $\mu$M of each primer, and 1.5 or 2.5 mM $MgCl_2$. Amplification was performed in GeneAmp 9700 96-Well PCR system (Applied Biosystems, Foster City, USA) or Veriti®96-Well thermal cycler (Applied Biosystems, Foster City,

USA). PCR was performed in two phases. In phase I, PCR was performed with an initial denaturation at 95 °C for 5 minutes, followed by 30 seconds at 95 °C, 45 seconds of annealing at optimised $T_m$ plus 5 °C with 1 °C decreased per cycle, and 45 seconds at 72 °C for 6 cycles. Phase II PCR was performed with an initial cycle of denaturation at 95 °C for 5 minutes, followed by 38 cycles of three steps: denaturation at 95 °C for 30 seconds, optimised $T_m$ for 45 seconds, and 72 °C for 45 seconds to allow primer elongation. An additional cycle of 72 °C for 10 minutes was added to allow final extension of primers.

#### 2.2.7.3 Asymmetric PCR for unlabelled probe melting curve analysis

Target regions of tag SNPs genotyped by unlabelled probe melting curve analysis were amplified by asymmetric PCR. The concentration of limiting to excess primers were used in the ratio of either 1:5 or 1:10. As a result, the single-stranded DNA complementary to unlabelled probe was preferentially amplified. Each reaction volume was 10 $\mu$l and contained 10 ng of genomic DNA, 0.2 mM of each dNTP, 0.2 unit of HotStarTaq Plus DNA polymerase, 1× PCR buffer, 0.2 $\mu$M of excess primer, 0.02 or 0.04 $\mu$M limiting primer, and 1.5 or 2.5 mM $MgCl_2$. Amplification was performed in GeneAmp 9700 96-Well PCR system (Applied Biosystems, Foster City, USA) or Veriti®96-Well thermal cycler (Applied Biosystems, Foster City, USA). PCR was performed with an initial cycle of denaturation at 95 °C for 5 minutes, followed by 50-60 cycles of three steps: denaturation at 95 °C for 30 seconds, 55-65 °C for 30-60 seconds annealing time, and 72 °C for 30-60 seconds for primer elongation. An additional cycle of 72 °C for 5 minutes was added to allow final extension of primers.

## 2.2.8 Electrophoresis

### 2.2.8.1 Agarose gel

Agarose gel was used to separate DNA fragments over 500bp for RFLP genotyping or to check size and specificity of PCR products. In general, a concentration of 2% agaorse gel was used for product or fragment size between 150bp to 500bp while a concentration of 1.5% agarose gel was used for product or fragment size over 500bp. PCR products were mixed with 6× loading dye in 5 to 1 ratio. DNA ladder obtained from Invitrogen (1kb Plus DNA Ladder; Carlsbad, CA, USA) was loaded and used as reference size determination of PCR products. Agarose gel electrophoresis was conducted with running time and voltage adjusted according to the size of PCR products and size of the gel in 0.5× TBE buffer. Agarose gel was stained with ethidium bromide (Sigma, St. Louis, USA) and gel bands were visualised by built-in ultra-violet transilluminator under Chemi Genius$^2$ Bio Imaging System (SynGene, Frederick, USA).

### 2.2.8.2 Polyacrylamide gel (PAGE) electrophoresis

PAGE was used to separate DNA fragments with size below 500bp for RFLP genotyping. Digested products (15 $\mu$l) were stained with 5 $\mu$l of 6× loading dye and 100× SYBR®Green I Nucleic Acid Gel Stain (Invitrogen, Carlsbad, CA, US) prepared in 9 to 1 ratio for 30 minutes. DNA ladder (1kb Plus DNA Ladder; Invitrogen, Carlsbad, CA, USA) was pre-stained similar to digested products and were loaded as reference size determination. Due to difference in fragment size of different tag SNPs, different concentration of PAGE was used. PAGE electrophoresis was conducted with running time and voltage adjusted according to the size of PCR products and gel concentration in 0.5× TBE buffer. Gel bands were visualised by built-in ultra-violet transilluminator with short band pass filter under Chemi Genius$^2$ Bio Imaging System (SynGene, Frederick, USA).

### 2.2.9 DNA sequencing

Genotypes obtained by RFLP and unlabelled probe melting curve analysis during optimisation stage were reconfirmed by direct sequencing using ABI®PRISM 3130 Genetic Analyzer (Applied Biosystems, Foster City, USA). At least two representative genotypes were selected for each tag SNP and were sequenced before genotyping patient samples. Patients with uncertain results obtained from RFLP analysis or unlabelled probe melting curve analysis were also sequenced to obtain genotypes.

Target regions of tag SNPs were first amplified using conventional PCR in a reaction volume of 10 $\mu$l. Specificity of PCR products (5 $\mu$l) was checked by agarose gel electrophoresis. Remaining PCR products (5 $\mu$l) were mixed with 0.5 unit of ExoI (New England Biolabs, Beverly, MA, USA) and 1 unit of SAP (GE Healthcare, Piscataway, USA) and incubated at 37 °C for 30 minutes for product purification. After purification, reaction mixture was incubated at 80 °C for 20 minutes for enzyme inactivation. Forward or reverse primer (0.01 $\mu$M), Big Dye terminator v1.1, and UltraPure$^{TM}$DNase/RNase-Free Distilled Water (Life Technologies, Rockville, USA) were added to purified PCR products. Reaction mixtures were incubated at 1 cycle of 96 °C for 1 minute, 37 cycles of 95 °C for 10 seconds, 50 °C, 55 °C, or 60 °C for 30 seconds, and one cycle 60 °C for 6 minutes.

PCR products were precipitated using an ethanol/sodium acetate precipitation method. Cycle sequencing products were mixed with 62.5 $\mu$l of 95% ethanol (Sigma, St. Louis, USA), 24.5 $\mu$l of UltraPure$^{TM}$DNase/RNase-Free Distilled Water (Life Technologies, Rockville, USA), and 3 $\mu$l of 3 M sodium acetate (Sigma-Aldrick, St. Louis, USA). Reaction mixtures were incubated in dark for 20 minutes at room temperature, followed by centrifugation at 14000 $g$ for 20 minutes. The supernatant was carefully discarded by pipetting. Cell pellet was mixed with 300 $\mu$l of 70%

ethanol (Sigma, St. Louis, USA), followed by centrifugation at 14000 $g$ for 5 minutes. The supernatant was carefully discarded by pipetting and any remaining liquid residue was dried using Savant DNA110 SpeedVac®concentrator (Thermo Fisher Scientific, Wilmington, USA) centrifuged for 15 minutes. Cell pellet was resuspended in 15 $\mu$l of Hi-Di$^{TM}$Formamide (Applied Biosystems, Foster City, CA, USA) and incubated in dark for 15 minutes. Direct sequencing was performed using ABI®PRISM 3130 Genetic Analyzer (Applied Biosystems, Foster City, USA) by capillary gel electrophoresis according to the manufacturer's protocol. Sequencing results were analyzed by Sequencing Analysis version 5.2 Patch 2 (Applied Biosystems, Foster City, USA), Sequence scanner version 1.0 (Applied Biosystems, Foster City, USA) and 4peaks version 1.7 (Nucleobytes B.V., Aalsmeer, Netherlands). Figure 2.2 illustrates sequencing results of three representation genotypes from one tag SNP.

Figure 2.2: Sequencing results of rs1800470 in *TGFβ1*. (a) Homozygous genotype CC. (b) Heterozygous genotype CC. (c) Homozygous genotype TT.

## 2.2.10 SNP genotyping

### 2.2.10.1 Restriction fragment length polymorphism (RFLP) analysis

PCR products of tag SNPs genotyped by RFLP were digested using restriction enzymes obtained either from MBI Fermentas (Vilnius, Lithuania) or New England Biolabs (Beverly, MA, USA) according to the manufacturers' recommendations. PCR products added with specific restriction enzymes were incubated up to 16 hours at optimal temperatures of the respective specific restriction enzymes to allow maximum activity. Restriction enzymes were inactivated at 80 °C for 20 minutes after incubation. Digested products (15 $\mu$l) were stained with 5 $\mu$l of 6× loading dye and 100× SYBR®Green I Nucleic Acid Gel Stain (Invitrogen, Carlsbad, CA, US) prepared in 9 to 1 ratio for 30 minutes. Digested fragments were separated by PAGE or agarose gel depending on the size of DNA fragments. Digested banding patterns are illustrated in Figure 2.3. An example gel picture of RFLP genotyping is shown in Figure 2.4.

### 2.2.10.2 Unlabelled probe melting curve analysis

Target regions of tag SNPs genotyped by unlabelled probe melting curve analysis were amplified by asymmetric PCR. PCR products added with 0.2 $\mu$M SYTO 9 green fluorescent nucleic acid stain (Invitrogen, Carlsbad, CA, USA) and 0.5 $\mu$M of 3-phosphorylated unlabelled probe were analysed with LightCycler 480 Real-time PCR System (Roche, Basel, Switzerland). DNA melting analysis was performed in three steps: an initial denaturation of 95 °C for 60 seconds at ramp rate 4.4 °C/second, followed by 50 °C for 60 seconds at ramp rate of 2.2 °C/second for probe hybridisation, and 95 °C at ramp rate 4.4 °C/second to determine melting behaviour of hybridised products by measuring fluorescence intensity. Acquisition of 5 data points per °C was used. Figure 2.5 illustrates an example result of genotyping by unlabelled probe melting curve analysis.

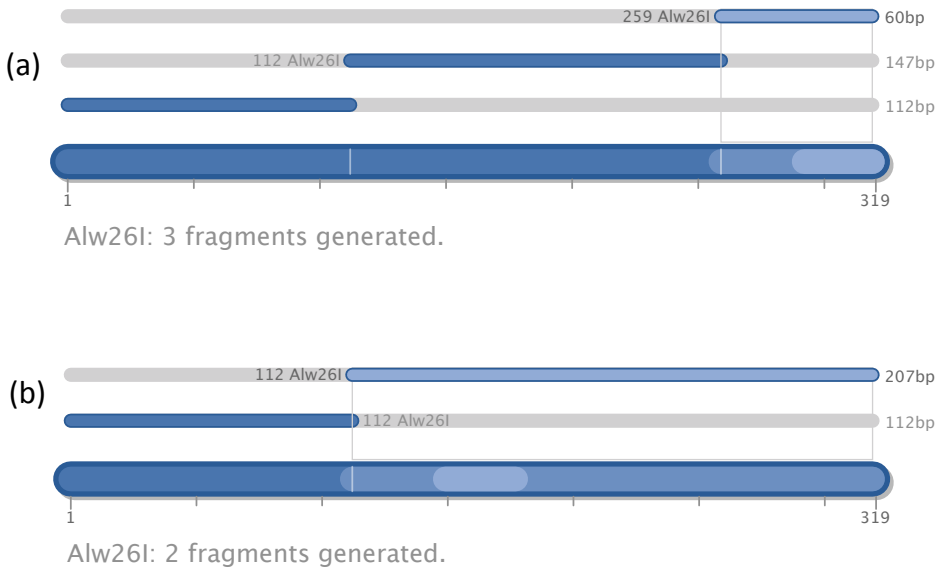


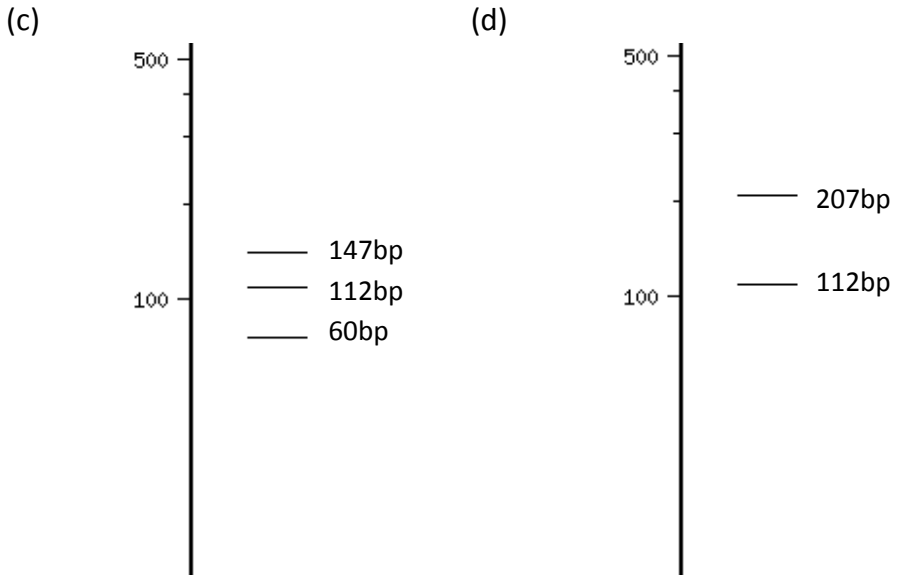


Figure 2.3: Genotyping of rs12983047 in *TGFβ1* by RFLP. (a) PCR products are digested with Alw26I and three fragments (60bp, 112bp and 147bp) are obtained for GG homozygote. (b) PCR products are digested with Alw26I and two fragments (112bp and 207bp) are obtained for CC homozygote. (c) The estimated banding pattern of GG homozygote. (d) The estimated banding pattern of CC homozygote.

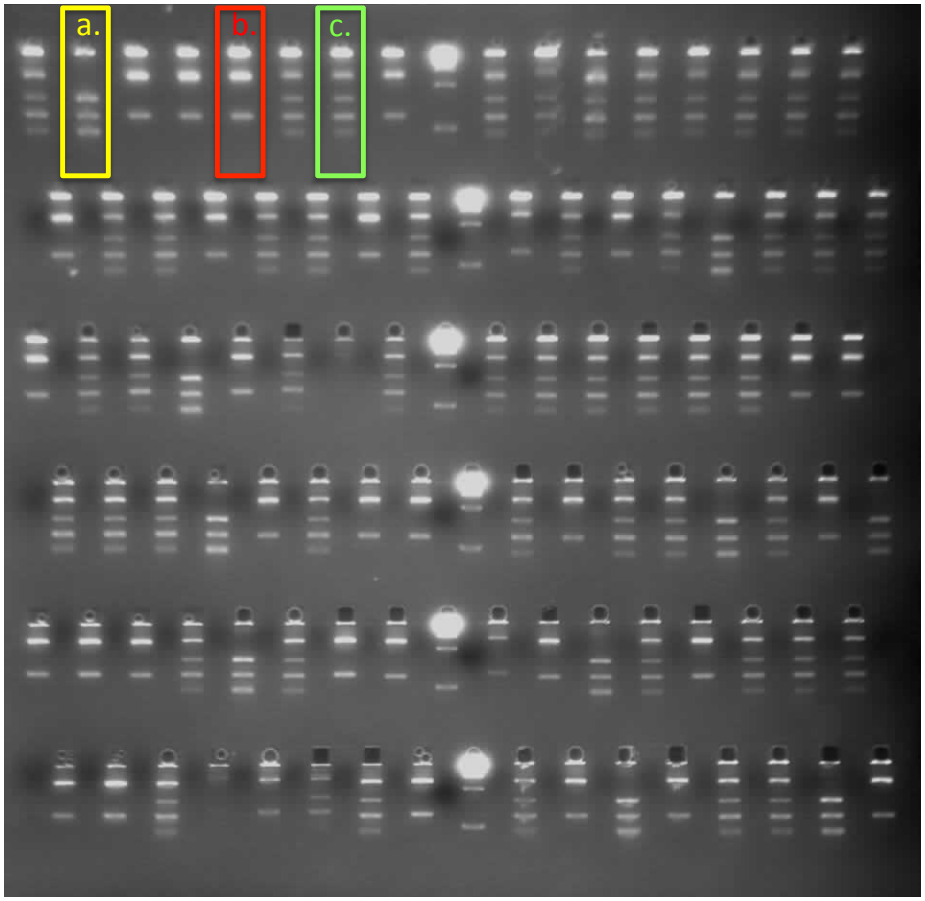


Figure 2.4: Genotyped results of rs12983047 in *TGFβ1* by RFLP. The 9th well of each row is loaded with DNA ladder. (a) GG homozygote. (b) CC homozygote. (c) GC heterozygote.

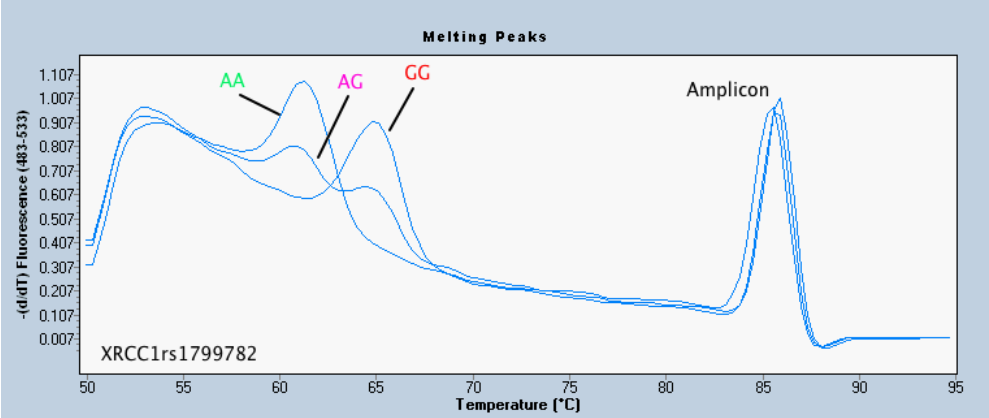


Figure 2.5: Genotyped results of rs1799782 from *XRCC1* by unlabelled probe melting curve analysis. Unlabelled probe is designed to match G allele in this example. Probe-amplicon duplex of homozygous genotype GG has a higher $T_m$ than probe-amplicon duplex of homozygous genotype AA. Two peaks are obtained for heterozygous GA.

## 2.3 Statistical analysis

HWE, single-marker and haplotype analyses were performed using PLINK version 1.07 (`http://pngu.mgh.harvard.edu/~purcell/plink/`). Clinical data were used as covariates in single-marker and haplotype analyses.

### 2.3.1 Clinical data

Due to numerous confounding factors, controls and cases were not matched in this study. The following collected clinical information was used as covariates in single-marker and haplotype analyses of acute complications: gender, sex, cancer staging, RT method, and treatment regimen. Besides the above clinical information, length of follow-up was also used as covariate in single-marker and haplotype analyses of chronic neck fibrosis.

### 2.3.2 Hardy-Weinberg equilibrium

Exact test implemented in PLINK was used to test for any deviation from HWE in controls and cases separately for all phenotypes. Deviations from HWE for controls may indicate many potential problems, such as genotyping errors, assortative mating, selection, and population stratification (Lewis and Knight, 2012). As a result, markers deviated from HWE ($P$ <0.001) were excluded for all association analyses.

### 2.3.3 Single-marker analysis

Single-marker analysis and the association of three phenotypes (acute skin reactions, acute mucositis and chronic neck fibrosis) were performed in PLINK using multivariate logistic regression analysis. Multiple testing was corrected based on

10,000 permutations to generate empirical $P$ ($P_{emp}$) values. ORs with 95% CI were also calculated for each genotype.

### 2.3.4 Haplotype analysis

Haplotype analysis and the association of three phenotypes (acute skin reactions, acute mucositis and chronic neck fibrosis) were performed in PLINK using multivariate logistic regression analysis. In order to obtain more information, all possible haplotypes were generated for each candidate gene using a sliding-window approach. Using sliding-window approach, all possible combinations of haplotypes were examined by shifting one SNP each time for a given window size n, whereas n is the number of SNPs of each candidate gene. ORs and asymptomatic P values ($P_{asym}$) of each haplotype were generated to investigate the association of each haplotype and radiation-induced complications. Multiple testing of haplotypes was corrected based on 10,000 permutations to generate $P_{emp}$ values. LD blocks were constructed based on combined allele frequencies of controls and cases with Haploview using solid spine of LD (SSLD) algorithm. SSLD algorithm constructed blocks based on the first and last markers in strong LD while intermediate markers within the block in weak or no LD (Barrett et al., 2005).

## 2.4 Computer Software

Several computer programs, databases, and online tools were used in this study. A summary of computer programs, databases, and online tools is shown in Table 2.3.

Table 2.3: Tools used in this study.

| Name | Type | Operating System | Version | Application | Sources/URL |
|---|---|---|---|---|---|
| 4peaks | Software | Mac | 1.7 | To perform DNA sequence analysis such as base calling | Nucleobytes B.V., Aalsmeer, Netherlands |
| DNA Sequencing Analysis Software | Software | Windows | 5.2 Patch 2 | To perform DNA sequence analysis such as base calling | Applied Biosystems, Foster City, CA, USA |
| Ensembl | Database | / | / | To obtain sequences of tag SNPs and SNPs information such as MAF in different ethnic groups | http://asia.ensembl.org/index.html |
| EnzymeX | Software | Mac | 3.1 | To predict all restriction enzyme recognition sites of tag SNPs within amplified regions | Nucleobytes B.V., Aalsmeer, Netherlands |
| Genetic power calculator | Online tool | / | / | To perform power calculation and sample size estimation | http://pngu.mgh.harvard.edu/~purcell/gpc/ |
| GeneSnap Software | Software | Windows | 6.04 | To capture gel pictures | SynGene, Frederick, USA |
| GeneWindow | Database | / | / | To obtain sequences of tag SNPs | http://genewindow.nci.nih.gov/ |
| Haploview | Software | Mac, Windows | 4.2 | To perform tag SNPs selection and generate LD plots based on genotype data | http://www.broadinstitute.org/haploview/haploview |
| HapMap | Database | / | release 27, phase II+III, Feb09 | To perform tag SNPs selection | http://hapmap.ncbi.nlm.nih.gov/ |
| LightCycler 480 Software | Software | Windows | 1.5.0 | To analyze melting curves for genotyping | Roche, Basel. Switzerland |
| NCBI | Database | / | / | To obtain sequences of tag SNPs and SNPs information such as MAF in different ethnic groups | http://www.ncbi.nlm.nih.gov/ |
| NEBcutter | Online tool | / | 2.0 | To predict all restriction enzyme recognition sites of tag SNPs within amplified regions | http://tools.neb.com/NEBcutter2/index.php |
| Oligo | Software | Windows | 6.57 | To design primers and probes | Molecular Biology Insights, Cascade, USA |
| PLINK | Software | Mac, Windows | 1.07 | To analyze genotype data | http://pngu.mgh.harvard.edu/~purcell/plink/ |
| PredicABEL (Based on R) | Software | Mac, Windows | 1.2-1 | To generate AUC using clinical information and genotype data | http://www.genabel.org/packages/PredictABEL |
| Primer-BLAST | Online tool | / | / | To search for all possibly mispriming sites of primers | http://www.ncbi.nlm.nih.gov/tools/primer-blast/ |
| R | Software | Mac, Windows | 2.15.2 | To run PredicABEL | http://www.r-project.org/ |
| R Studio$^{TM}$ | Software | Mac, Windows | 0.97.306 | To run PredicABEL | http://www.rstudio.com/ |
| Sequence Scanner | Software | Windows | 1.0 | To perform DNA sequence analysis such as base calling | Applied Biosystems, Foster City, CA, USA |
| SNP Function Prediction (FuncPred) | Online tool | / | / | To predict potential function role of tag SNPs | http://snpinfo.niehs.nih.gov/snpfunc.htm |
| TM Utility | Software | Windows | 1.3 | To estimate melting temperature of perfectly matched and mismatched probes | http://www.idahotech.com/downloads_up/index.html |
| WatCut | Online tool | / | / | To search for restriction enzymes for tag SNPs | http://watcut.uwaterloo.ca/watcut/watcut/template.php |

# Chapter 3

# Genetic association studies

## 3.1 Aims

The aims of this part were to investigate the association of genetic variants and haplotypes of six candidate genes (*ATM*, *SOD2*, *TGFβ1*, *TP53*, *XRCC1* and *XRCC3*) with acute and chronic post-RT complications in Chinese NPC patients.

## 3.2 Introduction

RT is the primary treatment for NPC with promising results. With the advancement of technology, higher overall survival (OS) rate and local control rate in NPC patients have been achieved by RT (Kam et al., 2004). However, radiation-induced acute normal tissue complications, such as skin reactions, mucositis and dysphagia, are unavoidable. In addition, radiation-induced damage may get severer over time and leads to chronic complications that affect the quality of life in cancer patients. Genetic factors, in addition to clinical and environmental factors, are thought to be one of the major contributors leading to individual variations in radiosensitiv-

ity despite the fact that patients received the same cancer treatment. Previous studies have investigated the association of SNPs in genes related to DNA repair and cell-cycle regulation pathways and various radiation-induced complications in different cancers. Reported SNPs may be used as universal biomarkers to predict various types of radiation-induced complications in cancer patients. Most published studies only investigated the functional variants and the association of radiation-induced complications in Caucasian patients with breast and prostate cancers. In the first part of this study, previously reported functional variants in six candidate genes, *ATM*, *SOD2*, *TGFβ1*, *TP53*, *XRCC1* and *XRCC3* and their association of radiation-induced complications (acute skin reactions, acute mucositis and chronic neck fibrosis) in Chinese NPC patients were investigated. In addition, tag SNPs were selected from each candidate genes to capture common variants from each candidate gene to perform single-marker association analysis and haplotype analysis.

## 3.3 Methodology

### 3.3.1 Subject recruitment

One hundred and twenty-eight Chinese NPC patients were recruited from the Department of Clinical Oncology, Queen Mary Hospital during their follow-up session (Section 2.2.1). Patients were classified into controls and cases based on classification criteria of each phenotype (Section 2.2.2).

### 3.3.2 SNP genotyping

Twenty-nine SNPs, including tag SNPs and reported functional variants, were selected from six candidate genes for this study. Tag SNPs were selected from International HapMap Project data (Rel 27 phase II+III, Feb09, on NCBI B36 assem-

bly, dbSNP b126) for Han Chinese subjects (`http://hapmap.ncbi.nlm.nih.gov/cgi-perl/gbrowse/hapmap27_B36/`) using Tagger implemented in Haploview (Section 2.2.4). Details of selected tag SNPs from each candidate gene is listed in Table 3.1. Twenty SNPs were genotyped using RFLP (Section 2.2.10.1) and eight SNPs were genotyped by unlabelled probe melting curve analysis (Section 2.2.10.2). One SNP (rs8064946) was genotyped by RFLP and unlabelled probe melting curve analysis. For this SNP, only samples with unrecognised digested patterns in RFLP were genotyped by unlabelled probe melting curve analysis. PCR conditions, primer and probe sequences and genotyping methods of tag SNPs are summarised in Table 3.3.3.

### 3.3.3 Statistical analysis

Single-marker and haplotype association analyses of each phenotype using genotyped data from 29 SNPs were performed with PLINK (Section 2.3). Multiple testing correction was performed with PLINK.

Table 3.1: Summary of selected tag SNPs from each candidate gene

| Gene | Total number of tag SNPs | Chromosome | rs number | Designation | Chromosome location (NCBI B36) |
|---|---|---|---|---|---|
| *ATM* | 4 | 11q22-q23 | rs228591 | ATM.S1 | 107602543 |
| Gene ID: 472 | | | rs600931 | ATM.S2 | 107622545 |
| | | | rs11212592 | ATM.S3 | 107724057 |
| | | | rs373759 | ATM.S4 | 107725867 |
| *SOD2* | 3 | 6q25.3 | rs4880 | SOD2.S1 | 160033862 |
| Gene ID: 6648 | | | rs5746136 | SOD2.S2 | 160023074 |
| | | | rs2842980 | SOD2.S3 | 160020106 |
| *TGFβ1* | 6 | 19q13.1 | rs1800469 | TGFB1.S1 | 46552136 |
| Gene ID: 7040 | | | rs1800470 | TGFB1.S2 | 46550761 |
| | | | rs2241716 | TGFB1.S3 | 46545926 |
| | | | rs4803455 | TGFB1.S4 | 46543349 |
| | | | rs111466345 | TGFB1.S5 | 46535301 |
| | | | rs12983047 | TGFB1.S6 | 46526339 |
| *TP53* | 4 | 17p13.1 | rs8064946 | TP53.S1 | 7530036 |
| Gene ID: 7157 | | | rs12602273 | TP53.S2 | 7523738 |
| | | | rs1042522 | TP53.S3 | 7520197 |
| | | | rs12951053 | TP53.S4 | 7518132 |
| *XRCC1* | 6 | 19q13.213.3 | rs3213282 | XRCC1.S1 | 48764720 |
| Gene ID: 7515 | | | rs12611088 | XRCC1.S2 | 48764642 |
| | | | rs1001581 | XRCC1.S3 | 48757228 |
| | | | rs3213344 | XRCC1.S4 | 48752493 |
| | | | rs1799782 | XRCC1.S5 | 48749414 |
| | | | rs25487 | XRCC1.S6 | 48747566 |
| *XRCC3* | 6 | 14q32.3 | rs1799794 | XRCC3.S1 | 103249020 |
| Gene ID: 7517 | | | rs861530 | XRCC3.S2 | 103243876 |
| | | | rs3212090 | XRCC3.S3 | 103238616 |
| | | | rs12432907 | XRCC3.S4 | 103238131 |
| | | | rs861539 | XRCC3.S5 | 103235506 |
| | | | rs861544 | XRCC3.S6 | 103232016 |

Table 3.2: Summary of genotyping methods, PCR conditions and sequences of primers and probes of selected tag SNPs

| Gene | rs number | Primer sequence[a,b,c] | Genotyping method | Primer (mM) | $Mg^{2+}$ | $T_m$ (°C) | Cycles | Size (bp) |
|---|---|---|---|---|---|---|---|---|
| ATM | rs228591 | P: $(T)_{16}$AAATGTCATTTTACTCCTATTGTTATGTGTT | RFLP | 0.3 | 2.5 | 55 | 30 | 202 |
| | | P: $(T)_{28}$GTAGACACATGTCATTTTGCTGAG | (AccI) | | | | | |
| | rs600931 | P: $(T)_{15}$CATTTTTACACTAGTTGAAGGGACT | RFLP | 0.3 | 2.5 | 58 | 35 | 180 |
| | | P: $(T)_{36}$ATTGATTCTCCCACCTGAGGCAA | (HinfI) | | | | | |
| | rs11212592 | P: ATATTGGATTTGAGGGACATTTTTGTAGTA | RFLP | 0.3 | 2.5 | 55 | 40 | 884 |
| | | P: CTGATTCTTAGCATCTACCTTTTTATAACT | (HplI) | | | | | |
| | rs373759 | P: $(T)_{34}$GGTACCATCCCTCCAATTCTTAG | RFLP | 0.3 | 1.5 | 55 | 32 | 185 |
| | | P: $(T)_{13}$GAGAGAGAAGGAAAAGTGGTGC | (BanI) | | | | | |
| SOD2 | rs4880 | P: CCAGCCTGCGTAGACGGT | UPr | 0.2 | 2.5 | 65 | 60 | 203 |
| | | P: CGTGGTGCTTGCTGTGGTG | | 0.02 | | | | |
| | | U: AGCCCAGATACCCCAAAGCCGGAGCCAG | | 0.5 | | | | |
| | rs5746136 | P: ATCTAGTCTTTTGCCCCAGTTAC | RFLP | 0.3 | 1.5 | 55 | 30 | 152 |
| | | P: $(T)_{21}$GTGACATCGACCAGAAGTATCAC | (TaqI) | | | | | |
| | rs2842980 | P: CCATCAAAGAGGTCTGCATTATGC | RFLP | 0.3 | 1.5 | 55 | 35 | 202 |
| | | P: $(T)_{26}$ATCAGATGATGTTTTTAAAGATATGACTGG | (DraI) | | | | | |
| *TGFβ1* | rs1800469 | P: TGACCCCAGCTAAGGCATG | RFLP | 0.3 | 1.5 | 55 | 35 | 962 |
| | | P: TTTTTCCTCTTCTCCCGACCAG | (Eco81I) | | | | | |
| | rs1800470 | P: TCACCAGCTCCATGTCGATA | UPr | 0.04 | 1.5 | 60 | 60 | 170 |
| | | P: ATCCCTGTTCGCGCTCTC | | 0.2 | | | | |
| | | U: CAGCAGCGGTAGCAGCAGCGGCAGCAGC | | 0.5 | | | | |
| | rs2241716 | P: $(T)_{25}$CGGATGAGGACATGAGCCAGAA | RFLP | 0.3 | 1.5 | 55 | 35 | 195 |
| | | P: $(T)_{27}$GATTGTAGGGTTTGTGTTCTTCCATC | (Bst5FI) | | | | | |
| | rs4803455 | P: TCACTGCAACCTCTGTGTCTT | RFLP | 0.2 | 2.5 | 55 | 35 | 304 |
| | | P: $(T)_{20}$CTGCATATTTGACACCCTGTATT | (TasI) | | | | | |
| | rs111466345 | P: ATGTCCAAGGGTCAGTCTATA | UPr | 0.1 | 2.5 | 55 | 50 | 183 |

Continued on next page

**Table 3.2 – continued from previous page**

| Gene | rs number | Primer sequence[a,b,c] | Genotyping method | Primer (mM) | $Mg^{2+}$ | $T_m$ (°C) | Cycles | Size (bp) |
|---|---|---|---|---|---|---|---|---|
| | | P: ACGACAGCTGGCCTGATTT | | 0.02 | | | | |
| | | U: CAAAGTTCTGGGATTACGGGCGTGAGCTA | | 0.5 | | | | |
| | rs12983047 | P: $(T)_{24}$ACAAATATTCACCTCTCAGAGCCG | RFLP | 0.3 | 1.5 | 55 | 30 | 319 |
| | | P: TGCGTGCATGACACTGTTTGAATC | (Alw26I) | | | | | |
| TP53 | rs8064946 | P: GGGACGATGAAAAGGGTCTGTG | RFLP | 0.3 | 1.5 | 55 | 30 | 319 |
| | | P: AGTTTCTTCCCATGCACCTGCC | (BsuRI) | | | | | |
| | or | | | | | | | |
| | | P: CGCTGTGTGTAAATGCCA | UPr | 0.2 | 2.5 | 55 | 55 | 105 |
| | | P: TGTTTCATTCCGCAGTTTCTT | | 0.04 | | | | |
| | | U: CGCGTACCGGGCACTTTGTGTCGTA | | 0.5 | | | | |
| | rs12602273 | P: $(T)_{37}$CAGCTGACTGAATAGATCCCTG | RFLP | 0.3 | 2.5 | 55 | 35 | 224 |
| | | P: $(T)_{18}$GTAAGAGCTCAACAAAGGTCAGC | (PvuII) | | | | | |
| | rs1042522 | P: $(T)_{12}$AGCTCCCAGAATACCAGAGGCTGCTCCGC | RFLP | 0.3 | 1.5 | 65 | 35 | 215 |
| | | P: $(T)_{32}$GCTGTCCGCGAATGCAAGAAGCCCAGA | (Bsh1236I) | | | | | |
| | rs12951053 | P: TGGGAGCAGTAAGGAGATT | UPr | 0.2 | 2.5 | 55 | 55 | 177 |
| | | P: ATCATCACACTGGAAGACTC | | 0.04 | | | | |
| | | U: CCTCTTACCGATTTCTGCCATACTACTACCC | | 0.5 | | | | |
| XRCC1 | rs3213282 | P: $(T)_{28}$AGGTGCCTAAGGGTATACACTAAAAAGA | RFLP | 0.3 | 2.5 | 58 | 35 | 178 |
| | | P: $(T)_{11}$AAACTGCTAATGGTGGTTGCCTCA | (Eco81I) | | | | | |
| | rs12611088 | P: GTGGTCTTCCTGGGTCATT | UPr | 0.2 | 2.5 | 55 | 55 | 140 |
| | | P: CAGTGTGCATCTCCAAAATAC | | 0.02 | | | | |
| | | U: TTAAAAAGGGATGGAGGCGGTAGGTCTATATG | | 0.5 | | | | |
| | rs1001581 | P: $(T)_{29}$GGTATGTGTGAGGTGGGCGC | RFLP | 0.1 | 1.5 | 71-65, 65 | 6, 38 | 261 |
| | | P: $(T)_{41}$GGGCTCGCGGTGGGACCT | (Bsh1236I) | | | | | |
| | rs3213344 | P: $(T)_{21}$CCTGTCTGTCTTGGCCTTGGCTT | RFLP | 0.1 | 2.5 | 60 | 35 | 188 |
| | | P: $(T)_{20}$GGCCTCAGCTTGGGTTTTTCCATG | (StyI) | | | | | |

Continued on next page

**Table 3.2 – continued from previous page**

| Gene | rs number | Primer sequence[a,b,c] | Genotyping method | Primer (mM) | $Mg^{2+}$ | $T_m$ (°C) | Cycles | Size (bp) |
|---|---|---|---|---|---|---|---|---|
| | rs1799782 | P: CCTTGCGGGACCTTAGAA | UPr | 0.2 | 2.5 | 55 | 55 | 175 |
| | | P: CTA<u>T</u>GTCTCAACCCTACTCA | | 0.02 | | | | |
| | | U: ATGT<u>A</u>TTGTTGATCCGGCTGAAGAAGAGTGC | | 0.5 | | | | |
| | rs25487 | P: TTCCCAGCACAGGATAAGGAGC | RFLP | 0.1 | 1.5 | 64-58, 58 | 6, 38 | 181 |
| | | P: $(T)_{39}$CCAAGTACAGCC<u>G</u>GGTCCTA | (MspI) | | | | | |
| XRCC3 | rs1799794 | P: CACTGACGGATAACAGACTCAC | RFLP | 0.3 | 1.5 | 55 | 30 | 282 |
| | | P: $(T)_{14}$GATGGAAGGTTGCTAAGAGGAA | (BseGI) | | | | | |
| | rs861530 | P: $(T)_{25}$GATGCCCTGGGGTGCTGAACAGT | RFLP | 0.3 | 1.5 | 58 | 30 | 296 |
| | | P: $(T)_{7}$GCTGCTCCTCCCGGCCCA | (Bsh1236I) | | | | | |
| | rs3212090 | P: CACCATCTGTCAACCTTGC | UPr | 0.02 | 2.5 | 55 | 55 | 179 |
| | | P: GGGAAACCAACACAGCTAT | | 0.2 | | | | |
| | | U: ATGAAGACGGAGTGGGGAAGAGAAGCC | | 0.5 | | | | |
| | rs12432907 | P:CTTACTTGCCTTTGGTCAG | UPr | 0.2 | 2.5 | 55 | 60 | 99 |
| | | P: TATAGACATCATCCTGGGAG | | 0.02 | | | | |
| | | U: GTAGAAAAGACGCAGAAGAAAAGATGGGAC | | 0.5 | | | | |
| | rs861539 | P: $(T)_{21}$GGCTC<u>A</u>CCTGGTGGTCAT | RFLP | 0.3 | 2.5 | 60 | 35 | 182 |
| | | P: $(T)_{35}$GCACTGCTCAGCTCAC<u>A</u>CAG | (DraIII) | | | | | |
| | rs861544 | P: GCGGCAAGGGAATCTGAGTA | RFLP | 0.3 | 1.5 | 55 | 30 | 249 |
| | | P: $(T)_{17}$<u>GG</u>CGCAGTGATTATTTTGACAG | (HphI) | | | | | |

**Abbreviation**: P = Primer; RFLP = Restriction fragment length polymorphism; U = Unlabelled probe; UPr = Unlabelled Probe Melting Analysis; $T_m$ = Annealing temperature.

[a] A Poly-T tail was added to the 5 end of some primers to enhance the size difference in digested fragment.

[b] Mismatched bases were underlined. Mismatches were introduced to avoid hairpins formation, to avoid formation of primer dimers, or to create restriction sites.

[c] The 3' end of the probe is either phosphorylated or added with a poly-A tail to prevent probe extension during amplification.

## 3.4 Results

### 3.4.1 Acute skin reactions

#### 3.4.1.1 Clinical characteristics of included patients

One hundred and seventeen Chinese NPC patients were included in this part of analysis. Patients were classified into controls and cases according to the highest grade of **acute skin reactions** recorded during RT (Section 2.2.2.1). Fifty patients were classified as controls and 67 patients were classified as cases. Clinical characteristics of recruited patients are summarised in Table 3.3. There was no significant difference of clinical characteristics between controls and cases ($P$>0.05).

#### 3.4.1.2 Single-marker analysis

All SNPs were successfully genotyped and were tested for HWE. No deviation from HWE was found in all SNPs for controls ($P$>0.001). As a results, all SNPs were included in single-marker analysis. Results of single-marker association analysis are shown in Table 3.5. None of the tag SNPs showed any association to radiation-induced acute skin reactions.

Table 3.3: Clinical characteristics of recruited patients in acute skin reactions

| Group | Control (n=50) | Case (n=67) | *P* |
|---|---|---|---|
| Clinical Variables | Mean (SD) | | |
| Age | 52.76 (10.94) | 52.76 (9.92) | 0.9995 |
| | Frequency (%) | | |
| Sex | | | 0.6990 |
| Male | 36 (72.0%) | 46 (68.7%) | |
| Female | 14 (28.0%) | 21 (31.3%) | |
| Stage (TMN) | | | 0.2553 |
| I | 10 (20.0%) | 5 (7.5%) | |
| II | 12 (24.0%) | 19 (28.4%) | |
| III | 18 (36.0%) | 27 (40.3%) | |
| IV | 8 (16.0%) | 13 (19.4%) | |
| Unavailable | 2 (4.0%) | 3 (4.5%) | |
| Radiotherapy | | | 0.5130 |
| CRT | 15 (30.0%) | 24 (35.8%) | |
| IMRT | 35 (70.0%) | 43 (64.2%) | |
| Chemotherapy | 27 (54.0%) | 36 (53.7%) | 0.9772 |

Table 3.4: Summary statistics of acute skin reactions

| | | | | | Genotype Counts 11/12/22 | | MAF | | HWE $P$ value | |
|---|---|---|---|---|---|---|---|---|---|---|
| Gene | SNP | | A1 | A2 | Controls | Cases | Controls | Cases | Controls | Cases |
| *ATM* | rs228591 | ATM.S1 | A | G | 13/28/9 | 30/24/13 | 0.4600 | 0.3731 | 0.5678 | 0.0667 |
| | rs600931 | ATM.S2 | C | T | 11/30/9 | 29/25/13 | 0.4800 | 0.3806 | 0.2554 | 0.1176 |
| | rs11212592 | ATM.S3 | A | G | 25/22/3 | 44/20/3 | 0.2800 | 0.1940 | 0.7291 | 0.6981 |
| | rs373759 | ATM.S4 | C | T | 21/23/6 | 37/24/6 | 0.3500 | 0.2687 | 1.0000 | 0.5329 |
| *SOD2* | rs4880 | SOD2.S1 | T | C | 36/13/1 | 55/11/1 | 0.1500 | 0.0970 | 1.0000 | 0.4743 |
| | rs5746136 | SOD2.S2 | G | A | 19/23/8 | 23/28/16 | 0.3900 | 0.4478 | 0.7738 | 0.2199 |
| | rs2842980 | SOD2.S3 | A | T | 14/23/13 | 23/27/17 | 0.4900 | 0.4552 | 0.5788 | 0.1405 |
| *TGFβ1* | rs1800469 | TGFB1.S1 | T | C | 18/27/5 | 23/32/12 | 0.3700 | 0.4179 | 0.3678 | 1.0000 |
| | rs1800470 | TGFB1.S2 | C | T | 17/28/5 | 23/32/12 | 0.3800 | 0.4179 | 0.2410 | 1.0000 |
| | rs2241716 | TGFB1.S3 | G | A | 27/22/1 | 36/25/6 | 0.2400 | 0.2761 | 0.2487 | 0.5515 |
| | rs4803455 | TGFB1.S4 | C | A | 25/19/6 | 27/28/12 | 0.3100 | 0.3881 | 0.5074 | 0.3144 |
| | rs11466345 | TGFB1.S5 | A | G | 23/25/2 | 31/29/7 | 0.2900 | 0.3209 | 0.1828 | 1.0000 |
| | rs12983047 | TGFB1.S6 | T | C | 19/27/4 | 23/30/14 | 0.3500 | 0.4328 | 0.3480 | 0.4637 |
| *TP53* | rs8064946 | TP53.S1 | C | G | 22/24/4 | 31/27/9 | 0.3200 | 0.3358 | 0.7442 | 0.4202 |
| | rs12602273 | TP53.S2 | G | C | 24/22/4 | 31/29/7 | 0.3000 | 0.3209 | 1.0000 | 1.0000 |
| | rs1042522 | TP53.S3 | G | C | 13/26/11 | 24/29/14 | 0.4800 | 0.4254 | 1.0000 | 0.3301 |
| | rs12951053 | TP53.S4 | T | G | 22/24/4 | 31/26/10 | 0.3200 | 0.3433 | 0.7442 | 0.2800 |
| *XRCC1* | rs3213282 | XRCC1.S1 | G | C | 26/21/3 | 40/25/2 | 0.2700 | 0.2164 | 1.0000 | 0.7171 |
| | rs12611088 | XRCC1.S2 | C | T | 31/17/2 | 36/25/6 | 0.2100 | 0.2761 | 1.0000 | 0.5515 |
| | rs1001581 | XRCC1.S3 | G | A | 24/22/4 | 21/37/9 | 0.3000 | 0.4104 | 1.0000 | 0.3180 |
| | rs3213344 | XRCC1.S4 | C | G | 26/20/4 | 37/24/6 | 0.2800 | 0.2687 | 1.0000 | 0.5329 |
| | rs1799782 | XRCC1.S5 | C | T | 26/20/4 | 38/23/6 | 0.2800 | 0.2612 | 1.0000 | 0.3524 |
| | rs25487 | XRCC1.S6 | G | A | 29/19/2 | 35/27/5 | 0.2300 | 0.2761 | 1.0000 | 1.0000 |
| *XRCC3* | rs1799794 | XRCC3.S1 | A | G | 12/30/8 | 24/28/15 | 0.4600 | 0.4328 | 0.2524 | 0.2215 |
| | rs861530 | XRCC3.S2 | A | G | 11/29/10 | 17/34/16 | 0.4900 | 0.4925 | 0.3950 | 1.0000 |
| | rs3212090 | XRCC3.S3 | G | A | 18/25/6 | 24/32/11 | 0.3776 | 0.4030 | 0.5594 | 1.0000 |
| | rs12432907 | XRCC3.S4 | G | A | 12/28/10 | 22/30/15 | 0.4800 | 0.4478 | 0.5703 | 0.2215 |
| | rs861539 | XRCC3.S5 | C | T | 43/7/0 | 58/8/1 | 0.0700 | 0.0746 | 1.0000 | 0.3036 |
| | rs861544 | XRCC3.S6 | C | T | 11/35/4 | 18/40/9 | 0.4300 | 0.4328 | 0.0040 | 0.1335 |

**Abbreviation**: SNP = single nucleotide polymorphism; A1 = major allele; A2 = minor allele; MAF = minor allele frequency.

Table 3.5: Single-marker association analysis using additive model of acute skin reactions

| Gene | SNP | | OR (95% CI) | | $P_{asym}$ | $P_{emp}$ |
|---|---|---|---|---|---|---|
| *ATM* | rs228591 | ATM.S1 | 0.70 | (0.41-1.19) | 0.1945 | 0.9783 |
| | rs600931 | ATM.S2 | 0.65 | (0.38-1.12) | 0.1295 | 0.9034 |
| | rs11212592 | ATM.S3 | 0.54 | (0.28-1.05) | 0.0761 | 0.7452 |
| | rs373759 | ATM.S4 | 0.65 | (0.36-1.17) | 0.1598 | 0.9524 |
| *SOD2* | rs4880 | SOD2.S1 | 0.55 | (0.24-1.24) | 0.1631 | 0.9499 |
| | rs5746136 | SOD2.S2 | 1.31 | (0.78-2.21) | 0.3157 | 0.9989 |
| | rs2842980 | SOD2.S3 | 0.87 | (0.53-1.44) | 0.6002 | 1.0000 |
| *TP53* | rs8064946 | TP53.S1 | 1.11 | (0.63-1.93) | 0.7228 | 1.0000 |
| | rs12602273 | TP53.S2 | 1.15 | (0.64-2.05) | 0.6484 | 1.0000 |
| | rs1042522 | TP53.S3 | 0.79 | (0.47-1.35) | 0.4114 | 0.9998 |
| | rs12951053 | TP53.S4 | 1.11 | (0.64-1.94) | 0.7209 | 1.0000 |
| *TGFβ1* | rs1800469 | TGFB1.S1 | 1.27 | (0.73-2.21) | 0.4008 | 0.9998 |
| | rs1800470 | TGFB1.S2 | 1.24 | (0.71-2.16) | 0.4572 | 1.0000 |
| | rs2241716 | TGFB1.S3 | 1.23 | (0.67-2.29) | 0.5168 | 1.0000 |
| | rs4803455 | TGFB1.S4 | 1.32 | (0.78-2.25) | 0.3149 | 0.9986 |
| | rs11466345 | TGFB1.S5 | 1.24 | (0.67-2.28) | 0.5131 | 1.0000 |
| | rs12983047 | TGFB1.S6 | 1.44 | (0.82-2.52) | 0.2070 | 0.9854 |
| *XRCC1* | rs3213282 | XRCC1.S1 | 0.73 | (0.38-1.40) | 0.3558 | 0.9995 |
| | rs12611088 | XRCC1.S2 | 1.39 | (0.74-2.61) | 0.3137 | 0.9986 |
| | rs1001581 | XRCC1.S3 | 1.71 | (0.93-3.15) | 0.0885 | 0.8115 |
| | rs3213344 | XRCC1.S4 | 0.95 | (0.53-1.70) | 0.8678 | 1.0000 |
| | rs1799782 | XRCC1.S5 | 0.92 | (0.52-1.65) | 0.8016 | 1.0000 |
| | rs25487 | XRCC1.S6 | 1.25 | (0.67-2.34) | 0.4958 | 1.0000 |
| *XRCC3* | rs1799794 | XRCC3.S1 | 0.89 | (0.59-1.52) | 0.6832 | 1.0000 |
| | rs861530 | XRCC3.S2 | 1.05 | (0.60-1.83) | 0.8711 | 1.0000 |
| | rs3212090 | XRCC3.S3 | 1.17 | (0.70-2.03) | 0.5975 | 1.0000 |
| | rs12432907 | XRCC3.S4 | 0.86 | (0.50-1.48) | 0.6079 | 1.0000 |
| | rs861539 | XRCC3.S5 | 1.04 | (0.38-2.81) | 0.9476 | 1.0000 |
| | rs861544 | XRCC3.S6 | 1.05 | (0.55-2.01) | 0.8903 | 1.0000 |

**Abbreviation**: SNP = single nucleotide polymorphism; OR = Odd ratio; CI = Confidence interval; $P_{asym}$ = asymptotic P value; $P_{emp}$ = empirical P value.
OR is calculated using major allele (A1) as reference. Refer to Table 3.4 for the major allele of each SNP.

#### 3.4.1.3 Haplotype analysis

Controls and cases were examined together to construct a LD map of each gene. LD plots of *ATM*, *SOD2*, *TGFβ1*, *TP53*, *XRCC1*, and *XRCC3* were constructed by Haploview and are shown in Figure 3.1-3.6. LD was expressed as $r^2$. LD blocks were constructed using SSLD algorithm (Section 2.3.4). One haplotype block was constructed for *ATM*, *SOD2*, *TP53*, *XRCC1*, and *XRCC3*. Two 8-kb haplotype blocks were constructed for *TGFβ1*. The haplotype blocks of *ATM*, *SOD2*, *TP53*, *XRCC1*, and *XRCC3* spanned 123 kb, 13 kb, 11 kb, 17 kb and 17 kb, respectively.

Haplotypes of all sizes were generated by PLINK (Section 2.3.4) and the results are summarised in Table 3.6. Six sliding windows were generated for *SOD2*. For *ATM* and *TP53*, 10 sliding windows were generated for each gene. Twenty-one sliding windows were generated for *TGFβ1*, *XRCC1*, and *XRCC3*. In total, 89 haplotype windows were generated for six candidate genes. The 2-SNP haplotype window (TGFB1.S5-S6) from *TGFβ1* showed significant association before multiple testing correction (Omnibus test $P_{asym} < 0.05$). However, significance was lost after 10,000 permutations. No significant difference was found in all sizes of haplotype windows for all candidate genes between controls and cases (Omnibus test $P_{emp} > 0.05$).

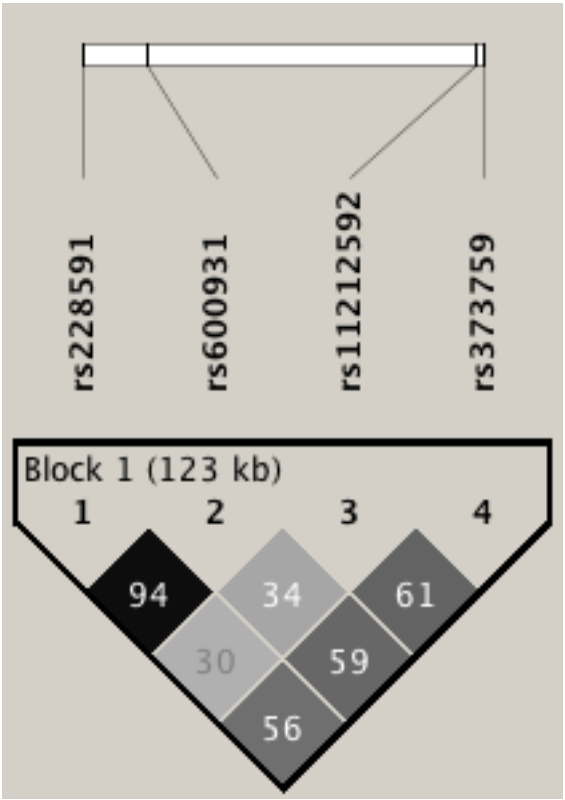


Figure 3.1: LD plot of *ATM* gene in NPC patients (acute skin toxicity and acute mucositis). LD plot is constructed by Haploview using the solid spine of LD algorithm. LD is expressed as $r^2$. One haplotype block is identified.

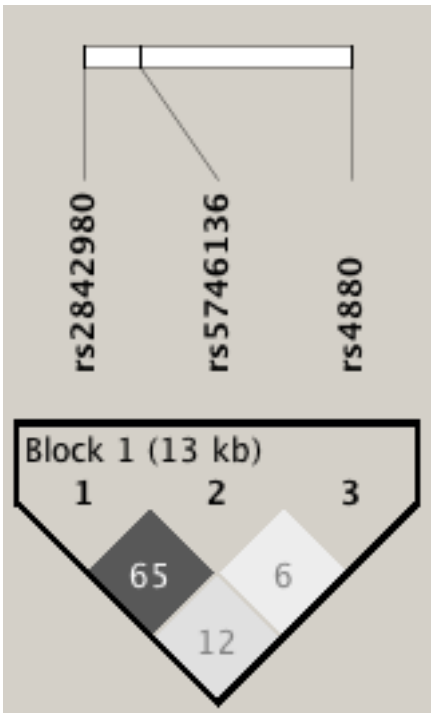


Figure 3.2: LD plot of *SOD2* gene in NPC patients (acute skin toxicity and acute mucositis). LD plot is constructed by Haploview using the solid spine of LD algorithm. LD is expressed as $r^2$. One haplotype block is identified.

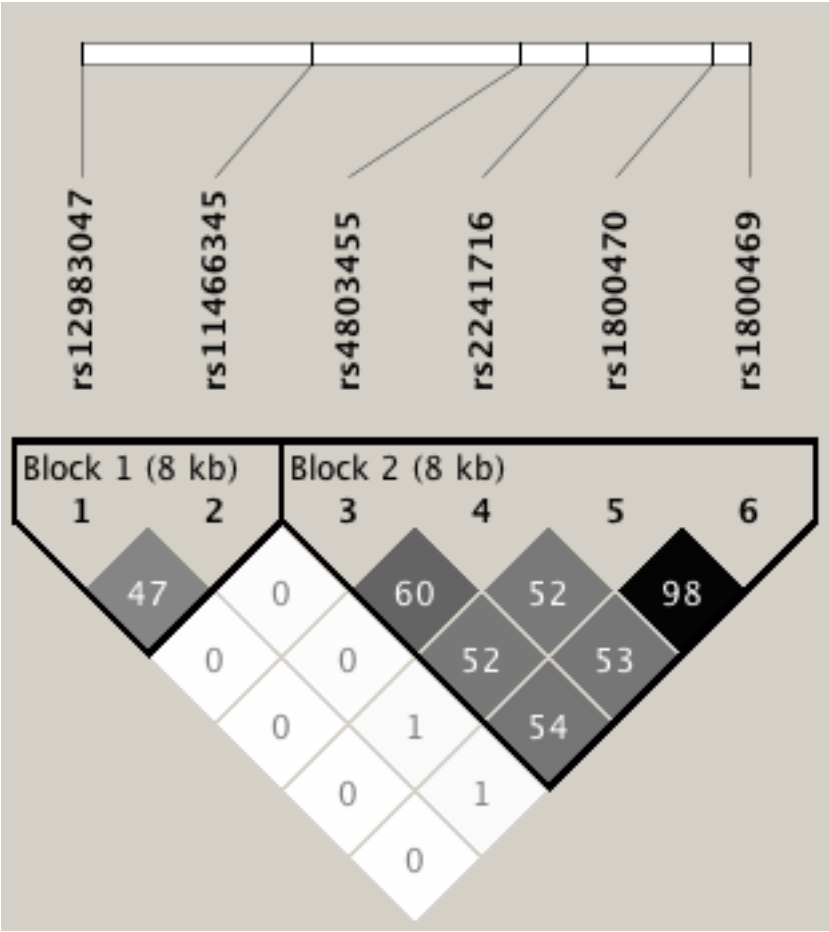


Figure 3.3: LD plot of *TGFβ1* gene in NPC patients (acute skin toxicity and acute mucositis). LD plot is constructed by Haploview using the solid spine of LD algorithm. LD is expressed as $r^2$. Two haplotype blocks are identified.

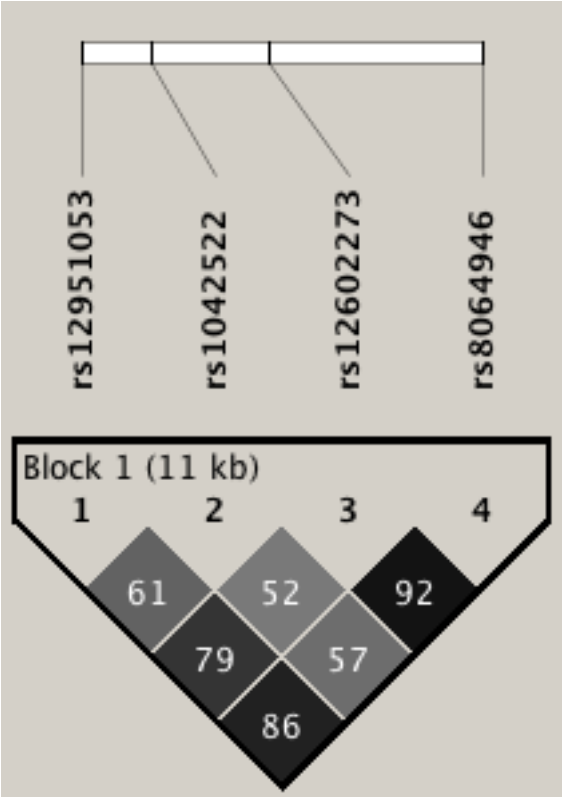


Figure 3.4: LD plot of *TP53* gene in NPC patients (acute skin toxicity and acute mucositis). LD plot is constructed by Haploview using the solid spine of LD algorithm. LD is expressed as $r^2$. One haplotype block is identified.

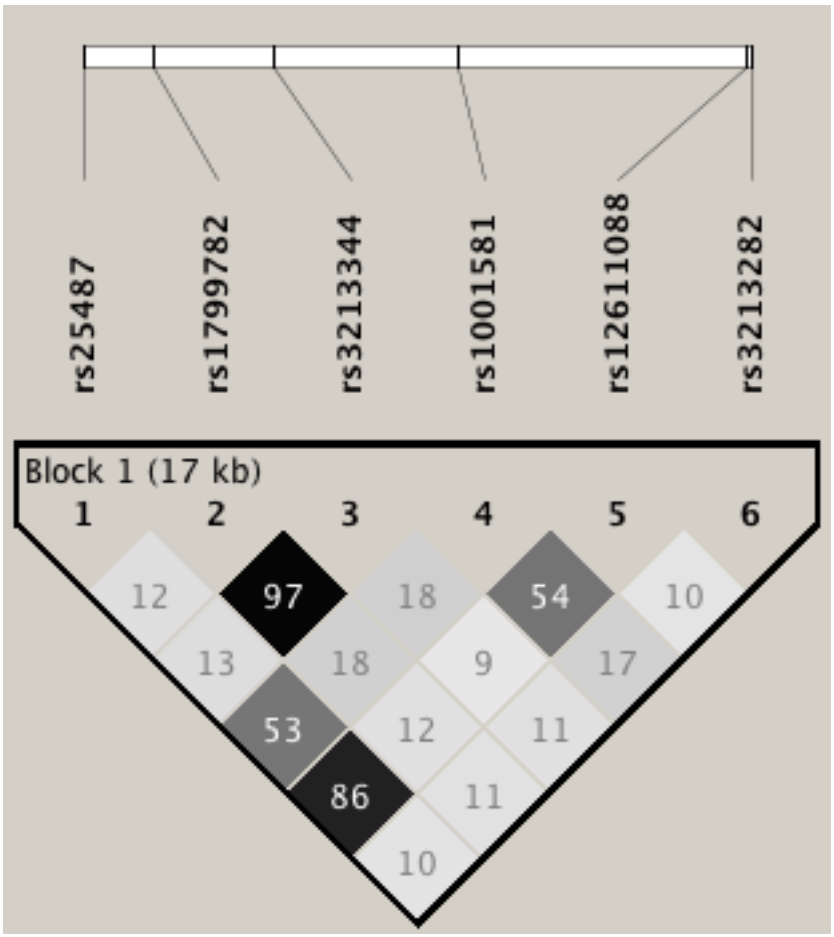


Figure 3.5: LD plot of *XRCC1* gene in NPC patients (acute skin toxicity and acute mucositis). LD plot is constructed by Haploview using the solid spine of LD algorithm. LD is expressed as $r^2$. One haplotype block is identified.

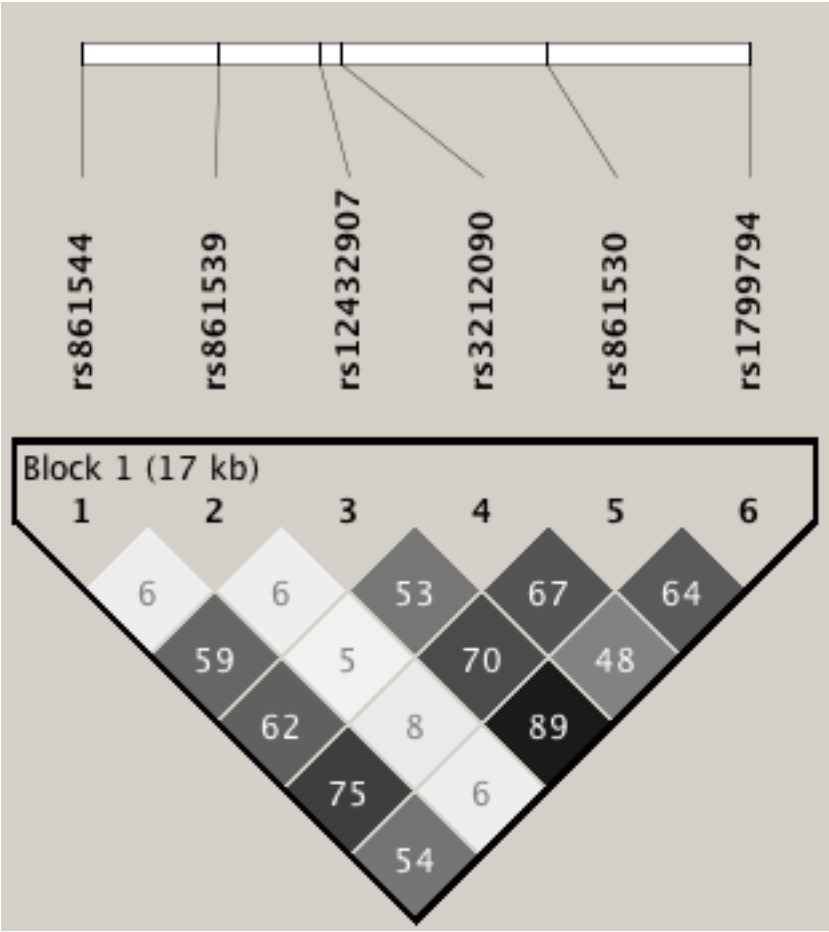


Figure 3.6: LD plot of *XRCC3* gene in NPC patients (acute skin toxicity and acute mucositis). LD plot is constructed by Haploview using the solid spine of LD algorithm. LD is expressed as $r^2$. One haplotype block is identified.

Table 3.6: Summary of sliding-window haplotype analysis based on omnibus test for acute skin reactions

| | | | SW | The most significant omnibus test | | |
|---|---|---|---|---|---|---|
| Gene | NSNP | First SW | Last SW | SW | $P_{asym}$ | $P_{emp}$ |
| *ATM* | 2 | ATM.S1..ATM.S2 | ATM.S3..ATM.S4 | ATM.S1..ATM.S2 | 0.0868 | 0.4345 |
| | 3 | ATM.S1..ATM.S3 | ATM.S2..ATM.S4 | ATM.S1..ATM.S3 | 0.1802 | 0.5373 |
| | 4 | ATM.S1..ATM.S4 | ATM.S1..ATM.S4 | ATM.S1..ATM.S4 | 0.2975 | 0.7193 |
| *SOD2* | 2 | SOD2.S1..SOD2.S2 | SOD2.S2..SOD2.S3 | SOD2.S1..SOD2.S2 | 0.2692 | 0.5428 |
| | 3 | SOD2.S1..SOD2.S3 | SOD2.S1..SOD2.S3 | SOD2.S1..SOD2.S3 | 0.2284 | 0.5293 |
| *TGFβ1* | 2 | TGFB1.S1..TGFB1.S2 | TGFB1.S5..TGFB1.S6 | TGFB1.S5..TGFB1.S6 | 0.0248 | 0.1880 |
| | 3 | TGFB1.S1..TGFB1.S3 | TGFB1.S4..TGFB1.S6 | TGFB1.S4..TGFB1.S6 | 0.1068 | 0.7247 |
| | 4 | TGFB1.S1..TGFB1.S4 | TGFB1.S3..TGFB1.S6 | TGFB1.S3..TGFB1.S6 | 0.0644 | 0.5432 |
| | 5 | TGFB1.S1..TGFB1.S5 | TGFB1.S2..TGFB1.S6 | TGFB1.S2..TGFB1.S6 | 0.2919 | 0.9626 |
| | 6 | TGFB1.S1..TGFB1.S6 | TGFB1.S1..TGFB1.S6 | TGFB1.S1..TGFB1.S6 | 0.3436 | 0.9759 |
| *TP53* | 2 | TP53.S1..TP53.S2 | TP53.S3..TP53.S4 | TP53.S2..TP53.S3 | 0.1151 | 0.2617 |
| | 3 | TP53.S1..TP53.S3 | TP53.S2..TP53.S4 | TP53.S2..TP53.S4 | 0.1327 | 0.3501 |
| | 4 | TP53.S1..TP53.S4 | TP53.S1..TP53.S4 | TP53.S1..TP53.S4 | 0.1306 | 0.5247 |
| *XRCC1* | 2 | XRCC1.S1..XRCC1.S2 | XRCC1.S5..XRCC1.S6 | XRCC1.S2..XRCC1.S3 | 0.1878 | 0.5841 |
| | 3 | XRCC1.S1..XRCC1.S3 | XRCC1.S4..XRCC1.S6 | XRCC1.S3..XRCC1.S5 | 0.1863 | 0.6956 |
| | 4 | XRCC1.S1..XRCC1.S4 | XRCC1.S3..XRCC1.S6 | XRCC1.S2..XRCC1.S5 | 0.2270 | 0.7447 |
| | 5 | XRCC1.S1..XRCC1.S5 | XRCC1.S2..XRCC1.S6 | XRCC1.S2..XRCC1.S6 | 0.2770 | 0.8728 |
| | 6 | XRCC1.S1..XRCC1.S6 | XRCC1.S1..XRCC1.S6 | XRCC1.S1..XRCC1.S6 | 0.4278 | 0.9544 |
| *XRCC3* | 2 | XRCC3.S1..XRCC3.S2 | XRCC3.S5..XRCC3.S6 | XRCC3.S5..XRCC3.S6 | 0.7393 | 1.0000 |
| | 3 | XRCC3.S1..XRCC3.S3 | XRCC3.S4..XRCC3.S6 | XRCC3.S2..XRCC3.S4 | 0.7973 | 1.0000 |
| | 4 | XRCC3.S1..XRCC3.S4 | XRCC3.S3..XRCC3.S6 | XRCC3.S1..XRCC3.S4 | 0.5174 | 0.9783 |
| | 5 | XRCC3.S1..XRCC3.S5 | XRCC3.S2..XRCC3.S6 | XRCC3.S1..XRCC3.S5 | 0.4915 | 0.9916 |
| | 6 | XRCC3.S1..XRCC3.S6 | XRCC3.S1..XRCC3.S6 | XRCC3.S1..XRCC3.S6 | 0.7480 | 1.0000 |

**Abbreviation**: SW = Sliding window; NSNP = number of SNPs in this haplotype window; $P_{asym}$ = asymptotic P value; $P_{emp}$ = empirical P value.

The SW is indicated as GENE.Sx...GENE.Sy, where GENE is the name of candidate gene, Sx is the first SNP and Sy is the last SNP of the SW. For example, TP53.S1..TP53.S3 represents the sliding window TP53.S1-S2-S3 (rs8064946-rs12602273-rs1042522) of *TP53* gene. Please refer to Table 3.1 for SNP identity.

## 3.4.2 Acute mucositis

### 3.4.2.1 Clinical characteristics of included patients

One hundred and seventeen Chinese NPC patients were included in this part of analysis. This group of patients was the same group of patients from the previous section investigating the genetic association of acute skin reactions (Section 3.4.1.1). Patients were classified into controls and cases according to the highest grade of **acute mucositis** recorded during RT (Section 2.2.2.1). Forty patients were classified as controls and 77 patients were classified as cases. Clinical characteristics of recruited patients are summarised in Table 3.7. There were no significant difference of clinical characteristics between controls and cases ($P$>0.05).

### 3.4.2.2 Single-marker analysis

All SNPs were successfully genotyped and were tested for HWE. No deviation from HWE was found in all SNPs for controls ($P$>0.001). As a results, all SNPs were included in single-marker analysis. Results of single-marker association analysis are shown in Table 3.9. One SNP from *XRCC3* (rs861539) and two SNPs from *TP53* (rs8064946 and rs12602273) showed significant association to radiation-induced mucositis before multiple testing correction ($P_{asym}$<0.05). However, significance did not survive after multiple-testing correction based on 10,000 permutations. None of the remaining tag SNPs of all candidate genes showed any association to radiation-induced acute mucositis.

Table 3.7: Clinical characteristics of recruited patients in acute mucositis

| Group | | Control (n=40) | Case (n=77) | *P* |
|---|---|---|---|---|
| Clinical Variables | | Mean (SD) | | |
| Age | | 51.58 (12.08) | 53.32 (9.31) | 0.4146 |
| | | Frequency (%) | | |
| Sex | | | | 0.4071 |
| | Male | 30 (75.0%) | 52 (67.5%) | |
| | Female | 10 (25.0%) | 25 (32.5%) | |
| Stage (TMN) | | | | 0.0613 |
| | I | 9 (22.5%) | 6 (7.8%) | |
| | II | 5 (12.5%) | 26 (33.7%) | |
| | III | 16 (40.0%) | 29 (37.7%) | |
| | IV | 6 (15.0%) | 15 (19.5%) | |
| | Unavailable | 4 (10.0%) | 1 (1.3%) | |
| Radiotherapy | | | | 0.1318 |
| | CRT | 17 (42.5%) | 22 (28.6%) | |
| | IMRT | 23 (57.5%) | 55 (71.4%) | |
| Chemotherapy | | 19 (47.5%) | 44 (57.1%) | 0.3252 |

Table 3.8: Summary statistics of acute mucositis

| | | | | | Genotype Counts 11/12/22 | | MAF | | HWE $P$ value | |
|---|---|---|---|---|---|---|---|---|---|---|
| Gene | SNP | | A1 | A2 | Controls | Cases | Controls | Cases | Controls | Cases |
| *ATM* | rs228591 | ATM.S1 | A | G | 14/22/4 | 29/30/18 | 0.3750 | 0.4286 | 0.4974 | 0.1015 |
| | rs600931 | ATM.S2 | C | T | 13/23/4 | 27/32/18 | 0.3875 | 0.4416 | 0.3160 | 0.1705 |
| | rs11212592 | ATM.S3 | A | G | 27/12/1 | 42/30/5 | 0.1750 | 0.2597 | 1.0000 | 1.0000 |
| | rs373759 | ATM.S4 | C | T | 20/19/1 | 38/28/11 | 0.2625 | 0.3247 | 0.2373 | 0.1279 |
| *SOD2* | rs4880 | SOD2.S1 | T | C | 29/11/0 | 62/13/2 | 0.1375 | 0.1104 | 1.0000 | 0.2154 |
| | rs5746136 | SOD2.S2 | G | A | 14/20/6 | 28/31/18 | 0.4000 | 0.4351 | 1.0000 | 0.1103 |
| | rs2842980 | SOD2.S3 | A | T | 11/17/12 | 26/33/18 | 0.4875 | 0.4481 | 0.3535 | 0.2530 |
| *TGFβ1* | rs1800469 | TGFB1.S1 | T | C | 14/18/8 | 27/41/9 | 0.4250 | 0.3831 | 0.7457 | 0.3393 |
| | rs1800470 | TGFB1.S2 | C | T | 13/19/8 | 27/41/9 | 0.4375 | 0.3831 | 1.0000 | 0.3393 |
| | rs2241716 | TGFB1.S3 | G | A | 22/13/5 | 41/34/2 | 0.2875 | 0.2468 | 0.2428 | 0.1332 |
| | rs4803455 | TGFB1.S4 | C | A | 20/12/8 | 35/35/10 | 0.3500 | 0.3571 | 0.0372 | 1.0000 |
| | rs11466345 | TGFB1.S5 | A | G | 14/24/2 | 40/30/7 | 0.3500 | 0.2857 | 0.0807 | 0.7795 |
| | rs12983047 | TGFB1.S6 | T | C | 9/23/8 | 33/34/10 | 0.4875 | 0.3506 | 0.5260 | 0.8042 |
| *TP53* | rs8064946 | TP53.S1 | C | G | 23/14/3 | 30/37/10 | 0.2500 | 0.3701 | 0.6784 | 1.0000 |
| | rs12602273 | TP53.S2 | G | C | 24/13/3 | 31/38/8 | 0.2375 | 0.3506 | 0.6589 | 0.6172 |
| | rs1042522 | TP53.S3 | G | C | 15/17/8 | 22/38/17 | 0.4125 | 0.4675 | 0.5145 | 1.0000 |
| | rs12951053 | TP53.S4 | T | G | 24/11/5 | 29/39/9 | 0.2625 | 0.3701 | 0.0942 | 0.6244 |
| *XRCC1* | rs3213282 | XRCC1.S1 | G | C | 20/16/4 | 46/30/1 | 0.3000 | 0.2078 | 0.7179 | 0.1684 |
| | rs12611088 | XRCC1.S2 | C | T | 23/14/3 | 44/28/5 | 0.2500 | 0.2468 | 0.6784 | 0.7672 |
| | rs1001581 | XRCC1.S3 | G | A | 16/21/3 | 29/38/10 | 0.3375 | 0.3766 | 0.4775 | 0.8089 |
| | rs3213344 | XRCC1.S4 | C | G | 22/14/4 | 41/30/6 | 0.2750 | 0.2727 | 0.4388 | 1.0000 |
| | rs1799782 | XRCC1.S5 | C | T | 23/13/4 | 41/30/6 | 0.2625 | 0.2727 | 0.4086 | 1.0000 |
| | rs25487 | XRCC1.S6 | G | A | 21/17/2 | 43/29/5 | 0.2625 | 0.2532 | 0.6999 | 1.0000 |
| *XRCC3* | rs1799794 | XRCC3.S1 | A | G | 15/18/7 | 21/40/16 | 0.4000 | 0.4675 | 0.7443 | 0.8202 |
| | rs861530 | XRCC3.S2 | A | G | 8/20/12 | 20/43/14 | 0.4500 | 0.4610 | 1.0000 | 0.3610 |
| | rs3212090 | XRCC3.S3 | G | A | 14/20/6 | 28/38/11 | 0.4000 | 0.3896 | 1.0000 | 0.8146 |
| | rs12432907 | XRCC3.S4 | G | A | 14/18/8 | 22/38/17 | 0.4250 | 0.4675 | 0.7457 | 1.0000 |
| | rs861539 | XRCC3.S5 | C | T | 30/9/1 | 71/6/0 | 0.1375 | 0.0390 | 0.5481 | 1.0000 |
| | rs861544 | XRCC3.S6 | C | T | 9/25/6 | 20/50/7 | 0.4625 | 0.4156 | 0.2004 | 0.0047 |

**Abbreviation**: SNP = single nucleotide polymorphism; A1 = major allele; A2 = minor allele; MAF = minor allele frequency.

Table 3.9: Single-marker association analysis using additive model of acute mucositis

| Gene | SNP | | OR (95% CI) | | $P_{asym}$ | $P_{emp}$ |
|---|---|---|---|---|---|---|
| *ATM* | rs228591 | ATM.S1 | 1.36 | (0.76-2.45) | 0.3173 | 0.9986 |
| | rs600931 | ATM.S2 | 1.42 | (0.77-2.60) | 0.2712 | 0.9957 |
| | rs11212592 | ATM.S3 | 1.68 | (0.80-3.52) | 0.1749 | 0.9643 |
| | rs373759 | ATM.S4 | 1.50 | (0.79-2.86) | 0.2233 | 0.9877 |
| *SOD2* | rs4880 | SOD2.S1 | 0.90 | (0.38-2.11) | 0.8143 | 1.0000 |
| | rs5746136 | SOD2.S2 | 1.06 | (0.61-1.82) | 0.8560 | 1.0000 |
| | rs2842980 | SOD2.S3 | 0.80 | (0.47-1.36) | 0.4202 | 0.9999 |
| *TP53* | rs8064946 | TP53.S1 | 1.95 | (1.01-3.74) | 0.0469 | 0.5838 |
| | rs12602273 | TP53.S2 | 2.00 | (1.01-3.95) | 0.0492 | 0.5978 |
| | rs1042522 | TP53.S3 | 1.30 | (0.73-2.31) | 0.3770 | 0.9997 |
| | rs12951053 | TP53.S4 | 1.78 | (0.95-3.35) | 0.0781 | 0.7639 |
| *TGFβ1* | rs1800469 | TGFB1.S1 | 0.80 | (0.44-1.44) | 0.4680 | 1.0000 |
| | rs1800470 | TGFB1.S2 | 0.77 | (0.43-1.41) | 0.4202 | 0.9999 |
| | rs2241716 | TGFB1.S3 | 0.74 | (0.39-1.41) | 0.3767 | 0.9995 |
| | rs4803455 | TGFB1.S4 | 0.93 | (0.53-1.64) | 0.8126 | 1.0000 |
| | rs11466345 | TGFB1.S5 | 0.79 | (0.42-1.49) | 0.4657 | 1.0000 |
| | rs12983047 | TGFB1.S6 | 0.55 | (0.30-1.01) | 0.0568 | 0.6473 |
| *XRCC1* | rs3213282 | XRCC1.S1 | 0.61 | (0.30-1.23) | 0.1848 | 0.9665 |
| | rs12611088 | XRCC1.S2 | 1.12 | (0.58-2.17) | 0.7510 | 1.0000 |
| | rs1001581 | XRCC1.S3 | 1.30 | (0.69-2.48) | 0.4415 | 1.0000 |
| | rs3213344 | XRCC1.S4 | 0.90 | (0.48-1.68) | 0.7447 | 1.0000 |
| | rs1799782 | XRCC1.S5 | 0.93 | (0.50-1.76) | 0.8370 | 1.0000 |
| | rs25487 | XRCC1.S6 | 1.01 | (0.52-1.96) | 0.9841 | 1.0000 |
| *XRCC3* | rs1799794 | XRCC3.S1 | 1.38 | (0.76-2.49) | 0.3015 | 0.9977 |
| | rs861530 | XRCC3.S2 | 0.63 | (0.35-1.17) | 0.1486 | 0.9420 |
| | rs3212090 | XRCC3.S3 | 0.95 | (0.52-1.71) | 0.8549 | 1.0000 |
| | rs12432907 | XRCC3.S4 | 1.26 | (0.70-2.27) | 0.4662 | 1.0000 |
| | rs861539 | XRCC3.S5 | 0.20 | (0.07-0.63) | 0.0035 | 0.1037 |
| | rs861544 | XRCC3.S6 | 0.75 | (0.37-1.49) | 0.4150 | 0.9999 |

**Abbreviation**: SNP = single nucleotide polymorphism; OR = Odd ratio; CI = Confidence interval; $P_{asym}$ = asymptotic P value; $P_{emp}$ = empirical P value.
OR is calculated using major allele (A1) as reference. Refer to Table 3.8 for the major allele of each SNP.

#### 3.4.2.3 Haplotype analysis

LD blocks were constructed using SSLD algorithm (Section 2.3.4). LD was expressed as $r^2$. Controls and cases were examined together to construct a LD map of each gene. Since the same group of patients from Section 3.4.1.1 was included in this part of analysis, LD plots of *ATM*, *SOD2*, *TGFβ1*, *TP53*, *XRCC1* and *XRCC3* are referred to LD plots constructed in the previous section (Figure 3.1-3.6). One haplotype block was constructed for *ATM*, *SOD2*, *TP53*, *XRCC1*, and *XRCC3*. Two haplotype blocks were constructed for *TGFβ1*. The haplotype blocks of *ATM*, *SOD2*, *TP53*, *XRCC1*, and *XRCC3* spanned 123 kb, 13 kb, 11 kb, 17 kb and 17 kb, respectively. Two 8-kb haplotype blocks were constructed for *TGFβ1*.

Haplotypes of all sizes were generated by PLINK (Section 2.3.4) and the results are summarised in Table 3.10. Six sliding windows were generated for *SOD2*. For *ATM* and *TP53*, 10 sliding windows were generated for each gene. Twenty-one sliding windows were generated for *TGFβ1*, *XRCC1*, and *XRCC3*. In total, 89 haplotype windows were generated for six candidate genes. The 2-SNP haplotype window (XRCC3.S4-S5), 3-SNP haplotype window (XRCC3.S3-S5), 4-SNP haplotype window (XRCC3.S2-S5), and 5-SNP haplotype window (XRCC3.S1-S5) from *XRCC3* showed significant association before multiple testing correction (Omnibus test $P_{asym}<0.05$). However, none of the significant level survived after 10,000 permutations. No significant difference was found in all sizes of haplotype windows for all candidate genes between controls and cases (Omnibus test $P_{emp}>0.05$).

Table 3.10: Summary of sliding-window haplotype analysis based on omnibus test for acute mucositis

| | | | SW | The most significant omnibus test | | |
|---|---|---|---|---|---|---|
| Gene | NSNP | First SW | Last SW | SW | $P_{asym}$ | $P_{emp}$ |
| *ATM* | 2 | ATM.S1..ATM.S2 | ATM.S3..ATM.S4 | ATM.S1..ATM.S2 | 0.3717 | 0.8539 |
| | 3 | ATM.S1..ATM.S3 | ATM.S2..ATM.S4 | ATM.S1..ATM.S3 | 0.4459 | 0.8770 |
| | 4 | ATM.S1..ATM.S4 | ATM.S1..ATM.S4 | ATM.S1..ATM.S4 | 0.6450 | 0.9744 |
| *SOD2* | 2 | SOD2.S1..SOD2.S2 | SOD2.S2..SOD2.S3 | SOD2.S2..SOD2.S3 | 0.5257 | 0.8394 |
| | 3 | SOD2.S1..SOD2.S3 | SOD2.S1..SOD2.S3 | SOD2.S1..SOD2.S3 | 0.5796 | 0.9129 |
| *TGFβ1* | 2 | TGFB1.S1..TGFB1.S2 | TGFB1.S5..TGFB1.S6 | TGFB1.S5..TGFB1.S6 | 0.1657 | 0.6502 |
| | 3 | TGFB1.S1..TGFB1.S3 | TGFB1.S4..TGFB1.S6 | TGFB1.S4..TGFB1.S6 | 0.3367 | 0.9526 |
| | 4 | TGFB1.S1..TGFB1.S4 | TGFB1.S3..TGFB1.S6 | TGFB1.S3..TGFB1.S6 | 0.4053 | 0.9636 |
| | 5 | TGFB1.S1..TGFB1.S5 | TGFB1.S2..TGFB1.S6 | TGFB1.S2..TGFB1.S6 | 0.6641 | 0.9999 |
| | 6 | TGFB1.S1..TGFB1.S6 | TGFB1.S1..TGFB1.S6 | TGFB1.S1..TGFB1.S6 | 0.7245 | 1.0000 |
| *TP53* | 2 | TP53.S1..TP53.S2 | TP53.S3..TP53.S4 | TP53.S1..TP53.S2 | 0.0733 | 0.3053 |
| | 3 | TP53.S1..TP53.S3 | TP53.S2..TP53.S4 | TP53.S1..TP53.S3 | 0.1063 | 0.3716 |
| | 4 | TP53.S1..TP53.S4 | TP53.S1..TP53.S4 | TP53.S1..TP53.S4 | 0.1320 | 0.5281 |
| *XRCC1* | 2 | XRCC1.S1..XRCC1.S2 | XRCC1.S5..XRCC1.S6 | XRCC1.S1..XRCC1.S2 | 0.4026 | 0.8614 |
| | 3 | XRCC1.S1..XRCC1.S3 | XRCC1.S4..XRCC1.S6 | XRCC1.S1..XRCC1.S3 | 0.4893 | 0.9287 |
| | 4 | XRCC1.S1..XRCC1.S4 | XRCC1.S3..XRCC1.S6 | XRCC1.S1..XRCC1.S4 | 0.6164 | 0.9883 |
| | 5 | XRCC1.S1..XRCC1.S5 | XRCC1.S2..XRCC1.S6 | XRCC1.S1..XRCC1.S5 | 0.6174 | 0.9884 |
| | 6 | XRCC1.S1..XRCC1.S6 | XRCC1.S1..XRCC1.S6 | XRCC1.S1..XRCC1.S6 | 0.4677 | 0.9708 |
| *XRCC3* | 2 | XRCC3.S1..XRCC3.S2 | XRCC3.S5..XRCC3.S6 | XRCC3.S4..XRCC3.S5 | 0.0151 | 0.0805 |
| | 3 | XRCC3.S1..XRCC3.S3 | XRCC3.S4..XRCC3.S6 | XRCC3.S3..XRCC3.S5 | 0.0111 | 0.0680 |
| | 4 | XRCC3.S1..XRCC3.S4 | XRCC3.S3..XRCC3.S6 | XRCC3.S2..XRCC3.S5 | 0.0270 | 0.3531 |
| | 5 | XRCC3.S1..XRCC3.S5 | XRCC3.S2..XRCC3.S6 | XRCC3.S1..XRCC3.S5 | 0.0362 | 0.4721 |
| | 6 | XRCC3.S1..XRCC3.S6 | XRCC3.S1..XRCC3.S6 | XRCC3.S1..XRCC3.S6 | 0.0657 | 0.6295 |

**Abbreviation**: SW = Sliding window; NSNP = number of SNPs in this haplotype window; $P_{asym}$ = asymptotic P value; $P_{emp}$ = empirical P value.

The SW is indicated as GENE.Sx...GENE.Sy, where GENE is the name of candidate gene, Sx is the first SNP and Sy is the last SNP of the SW. For example, TP53.S1..TP53.S3 represents the sliding window TP53.S1-S2-S3 (rs8064946-rs12602273-rs1042522) of *TP53* gene. Please refer to Table 3.1 for SNP identity.

### 3.4.3 Chronic skin fibrosis

#### 3.4.3.1 Clinical characteristics of included patients

One hundred and twenty Chinese NPC patients were included in this part of analysis. Patients were classified into controls and cases according to the highest grade of **chronic skin reactions** recorded during RT (Section 2.2.2.2). Ninety-one patients were classified as controls and twenty-nine patients were classified as cases. Clinical characteristics of recruited patients are summarised in Table 3.11. There was no significant difference in the mean age, cancer stagings, and the number of patients received chemotherapy between controls and cases ($P$>0.05). The length of follow up and the number of males and females were significant difference between controls and cases ($P$<0.01).

#### 3.4.3.2 Single-marker analysis

All SNPs were successfully genotyped and were tested for HWE. No deviation from HWE was found in all SNPs for controls ($P$>0.001). As a results, all SNPs were included in single marker analysis. Results of single-marker association analysis are shown in Table 3.13. One SNP from *XRCC3* (rs861539) showed significant association to radiation-induced chronic neck fibrosis before multiple testing correction ($P_{asym}$<0.05). However, significance did not survive after multiple testing correction based on 10,000 permutations. None of the remaining tag SNPs of all candidate genes showed any association to radiation-induced chronic neck fibrosis.

Table 3.11: Clinical characteristics of recruited patients in chronic neck fibrosis

| Group | | Control (n=91) | Case (n=29) | *P* |
|---|---|---|---|---|
| Clinical Variables | | Mean (SD) | | |
| Follow up years | | 8.13 (5.57) | 12.38 (5.15) | 0.0004 |
| Age | | 53.0 (10.50) | 55.6 (8.90) | 0.2491 |
| | | Frequency (%) | | |
| Sex | | | | 0.0333 |
| | Male | 69 (75.8%) | 16 (55.2%) | |
| | Female | 22 (24.2%) | 13 (44.8%) | |
| Stage (TMN) | | | | 0.6453 |
| | I | 16 (17.6%) | 0 (0.0%) | |
| | II | 26 (28.6%) | 6 (20.7%) | |
| | III | 29 (31.9%) | 15 (51.7%) | |
| | IV | 17 (17.6%) | 4 (13.8%) | |
| | Unavailable | 4 (4.4%) | 4 (13.8%) | |
| Radiotherapy | | | | 0.0003 |
| | CRT | 26 (28.6%) | 19 (65.5%) | |
| | IMRT | 65 (71.4%) | 10 (34.5%) | |
| Chemotherapy | | 46 (55.6%) | 15 (51.7%) | 0.9132 |

Table 3.12: Summary statistics of chronic neck fibrosis

| | | | | | Genotype Counts 11/12/22 | | MAF | | HWE $P$ value | |
|---|---|---|---|---|---|---|---|---|---|---|
| Gene | SNP | | A1 | A2 | Controls | Cases | Controls | Cases | Controls | Cases |
| *ATM* | rs228591 | ATM.S1 | A | G | 33/39/19 | 11/12/6 | 0.4231 | 0.4138 | 0.2826 | 0.4548 |
| | rs600931 | ATM.S2 | C | T | 32/40/19 | 9/14/6 | 0.4286 | 0.4483 | 0.3910 | 1.0000 |
| | rs11212592 | ATM.S3 | A | G | 58/30/3 | 12/12/5 | 0.1978 | 0.3793 | 1.0000 | 0.6915 |
| | rs373759 | ATM.S4 | C | T | 49/34/8 | 11/12/6 | 0.2747 | 0.4138 | 0.5987 | 0.4548 |
| *SOD2* | rs4880 | SOD2.S1 | T | C | 73/17/1 | 18/10/1 | 0.1044 | 0.2069 | 1.0000 | 1.0000 |
| | rs5746136 | SOD2.S2 | G | A | 32/36/23 | 8/19/2 | 0.4505 | 0.3966 | 0.0581 | 0.1154 |
| | rs2842980 | SOD2.S3 | A | T | 32/35/24 | 9/15/5 | 0.4560 | 0.4310 | 0.0350 | 1.0000 |
| *TGFβ1* | rs1800469 | TGFB1.S1 | T | C | 33/42/16 | 6/20/3 | 0.4066 | 0.4483 | 0.6681 | 0.0627 |
| | rs1800470 | TGFB1.S2 | C | T | 32/43/16 | 6/20/3 | 0.4121 | 0.4483 | 0.8300 | 0.0627 |
| | rs2241716 | TGFB1.S3 | G | A | 46/38/7 | 17/10/2 | 0.2857 | 0.2414 | 1.0000 | 0.6437 |
| | rs4803455 | TGFB1.S4 | C | A | 40/37/14 | 12/12/5 | 0.3571 | 0.3793 | 0.2625 | 0.6915 |
| | rs11466345 | TGFB1.S5 | A | G | 48/36/7 | 9/18/2 | 0.2747 | 0.3793 | 1.0000 | 0.1322 |
| | rs12983047 | TGFB1.S6 | T | C | 36/44/11 | 8/15/6 | 0.3626 | 0.4655 | 0.8208 | 1.0000 |
| *TP53* | rs8064946 | TP53.S1 | C | G | 39/40/12 | 15/13/1 | 0.3516 | 0.2586 | 0.8179 | 0.6356 |
| | rs12602273 | TP53.S2 | G | C | 41/40/10 | 16/12/1 | 0.3297 | 0.2414 | 1.0000 | 1.0000 |
| | rs1042522 | TP53.S3 | G | C | 25/47/19 | 13/9/7 | 0.4670 | 0.3966 | 0.8340 | 0.0617 |
| | rs12951053 | TP53.S4 | T | G | 39/41/11 | 15/10/4 | 0.3462 | 0.3103 | 1.0000 | 0.3822 |
| *XRCC1* | rs3213282 | XRCC1.S1 | G | C | 52/35/4 | 16/11/2 | 0.2363 | 0.2586 | 0.7711 | 1.0000 |
| | rs12611088 | XRCC1.S2 | C | T | 51/33/7 | 17/11/1 | 0.2582 | 0.2241 | 0.5897 | 1.0000 |
| | rs1001581 | XRCC1.S3 | G | A | 34/46/11 | 12/13/4 | 0.3736 | 0.3621 | 0.5088 | 1.0000 |
| | rs3213344 | XRCC1.S4 | C | G | 51/32/8 | 16/11/2 | 0.2637 | 0.2586 | 0.4166 | 1.0000 |
| | rs1799782 | XRCC1.S5 | C | T | 52/31/8 | 16/11/2 | 0.2582 | 0.2586 | 0.2812 | 1.0000 |
| | rs25487 | XRCC1.S6 | G | A | 50/35/6 | 15/13/1 | 0.2582 | 0.2586 | 1.0000 | 0.6356 |
| *XRCC3* | rs1799794 | XRCC3.S1 | A | G | 24/50/17 | 13/10/6 | 0.4615 | 0.3793 | 0.4002 | 0.2312 |
| | rs861530 | XRCC3.S2 | A | G | 20/52/19 | 8/13/8 | 0.4945 | 0.5000 | 0.2125 | 0.7099 |
| | rs3212090 | XRCC3.S3 | G | A | 32/44/15 | 11/16/2 | 0.4066 | 0.3448 | 1.0000 | 0.4131 |
| | rs12432907 | XRCC3.S4 | G | A | 26/47/18 | 11/11/7 | 0.4560 | 0.4310 | 0.8330 | 0.2604 |
| | rs861539 | XRCC3.S5 | C | T | 82/8/1 | 21/8/0 | 0.0550 | 0.1379 | 0.2297 | 1.0000 |
| | rs861544 | XRCC3.S6 | C | T | 22/59/10 | 8/18/3 | 0.4341 | 0.4138 | 0.0030 | 0.2498 |

**Abbreviation**: SNP = single nucleotide polymorphism; A1 = major allele; A2 = minor allele; MAF = minor allele frequency.

Table 3.13: Single-marker association analysis using additive model of chronic neck fibrosis

| Gene | SNP | | OR (95% CI) | | $P_{asym}$ | $P_{emp}$ |
|---|---|---|---|---|---|---|
| *ATM* | rs228591 | ATM.S1 | 0.72 | (0.37-1.40) | 0.3508 | 0.9994 |
| | rs600931 | ATM.S2 | 0.80 | (0.41-1.57) | 0.5253 | 1.0000 |
| | rs11212592 | ATM.S3 | 1.82 | (0.87-3.82) | 0.1225 | 0.8893 |
| | rs373759 | ATM.S4 | 1.32 | (0.68-2.57) | 0.4291 | 0.9999 |
| *SOD2* | rs4880 | SOD2.S1 | 1.69 | (0.68-4.20) | 0.2852 | 0.9957 |
| | rs5746136 | SOD2.S2 | 0.71 | (0.35-1.42) | 0.3489 | 0.9994 |
| | rs2842980 | SOD2.S3 | 1.09 | (0.58-2.05) | 0.7904 | 1.0000 |
| *TP53* | rs8064946 | TP53.S1 | 0.66 | (0.31-1.39) | 0.2909 | 0.9969 |
| | rs12602273 | TP53.S2 | 0.68 | (0.32-1.45) | 0.3409 | 0.9991 |
| | rs1042522 | TP53.S3 | 0.73 | (0.38-1.39) | 0.3566 | 0.9994 |
| | rs12951053 | TP53.S4 | 0.90 | (0.45-1.81) | 0.7748 | 1.0000 |
| *TGFβ1* | rs1800469 | TGFB1.S1 | 1.16 | (0.57-2.35) | 0.7058 | 1.0000 |
| | rs1800470 | TGFB1.S2 | 1.12 | (0.54-2.29) | 0.7741 | 1.0000 |
| | rs2241716 | TGFB1.S3 | 0.72 | (0.33-1.57) | 0.4258 | 0.9999 |
| | rs4803455 | TGFB1.S4 | 0.99 | (0.51-1.92) | 0.9837 | 1.0000 |
| | rs11466345 | TGFB1.S5 | 1.99 | (0.95-4.18) | 0.0744 | 0.7449 |
| | rs12983047 | TGFB1.S6 | 1.75 | (0.89-3.44) | 0.1139 | 0.8727 |
| *XRCC1* | rs3213282 | XRCC1.S1 | 1.19 | (0.53-2.65) | 0.6975 | 0.9899 |
| | rs12611088 | XRCC1.S2 | 0.59 | (0.25-1.36) | 0.2345 | 0.6137 |
| | rs1001581 | XRCC1.S3 | 0.67 | (0.32-1.39) | 0.2900 | 0.7165 |
| | rs3213344 | XRCC1.S4 | 1.34 | (0.64-2.82) | 0.4430 | 0.8889 |
| | rs1799782 | XRCC1.S5 | 1.40 | (0.67-2.94) | 0.3833 | 0.8289 |
| | rs25487 | XRCC1.S6 | 0.80 | (0.36-1.79) | 0.6099 | 0.9705 |
| *XRCC3* | rs1799794 | XRCC3.S1 | 0.65 | (0.32-1.31) | 0.2408 | 0.5839 |
| | rs861530 | XRCC3.S2 | 1.08 | (0.55-2.13) | 0.8371 | 0.9992 |
| | rs3212090 | XRCC3.S3 | 0.68 | (0.33-1.39) | 0.2959 | 0.6733 |
| | rs12432907 | XRCC3.S4 | 0.82 | (0.42-1.62) | 0.5821 | 0.9502 |
| | rs861539 | XRCC3.S5 | 3.88 | (1.25-12.07) | 0.0116 | 0.0632 |
| | rs861544 | XRCC3.S6 | 0.94 | (0.43-2.05) | 0.8795 | 0.9999 |

**Abbreviation**: SNP = single nucleotide polymorphism; OR = Odd ratio; CI = Confidence interval; $P_{asym}$ = asymptotic P value; $P_{emp}$ = empirical P value.
OR is calculated using major allele (A1) as reference. Refer to Table 3.12 for the major allele of each SNP.

#### 3.4.3.3 Haplotype analysis

Controls and cases were examined together to construct a LD map of each gene. LD plots of *ATM*, *SOD2*, *TGFβ1*, *TP53*, *XRCC1*, and *XRCC3* were constructed by Haploview and are shown in Figure 3.7-3.12. LD was expressed as $r^2$. LD blocks were constructed using SSLD algorithm (Section 2.3.4). One haplotype block was constructed for *ATM*, *SOD2*, *TP53*, *XRCC1* and *XRCC3*. The haplotype blocks of *ATM*, *SOD2*, *TP53*, *XRCC1* and *XRCC3* spanned 123 kb, 13 kb, 11 kb, 17 kb and 17 kb, respectively. Two 8-kb haplotype blocks were constructed for *TGFβ1*.

Haplotypes of all sizes were generated by PLINK (Section 2.3.4) and the results are summarised in Table 3.14. Six sliding windows were generated for *SOD2*. For *ATM* and *TP53*, 10 sliding windows were generated for each gene. Twenty-one sliding windows were generated for *TGFβ1*, *XRCC1*, and *XRCC3*. In total, 89 haplotype windows were generated for six candidate genes. The 2-SNP haplotype window (XRCC3.S5-S6), 4-SNP haplotype window (XRCC3.S1-S4), and 6-SNP haplotype window (XRCC3.S1-S6) from *XRCC3* showed significant association before multiple testing correction (Omnibus test $P_{asym}<0.05$). However, significant level was lost after 10,000 permutations. No significant difference was found in all sizes of haplotype windows for all candidate genes between controls and cases (Omnibus test $P_{emp}>0.05$).

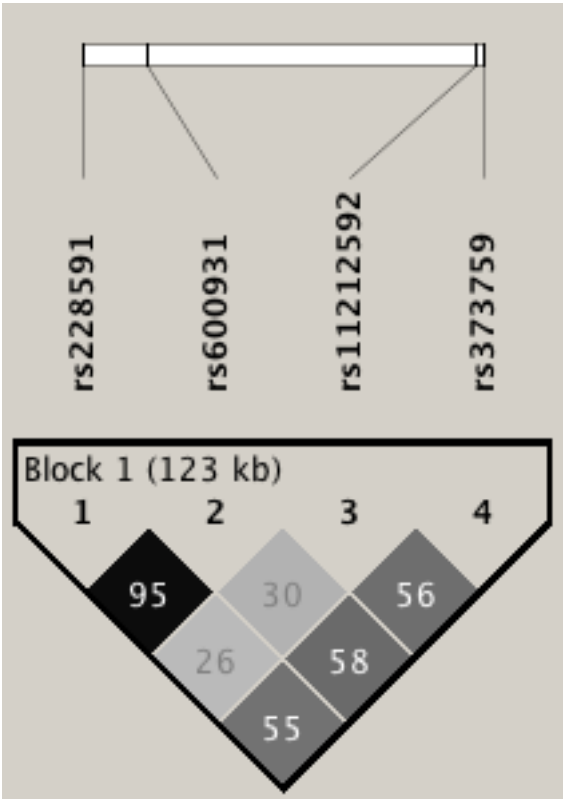


Figure 3.7: LD plot of *ATM* gene in NPC patients (chronic neck fibrosis). LD plot is constructed by Haploview using the solid spine of LD algorithm. LD is expressed as $r^2$. One haplotype block is identified.

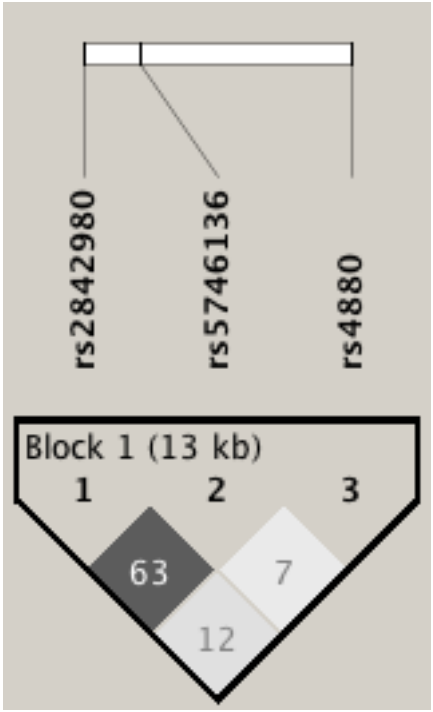


Figure 3.8: LD plot of *SOD2* gene in NPC patients (chronic neck fibrosis). LD plot is constructed by Haploview using the solid spine of LD algorithm. LD is expressed as $r^2$. One haplotype block is identified.

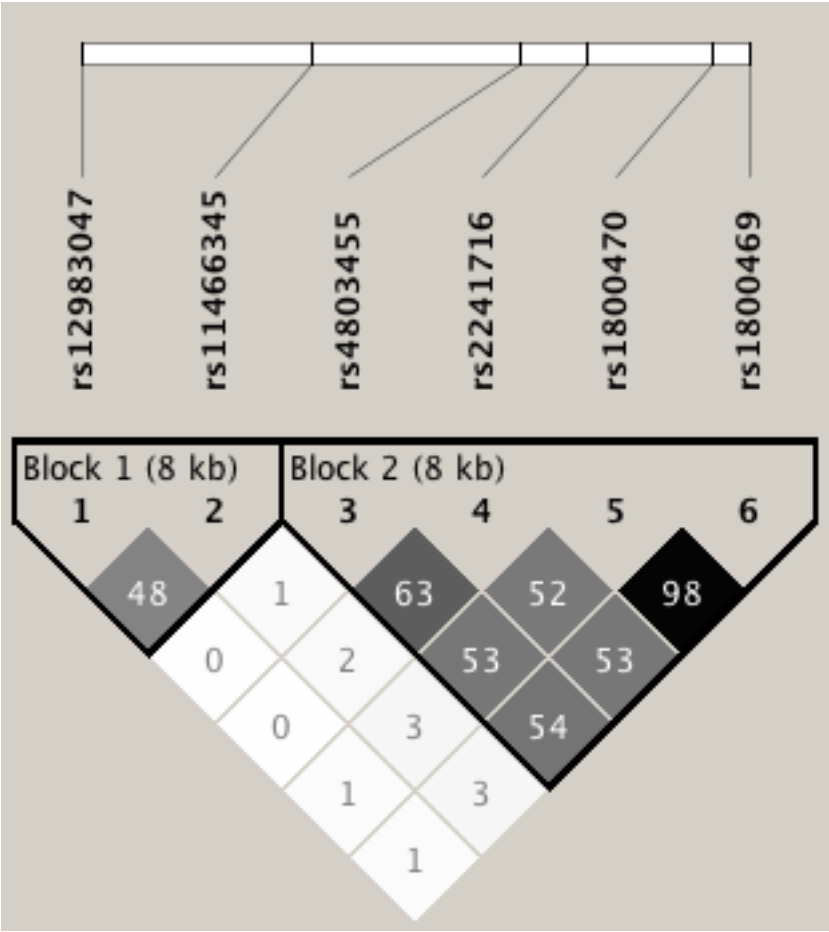


Figure 3.9: LD plot of *TGFβ1* gene in NPC patients (chronic neck fibrosis). LD plot is constructed by Haploview using the solid spine of LD algorithm. LD is expressed as $r^2$. Two haplotype blocks are identified.

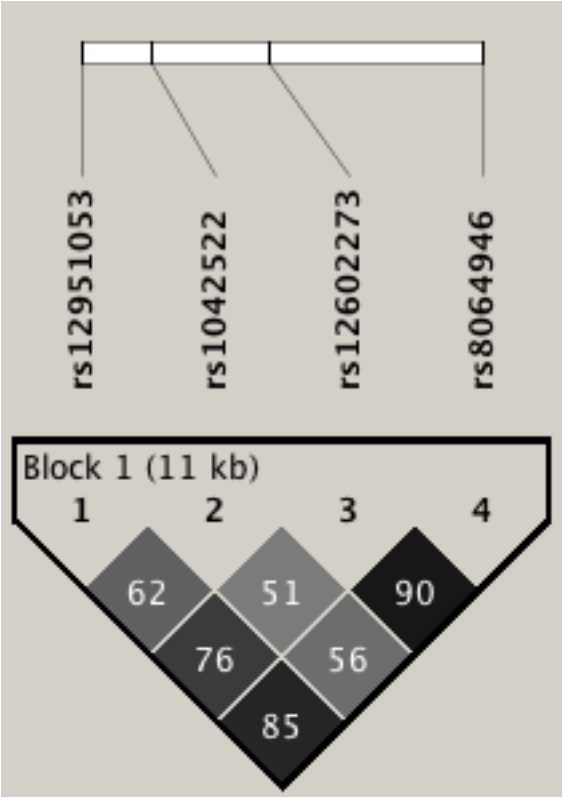


Figure 3.10: LD plot of *TP53* gene in NPC patients (chronic neck fibrosis). LD plot is constructed by Haploview using the solid spine of LD algorithm. LD is expressed as $r^2$. One haplotype block is identified.

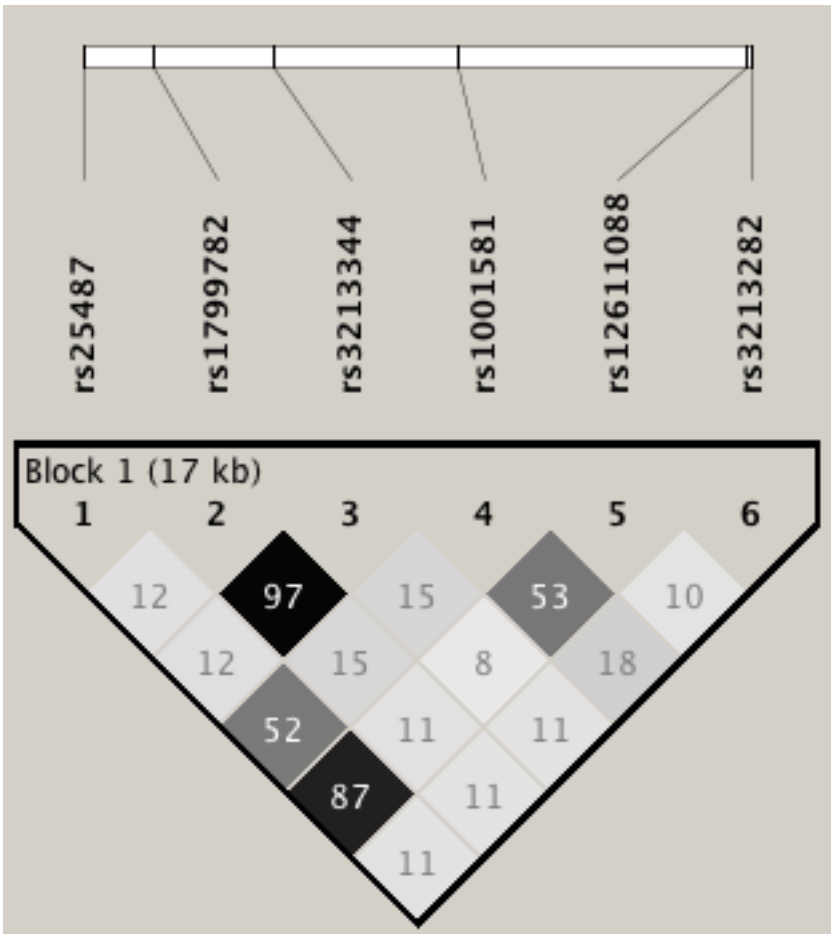


Figure 3.11: LD plot of *XRCC1* gene in NPC patients (chronic neck fibrosis). LD plot is constructed by Haploview using the solid spine of LD algorithm. LD is expressed as $r^2$. One haplotype block is identified.

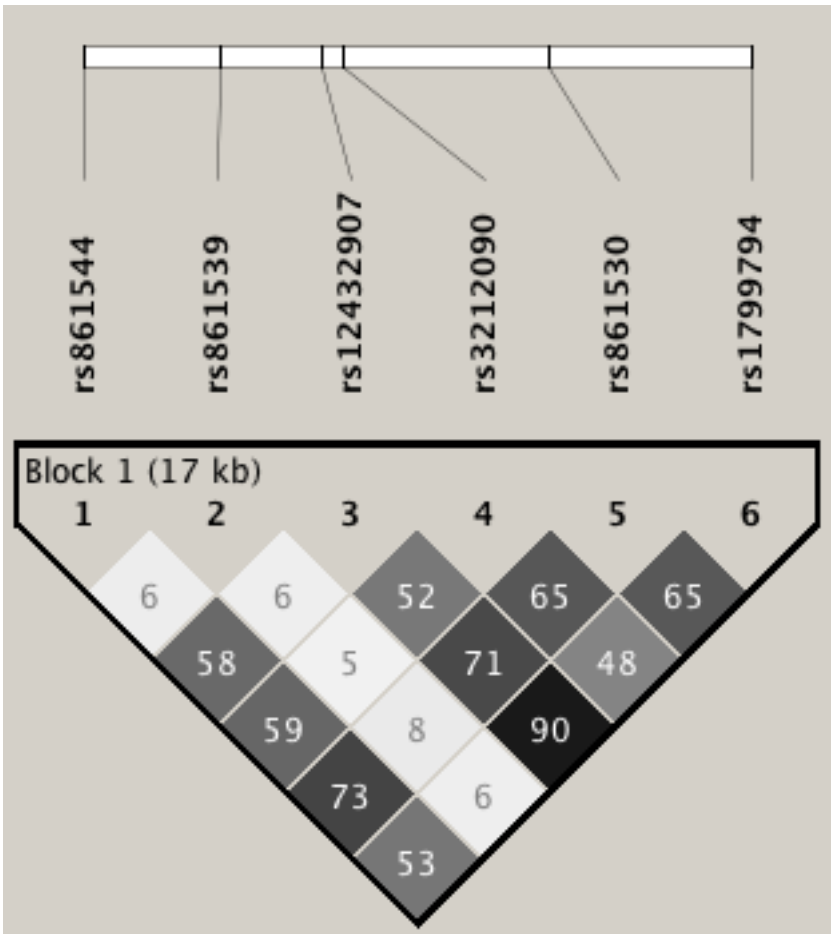


Figure 3.12: LD plot of *XRCC3* gene in NPC patients (chronic neck fibrosis). LD plot is constructed by Haploview using the solid spine of LD algorithm. LD is expressed as $r^2$. One haplotype block is identified.

Table 3.14: Summary of sliding-window haplotype analysis based on omnibus test for chronic neck fibrosis

| | | | SW | The most significant omnibus test | | |
|---|---|---|---|---|---|---|
| Gene | NSNP | First SW | Last SW | SW | $P_{asym}$ | $P_{emp}$ |
| *ATM* | 2 | ATM.S1..ATM.S2 | ATM.S3..ATM.S4 | ATM.S2..ATM.S3 | 0.0939 | 0.3137 |
| | 3 | ATM.S1..ATM.S3 | ATM.S2..ATM.S4 | ATM.S1..ATM.S3 | 0.0958 | 0.3277 |
| | 4 | ATM.S1..ATM.S4 | ATM.S1..ATM.S4 | ATM.S1..ATM.S4 | 0.1486 | 0.4747 |
| *SOD2* | 2 | SOD2.S1..SOD2.S2 | SOD2.S2..SOD2.S3 | SOD2.S1..SOD2.S2 | 0.4479 | 0.7562 |
| | 3 | SOD2.S1..SOD2.S3 | SOD2.S1..SOD2.S3 | SOD2.S1..SOD2.S3 | 0.4648 | 0.8596 |
| *TGFβ1* | 2 | TGFB1.S1..TGFB1.S2 | TGFB1.S5..TGFB1.S6 | TGFB1.S5..TGFB1.S6 | 0.1356 | 0.5892 |
| | 3 | TGFB1.S1..TGFB1.S3 | TGFB1.S4..TGFB1.S6 | TGFB1.S4..TGFB1.S6 | 0.1201 | 0.7381 |
| | 4 | TGFB1.S1..TGFB1.S4 | TGFB1.S3..TGFB1.S6 | TGFB1.S2..TGFB1.S5 | 0.1424 | 0.9306 |
| | 5 | TGFB1.S1..TGFB1.S5 | TGFB1.S2..TGFB1.S6 | TGFB1.S1..TGFB1.S5 | 0.0827 | 0.8519 |
| | 6 | TGFB1.S1..TGFB1.S6 | TGFB1.S1..TGFB1.S6 | TGFB1.S1..TGFB1.S6 | 0.2331 | 0.9640 |
| *TP53* | 2 | TP53.S1..TP53.S2 | TP53.S3..TP53.S4 | TP53.S1..TP53.S2 | 0.4194 | 0.8629 |
| | 3 | TP53.S1..TP53.S3 | TP53.S2..TP53.S4 | TP53.S2..TP53.S4 | 0.4512 | 0.8133 |
| | 4 | TP53.S1..TP53.S4 | TP53.S1..TP53.S4 | TP53.S1..TP53.S4 | 0.2669 | 0.7161 |
| *XRCC1* | 2 | XRCC1.S1..XRCC1.S2 | XRCC1.S5..XRCC1.S6 | XRCC1.S4..XRCC1.S5 | 0.4500 | 0.9159 |
| | 3 | XRCC1.S1..XRCC1.S3 | XRCC1.S4..XRCC1.S6 | XRCC1.S2..XRCC1.S4 | 0.2924 | 0.8450 |
| | 4 | XRCC1.S1..XRCC1.S4 | XRCC1.S3..XRCC1.S6 | XRCC1.S2..XRCC1.S5 | 0.2925 | 0.8450 |
| | 5 | XRCC1.S1..XRCC1.S5 | XRCC1.S2..XRCC1.S6 | XRCC1.S2..XRCC1.S6 | 0.0877 | 0.5960 |
| | 6 | XRCC1.S1..XRCC1.S6 | XRCC1.S1..XRCC1.S6 | XRCC1.S1..XRCC1.S6 | 0.2633 | 0.8891 |
| *XRCC3* | 2 | XRCC3.S1..XRCC3.S2 | XRCC3.S5..XRCC3.S6 | XRCC3.S5..XRCC3.S6 | 0.0147 | 0.1944 |
| | 3 | XRCC3.S1..XRCC3.S3 | XRCC3.S4..XRCC3.S6 | XRCC3.S1..XRCC3.S3 | 0.0561 | 0.3531 |
| | 4 | XRCC3.S1..XRCC3.S4 | XRCC3.S3..XRCC3.S6 | XRCC3.S1..XRCC3.S4 | 0.0301 | 0.3231 |
| | 5 | XRCC3.S1..XRCC3.S5 | XRCC3.S2..XRCC3.S6 | XRCC3.S2..XRCC3.S6 | 0.1132 | 0.6833 |
| | 6 | XRCC3.S1..XRCC3.S6 | XRCC3.S1..XRCC3.S6 | XRCC3.S1..XRCC3.S6 | 0.0339 | 0.4571 |

**Abbreviation**: SW = Sliding window; NSNP = number of SNPs in this haplotype window; $P_{asym}$ = asymptotic P value; $P_{emp}$ = empirical P value.

The SW is indicated as GENE.Sx...GENE.Sy, where GENE is the name of candidate gene, Sx is the first SNP and Sy is the last SNP of the SW. For example, TP53.S1..TP53.S3 represents the sliding window TP53.S1-S2-S3 (rs8064946-rs12602273-rs1042522) of *TP53* gene. Please refer to Table 3.1 for SNP identity.

## 3.5 Discussion

Normal tissue complications, regardless of severity, affect all cancer patients receiving RT as cancer treatment. As a result, individual customisation of cancer treatment to improve treatment prognosis and quality of life can be achieved by understanding the underlying mechanism that leads to individual variations in normal tissue radiosensitivity. Extreme hypersensitivity in genetic disorders, such as ataxia telangiectasia or Fanconi's anaemia, is caused by rare truncated proteins. However, unlike Mendelian diseases, variation in normal tissue sensitivity is a phenomenon of complex traits rather than rare functional mutants. Common variants may also have important roles in the development of severe radiation sensitivity. In order to obtain more comprehensive information about the role of common genetic variants in the development of severe radiation-induced complications, functional SNPs and tag SNPs were selected from six candidate genes. Candidate-gene selection was based on published functional variants with positive association in various types of radiation-induced complications in cancer patients. Selected candidate genes, *ATM*, *SOD2*, *TGFβ1*, *TP53*, *XRCC1* and *XRCC3* are involved in DNA repair and cell-cycle regulation pathways.

As mentioned previously, ATM mutant is the cause of hypersensitivity to radiation in the genetic disorder ataxia telangiectasia. As a result, it was hypothesised that common genetic variants in *ATM* may contribute to individual variations in radiation susceptibility. *SOD2* is involved in removing ROS generated during radiation-induced damage while *XRCC1* and *XRCC3* repair DNA damage. Tumour suppressor p53 is encoded by *TP53*, which controls cell fate so that apoptotis is induced when damage is beyond repair. Besides common variants, previously reported functional SNPs, including rs4880 (Val16Ala) from *SOD2*, rs1042522 (Arg72Pro) from *TP53*, rs1800470 (Leu10Pro) from *TGFβ1*, rs1799782

(Arg194Trp) and rs25487 (Arg399Gln) from *XRCC1*, and rs861539 (Thr241Met) from *XRCC3* were genotyped to investigate the association of radiation-induced toxicities in Chinese NPC patients in this study. Significant association between radiation-induced complications and rs1801516 (Asp1853Asn), a functional genetic variant from *ATM*, has also been reported. However, due to a low MAF (<0.1), this SNP was not examined in this study.

Single-marker analysis and haplotype analysis of all possible sizes were performed to study the risk effect. None of the tag SNPs from *ATM*, *SOD2* and *XRCC1* showed significant association to any radiation-induced complications in single-marker or haplotype analyses. Three SNPs (rs8064946 and rs12602273 in *TP53*, and rs861539 in *XRCC3*) showed significant association to acute mucositis ($P_{asym}$ <0.05). One of the three SNPs (rs861539 in *XRCC3*) also showed significant association to chronic neck fibrosis ($P_{asym}$<0.05). Haplotype analyses showed significant association of acute skin reactions and haplotype of *TGFβ1* ($P_{asym}$<0.05). Significant association between acute mucositis and chronic neck fibrosis and haplotypes of *XRCC3* were also demonstrated ($P_{asym}$<0.05). Permutation was performed to mitigate the occurrence of false positive findings arising from random chance and multiple comparisons. None of these significant associations survived after multiple testing correction ($P_{emp}$>0.05).

Association of significant results failed to be replicated owing to between-study variations and small sample size. For instance, *XRCC1* is one of the genetic predispositions in breast cancer development (Moullan et al., 2003). Severe radiation-induced side effects were significantly higher in breast cancers with genetic variant rs25487 from *XRCC1* due to reduced level of repair ability (Moullan et al., 2003; Sterpone et al., 2010). In contrast, studies investigated the same *XRCC1* variant with relatively larger cohorts reported no significant association (Chang-Claude

et al., 2009; Popanda et al., 2009; Suga et al., 2007). Genetic variant rs1801516 from *ATM* was associated with increased risk of subcutaneous fibrosis in breast cancer patients. However, this association was not replicated by the same research group (Andreassen et al., 2006a,b). In addition, conflicting results have been reported with some studies demonstrating protective effect and risk effect of the same allele of the same SNP (Andreassen and Alsner, 2009). Despite the between-study variations such as selected cancer types, methodologies, candidate-gene selection, and allele frequencies in different ethnic groups, our results were in line with recently published replication and validation studies with large cohorts using similar classification criteria for controls and cases (Barnett et al., 2012a; Chang-Claude et al., 2009; Popanda et al., 2009; Talbot et al., 2012). The combined evidences suggested that the major limitation of this study, as well as other published studies, is the small sample size with lack of statistical power to detect SNPs with small to modest effects. Moreover, the number of candidate genes selected in this study may not be enough to investigate the complex phenomenon of radiation-induced complications. Although this study has higher coverage of candidate genes compared to most of the published studies, causal variants may not be captured by genotyped tag SNPs, particularly rare variants with MAF$<$0.1. Future studies should be performed in much larger cohorts to reduce the possibility of false positive and false negative findings. Studies with a larger cohort also enhance the characterisation of genetic profiles by comparing patients with different levels of radiation toxicities through subgroup analysis.

Alternatively, sample size limitation can be overcome by pooling data from studies with similar experimental settings through meta-analysis. Association of late skin toxicities and genetic variant rs1800469, located at the promoter region of *TGF$\beta$1*, was investigated in a recently published meta-analysis (Barnett et al., 2012b). Eleven cohorts with over two thousand breast cancers were included. Detailed

clinical information from each cohort was used as covariates. No significant association was reported in this meta-analysis as well as results from our group. It is unlikely that severity of radiation-induced skin reaction is contributed by a single genetic variant. On the other hand, radiation-induced mucositis is specific to head and neck cancer patients during RT. In the next chapter, a meta-analysis was performed to confirm association of genetic variants from *XRCC1* and *XRCC3*, regardless of significant or non-significant findings, reported by other research groups.

## 3.6 Conclusion

In this study, association of radiation-induced complications in six candidate genes was investigated. None of the candidate genes was found to be associated with any radiation-induced complications in Chinese NPC patients. Tag SNPs may not be ideal universal biomarkers in predicting individual general risk of radiation-induced toxicities. Future studies including more candidate genes with larger sample size are needed to further investigate the role of genetic variants in radiation-induced complications.

# Part II

# Meta-analysis

# Chapter 4

# Meta-analysis

## 4.1 Aims

The aims of this part were to identify genetic association studies that focused on radiation-induced acute mucositis in head and neck cancer patients from existing literature and to perform a meta-analysis.

## 4.2 Introduction

Dermatitis and mucositis are common acute complications induced by RT in head and neck cancer patients. Unlike dermatitis, which may occur in any type of cancers that requiring RT as treatment, mucositis is a type of tissue-specific toxicity that is mainly induced by RT in head and neck cancer patients. Incidence of radiation-induced mucositis is around 80-100% in head and neck cancer patients (Logan, 2009). If chemotherapy is used concurrently with RT, the prevalence of grade 3 mucositis in head and neck cancer patients may reach up to 50% (Logan, 2009). Development of radiation-induced ulcerative mucositis may lead

to hospitalisation, use of tube feeding, and affect cancer treatment efficacy due to treatment postponement or termination. Age, body weight, gender, genetic factors, and underlying health issues are considered as possible risk factors in the development of radiation-induced mucositis (Sonis, 2009). Among these risk factors, genetic association studies investigating the role of SNPs and individual normal tissue radiation sensitivity have been increasing. However, the majority of published studies mainly focused on breast and prostate cancers in Caucasians (Andreassen and Alsner, 2009; Lee et al., 2012). Recent systematic review identified 7 studies performed in head and neck cancer patients and assessed various clinical endpoints (Ghazali et al., 2012). Association of genetic variants in *XRCC1* and radiation-induced mucositis has been recently reported in Chinese NPC patients (Li et al., 2013). As mentioned before, *XRCC1* and *XRCC3* are genes involved in DNA repair. Changes in functional variants, such as missense mutations, may affect individual normal tissue susceptibility to radiation. The sample size in most published studies using candidate-gene approach is small and hence the studies are under-powered. Since mucositis is a type of tissue-specific toxicity in head and neck cancer patients, a meta-analysis was performed to investigate the association of SNPs in *XRCC1* and *XRCC3* and radiation-induced mucositis in head and neck cancer patients. Existing literature and local studies performed in Chinese population were identified through three databases. Genotype data of these studies, including data in this project, were analysed.

## 4.3 Methods

### 4.3.1 Phenotype definition

Patients with mucositis of grade 0-1 during RT was classified as controls. Patients with mucositis grade 2 or above during RT was classified as cases. Patient classifi-

cation was based on any three commonly used systems, including CTCAE, acute radiation morbidity scoring criteria by RTOG, and WHO handbook for reporting results of cancer treatment.

### 4.3.2 Search strategy

Three databases were chosen for comprehensive search of published literature. These databases included PubMed, Scopus and a Chinese database called China National Knowledge Infrastructure (CNKI) to locate local studies in Chinese population. Three sets of predefined keywords were used in searching literature. The first set of keywords included reference SNP ID numbers (rs numbers) from *XRCC1* and *XRCC3*. The second set of keywords included words related to radiation toxicities, types of head and neck cancers, and genetic variants. The third set of keywords included gene name, words related to radiation toxicities, and types of head and neck cancers. Due to the sensitivity of different databases, all three sets of keywords were used in PubMed and Scopus, and only the first set of keywords was used in CNKI to perform literature search. Comprehensive search of published literatures was performed in Mar 2013. Articles published before Jan 1997 were excluded owing to limited electronic availability. A summary of keywords is listed in Table 4.1. Manual screening was performed to identify any potential eligible studies from the cited references of retrieved articles.

Table 4.1: Keywords used in literature search

| | Keywords | Databases |
|---|---|---|
| Set 1 | rs3213282 OR rs12611088 OR rs1001581 OR rs3213344 OR rs1799782 OR rs25487 OR rs1799794 OR rs861530 or rs3212090 OR rs861539 OR rs861544 | CNKI, PubMed and Scopus |
| Set 2 | (Radiotherapy OR radiation OR radiation therapy OR irradiation OR radiation-induced OR radiosensitivit* OR hypersensitivit* OR radiotoxicit*) AND (head and neck OR HNC OR NPC OR nasopharyngeal OR nasopharynx OR esophageal OR esophagus OR Oral OR oral cavity OR oropharynx OR oropharyngeal OR hypopharynx OR hypopharyngeal OR larynx OR laryngeal OR throat OR nasal cavity OR paranasal sinus OR trachea OR tracheal OR tongue OR tonsil OR thyroid OR salivary glands) AND (Cancer OR carcinoma) AND (Polymorphism* OR SNP OR SNPs OR variant* OR variation* OR mutation* OR predictor* OR determinant* OR allele* OR haplotype*) AND (Response* OR reaction* OR side effect* OR complication* OR toxicit* OR mucositis OR injur*) | PubMed, Scopus |
| Set 3 | (XRCC1 OR XRCC3) AND (Radiotherapy OR radiation OR radiation therapy OR irradiation OR radiation-induced OR radiosensitivit* OR hypersensitivit* OR radiotoxicit*) AND (head and neck OR HNC OR NPC OR nasopharyngeal OR nasopharynx OR esophageal OR esophagus OR oral OR oral cavity OR oropharynx OR oropharyngeal OR hypopharynx OR hypopharyngeal OR larynx OR laryngeal OR throat OR nasal cavity OR paranasal sinus OR trachea OR tracheal OR tongue OR tonsil OR thyroid OR salivary glands) AND (Cancer OR carcinoma) | PubMed, Scopus |

### 4.3.3 Study selection

Two reviewers (Cheuk I and Tian F) performed literature search from three databases. Articles retrieved from three databases were examined independently by these two reviewers. Duplicates were removed after all retrieved articles were merged. Preliminary screening was performed based on title and abstract of the remaining articles. Full-text articles were retrieved for all potential eligible studies and assessed for compliance with the predefined inclusion and exclusion criteria. Eligible studies must be prospective, cross-sectional, or retrospective case-control genetic association studies or abstracts that included head and neck cancer patients with sufficient polymorphism data from *XRCC1* and *XRCC3*. Additional data or information required for data analysis was requested from potentially eligible studies. Abstracts without sufficient information, meta-analysis and review articles were excluded. The detailed inclusion and exclusion criteria are listed in Table 4.2. Results of two reviewers were compared to investigate any discrepancy. Disagreement between two reviewers was resolved by a third reviewer (Wu V) if the two reviewers could not reach a consensus.

Table 4.2: Detailed inclusion/exclusion criteria of eligible studies

| | Inclusions | Exclusions |
|---|---|---|
| Participants | Head and neck cancers<br>• oral cavity<br>• nasopharynx<br>• pharynx<br>• larynx<br>• nasal cavity<br>• paranasal sinuses<br>• trachea<br>• tongue<br>• tonsil<br>• thyroid<br>• salivary glands<br>• cervical esophagus | Diseases other than head and neck cancers, and esophageal cancer<br>No previous history of radiation treatment and/or surgery and/or chemotherapy |
| Types of Studies | Case-control studies<br>• Prospective<br>• Cross-sectional<br>• Retrospective<br>Human studies<br>Genetic association studies | Study without control sample<br>Studies with overlapping data<br>Animal study and studies using cell lines |
| Types of information | Abstracts or unpublished work with sufficient information<br>Original research articles<br>Abstracts or unpublished works without sufficient information | Review<br>Meta-analysis |
| Outcomes to be measured | *XRCC1* and/or *XRCC3* polymorphism data<br>• Allelic count<br>• Genotypic count<br>• Odd ratio | Non-XRCC1/XRCC3 polymorphism data |
| Period covered | Jan 1997 to Mar 2013 | Before Jan 1997 |

### 4.3.4 Data abstraction

Standardised data abstraction form was used to record relevant data from all eligible studies. Data abstraction form contained the following fields: last name of first author, publication year, country of origin, ethnicity of the study population, cancer type, study design, treatment, genotyping method, grading system used to assess acute radiation-induced toxicities, control and case classifications, total number of controls and cases, covariates, and genotype distribution. Exact test was used to test for any deviation of HWE in controls in all eligible studies.

### 4.3.5 Statistical analysis

Meta-analysis was performed using the software RevMan (version 5.2; `http://ims.cochrane.org/revman`). $I^2$ statistics was used to determine statistical heterogeneity between studies. $I^2$ statistics is defined as the percentage of between-study variations contributed by statistical heterogeneity instead of chance based on degree of freedom (df) and chi-square statistics (Q) (Higgins and Green, 2011):

$$I^2 = (Q\text{-}df)/Q \times 100\%$$

$I^2$ statistics was interpreted according to guidelines established by the Cochrane collaboration (Higgins and Green, 2011). Heterogeneity between studies might not be important if $I^2$ <40%; $I^2$ of 30% to 60% indicates moderate heterogeneity was present between studies; $I^2$ of 50% to 90% indicates substantial heterogeneity present between studies; and $I^2$ of 75% to 100% indicates considerable heterogeneity between studies. Either fixed-effect or random-effect models was used to estimate odd ratios (ORs) and 95% confidence intervals (CI) for each study. Model selection was based on $I^2$: fixed-effect model if $I^2 \leq$40% and random-effect model

if $I^2$ >40%. The Mantel-Haenszel (M-H) method was the default method to calculate weighted ORs of dichotomous outcome in both fixed-effect and random-effect models in RevMan. Since the mechanism of normal tissue toxicities induced by SNPs is unknown, ORs and 95% CIs were calculated based on dominant model, recessive model, and allelic model for each study and across all populations under study.

## 4.4 Results

### 4.4.1 Study selection

After literature search, 312 articles were retrieved from the three databases. One additional article was identified through another source. All retrieved articles were screened for duplication and 79 duplicates were excluded. Abstract and titles of the remaining 234 articles were screened. Four potentially eligible articles were identified and full text were retrieved to assess eligibility. Based on the inclusion and exclusion criteria, one study was excluded. Authors of the remaining studies were contacted to request additional information if not provided in the full-text articles. One study was further excluded because of insufficient data. In total, two published studies, in addition to genotype data from this project, were included in the meta-analysis (Li et al., 2013; Pratesi et al., 2011). The workflow of literature search is summarised in Figure 4.1.

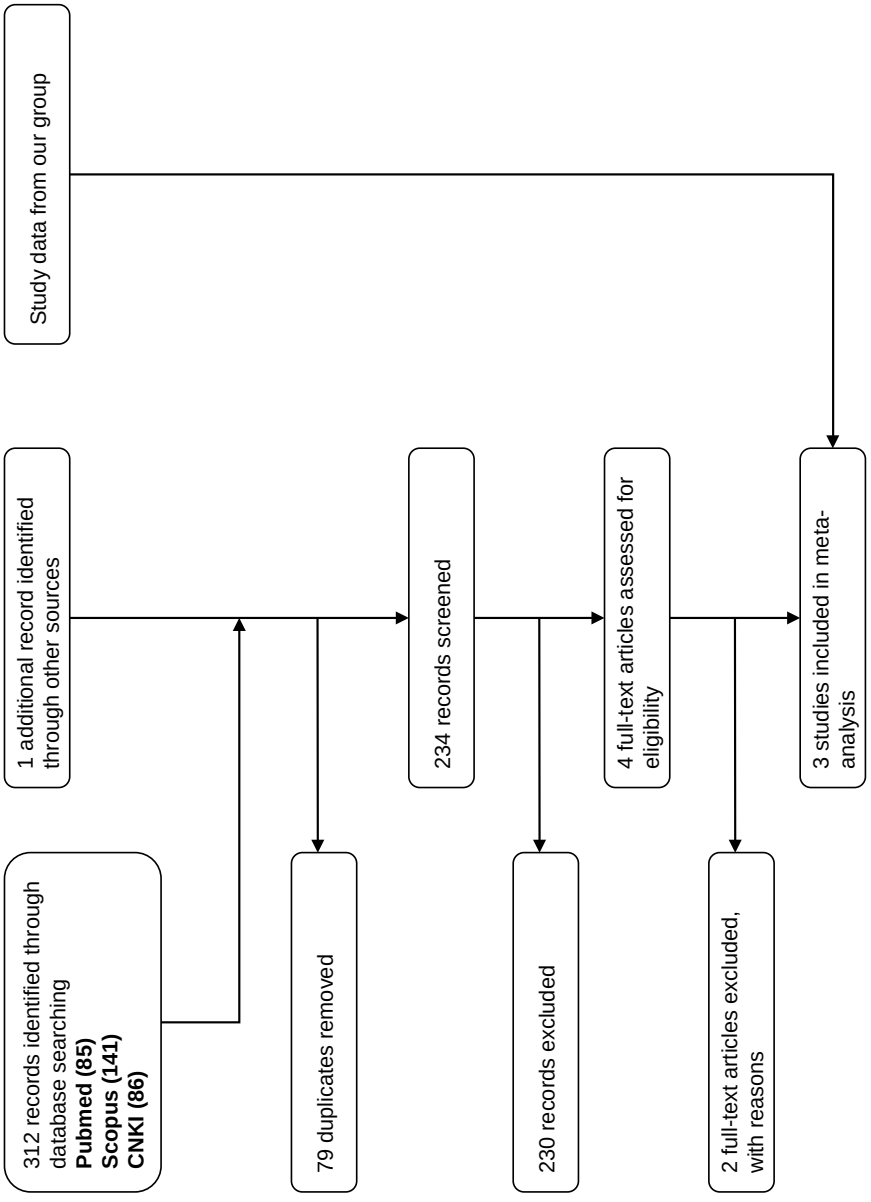


Figure 4.1: The workflow of literature search.

### 4.4.2 Study characteristics

Data from two eligible studies and data from this project were further evaluated. All studies were case-control studies. The total number of patients in these three studies was 332. Two studies included only Chinese NPC patients and the third study included Italian patients with head and neck cancer. To assess severity of radiation-induced mucositis, two studies used CTCAE and one study used acute radiation morbidity scoring criteria by RTOG. One study classified controls as patients with grade 0-2 radiation-induced mucositis while the other two studies classified controls as patients with grade 0-1 radiation-induced mucositis. Genotype distribution was obtained from these studies for outcome measure reclassification. Three functional variants, Arg194Trp (rs1799782), Gln399Arg (rs25487), and Thr241Met (rs861539) were investigated in at least two studies. Two SNPs (rs1799782 and rs25487) were located in *XRCC1*, and rs861539 was located in *XRCC3*. Data were extracted for further analysis. Study characteristics are summarised in Table 4.3.

Table 4.3: Characteristics of included studies

| **First author** | Cheuk | Li | Pratesi |
|---|---|---|---|
| **Year of Publication** | / | 2013 | 2011 |
| **Origin** | HKSAR | China | Italy |
| **Study Design** | Case-control | Case-control | Case-control |
| **Cancer type** | NPC | NPC | Head and neck cancers |
| **Control Classification** | Grade 0-1 | Grade 0-2 | Grade 0-1 |
| **Case Classification** | Grade 2 or above | Grade 3 or above | Grade 2 or above |
| **XRCC1 SNPs** | rs3213282, rs12611088, rs1001581, rs3213344, rs1799782, rs25487 | rs1799782, rs25487* | rs25487* |
| **XRCC3 SNPs** | rs1799794, rs861530, rs3212090, rs861539, rs861544 | / | rs861539 |
| **Treatment method** | RT/CRT | RT/CRT | RT/CRT |
| **Period of recruitment** | May 2010 - Sep 2011 | Nov 2009 - Dec 2010 | Jun 2009 - Sep 2010 |
| **Genotyping method** | RFLP, UPr | RFLP | UPr |
| **Covariates listed (if any)** | Age, sex, RT method, chemotherapy, stage | Age, sex, smoking, alcohol drinking, BMI, stage, RT method, dose | Chemotherapy, BED |
| **Sample size** | Total : 117<br>Control:40<br>Case: 77 | Total : 114<br>Control: 66<br>Case: 48 | Total : 101<br>Control: 33<br>Case: 68 |

**Abbreviation**: HKSAR = Hong Kong Special Administrative Region; RT = Radiotherapy; CRT = Concurrent chemotherapy and radiotherapy; RFLP = Restriction fragment length polymorphism; UPr = Unlabelled Probe Melting Analysis.
* Significant association with radiation-induced mucositis was reported.

### 4.4.3 Data analysis

Controls and cases were reclassified for one study based on genotype data and clinical characterisitics obtained from Li *et al.* Distribution of allele counts in controls and cases are shown in Table 4.4. Assessment of risk of bias was not performed due to the limited number of studies included. All the three functional SNPs were tested for deviation from HWE. Both rs1799782 and rs861539 were in HWE in all included studies. Deviation of HWE was found in rs25487 in one study. ORs for the combined population were obtained for all SNPs. Subgroup analysis was performed for rs25487 for Chinese populations from the two studies.

Table 4.4: Distribution of alleles in controls and cases after reclassification in three studies

| Study and functional SNP of interest | HWE in Controls ($P$>0.01) | Control (Grade 0-1) | | | Case (Grade 2 or above) | | |
|---|---|---|---|---|---|---|---|
| rs1799782 (XRCC1 c.580C>T p.Arg194Trp) | | 1 (C) | 2 (T) | Total | 1 (C) | 2 (T) | Total |
| Cheuk 2013 | Yes | 59 | 21 | 80 | 112 | 42 | 154 |
| Li 2013 | Yes | 32 | 16 | 48 | 130 | 50 | 180 |
| Total allele counts | | 91 | 37 | 128 | 242 | 92 | 334 |
| rs25487 (XRCC1 c.1196 A>G p.Gln399Arg) | | 1 ( G ) | 2 ( A ) | Total | 1 ( G ) | 2 ( A ) | Total |
| Cheuk 2013 | Yes | 59 | 21 | 80 | 115 | 39 | 154 |
| Li 2013 | Yes | 37 | 11 | 48 | 131 | 49 | 180 |
| Pratesi 2011 | No | 47 | 19 | 66 | 77 | 59 | 136 |
| Total allele counts | | 143 | 51 | 194 | 323 | 147 | 470 |
| rs861539 (XRCC3 c.722 C>T p.Thr241Met) | | 1 (C) | 2 (T) | Total | 1 (C) | 2 (T) | Total |
| Cheuk 2013 | Yes | 69 | 11 | 80 | 148 | 6 | 154 |
| Pratesi 2011 | Yes | 36 | 30 | 66 | 69 | 67 | 136 |
| Total allele counts | | 105 | 41 | 146 | 217 | 73 | 290 |

#### 4.4.3.1 Dominant model

$I^2$ was 0%, 0%, and 2% for rs1799782, rs25487, and rs861539 respectively. Fixed-effect model was used to obtain ORs for all three SNPs. Z score and OR of rs1799782 were 0.06 ($P$=0.95) and 1.04 (95% CI 0.34, 3.14). Z score and OR of rs25487 were 0.42 ($P$=0.67) and 0.85 (95% CI 0.40, 1.80). Z score and OR of rs861539 were 0.45 ($P$=0.65) and 1.22 (95% CI 0.51, 2.94). Forest plots of rs1799782 (Figure 4.2), rs25487 (Figure 4.3), and rs861539 (Figure 4.4) summarise the results of meta-analysis.

$I^2$ of rs25487 was 0% in the Asian subgroup analysis. As a result, a fixed-effect model was used to estimate OR. Forest plot of this subgroup is shown in Figure 4.5. Z score and OR of subgroup analysis were 0.41 ($P$=0.68) and 1.26 (95% CI 0.42, 3.78). Overall, there was no significant association for all SNPs in overall population analysis and subgroup analysis.

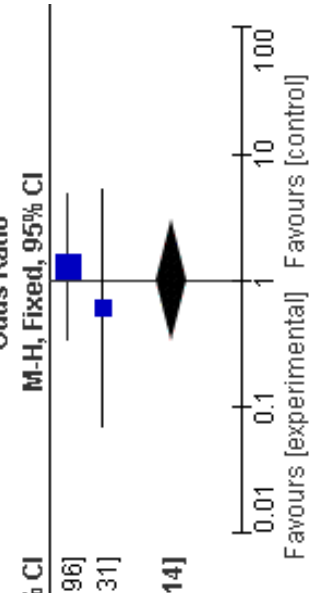


Figure 4.2: Forest plot of rs1799782 in the *XRCC1* gene under a dominant model.

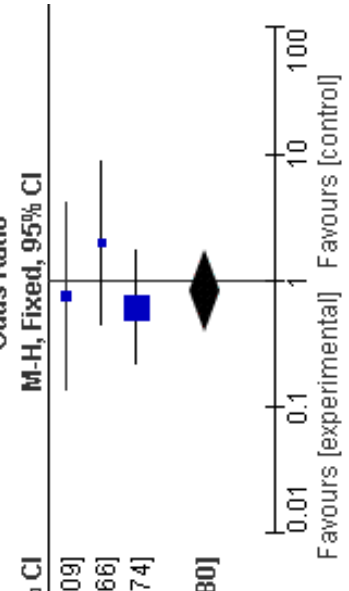


Figure 4.3: Forest plot of rs25487 in the *XRCC1* gene under a dominant model.

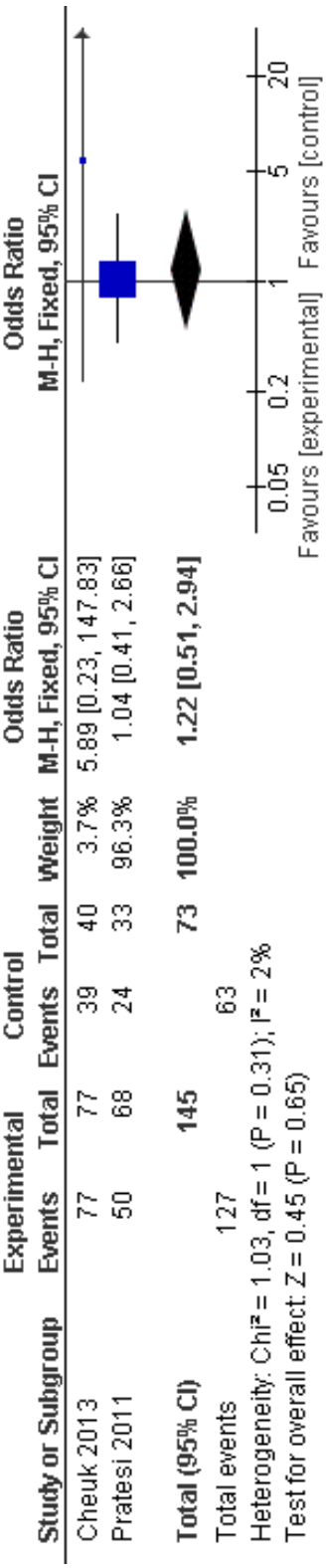


Figure 4.4: Forest plot of rs861539 in the *XRCC3* gene under a dominant model.

| Study or Subgroup | Experimental Events | Experimental Total | Control Events | Control Total | Weight | Odds Ratio M-H, Fixed, 95% CI |
|---|---|---|---|---|---|---|
| Cheuk 2013 | 72 | 77 | 38 | 40 | 59.5% | 0.76 [0.14, 4.09] |
| Li 2013 | 84 | 90 | 21 | 24 | 40.5% | 2.00 [0.46, 8.66] |
| Pratesi 2011 | 50 | 68 | 27 | 33 | 0.0% | 0.62 [0.22, 1.74] |
| **Total (95% CI)** | | **167** | | **64** | **100.0%** | **1.26 [0.42, 3.78]** |
| Total events | 156 | | 59 | | | |

Heterogeneity: Chi² = 0.73, df = 1 (P = 0.39); I² = 0%
Test for overall effect: Z = 0.41 (P = 0.68)

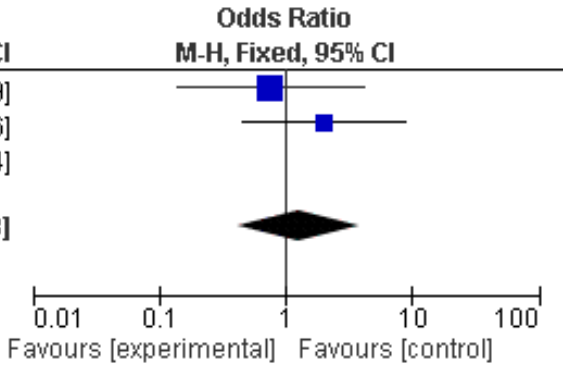


Figure 4.5: Forest plot of a subgroup analysis of rs25487 in the *XRCC1* gene under a dominant model.

#### 4.4.3.2 Recessive model

$I^2$ was 29%, 0%, and 85% for rs1799782, rs25487, and rs861539 respectively. Fixed-effect model was used to obtain ORs for rs1799782 and rs25487 while random-effect model was used to obtain OR for rs861539. Z score and OR of rs1799782 were 0.43 ($P$=0.66) and 1.14 (95% CI 0.63, 2.04). Z score and OR of rs25487 were 0.76 ($P$=0.44) and 0.83 (95% CI 0.51, 1.34). Z score and OR of rs861539 were 0.46 ($P$=0.64) and 1.53 (95% CI 0.25, 9.23). Forest plots of rs1799782 (Figure 4.6), rs25487 (Figure 4.7), and rs861539 (Figure 4.8) summarise the results of meta-analysis.

$I^2$ of rs25487 was 30% in the Asian subgroup analysis. As a result, a fixed-effect model was used to estimate OR. Forest plot of this subgroup is shown in Figure 4.9. Z score and OR of subgroup analysis were 0.55 ($P$=0.58) and 0.85 (95% CI 0.47, 1.52). Overall, there was no significant association for all SNPs in overall population analysis and subgroup analysis.

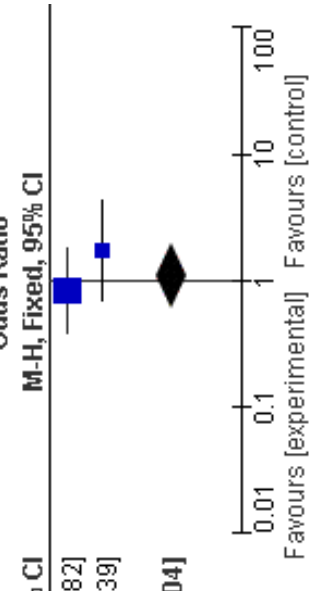


Figure 4.6: Forest plot of rs1799782 in the *XRCC1* gene under a recessive model.

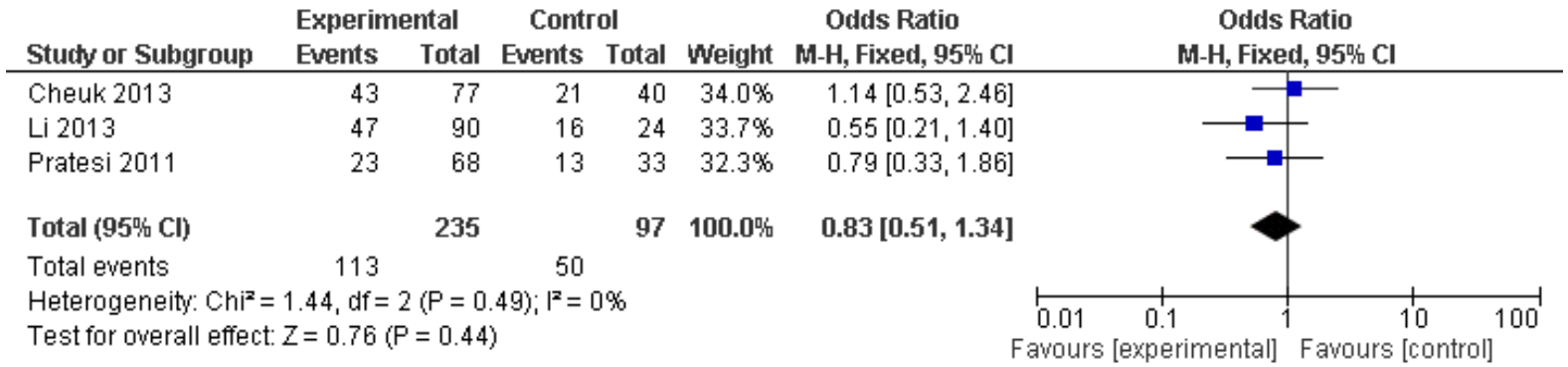


Figure 4.7: Forest plot of rs25487 in the *XRCC1* gene under a recessive model.

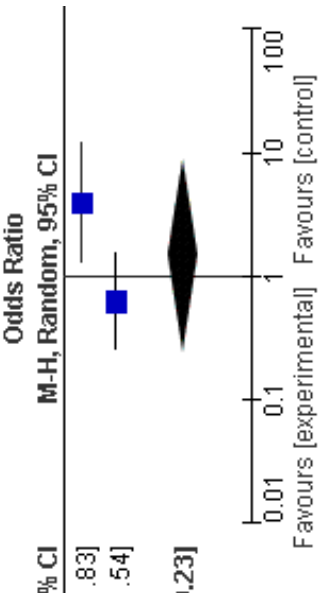


Figure 4.8: Forest plot of rs861539 in the *XRCC3* gene under a recessive model.

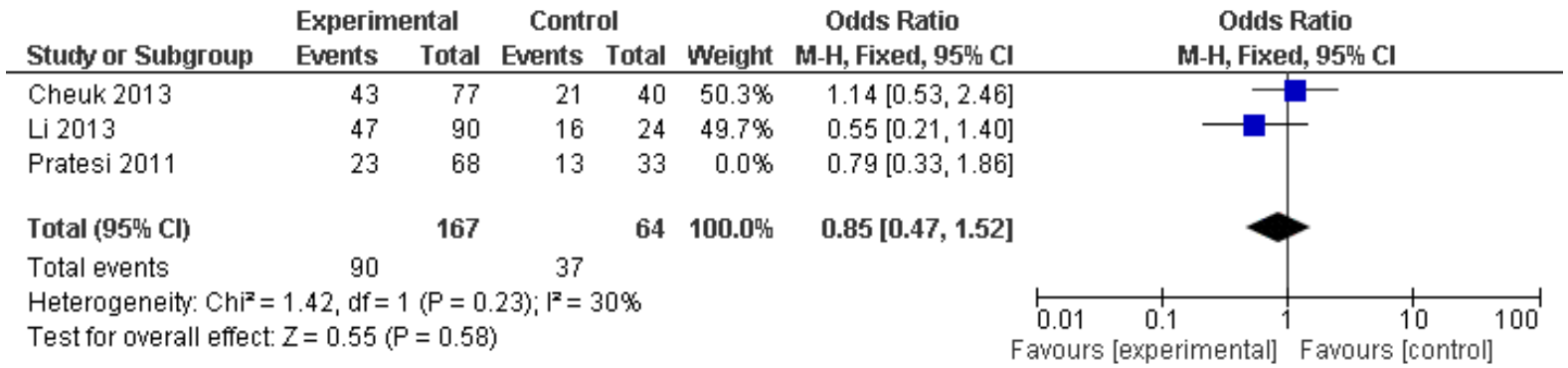


Figure 4.9: Forest plot of a subgroup analysis of rs25487 in the *XRCC1* gene under a recessive model.

#### 4.4.3.3 Allelic model

$I^2$ was 0%, 15%, and 84% for rs1799782, rs25487, and rs861539 respectively. Fixed-effect model was used to obtain ORs for rs1799782 and rs25487 while random-effect model was used to obtain OR for rs861539. Z score and OR of rs1799782 were 0.37 ($P$=0.71) and 1.09 (95% CI 0.69, 1.72). Z score and OR of rs25487 were 1.43 ($P$=0.15) and 0.76 (95% CI 0.52, 1.11). Z score and OR of rs861539 were 0.72 ($P$=0.17) and 1.73 (95% CI 0.39, 7.64). Forest plots of rs1799782 (Figure 4.10), rs25487 (Figure 4.11), and rs861539 (Figure 4.12) summarise the results of meta-analysis.

$I^2$ of rs25487 was 0% in the Asian subgroup analysis. As a result, a fixed-effect model was used to estimate OR. Forest plot of this subgroup is shown in Figure 4.13. Z score and OR of subgroup analysis were 0.27 ($P$=0.78) and 0.94 (95% CI 0.58, 1.50). Overall, there was no significant association for all SNPs in overall population analysis and subgroup analysis.

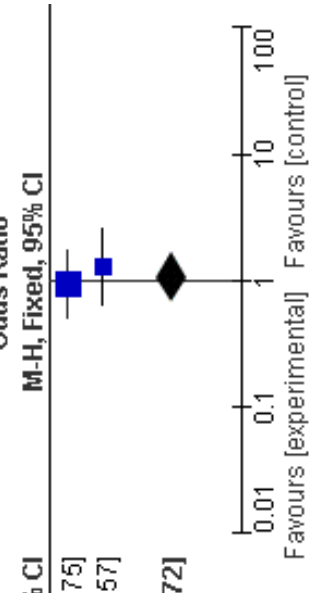


Figure 4.10: Forest plot of rs1799782 in the *XRCC1* gene under an allelic model.

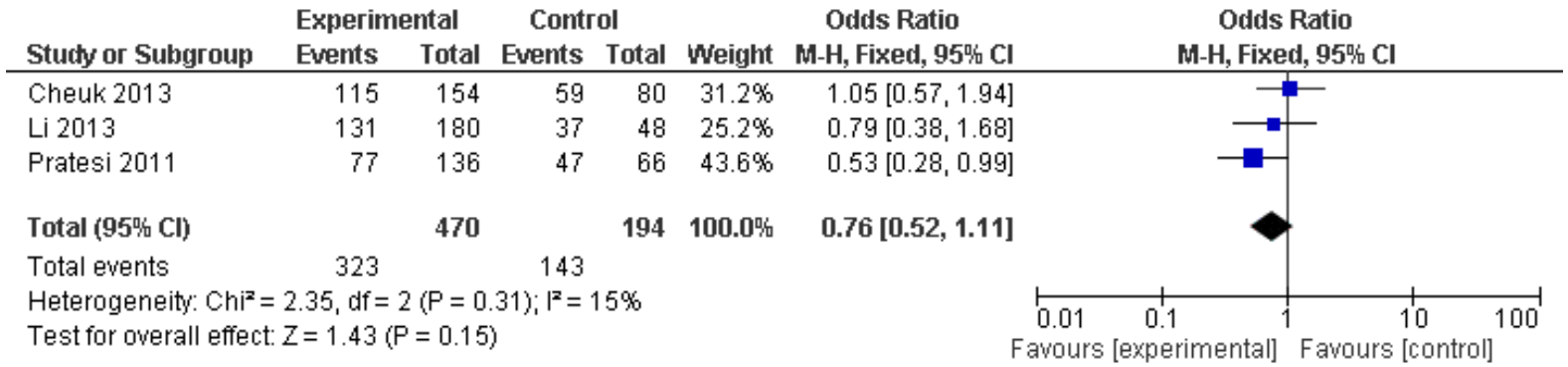


Figure 4.11: Forest plot of rs25487 in the *XRCC1* gene under an allelic model.

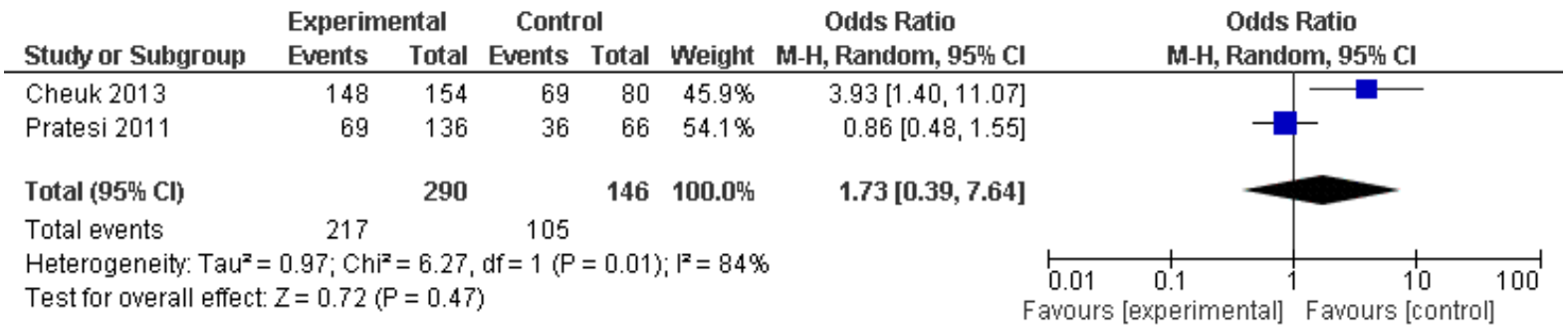


Figure 4.12: Forest plot of rs861539 in the *XRCC3* gene under an allelic model.

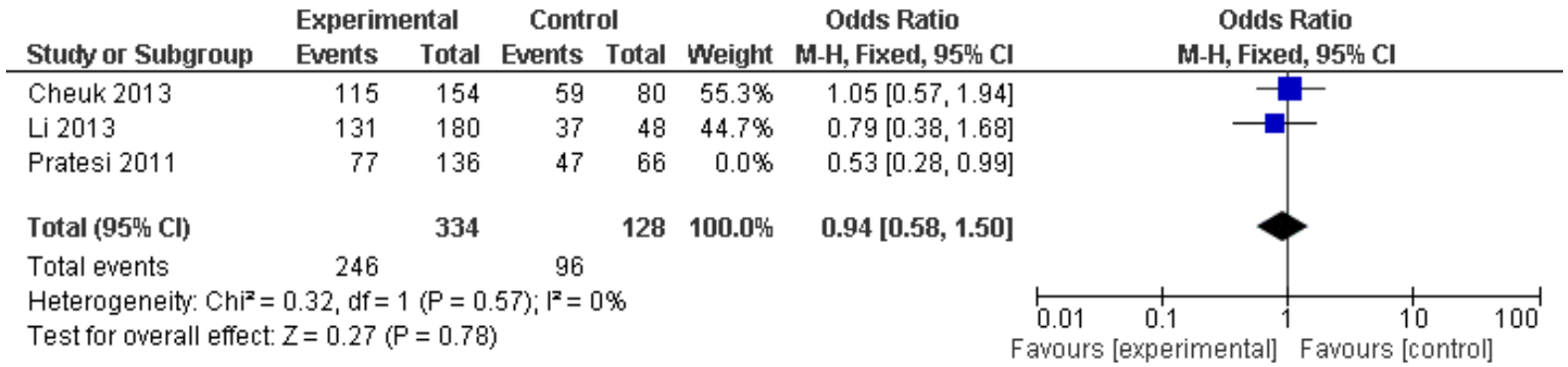


Figure 4.13: Forest plot of a subgroup analysis of rs25487 under an allelic model.

## 4.5 Discussion

Mucositis is one of the common radiation toxicities induced by RT in head and neck cancer patients. As mentioned previously, radiation-induced mucositis is the result of complex biological events that involved many signalling pathways (Sonis, 2009). Association between DNA repair genes such as *XRCC1* and *XRCC3* and various radiation-induced toxicities in many cancer types have been reported. Owing to small sample sizes, larger cohort studies could not replicate previously reported significant findings (Andreassen and Alsner, 2009; Barnett et al., 2012a). In addition, variations of study design may also lead to inconsistent findings. In order to overcome the sample size limitation and to detect between-study heterogeneity, meta-analysis of published literature with similar study design can be performed. Meta-analysis is a statistical tool to combine existing literature systematically to increase statistical power (Berman and Parker, 2002). By analysing results from an adequate number of studies through meta-analysis, more robust conclusion can be obtained (Nakaoka and Inoue, 2009).

In this meta-analysis, two published studies with adequate data, in addition to the data from the first part of this study, were combined to investigate the association of radiation-induced mucositis in 332 head and neck cancer patients and three functional SNPs from *XRCC1* and *XRCC3*. Two functional SNPs (rs1799782 and rs25487) are located in *XRCC1* and one functional SNP (rs861539) is located in *XRCC3*. No association of these SNPs and radiation-induced mucositis was found in this meta-analysis.

Under HWE, expected genotype frequencies could be calculated from allele frequencies (Wittke-Thompson et al., 2005). Case-control study is the simplest study design to compare the frequency of genetic variations in individuals with or with-

out a disease of interest. Deviation of HWE may be caused by many reasons such as random chances, genotyping errors, assortative mating, selection, and population stratification (Lewis and Knight, 2012). Controls in case-control studies should be in HWE although there is no standard guidelines for rejecting any deviated SNP (Lewis and Knight, 2012). Deviation from HWE is commonly used for checking the quality of genotyping (Lewis and Knight, 2012). In this project, DNA samples from the general population were obtained for genotyping and results were verified by sequencing to meet 100% concordance before genotyping all controls and cases. In the study by Li *et al.*, 10% of randomly selected samples were sequenced. Verification of genotyping results was not mentioned in study by Pratesi *et al.* Nevertheless, deviation of HWE was not detected in all included studies in this meta-analysis ($P$>0.001).

In this meta-analysis, two Asian populations and one European population were included. Subgroup analysis of rs25487 was further performed in Asian populations to investigate the effect of functional SNPs in specific population. No significant association was found in all SNPs in overall population analysis and subgroup analysis. The effects of these SNPs may be too modest, or may not be the causal variants of radiation-induced mucositis.

Discrepancy of allele frequencies and studied cancer types maybe the major contributors of between-study heterogeneity. Except for rs861539, the $I^2$ values of rs25487 and rs1799782 for overall population analysis and subgroup analysis were low in all models ($I^2$ <40%). The allele frequencies of the major allele of rs1799782 (C), rs25487 (G), and rs861539 (C) in Han Chinese were 0.556, 0.726, and 0.942 respectively. The allele frequencies of the major allele of rs1799782 (C), rs25487 (G), and rs861539 (C) in Caucasians were 0.850, 0.634, and 0.571 respectively. The large discrepancy in the allele frequencies of rs861539 in two ethnic groups

leads to the large heterogeneity obtained in recessive model ($I^2$=85%) and allelic model ($I^2$=84%). Radiation-induced mucositis occurs in all head and neck cancer patients treated by RT. Since seven types of head and neck cancer patients were included in the European population while only NPC patients were included in both Asian populations, slight variations in radiotherapy techniques and stagings may introduce between-study heterogeneity.

CTCAE, acute radiation morbidity scoring criteria by RTOG, and WHO handbook for reporting results of cancer treatment are the three most commonly used systems to assess severity of mucositis during cancer treatments (Sciubba and Goldenberg, 2006). In this meta-analysis, patients were classified as cases with mucositis of grade 2 or above based on any of the three systems. Genotype data were obtained from Li *et al.* for reclassifying patients for this meta-analysis. Misclassification of mucositis severity may occur due to subjective nature of these grading systems. Heterogeneity between studies may be introduced and leads to false positive findings. Using distinct clinical end points such as toxicity-specific description, or normalising toxicity scores in each study by z-statistics may be beneficial in combining data across clinical trials and conducting meta-analysis (Andreassen et al., 2012b; Ghazali et al., 2012).

The first unbiased meta-analysis investigated the association rs1800469 from *TGFβ1*, one of the most extensively studied SNPs, and radiation-induced skin toxicities in 11 cohorts with 2782 breast cancer patients, could not confirm previously reported significant findings (Barnett et al., 2012b). A validation study in breast cancer patients investigated the association of 92 SNPs in 46 genes and overall toxicity also reported no significant finding (Barnett et al., 2012a). These findings suggested that significant findings from small-scale studies may be false-positive and individual SNPs may not be universal biomarkers for all types of toxicities

found in different cancers. Since the effect size of causal variants may be too small to detect, future studies should be performed in a larger cohort of patients. Besides international cooperation, data can be pooled to increase the sample size from published studies. Data pooling may be beneficial in identifying non-disease specific and ethnic group specific biomarkers in cancer patients.

Palifermin is a KGF recombinant protein that is the only intervention approved in relieving oral mucositis in haematologic cancer patients receiving intensive treatment (Sonis, 2009). Incidence of severe oral mucositis in head and neck cancer patients was reduced from 67% and 69% to 51% and 54% in two clinical trials using palifermin (Han et al., 2013). By identifying high-risk patients using various approaches, these drugs could be used specifically for this group of high-risk patients to reduce the severity of oral mucositis to improve overall treatment efficacy and quality of life in future.

## 4.6 Limitations

The major limitation of this meta-analysis is the small number of included studies. Since adequate data were not available in some published literature, only data from this project and two published studies were analysed. As a result, future meta-analysis is needed when more data are available. Clinical factors were not included as covariates when performing this meta-analysis. Clinical factors such as age, body mass, ethnicity and gender are potential risk factors, in addition to genetic factors, that contribute to variations in radiation sensitivity between individuals (Sonis, 2009). These factors may have impact on the magnitude of overall ORs in each study. In order to improve data extraction across studies to perform meta-analysis, standardised data collection form should be used to improve reporting clinical variables and genetic information. Guidelines such as Quantitative

Analyses of Normal Tissue Effects in the Clinic (QUANTEC) and Strengthening the Reporting of Genetic Association studies (STREGA) recommendations should be followed when reporting treatment methods, clinical information and results from association studies (Bentzen et al., 2010; Little et al., 2009). With the use of QUANTEC and STREGA recommendations, heterogeneity between studies due to study design could be reduced and unbiased meta-analysis could be performed.

## 4.7 Conclusions

In summary, meta-analysis of overall population and subgroup were conducted and previously reported significant findings could not be confirmed. Future studies should investigate the effect of SNPs using GWAS approach to identify predictive biomarkers for radiation-induced mucositis, as well as other radiation-induced toxicities, to establish individual customisation of cancer treatment and to improve patient care during RT treatment.

# Part III

# Predictive assay

# Chapter 5

# Materials and Methods

## 5.1 Chemicals and reagents

Culture medium and all buffer solutions used in subsequent experiments were prepared using water purified by reverse osmosis (Millipore, Bedford, USA). Reagents for cell culture experiments were filter sterilised using 0.22 $\mu$m Nalgene®75 mm bottle-top filter (Nalgene$^{TM}$, NY, USA) before use.

### 5.1.1 Isolation of peripheral blood mononuclear cells

Histopaque®-1077 (Sigma-Aldrich, St. Louis, USA) was used in density-gradient centrifugation to isolate peripheral blood mononuclear cells (PBMCs).

### 5.1.2 Reagents used in cell culture

Certified faetal bovine serum (FBS), Dulbecco's PBS solution, RPMI-1640 and trypan blue were obtained from Gibco®(Life technologies, Carlsbad, CA, USA). Culture-grade dimethyl sulfoxide (DMSO) was obtained from Sigma (St. Louis,

USA). Crystal violet was obtained from VMR international (Poole, England). Glacial acetic acid was obtained from Panreac (Barcelona, Spain).

### 5.1.3 Reagents used in flow cytometry

FITC Annexin V-PI kit was obtained from BD Bioscience (San Jose, CA, USA). FITC annexin V, PI, and Annexin-V binding buffer (10×) were included in this kit.

## 5.2 Methods

The workflow is summarised in Figure 5.1.

## 5.3 Patient recruitment

This study followed the Declaration of Helsinki and ethics approval was obtained from the Human Subjects Ethics Sub-Committee, the Hong Kong Polytechnic University, and the Kowloon West Cluster Research Ethics Committee (REC Reference: KW/EX-12-025(48-08)) prior to any subject recruitment. All subjects were recruited from the Department of Oncology, Princess Margaret Hospital from June 2012 to August 2013. Recruited subjects were Chinese NPC patients, aged 18 or above with no history of other cancers and cancer treatment. Detailed patient recruitment criteria was shown in Table 5.1. Recruited subjects were explained with the related information. A written consent was obtained from each subject before joining the study. The following patients' related clinical information was provided by a project research assistant: date of birth, age, sex, admission date, stage of disease, RT method, treatment start and end dates, treatment regimen, highest grade of all acute induced complications, last date of seeing the patient,

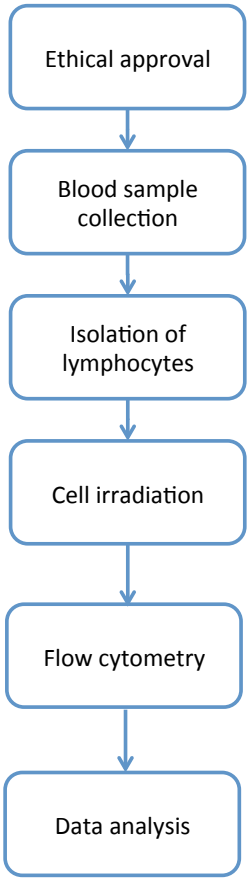


Figure 5.1: The workflow of cell irradiation experiment.

and any cancer-related medical history. Heparinised blood samples were kept at 4 °C and were processed within 24 hours after collection.

Table 5.1: Detailed inclusion/exclusion criteria of patient recruitment

| | Inclusions | Exclusions |
|---|---|---|
| Participants | NPC patients with no distant metastasis | Diseases other than NPC or NPC patients with multiple cancers or distant metastasis |
| Ethnicity | Chinese | Non-Chinese |
| Age | 18 or above | Below 18 |
| Treatment method | Never receive any cancer treatment | Previously treated with radiation therapy, chemotherapy, or surgery |

### 5.3.1 Normal group and sensitive group classification

#### 5.3.1.1 Acute skin reactions and acute mucositis

Patients were divided into normal group (grade 0-1) and sensitive group (grade 2 or above) based on acute radiation morbidity scoring criteria published by RTOG.

### 5.3.2 Isolation of peripheral blood mononuclear cells

#### 5.3.2.1 Reference samples

Blood samples containing mainly white cell fraction (buffy coat) from blood donors were used as reference samples in this study. Buffy coat was diluted with PBS in a ratio of 1 to 3. PBMCs were separated by density-gradient centrifugation at 2000 rpm for 20 minutes using Histopaque®-1077 at room temperature with brake off. Isolated PBMCs were washed with 40ml PBS by centrifugation at 1500 rpm for 10 minutes. Supernatant was discarded and cell pellet resuspended in freezing medium containing 90%FBS and 10%DMSO. Resuspended cells were cryopreserved at -80 °C using freezing container Mr. Frosty (Nalgene$^{TM}$, NY, USA) with cooling rate -1 °C/min. Frozen PBMCs were stored in liquid nitrogen.

#### 5.3.2.2 Patient samples

Three millilitres of heparinised blood were centrifuged at 3500 rpm for 10 minutes. Plasma was stored and the remaining white cells and red blood cells were diluted with PBS in a ratio of 1 to 3. PBMCs were separated by density-gradient centrifugation at 2000 rpm for 20 minutes using Histopaque®-1077 at room temperature with brake off. Isolated PBMCs were washed with 10 ml PBS by centrifugation at 1500 rpm for 10 minutes. Supernatant was discarded and cell pellet resuspended in freezing medium containing 90%FBS and 10% DMSO. Resuspended cells were cryopreserved at -80 °C using freezing container Mr. Frosty (Nalgene$^{TM}$, NY, USA)

with cooling rate -1 °C/min. Frozen PBMCs were stored in liquid nitrogen.

### 5.3.3 PBMC preparation

Complete medium (RPMI 1640 containing 10% (v/v) FBS) was incubated at 37 °C before use. PBMCs retrieved from liquid nitrogen were rapidly thawed at 37 °C. Thawed PBMCs were washed with complete medium by centrifugation at 1000 rpm for 10 minutes to remove freezing medium. Supernatant was discarded and cell pellet resuspended in complete medium. Cell counting and cell viability check by Trypan blue were performed under inverted microscope (Nikon Eclipse TS100 Microscope, NY, USA). Cell viability was calculated using the following formula:

Viability = Number of viable cells ÷ (Number of viable cells + Number of dead cells).

Samples with viability less than 80% were excluded in the subsequent experiment. Cell suspension was incubated at 37 °C in a humidified atmosphere containing 5% $CO_2$ for up to 18 hours (Direct Heat $CO_2$ Incubators; Thermo Fisher Scientific, Wilmington, USA). Cells were washed using the same procedure 3 hours before cell irradiation and resuspeneded in complete medium with cell concentration of $10^6$ cells/ml. Cell suspension was dispensed into 2 ml microcentrifuge tube and microcentrifuge tubes were then wrapped with parafilm. Microcentrifuge tubes containing cell suspension were kept at 4 °C and were transferred to Princess Margaret Hospital for irradiation within 1 hour.

### 5.3.4 PBMC irradiation

#### 5.3.4.1 Cell irradiation

Twelve aliquots of each reference sample were divided into 3 groups (0 Gy, 2 Gy, 8 Gy). For patient samples, three aliquots of each sample were divided into 3 groups (0 Gy, 2 Gy, 8 Gy). Aliquots were irradiated at 0 Gy (no irradiation), 2 Gy, or 8 Gy using Varian Clinac®6EX linear accelerator (Palo Alto, USA) according to the set-up shown in Figure 5.2 and Figure 5.3. Three parameters were used to calculate the radiation dose to cell vials using the machine provided data: radiation field size, source-to-surface distance, and surface-to-vial distance. Irradiated cell vials were transferred back to the Department of Health technology and Informatics, the Hong Kong Polytechnic University, within 1 hour after irradiation.

For **reference** samples, aliquots of each sample receiving the same dose were pooled in 25 $cm^2$ cell culture flask and were incubated at 37 °C in a humidified atmosphere containing 5% $CO_2$. Cell suspensions were taken from the flask at 2 hours, 6 hours and 18 hours after irradiation. For **patient** samples, aliquots of each sample receiving the same dose were pooled in 12-well cell culture plate and were incubated at 37 °C in a humidified atmosphere containing 5% $CO_2$. Cell suspensions were taken from the flask at 2 hours, 6 hours and 18 hours after irradiation.

According to manufacturer's recommendation, $10^6$ cells were centrifuged and resuspended in 1× Annexin V binding buffer and was stained with 2 $\mu$l of FITC Annexin V and 2 $\mu$l of PI. Stained cells were incubated in dark for 10 minutes. Radiation-induced apoptosis was assessed by a two-laser FC500 flow cytometer (Beckman Coulter, USA). Flow data were analysed by the CXP software (Beckman Coulter, USA).

#### 5.3.4.2 Definition of radiation-induced apoptosis

Cells that are undergoing early apoptosis are Annexin V-positive and PI-negative. Cells that are undergoing late apoptosis are both Annexin V-Positive and PI-positive. Total apoptosis is the sum of cells undergoing early and late apoptosis. Radiation-induced apoptosis was calculated by subtracting percentage of total apoptosis at 2 Gy or 8 Gy from baseline, in which the baseline was the percentage of spontaneous PBMCs apoptosis at 0 Gy (no irradiation).

## 5.4 Statistical analysis

Radiation-induced apoptosis between reference samples and cancer patients was analysed by two-way ANOVA. Radiation-induced apoptosis between normal and sensitive groups at different radiation doses was analysed by two-way ANOVA.

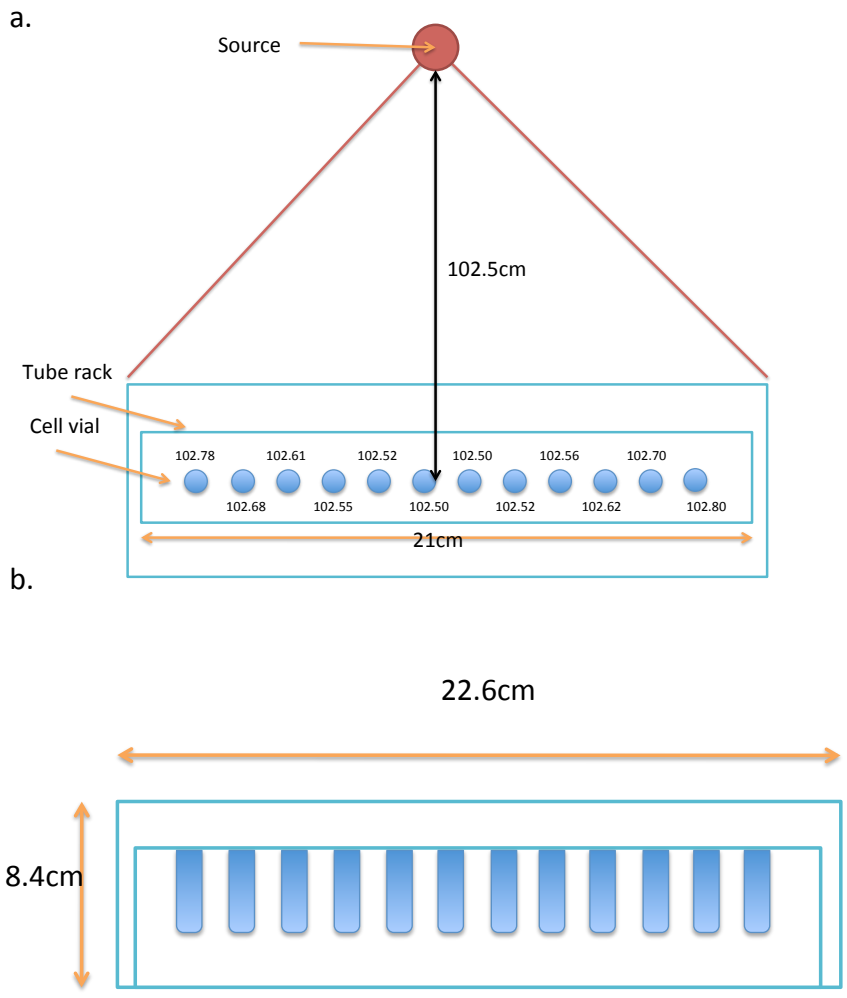


Figure 5.2: Aerial view (a) and side view (b) of cell irradiation model. The distance between each cell vial and source was represented in centimetre.

a.

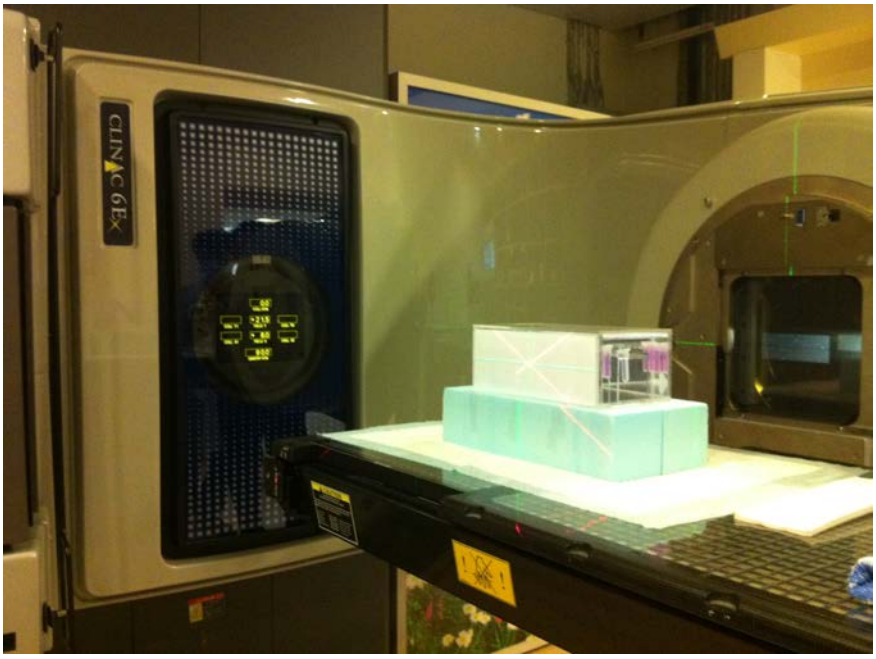


b.

Figure 5.3: Setting of linear accelerator. (a) Set up condition for cell irradiation. (b) Close view of the box containing resuspended cells.

# Chapter 6

# Predictive assays

## 6.1 Aims

The aim of this section was to investigate whether PBMCs apoptosis induced by *in vitro* radiation may be used as a biological marker in predicting the occurrence of severe radiation-induced acute complications in Chinese NPC patients.

## 6.2 Introduction

Besides identification of causal genetic variants, cell-based prediction assays, such as quantification of radiation-induced apoptosis in fibroblasts or PBMCs derived from cancer patients, have been explored to differentiate normal and hypersensitive cancer patients before RT treatment. Patients with genetic disorder ataxia telangiectasia (AT) are hypersensitive to ionising radiation (Section 1.6.1). The percentage of radiation-induced apoptosis in PBMCs derived from AT patients was lower when compared to healthy individuals (Crompton et al., 1999). The percentage of radiation-induced apoptosis in PBMCs derived from hypersensitive

cancer patients also obtained similar findings (Crompton et al., 1999). One of the major concerns is the reproducibility of these assays affected by variations in treatment doses, use of cell types, and classification of radiosensitivity. In addition, most studies were performed in breast cancer patients or patient cohort with various types of cancer focusing mainly on radiation-induced skin toxicity. Lack of information is available particularly to head and neck cancer specific toxicity such as mucositis. In this study, the correlation between acute complications (skin reactions and mucositis) and the percentage of radiation-induced apoptosis in isolated PBMCs from Chinese NPC patients was investigated.

## 6.3 Methodology

### 6.3.1 Patient recruitment

Thirty Chinese NPC patients were recruited at the Department of Oncology, Princess Margaret Hospital (Section 5.3) before the start of any cancer treatment. Patients were classified into normal group or sensitive group based on the classification criteria of each phenoytpe (Section 5.3.1). Twenty seven blood samples from anonymous blood donors were used as reference samples.

### 6.3.2 Radiation-induced apoptosis

PBMCs were isolated from heparinised blood of each patient within 24 hours after collection (Section 5.3.2.2). For logistic reason, PBMCs from healthy individuals and patients were stored in liquid nitrogen and cell irradiation experiments were performed in June and July 2013. Frozen PBMCs were thawed, washed and incubated with complete medium 18 hours before cell irradiation (Section 5.3.3). Aliquots containing $1 \times 10^6$/ml PBMCs in complete medium were irradiated at 0 Gy, 2 Gy and 8 Gy. Apoptosis was determined by FITC Annexin V-PI kit (BD

Bioscience, San Jose, CA, USA). Flow cytometry was performed using FC500 Flow cytometer (Beckman Coulter, USA). Radiation-induced apoptosis was quantified by the CXP software (Beckman Coulter, USA) (Section 5.3.4)

### 6.3.3 Data analysis

Percentages of live cells, cells entering early apoptosis, and cells undergoing late apoptosis were compared between reference samples and patient samples (Section 5.3.4.2 and 5.4).

## 6.4 Results

### 6.4.1 Subject recruitment

Six reference samples were excluded from analysis because of low cell viability (<80%). Two reference samples were used in pilot studies for protocol optimisation. Thus, these samples were not included in this analysis. One patient sample was excluded due to the patient did not receive RT treatment. One patient sample was excluded because RT treatment was administered in a private hospital with no RT response recorded. Seven patient samples were not included in this analysis since RT treatment has not yet completed or had not commenced at the time of analysis. In total, 19 reference samples and 21 patient samples were included in this analysis. A summary of patient clinical characteristics is shown in Table 6.1. Summary statistics of acute toxicities observed in included patients are shown in Table 6.2.

### 6.4.2 Quantification of radiation-induced apoptosis using flow cytometry

Irradiated PBMCs were stained with Annexin V and PI to differentiate live cells, cells undergoing early apoptosis, and cells undergoing late apoptosis (Section 1.5.3.4 and 1.8). Figure 6.1 is a scatterplot showing the locations of these cell populations.

#### 6.4.2.1 Time point selection

Total apoptosis is the sum of cells undergoing early apoptosis and cells undergoing late apoptosis (Section 5.3.4.2). Total apoptosis of reference samples was measured at three time points (2h, 6h, and 18h) following 0 Gy, 2 Gy and 8 Gy irradiation. Total apoptosis at baseline (0 Gy) showed no significant difference at all time points. Total apoptosis of reference samples irradiated at 2 Gy and 8 Gy, measured at 2 hours and 6 hours showed no significant difference. Total apoptosis showed significant difference at 2 Gy and 8 Gy between 2 hours and 18 hours post treatment ($P<0.05$). Therefore, measurement of total apoptosis 6 hours post-treatment was not performed for patient samples. Distribution of total apoptosis is shown in Figure 6.2.

#### 6.4.2.2 Total apoptosis in reference samples and patients

Total apoptosis of reference samples and patient samples 2 hours and 18 hours post-irradiation are shown in Figure 6.3a and 6.3b. No significant difference of total apoptosis was found between reference samples (n=19) and patient samples (n=21) at baseline and 18 hours post-irradiation ($P>0.05$).

#### 6.4.2.3 Radiation-induced apoptosis in normal group and sensitive group

Patients were considered as normal or sensitive according to criteria mentioned in Section 5.3.1.1. Radiation-induced apoptosis at each dose was calculated for both groups by subtracting total apoptosis at baseline (0 Gy) (Section 5.3.4.2, Table 6.3). Radiation-induced apoptosis increased over time in both groups ($P<0.05$) (Figure 6.4). Radiation-induced apoptosis increased with higher dose of radiation for both groups in acute skin reactions and sensitive group in acute mucositis ($P<0.05$). No significant change of radiation-induced apoptosis in normal group of acute mucositis was found ($P=0.3733$). There was no significant difference of radiation-induced apoptosis between normal group and sensitive group ($P>0.05$).

Table 6.1: Clinical characteristics of recruited patients in this study

| | | Patients | Percentages (%) |
|---|---|---|---|
| Age | | | |
| | Min | 38 | |
| | Median | 52 | |
| | Max | 78 | |
| Sex | | | |
| | Male | 15 | 71.4% |
| | Female | 6 | 28.6% |
| Histology of NPC | | | |
| | Type II | 2 | 9.5% |
| | Type III | 19 | 90.5% |
| Stage | | | |
| | I | 3 | 14.3% |
| | IIB | 1 | 4.8% |
| | III | 8 | 38.1% |
| | IVA | 6 | 28.5% |
| | IVB | 2 | 9.5% |
| | IVC | 1 | 4.8% |
| Treatment | | | |
| | RT Only | 5 | 23.8% |
| | CRT | 16 | 76.2% |

**Abbreviation**: RT = Radiotherapy; CRT = Concurrent chemotherapy and radiotherapy.

Table 6.2: A summary of acute toxicities observed in 21 patients recruited for this study

| | Grade | | | |
|---|---|---|---|---|
| Acute toxicity | 0 | 1 | 2 | 3 |
| Skin reaction | 5 (23.8%) | 7 (33.3%) | 7 (33.3%) | 2 (9.5%) |
| Mucositis | 2 (9.5%) | 3 (14.3%) | 9 (42.3%) | 7 (33.3%) |

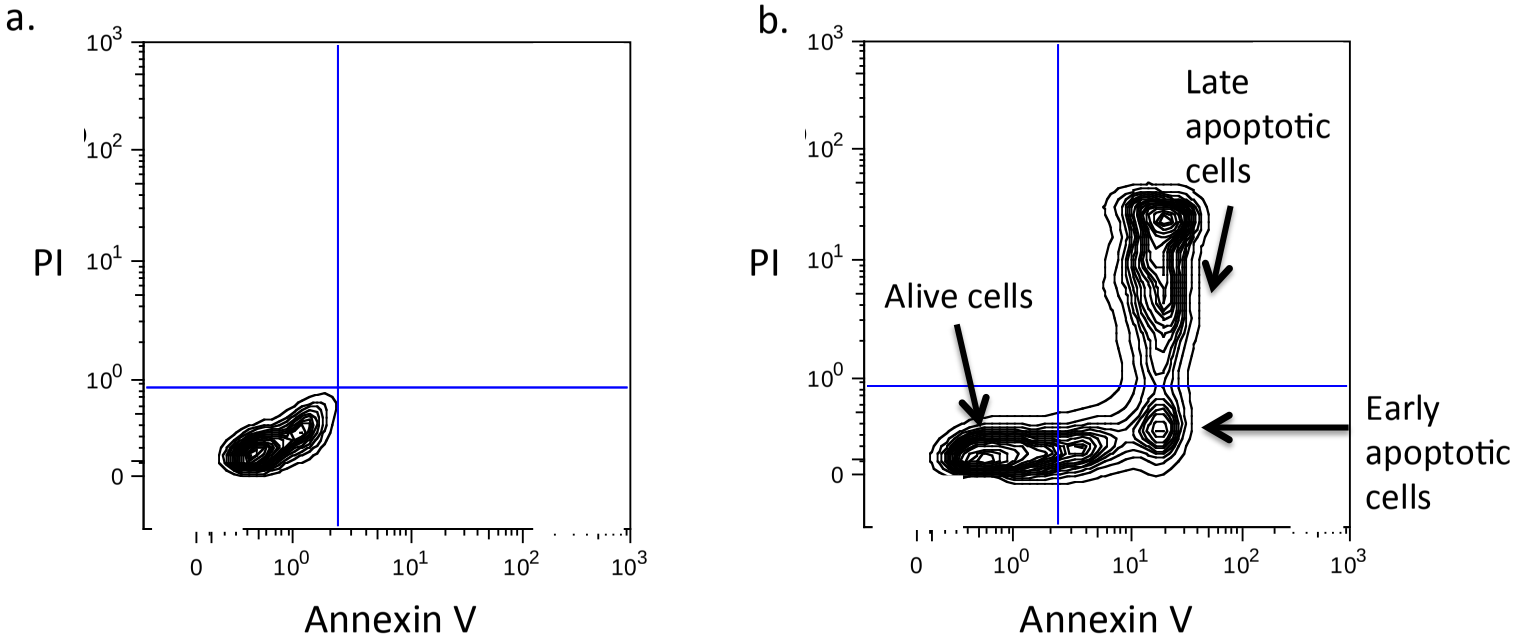


Figure 6.1: A scatterplot showing three cell populations. The x-axis indicates the fluorescence intensity of propidium iodide while the y-axis shows the fluorescence intensity of annexin V. Note the logarithmic scales for both axes. (a) Unstained control. (b) Cells undergoing apoptosis are stained with Annexin V and PI. Three populations are identified and are indicated by arrows.

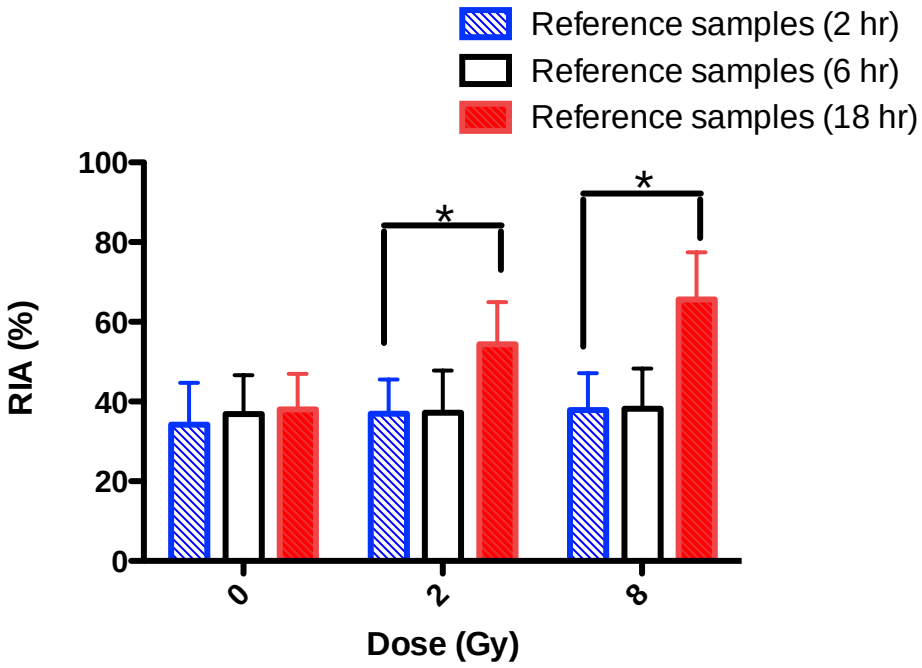


Figure 6.2: Percentage of total radiation-induced apoptosis (RIA) versus Dose in reference samples (n=19). No significant difference was found between 2 hours and 6 hours after radiation for all time points at all dosages ($P>0.05$). Significant difference was found between 2 hours and 18 hours after radiation for cells receiving 2 Gy and 8 Gy irradiation ($^*P<0.05$).

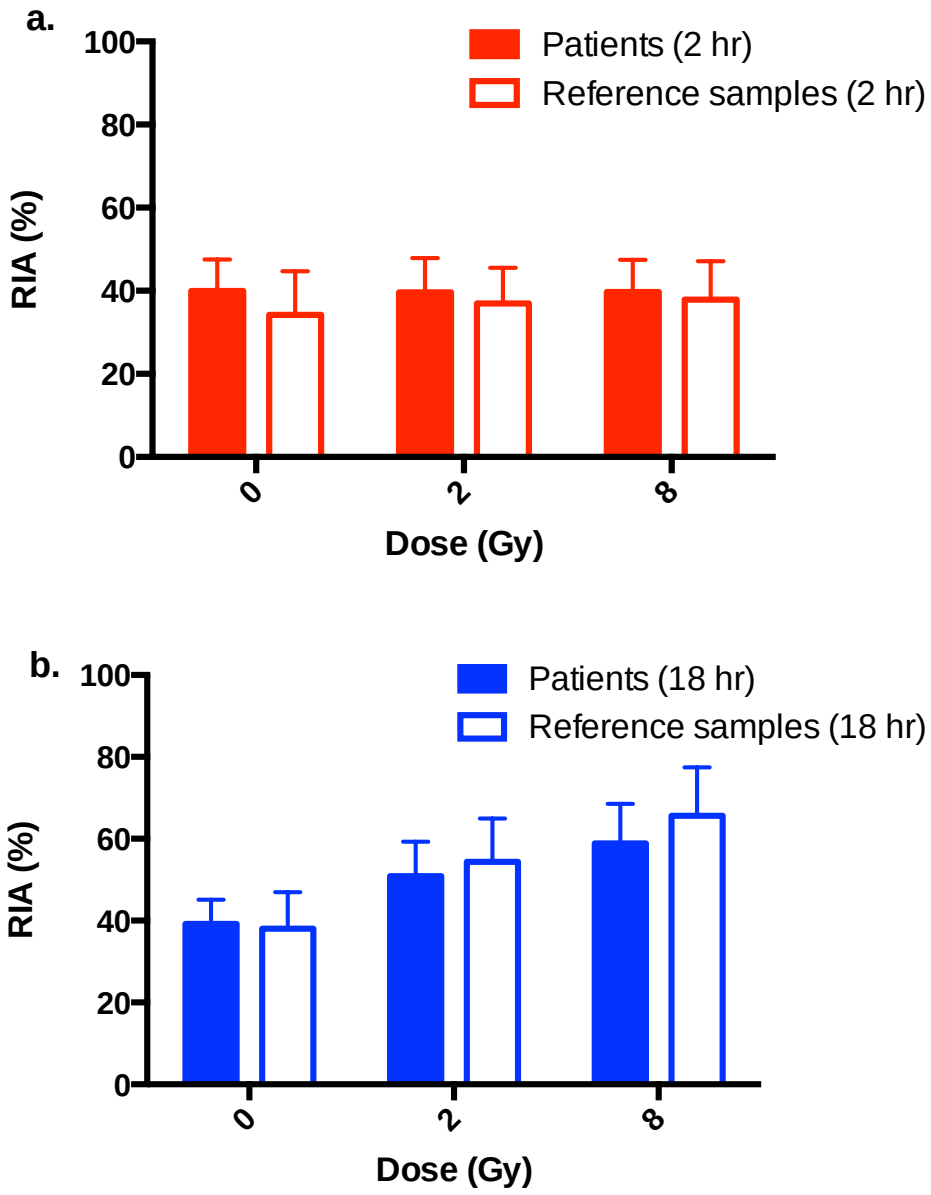


Figure 6.3: Percentage of total radiation-induced apoptosis (RIA) versus Dose in reference samples (n=19) and patient samples (n=21). (a) Percentage of total RIA was not significantly different between reference samples and patient samples 2 hours post-irradiation at all dosages ($P$>0.05). (b) Percentage of total apoptosis was not significantly different between reference samples and patient samples 18 hours post-irradiation at all dosages ($P$>0.05).

Table 6.3: A summary of radiation-induced apoptosis at 18 hours

| | Mean (SD), % | | | |
|---|---|---|---|---|
| | Skin | | Mucositis | |
| Dose (Gy) | Normal | Sensitive | Normal | Sensitive |
| 2 | 11.83 (4.39) | 11.53 (5.39) | 12.61 (2.69) | 11.38 (5.36) |
| 8 | 18.39 (7.18) | 20.92 (8.19) | 18.04 (7.11) | 19.89 (5.18) |

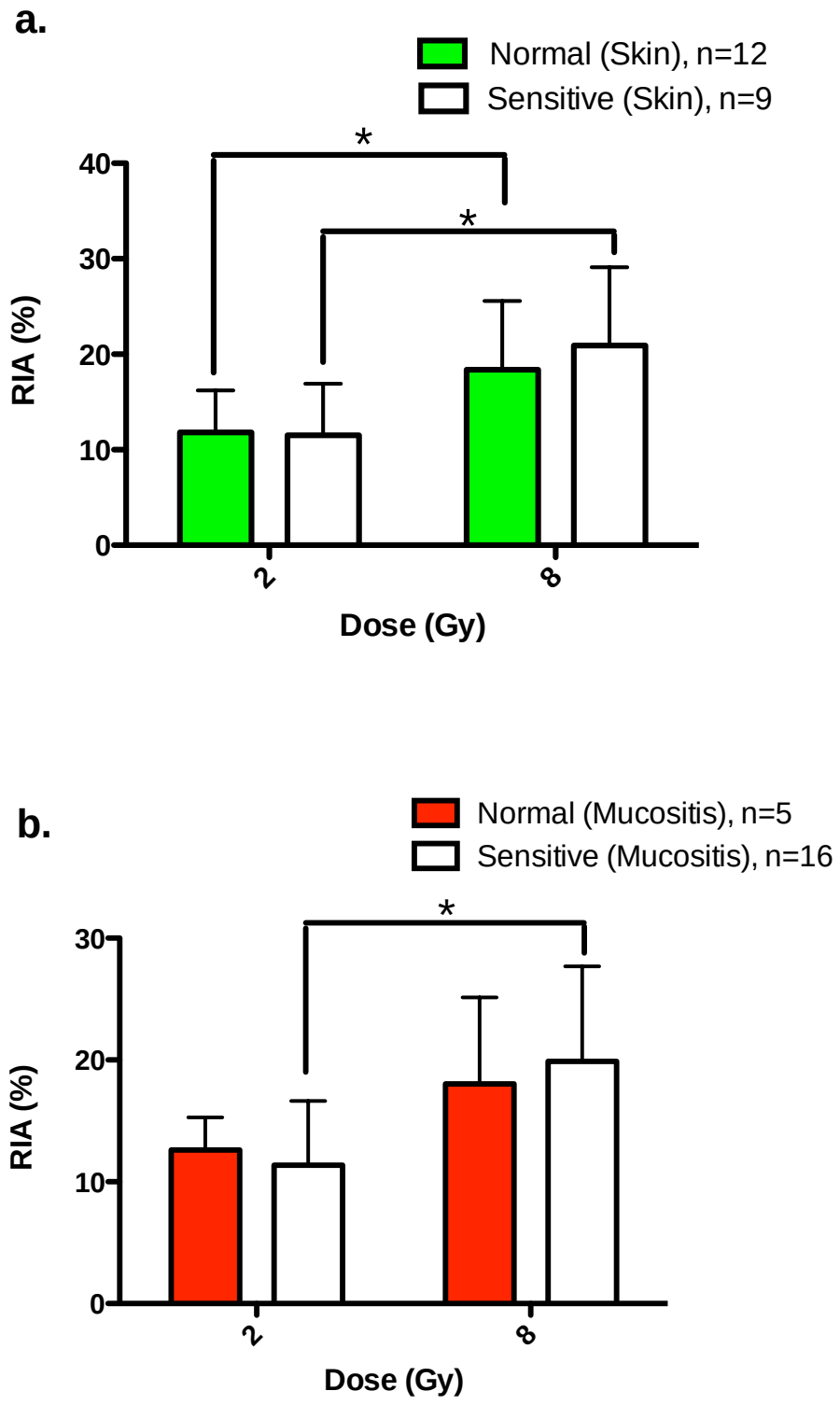


Figure 6.4: Percentage of radiation-induced apoptosis (RIA) in normal group and sensitive group. Percentage of total RIA increased over time. (a) Percentage of total RIA was significantly higher 18 hours after 8 Gy irradiation than 2 Gy irradiation in both normal and sensitive groups (acute skin toxicity) ($*P<0.05$). (b) Percentage of total RIA was significantly higher 18 hours after 8 Gy irradiation than 2 Gy irradiation in sensitive group only (acute mucositis) ($*P<0.05$).

## 6.5 Discussion

Cancer patients receiving similar protocol of cancer treatments show individual variations in the severity and types of radiation-induced toxicities. Personalised RT is one of the long-term goals in improving treatment effectiveness and reducing radiation-induced toxicities in cancer patients. Besides investigation of underlying genetic variants, cell-based predictive assays are attractive alternatives to differentiate cellular response during radiation between normal and radiosensitive cancer patients. One of the commonly used methods is quantification of radiation-induced apoptosis using flow cytometry (Henríquez-Hernández et al., 2012). In this study, correlation between radiation-induced apoptosis of PBMCs and acute radiation-induced complications in Chinese NPC patients was investigated.

Correlation of acute and late toxicities with radiation-induced damages has been reported although the underlying mechanism is still unclear (Bordon et al., 2009, 2010; Crompton et al., 1999; Henríquez-Hernández et al., 2011; Mariano Ruiz de Almodóvar et al., 2002; Núñez et al., 1998; Ozsahin et al., 2005; Pinar et al., 2010; Popanda et al., 2003; Schnarr et al., 2009; Sterpone et al., 2010; Wang et al., 2005a). While late toxicities affect the quality of life after treatment, acute toxicities affect the treatment experience and effectiveness of cancer patients. Since some studies were performed in a mixed population of cancer patient with incomparable toxicities, conclusions made by these studies may not be definitive.

As aforementioned, many assays have been used to establish a correlation of cellular response, such as initial DNA damages or apoptosis, with radiation hypersensitivity (Section 1.5.3). Conflicting results have been reported and attributed to between-study variations such as methods in assessing radiation-induced damages, use of cell types, studied cancer types, and study design.

Cultured fibroblasts, PBMCs, lymphocytes and lymphoblastoid cell lines (LCLs) are commonly used cell types in published studies. Cultured fibroblasts from patients are not the most suitable cell type used in studying individual radiosensitivity because of practical reasons (Section 1.5.3.1). Inter-laboratory comparison of lymphocytes and LCLs derived from healthy individuals and radiosensitive patients suggested that primary lymphocytes should be used instead of LCLs (Greve et al., 2012). LCLs are transformed from lymphocytes by using EBV. However, gene activity and metabolism of LCLs are different from lymphocytes after the immortalisation process (Greve et al., 2009). For instance, *p16* and *Rb* are tumour suppressor genes that are downregulated in this immortalisation process. As a result, physiological features of LCLs are different from those of the corresponding primary lymphocytes. No apoptosis was detected by annexin V after irradiation of LCLs. Alternative assays such as TUNEL assay also showed negative results (Greve et al., 2009).

Whole blood collected or PBMCs isolated from cancer patients retrospectively were used in other studies (Bordon et al., 2009, 2010; Henríquez-Hernández et al., 2011; Ozsahin et al., 2005; Pinar et al., 2010). Patients' clinical conditions, as well as cell culture conditions, may have great impact on the level of apoptosis. Increased levels of DNA fragmentations and micronuclei were observed after irradiation of PBMCs collected from previously RT-treated cancer patients (Djuzenova et al., 2006). Because of the presence of factors suck as cytokines, blood may have the ability to scavenge radiation-induced free radicals after *in vitro* blood irradiation. On the other hand, enhanced apoptosis is observed when isolated subpopulations of blood cells are irradiated (Wilkins et al., 2002b). It has been reported that oxidant-induced damages were unable to repair in cryopreserved PBMCs when compared with fresh PBMCs (Duthie et al., 2002). In this study, blood samples were collected before the start of RT. Radiosensitivity of cryopreserved PBMCs

used in this study may be affected by these confounding factors.

Owing to different levels of radiation sensitivity of different types of blood cells, cell types used in investigating radiosensitivity and radiation-induced damages vary. Some studies focused on monitoring particular subpopluations, such as $CD4^+$ and $CD8^+$ T-lymphocytes while other studies measured DNA damages in PBMCs (Bordon et al., 2009, 2010; Cornetta et al., 2006; Crompton et al., 1999; Djuzenova et al., 2006; Henríquez-Hernández et al., 2011; Ozsahin et al., 2005; Pinar et al., 2010; Popanda et al., 2003). Our results were in line with those studies focused on radiosensitivity of subpopulations with similar experimental protocol (Greve et al., 2012, 2009; Ozsahin et al., 2005). Initial DNA damages measured by pulsed-field gel electrophoresis (PFGE) were correlated with acute skin toxicities in breast cancer and head and neck cancer patients (Mariano Ruiz de Almodóvar et al., 2002; Núñez et al., 1998; Wang et al., 2005a). In contrast, lack of correlation between radiation-induced damages and acute skin reactions has also been reported by studies using the same approach (López et al., 2005; Strasser et al., 2007). Lack of correlation between acute skin reactions and DNA repair capacity using comet assay in breast cancer patients was also reported by Popanda *et al.* (2003) while significantly reduced DNA repair in patients with severe acute skin toxicity was found by Sterpone *et al.* (2010). Different time points used in various studies may also lead to discrepancies. While 18 hours after cell irradiation was the optimal time point used in this study to investigate radiation-induced damages, other studies performed measurements at different time points. Variations of time point selection in each study may be due to between-study variations such as dose selection and use of cell types. Therefore, different studies were incomparable because of difference in study design and methodologies.

## 6.6 Limitations

One of the major limitations of this study is the small sample size. Based on inter-laboratory comparisons, it is estimated that over 250 patients are required to differentiate normal and sensitive patients with small effect size in order to achieve 80% power (Greve et al., 2012). Due to different study design, our results were unable to compare with other published studies. The use of cryopreserved PBMCs instead of freshly isolated PBMCs may introduce substantial damages before *in vitro* cell irradation. DNA damages induced by freezing and thawing PBMCs may contribute to spontaneous apoptosis and cell shrinkages. Figure 6.5 illustrates cell populations of three reference samples before irradiation. An extra cell population of low forward scatter was found in some frozen samples when compared to freshly isolated PBMCs. Cell shrinkage and cell debris, which are the result of freeze-thawing processes of PBMCs, may contribute to these additional, non-radiation-related annexin V and PI positive cells. Since samples were irradiated and handled at two different locations, cells were unable to irradiate after freshly isolated from blood. Transportation of samples may also affect our results. Owing to limited samples, no replicate measure was performed in this study. Significant variations have been shown in repeat sample measurements using G2 assays, in which radiosensitivity was determined by measuring chromatid breaks during G2-phase of cell cycle after *in vitro* irradiation (Bryant et al., 2002; Chaudhry, 2008). Repeated measurements should be performed in the future to minimise within subject-variability.

This study is unable to monitor late radiation-induced effect because of time limitation. Since this will be prospective study, at least two years of post-treatment follow-up period is required to obtain information on late toxicity development. A mathematical model has been proposed by Bordon *et al.* to predict the de-

velopment of late toxicities induced by radiation (Bordon et al., 2009). Since acute toxicities and late side effects may be correlated, patients exhibiting severe acute toxicities should be monitored to investigate the correlation between radiation-induced apoptosis and late toxicities in the future. Investigation of radiation-induced damages using multiple assays on the same primary cells could be performed since each assay has its advantages and limitations.

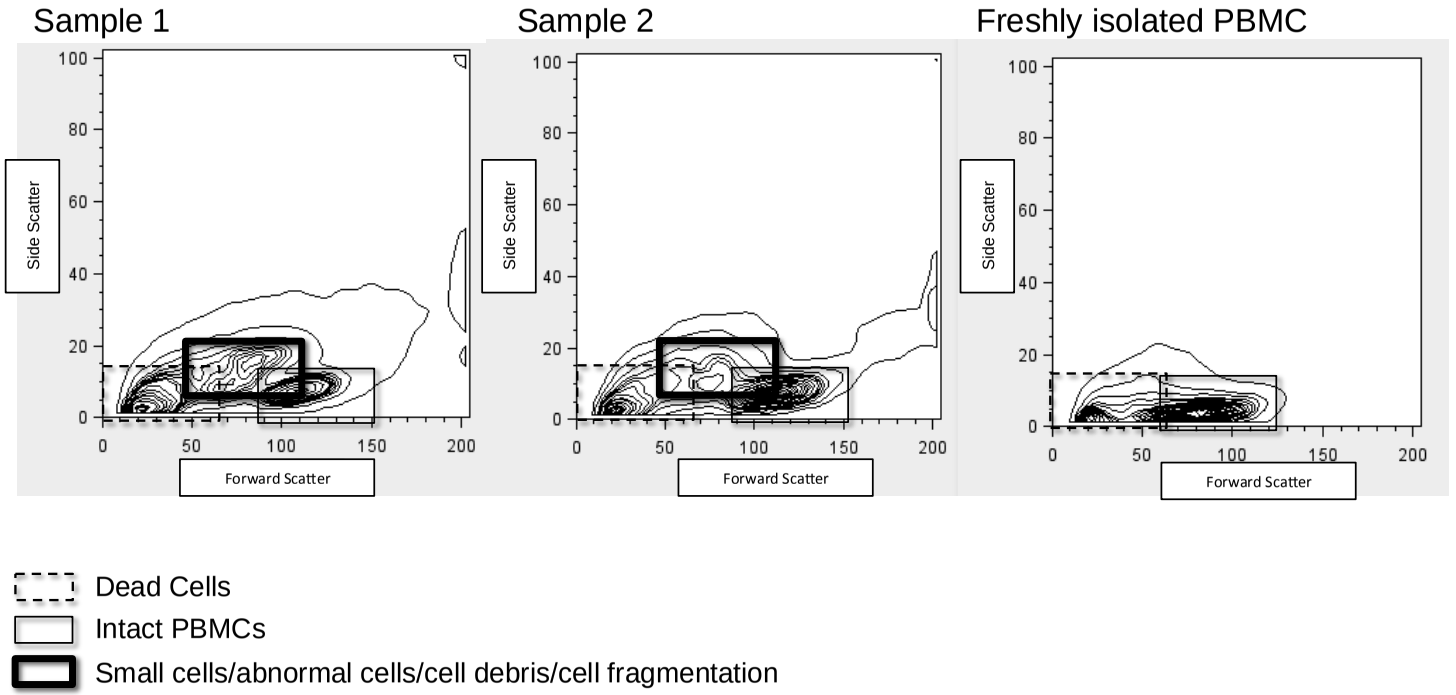


Figure 6.5: Cell populations of freshly isolated cells and cryopreserved cells. Sample 1 and sample 2 are cryopreserved PBMCs. Compared with freshly isolated PBMCs, an extra cell population is identified in both sample 1 and sample 2. This extra cell population represents cell debris, cell fragmentation, and shrinking cells.

## 6.7 Conclusion

In this prospective study, correlation between radiation-induced apoptosis and acute radiation-induced toxicities in Chinese NPC patients was investigated. Compared to patients with mild acute toxicities, reduced level of radiation-induced apoptosis in patients showing increased radiosensitivity was not found in this study. Future studies should include larger sample size to investigate radiation-induced DNA damages in different aspects with different types of assays. Patients with severe acute toxicities should be followed to monitor any development of late toxicities.

# Chapter 7

# Overall Discussion

NPC is an endemic cancer in Southern China, including Hong Kong. RT is the most effective primary treatment particularly for the undifferentiated type of NPC, which accounts for over 90% of the NPC cases (Wei and Sham, 2005). Effectiveness of RT is limited by the occurrence of acute radiation-induced toxicities, while physical health and quality of life are affected by the development of late toxicities. Information on NPC-related radiation-induced toxicities in Chinese population is is lacking, since research focus is slightly different based on different endemic cancers in different ethnic groups. Based on existing literatures, this study adopted several strategies to obtain genetic information retrospectively and cellular response prospectively from NPC patients. This is the ***first*** study investigating the potential predictiveness of clinical radiosensitivity based on genetic information and *in vitro* radiation-induced cellular apoptosis in local Chinese NPC patients.

## 7.1 Genetic variants in genes related to DNA repair and cell cycle regulation

Candidate-gene approach is the most common approach used in the research of radiation toxicities. Candidate-gene approach is a hypothesis-driven approach, in which candidate genes are selected based on their functional roles in particular pathways. Ionising radiation is the most effective agents to kill rapidly proliferative tumour cells. Normal tissues such as epithelial cells exposed to ionising radiation are also affected and this leads to various treatment-related toxicities. Pathways within the DNA damage response system, such as cell cycle checkpoints, DNA repair and cell death, are activated by radiation-induced damages (Jioner and van der Kogel, 2009). Six functional candidate genes in this DNA damage response system, *ATM*, *SOD2*, *TGFβ1*, *TP53*, *XRCC1* and *XRCC3*, were selected to investigate their genetic variants and association of various radiation-induced toxicities in NPC patients. Previous studies only focused on functional variants of candidate genes while the role of other common variants in individual variation of radiosensitivity is unknown. Besides previously reported functional variants, this study was able to captured common variants using tag SNPs and to construct haplotypes in local Chinese population. In order to avoid any false positive findings, permutation was performed for correction of multiple testing. Despite the fact that significant results were reported by other research groups, no association was found in any of the single-marker analysis and haplotype analysis for all phenotypes investigated in this study (Chapter 3).

### 7.1.1 Effect size and sample size

Several reasons and limitations may be the possible causes of non-significant results in this study. A power calculation is performed using results from this study to investigate the required number of controls and cases in 2 to 1 ratio to reach 80% power. With the high prevalence of acute skin reactions and mucositis (57% and 65% respectively), a minimum 4092 controls and 2046 cases are required to give sufficient statistical power (Table 7.1). Not surprisingly, a much larger sample size is required for the investigation of late toxicities with the prevalence of 24% of chronic neck fibrosis obtained in this study. Sample size limitation may be attributed to the loss of significance after multiple testing adjustment of selected SNPs.

A validation study with 99% power to detect a SNP with an MAF equal to 0.35 was published in 2012 (Barnett et al., 2012a). Ninety two SNPs in 46 genes were genotyped in 1613 breast cancer and prostate cancer patients. Our results were in line with this validation study that none of the reported SNPs showed significant association after adjustment for multiple testing comparisons. In addition, the first replication study using candidate-gene approach investigated adverse skin reactions in breast cancers was published in 2012 (Talbot et al., 2012). This study included three independent cohorts with a total 2036 breast cancer patients to capture 43 SNPs in 35 genes. Except rs1800629 located in the *TNFα* gene, Talbot *et al.* reported that none of the investigated SNPs was associated with overall late toxicities. Genetic variant rs1800629 (G>A) is located in the promoter region, 308 bp upstream of the transcription start site of the *TNFα* gene (Talbot et al., 2012). Talbot *et al.* also genotyped rs2857595, a SNP in high LD with rs1800629, in the third cohort with significant results. Since only European cohorts were involved in this replication study, it is not known whether these SNPs in the *TNFα*

gene are the surrogate of other SNPs located at a distant region or the causal variants associated with increased risk of radiation toxicities in all populations. It is important to note that significant effect of SNPs may be affected by other confounding factors, such as treatment parameters and clinical information, during univariate and multivariate analyses or their effect size (Barnett et al., 2012b). Effect size of common variants is likely to be small to modest, compared with effect size of rare variants (Figure7.1)(West et al., 2012; Wray et al., 2013). It seems that individual risk of a complex disease may be increased by the accumulative effect of multiple common variants (Wray et al., 2013).

Table 7.1: Sample size estimation based on observed data

| Parameters | Values |
|---|---|
| High risk allele frequency (A) | 0.34 |
| Prevalence of any post-RT complications | 0.57 |
| Genotype relative risk (Aa) | 1 |
| Genotype relative risk (AA) | 1.5 |
| Number of tag SNPs for this study | 29 |
| Ratio of cases to controls | 1:2 |
| Type 1 error | 0.05/29 = 0.00172 |
| User-defined Power | 80% |
| Minimum sample size estimated for experimental: control | 2046:4092 |

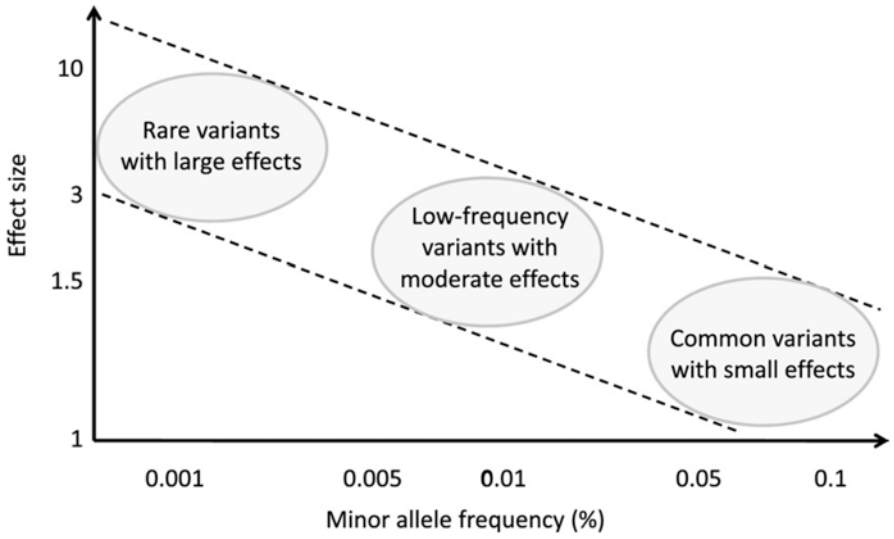


Figure 7.1: Relationship between allele frequency and effect size (West et al., 2012).

### 7.1.2 Multiple-SNP model based on genetic profile

A multiple-SNP model was proposed to establish correlation between the total number of risk alleles in candidate genes and the risk of developing severe late adverse reactions in matched case-control breast cancer patients (Azria et al., 2008). Azria *et al.* reported that breast cancer patients with 4 or more SNPs have higher risk of developing severe late adverse reactions. A preliminary analysis based on data from acute skin reactions in this study was performed. Instead of quantifying the number of risk alleles in individual patients, receiver operating characteristic (ROC) curves were constructed based on clinical data and genetic information obtained in this study to investigate the accumulative effect of common variants. All SNPs and clinical characteristics were included in generating this preliminary prediction model.

Predicted risks were calculated by PredictABEL package version 1.2-1 in R version 2.15.1 for windows using logistic regression analysis (Kundu et al., 2011). Area under ROC curves (AUC) was obtained and was used as a discrimination measure of acute skin reactions between controls and cases. Mann-Whitney U test was used to compared predicted risks between controls and cases. Distribution of predicted risks of controls and cases is shown in Figure 7.2b. Predicted risks from cases were significantly different from controls ($P<0.0001$). Summary statistics of predicted risk are shown in Table 7.2. Although there is some overlap between controls and cases, our constructed risk model is similar to the SNP model by Azria *et al.* (Figure 7.2a).

Three ROC curves were constructed and used as preliminary prediction analysis. Figure 7.3 illustrates the ROC curves constructed based on clinical factors only (Figure 7.3a), genetic factors only (Figure 7.3b), and both clinical and genetic factors (Figure 7.3c). AUC represents the predictive performance of each model.

AUC calculated based on clinical factors only, genetic factors only, both clinical and genetic factors was 0.7, 0.76, and 0.84 respectively. Our preliminary results indicated that although none of the genotyped SNPs in this study showed any correlation with acute skin toxicities, prediction model could be constructed based on accumulative effects of common genetic variants from pathways involved in DNA damage response system. Individual genetic profiles, in addition to comprehensive clinical information, may help in identifying high risk patients. Future study using another cohort of NPC patients should be conducted to validate this prediction model.

a.

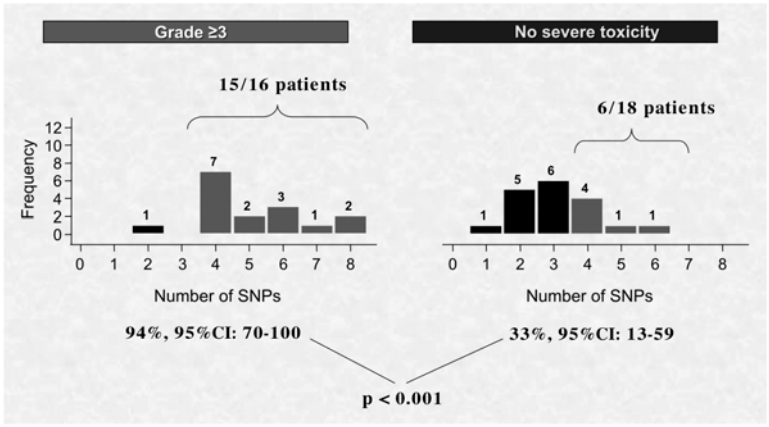


b.

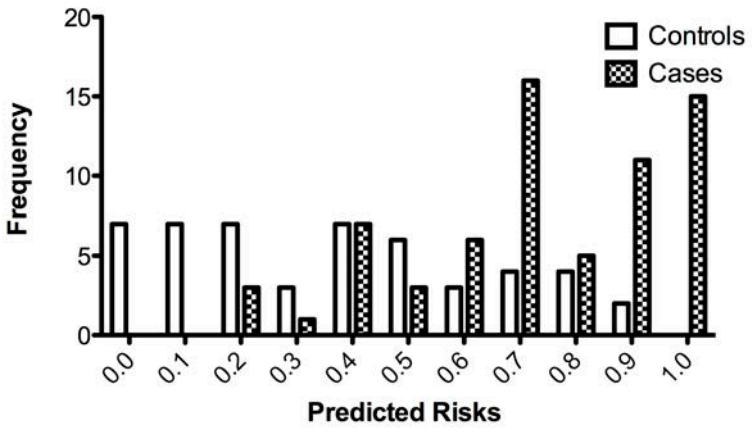


Figure 7.2: Distribution of the number of SNPs and predicted risks. (a) Distribution of the number of SNPs in the radiosensitive group (left) and control group (right) in study by Azria et al. (2008). (b) Distribution of predicted risks from controls and cases in this study. A similar pattern of left skewness of cases is observed.

Table 7.2: Summary statistics of predicted risk in controls and cases

| Group | Control | Case |
|---|---|---|
| Minimum | 7.49 x $10^{-9}$ | 0.20 |
| Maximum | 0.90 | 1.0 |
| Mean | 0.38 | 0.72 |
| SD | 0.27 | 0.21 |

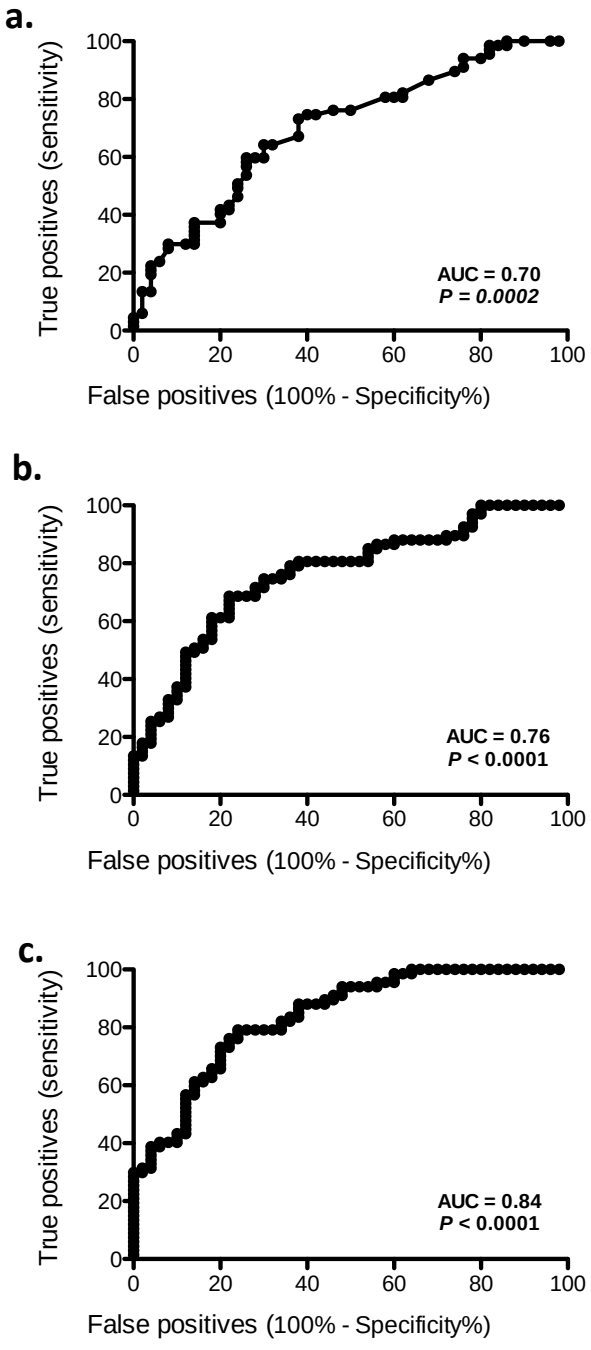


Figure 7.3: Receiver operating characteristic (ROC) curves. Three ROC curves are constructed to obtain area under ROC curves (AUC). (a) ROC curve constructed with clinical data only. (b) ROC curve constructed with genetic factors only. (c) ROC curve constructed with both clinical data and genetic factors.

## 7.2 Meta-analysis

As mentioned in a previous section, the sample size of this study is underpowered to detect SNPs with small to modest effect. Small sample size is one of the major limitations in conducting clinical research since it is difficult to recruit a large number of patients, especially when the number of participating hospitals is small. One way to overcome sample size limitation is to perform a meta-analysis by pooling data from studies with similar protocols. The first meta-analysis investigating the association of SNP rs1800469 in *TGFβ1* and late radiation-induced toxicities in breast cancer patients was published in 2012 (Barnett et al., 2012b). This meta-analysis included 2782 breast cancer patients from 11 cohorts to investigate late fibrosis and overall toxicities and used genetic information and clinical information by univariate and multivariate logistic regression analyses. Significant association between rs1800469 and either fibrosis or overall toxicities was not found in this unbiased meta-analysis.

Oral mucositis, on the other hand, is a type of radiation-induced toxicity specific to head and neck cancers. Information on genetic association and radiation-induced toxicities in head and neck cancer is still limited. Based on published literatures, two genes, *XRCC1* and *XRCC3*, were selected to perform a comprehensive literature search to investigate acute mucositis and genetic association in head and neck cancers. To the best of our knowledge, this is the ***first*** meta-analysis focusing on radiation-induced toxicities associated with head and neck cancer patients. Our results indicated that none of the SNPs from *XRCC1* and *XRCC3* showed significant association in overall population analysis and subgroup analysis (Chapter 4).

With the inclusion of two additional studies, the sample size in meta-analysis

was three-fold higher than our sample size in the candidate-gene association analysis. Although the grading systems of radiation toxicities are well established, classification of "severe" toxicities vary between studies. This variation may introduce significant heterogeneity when performing meta-analysis, in addition to other factors such as ethnic groups, treatment variations and genotyping methods. Besides the two included studies, two other studies identified through literature search were excluded because of insufficient information. Genotype information of non-significant results was not published. In order to enhance data pooling across different studies, standardised reporting guidelines should be used in the future. For example, the use of distinct clinical endpoints, such as erythema and ulceration, may be beneficial during data pooling process (Andreassen et al., 2012b).

Besides establishing standardised guidelines for reporting data, other approaches could also be used to increase sample size, to generate new hypothesis or new findings in meta-analysis. Diagnosis-focused approach and biology-focused approach are two approaches used in most published genetic association studies focusing on radiation-induced toxicities in cancer patients (Andreassen et al., 2012b). Studies adopting diagnosis-focus approach investigate various radiation-induced toxicities in a particular type of cancer. Investigation of genetic variants and the association of erectile function, bladder toxicity, and rectal bleeding in prostate cancer patients is an example of study using diagnosis-focused approach. On the other hand, studies using biology-focused approach investigate the association of genetic variants with non-cancer specific phenotype, such as skin toxicities, in patients with various types of cancers (Andreassen et al., 2012b).

A list of recommended data has been proposed for minimum requirement for data collection in conducting radiogenomic studies (West et al., 2012). This list consists of 37 items in 6 categories related to clinical characteristics, cancer staging,

treatment regimen and treatment-related toxicities. Proposed data collection list is shown in Table 7.3. With the use of recommended list and various research strategies to enhance data pooling, heterogeneity between studies, publication bias and other possible sources of variations can be identified in systematic meta-analysis. Future studies can be designed on the basis of findings and new hypothesis generated from meta-analysis to advance our understanding of the effect and predictiveness of genetic variants on radiation-induced toxicities.

Table 7.3: Recommended data collection list (West et al., 2012)

| Area | Data |
|---|---|
| Patient factors | Date of birth and date of start of radiotherapy to calculate age |
| | Ethnicity |
| | Sex |
| | Diabetes |
| | Rheumatoid arthritis and duration |
| | Systemic lupus erythematosus and duration |
| | Hypertension (use of hypertensive drugs) and duration |
| | Heart disease and duration |
| | Details of other chronic illnesses |
| | Weight and height at start of radiotherapy to calculate body mass index |
| | Smoking history |
| | Inflammatory bowel disease and duration for pelvic radiotherapy |
| | Breast size for breast cancer patients |
| Treatment | Previous surgery |
| | Use of chemotherapy |
| | Use of hormone therapy |
| Radiotherapy | Total dose |
| | Overall treatment time |
| | Dose per fraction |
| | Number of fractions |
| | Use and details of brachytherapy |
| | Use and details of boost |
| | Dose-volume histogram parameters considered relevant for each tumor site |
| Toxicity | Use of widely used scoring system preferable, for example, CTCAE |
| | Collection of physician/nurse reported data |
| | Collection of patient-reported outcomes using a validated scale |
| Cancer | Site |
| | Stage (TNM, overall) |
| | Tumor volume |
| | Grade |
| | Other cancer-specific information, for example, Gleason score for prostate cancers |
| Follow-up | Date of recurrence |
| | Date and grade of toxicity |
| | Date of death |
| | Date last seen |
| | Date of intercurrent death |
| | Date lost to follow-up |

Abbreviations: CTCAE, Common Terminology Criteria for Adverse Events; TNM, Tumor Node Metastasis.

## 7.3 Quantification of radiation-induced damage

Apoptosis can result from lethal DNA damages induced by ionising radiation (Jioner and van der Kogel, 2009). Several pathways and proteins are involved in response to DNA damages such as SSBs and DSBs. During ionising radiation, many cellular proteins, such as ATM, are activated by DSBs, which in turn lead to the activation of many other proteins such as p53, p21 and epigenetic changes such as phospharylation of H2AX, known as $\gamma$H2AX. H2AX belongs to H2A histone family and it is one of the components of the core nucleosome structure wrapped by DNA. Phosphorylated H2AX initiates various pathways related to DNA damage response such as checkpoint activation and apoptosis. Inhibition of ATM, defective phosphorylation of H2AX and other mutated proteins lead to extreme clinical radiosensitivity in genetic disorders (Jioner and van der Kogel, 2009).

Besides the investigation of cellular response in functional studies, direct response such as apoptosis and DNA damages are quantified using various types of assays to establish their correlations with increase radiosensitivity. Inverse correlation between radiation-induced apoptosis and severity of radiation-induced toxicities have been shown by many studies, but with conflicting results (Henríquez-Hernández et al., 2012). Initial DNA damages, on the other hand, also showed inverse correlation to the level of radiation-induced apoptosis (Pinar et al., 2010). Compared to techniques used to measure DNA damages, such as comet assay and PFGE, measurement performed with flow cytometry provides a more rapid, quantitative and less laborious method to directly identify cell response. With the use of various flow cytometry-based assays, using a flow cytometry-based detection method seems to be the most suitable way to apply in a clinical setting. As a result, quantification of apoptosis on PBMCs isolated from Chinese NPC patients

through *in vitro* irradiation by means of flow cytometry is the third approach adopted in this study. FITC-conjugated annexin V and PI were used to identify apoptotic cells induced by radiation. Although significant results have been reported (Henríquez-Hernández et al., 2012), our study was limited by the small sample size that overall findings indicated that difference of radiation-induced apoptosis between the normal and sensitive patients was undistinguishable.

Owing to inter-study variations such as in study design, sample size and definition of clinical endpoints as hypersensitivity (Section 6.5), findings are often conflicting or incomparable. Inter-laboratory comparisons were performed by the same research group (Greve et al., 2012, 2009). Three techniques used to measure radiation-induced cell death (Annexin V and PI) and induction and repair of DNA strand breaks (Comet Assay and induction of $\gamma$H2AX foci) were validated by five laboratories (Greve et al., 2012). Cryopreserved PBMCs and LCLs derived from the same group of cancer patients were used in five laboratories. Summary of assays performed by participating laboratories are shown in Table 7.4. None of the assays, either using PBMCs or LCLs, was able to distinguish age- and sex-matched, radiosensitive patients and non-radiosensitive patients even with the use of standardised protocols across all laboratories. Considerable inter-individual variations, either PBMCs or LCLs, were also reported. Based on previous findings and our results, the effect size of radiation-induced damages between radiosensitive and non-radiosensitive patients is likely to be small, unlike clinical features such as extreme radiosensitivity in genetic disorders. A larger sample size, in addition to detail clinical data as suggested in Section 7.2, is needed in order to categorise patients, no matter which assays and parameters are chosen to measure radiation-induced damages. Sample size and power calculation based on our study findinges was shown in Figure 7.4.

Table 7.4: Summary of assays used in inter-laboratory comparison study

| Assay | Parameters | Centre A | Centre B | Centre C | Centre D | Centre E |
|---|---|---|---|---|---|---|
| Annexin V/PI | Apoptosis | X | X | X | | |
| $\gamma$H2AX foci | Results of DNA DSBs | | X | X | | |
| Comet Assay | Induction and repair of DNA strand breaks | | | | X | X |

Assays performed by each participating centre are indicated as X. Total five laboratories were participated in the inter-laboratory validation study (Greve et al., 2012).

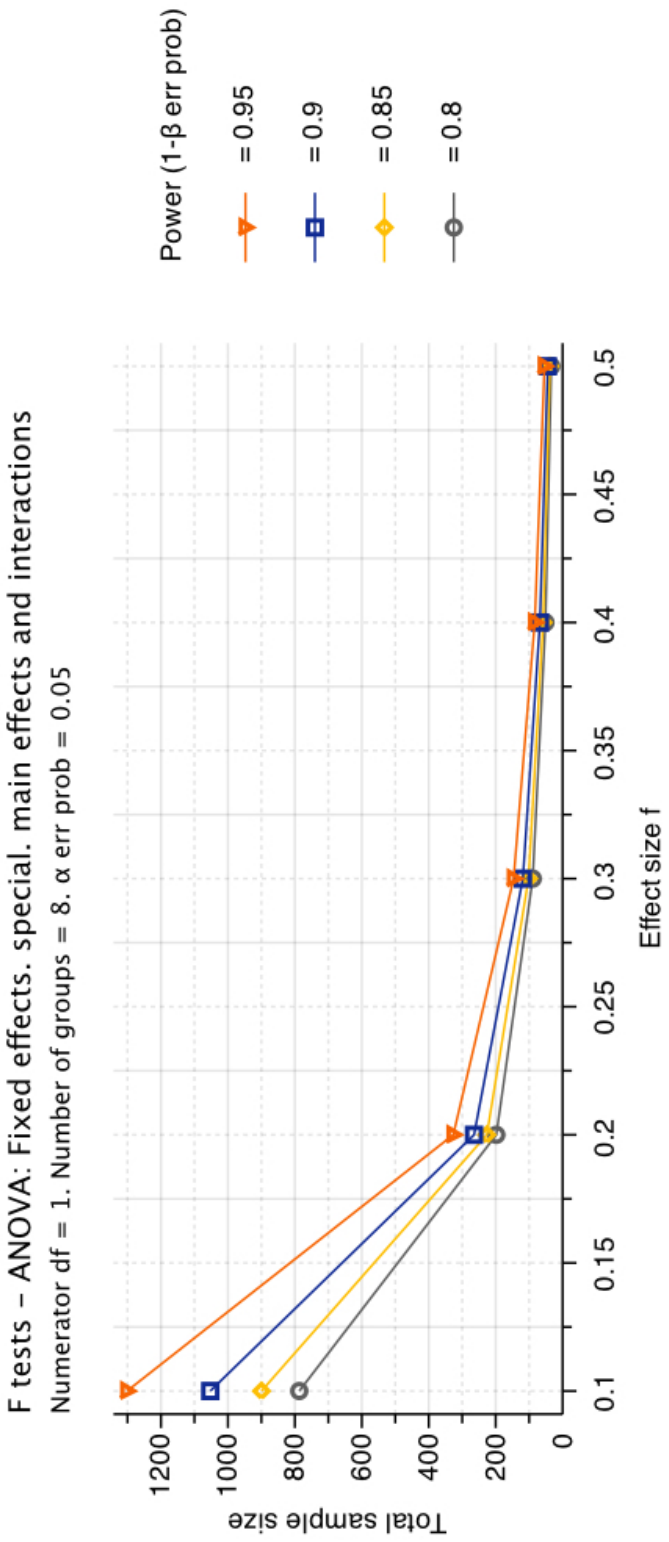


Figure 7.4: Sample size and power calculation based on observed data in predictive assay

## 7.4 Future direction

Our results of genetic association using a candidate-gene approach (Chapter 3), data pooled by meta-analysis (Chapter 4), and quantification of *in vitro* radiation-induced apoptosis (Chapter 6) support the notion that improvements should be made in order to apply these prediction methods clinically. Further studies should be performed with improvements based on our findings in order to achieve higher accuracy in prediction and differentiation of radiosensitive patients in the future.

### 7.4.1 Genome-wide association studies (GWAS)

The emergence of the GWAS era may help to obtain comprehensive individual SNP profile and improve our understanding of radiation-induced toxicities in different cancers. Common variants associated with many complex diseases have been identified through GWAS (Wray et al., 2013). The first GWAS in the field of radiogenomics was published in 2010 (Kerns et al., 2010). A cancer-type and possibly ethnic group-specific biomarker was identified in African prostate cancer patients (Kerns et al., 2010). This SNP (rs2268363) is located in follicle-stimulating hormone receptor (FSHR) gene that is associated with erectile dysfunction. A 2-stage GWAS composed of mixed ethnic populations, predominantly European ancestry, was published in 2013 by the same research group (Kerns et al., 2013). Findings from two GWAS suggested that SNPs associated with erectile dysfunctions in African ancentry may not have the same association in European ancentry because of variation in allelic frequencies in different ethnic groups (Kerns et al., 2013).

With the availability of high throughput genotyping, the number of GWAS has been increasing. Although small sample size is also a major limitation in GWAS, comprehensive genetic profile could be obtained from radiosensitive patients to narrow the selection of candidate genes for future association studies. Besides,

clinical endpoints such as fibrosis and telangiectasia are common toxicities in patients with different cancers. It is probably beneficial to perform combined and subgroup analyses by grouping patients with various cancers from different ethnic origins that suffered with the same clinical endpoint to overcome the sample size limitation and to enhance our understanding of underlying pathogenic mechanism.

### 7.4.2 International collaboration

The Radiogenomics Consortium established in 2009 is an international collaboration of research groups with interests in identifying genetic variants associated with radiation toxicities (West et al., 2010). As of May 2013, over 80 institutions in 19 countries are participating in this consortium (`http://epi.grants.cancer.gov/radiogenomics/`). International collaboration enables researchers to establish standardised guidelines, to increase sample sizes, and to conduct studies with adequate power when performing radiogenetics/radiogenomics studies. Overall population and subgroup analyses could also be performed to study the effect of genetic variants in different ethnic origins through International collaboration.

### 7.4.3 Gene expression profiles

Besides the investigation of radiation-induced toxicities in respect of genetic variations and direct radiation-induced cell response, gene expression profiling may be useful in understanding between-individual variations in radiation sensitivity. Gene expression levels between radiosensitive and non-radiosensitive patients revealed a large deviation of radiation response in two groups of individuals (Greve et al., 2012; Henríquez-Hernández et al., 2009; Mayer et al., 2011; Rødningen et al., 2008; Smirnov et al., 2009; Sonis et al., 2007; Svensson et al., 2006). Radiation-induced toxicities are not caused by rare mutations as Mendelian diseases such as

enzymatic deficiencies or truncated proteins, but the end result of complex traits involved in many signalling pathways (Sonis, 2009). Recent studies suggested that individual variations in gene expression may increase the risk of developing severe radiation-induced toxicities (Sonis, 2009). Gene expression levels showed 1.5-fold changes in over 3000 genes at 2 hours after irradiation. The most significant associated genes identified by linkage analysis are involved in cell cycle and apoptosis regulation (Greve et al., 2012; Smirnov et al., 2009). Other studies also identified genes involved in cell cycle regulation by comparing gene expression profiles of healthy individuals and cancer patients (Henríquez-Hernández et al., 2009; Mayer et al., 2011). Some regulators not previously known were identified in regulating changes in expression level during radiation (Smirnov et al., 2009). However, results were unable to replicate due to between-study variations such as cancer types, clinical endpoints, and radiation doses (Henríquez-Hernández et al., 2009; Mayer et al., 2011). With the availability of various bioinformatic tools, association of genetic data from GWAS and changes of gene expression levels can be interpreted using techniques such as quantitative levels of expression (eQTL) mapping (Cookson et al., 2009). This technique is particularly useful to interpret the effect or the role of genetic variants with unknown biological functions (Cookson et al., 2009). Using eQTL mapping, several *cis*-acting regulatory SNPs involved in complex diseases have been identified (Cookson et al., 2009). Further investigation is needed to extend and advance the understanding of complex genetic control in radiation-induced toxicities, not only limited to common genetic variations and direct radiation response at the cellular level, but also individual gene expression profiles (Henríquez-Hernández et al., 2009; Mayer et al., 2011; Svensson et al., 2006).

### 7.4.4 Other potential areas

#### 7.4.4.1 Epigenetic changes

DNA methylation and histone modification are epigenetic changes that are not detected by GWAS and measurement of radiation-induced response through apoptosis assays. Although investigation of epigenetic changes is of particular interests in many research studies, little is known about their role with regard to radiation toxicities (West et al., 2012). Phosphorylation of histone H2AX is an example of epigenetic changes in response to DNA damages. Increased radiosensitivity in H2AX-deficient mouse embryonic stem cells has been reported (Bassing et al., 2002). Variation in $\gamma$H2AX foci induction has been used to assess DNA strand damages by radiation in many studies although the findings are not definitive (Finnon et al., 2012).

Besides the investigation of histone modification, epigenetic changes induced by radiation have been assessed by *in vitro* studies using animal models or *in vitro* studies. DNA regions with high content of G and C dinucleotides, known as CG or CpG islands, are associated with transcription start sites that regulate gene expression (Jones, 2012). DNA methylation occurring at CpG islands leads to gene silencing in cancer cells. On the other hand, the function of methylated non-CpG islands is still unclear (Jones, 2012). Global genome methylation status were observed in lung tissue, but not liver and spleen tissues in mice 1 month after acute exposure to radiation (Pogribny et al., 2004). These findings suggested that epigenetic changes induced by radiation are dose-dependent, tissue-specific and related to DNA repair pathways (Pogribny et al., 2004). Epigenetic changes can be investigated alongside with gene expression levels in radiosensitive and non-radiosensitive individuals to unravel the mechanism of individual variations in radiation toxicities.

#### 7.4.4.2 Bystander effects and genomic instability of non-irradiated cells

Bystander effect is a phenomenon in which non-irradiated cells exhibit similar response as their neighbouring irradiated cells (Lorimore et al., 2003). These non-targeted effects are caused by intercellular communication mechanisms in which stress signals are transmitted from irradiated cells to non-irradiated cells (Azzam et al., 2013). Genomic instability was observed in irradiated cells, non-irradiated cells and their progeny. Reproductive potential of irradiated cells or bystander cells may persist up to six generations of cell replication that chromosome aberrations, enhanced death rate and lethal gene mutations have been observed in their progeny randomly (Lorimore et al., 2003). As a result, bystander effects and genomic instability may have a significant implication in evaluating radiation response in normal cells and cancer cells. A simplified version of transmission mechanism is illustrated in Figure 7.5.

#### 7.4.4.3 Apoptosis and autophagy

Apoptosis is type I programmed cell death mediated by proteins belonging to the B-cell lymphoma 2 (Bcl-2) family such as Bax and Bak (Moretti et al., 2007). However, little is known about the role of autophagy - type II programmed cell death - during radiation-induced cell death. Apoptosis mediated by Bax and Bak has been reported with contribution of less than 20% to radiation-induced cell death (Moretti et al., 2007). Autophagic cell death is well-characterised, although the exact regulation mechanism is still unclear (Moretti et al., 2007). Autophagy has been shown to have cell survival advantage under harsh conditions such as exposure to ionising radiation and nutrient depletion (Kuwahara et al., 2011; Wirawan et al., 2012). Since apoptosis and autophagy share many molecular regulators that are inter-connected in both pathways (Eisenberg-Lerner et al., 2009), quantifica-

tion of radiation-induced apoptosis may not be sufficient to distinguish patients with normal sensitivity and hypersensitivity to radiation. It will be interesting to investigate the potential role of autophagy in normal tissue radiosensitivity, as well as cancer cells radiosensitivity, to improve treatment outcome in future studies.

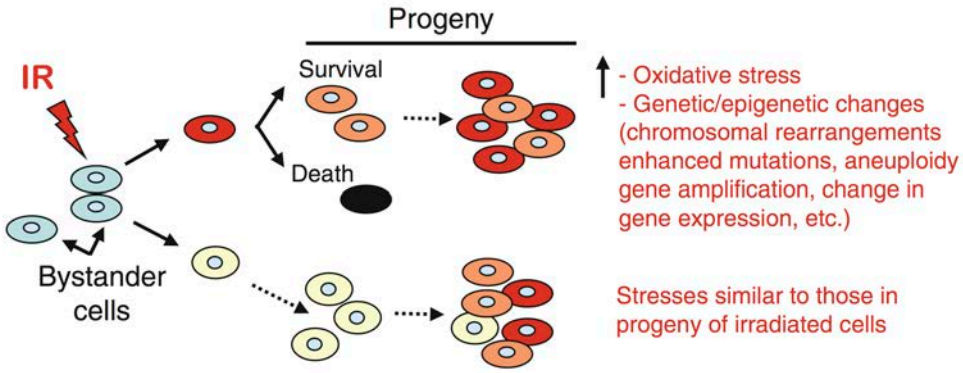


Figure 7.5: Bystander effects (non-targeted effects) induced by ionising radiation (IR). Apparent normal cells are shown in yellow. Dead cells are shown in black. Cells with different levels of damages such as genomic instability and mutations are shown in coral or red. Cell signals are transmitted from irradiated cells to nearby, non-irradiated/bystander cells. Progeny of irradiated cells and bystander cells may have similar radiation-induced response (Azzam et al., 2013).

# Chapter 8

# Summary and Conclusion

This study investigated the potential prediction of radiation-induced toxicities by means of three approaches in Chinese NPC patients. Tag SNPs and functional SNPs were selected from *ATM*, *SOD2*, *TGFβ1*, *TP53*, *XRCC1* and *XRCC3* and their role in contributing to individual variation of radiation-induced toxicities were investigated. This study is the ***first*** genetic association study investigating our local Chinese population. None of the investigated SNPs showed significant association after correction for multiple testing ($P$>0.05).

A meta-analysis was performed to investigate the association of genetic variants in *XRCC1* and *XRCC3* with radiation-induced mucositis, which occurs only in head and neck caner patients. Two studies were identified with adequate data from a comprehensive literature search. This study is the ***first*** meta-analysis focusing on radiation-induced mucositis in head and neck cancers. No association of *XRCC1* and *XRCC3* with radiation-induced mucositis was found in overall population analysis and subgroup analysis in dominant, recessive, and allelic models ($P$>0.05).

Quantification of radiation-induced apoptosis by using PBMCs isolated from cancer patients was the third approach used in study to differentiate radiosensitive and non-radiosensitive patients. PBMCs were irradiated at three radiation doses (0 Gy, 2 Gy, and 8 Gy). Percentage of radiation-induced apoptosis was measured 2 hours (baseline) and 18 hours by flow cytometry. No significant difference was found in the percentage of radiation-induced apoptosis between radiosensitive and non-radiosensitive patients ($P>0.05$).

The most apparent limitation of this study lies in the fact that inadequate number of NPC patients recruited. The present study has only explored two types of acute toxicities and one type of late toxicity due to the limited availability of clinical data. Individual variation in radiation sensitivity is the accumulation of small to modest effect contributed by genetic variants or DNA damage response pathways. Future studies with larger sample size are needed in order to overcome this limitation. Predicting individual susceptibility to radiation could be achieved with higher accuracy by generating individual SNP profile, in addition to more detailed clinical information. Quantification of radiation-induced apoptosis and monitoring gene expression changes may help to study radiation-induced effects at the cellular level at different time point in future.

# Appendix A

# Consent forms

# Research Study Information Sheet

**Title of Project:**
Role of genetic factors in post-radiotherapy complications in patients with Nasopharyngeal Carcinoma

**Principle Investigator:**
Dr. Vincent Wing-Cheung Wu
Department of Health Technology and Informatics, The Hong Kong Polytechnic University
Tel: 3400

**Co-investigators:**
Professor Shea-ping Yip
Department of Health Technology and Informatics, The Hong Kong Polytechnic University
Tel: 3400

Professor Dora LW Kwong
Department of Clinical Oncology, Li Ka Shing Faculty of Medicine
The University of Hong Kong
Tel: 2255

**Aims of the Project:**

This study aims to investigate how genetic variation affects the development of post-radiotherapy complications in NPC patient by genotyping related genetic information from NPC patients treated with different radiotherapy techniques.

**What do volunteers for the study have to do?**

If you volunteer for the study, you will be asked:

1. to sign an informed consent form that states you understand the information presented on this sheet and willing to participate in this study
2. to give some personal information (such as name, age) and information of your medical history. All information, results, and data will be kept confidential, and will only be accessed by the investigators
3. to donate 15 ml blood for DNA analysis

**Duration of examination**

The blood extraction will take about 5 minutes.

**Any medication involves in the study?**

No

**Is there any discomfort during the blood extraction?**

No. The potential hazards include pain and occasional bruising following venepuncture, but without serious consequences.

**Can a volunteer withdraw from the study?**

Yes, you can stop participating in the study at any time with no penalty.

**Any benefit to the volunteer?**

There is no intended clinical benefit to you from taking part in this study. Your participation will generate useful data for identifying patients with high risk of suffering various severe adverse effects before any treatment and provide better patient care to these patients in the future.

**Can I get more information on the study?**

Yes, contact Dr. Vincent Wu and he will try to answer any questions you may have.

**This study was approved by the Ethics Sub-Committee, Department of Health Technology and Informatics, the Hong Kong Polytechnic University. However, if you think there are any procedures that seem to be unethical, please do not hesitate to contact the Secretary of the Human Subjects Ethics Sub-committee of the Hong Kong Polytechnic University in writing c/o Human Resources Office of the University.**

# 研 究 資 料 詳 情 及 同 意 書

**研 究 題 目 ：**
遺 傳 因 素 對 鼻 咽 癌 病 人 在 接 受 強 度 調 控 放 射 療 法 或 一 般 放 射 療 法 並 發 症 的 影 響

**主 研 究 員 ：**
胡 永 祥 博 士
香 港 理 工 大 學 醫 療 科 技 及 資 訊 學 系
電 話 ：3400

**副 研 究 員 ：**
葉 社 平 教 授
香 港 理 工 大 學 醫 療 科 技 及 資 訊 學 系
電 話 ：3400

鄺 麗 雲 教 授
香 港 大 學 李 嘉 誠 醫 學 院 臨 床 腫 瘤 科
電 話 ：2255

**研 究 目 的 ：**

研 究 旨 在 探 討 基 因 變 異 如 何 影 響 放 射 療 法 後 併 發 症。

**自願參加者需要怎樣做？**

如你願意參加這項研究，你將會需要：

1. 簽署一張研究同意書以表示你明白本研究資料詳情和願意參加這項研究。

2. 提供一些個人資料，所有資料和研究結果將會保密和只許上列研究員參閱。

3. 接受一次抽血化驗(大約15毫升血液)作為有關你的基因分析。

**所需時間**

整個抽血過程大概需時5分鐘。

**這項研究需要使用藥物嗎？**

不需要。

**抽血會引起身體不適嗎？**

不會，但潛在的危險包括疼痛，靜脈穿刺後可能有瘀傷，但不會造成嚴重後果。

**參加者可否中途退出這項研究計劃？**

你可以隨時退出這項研究而不會有任何懲罰。

**參加者會否得到任何利益?**

您並不會因參與研究而得到直接利益。這個研究將有利於研究人員在未來找出高危患者並在作出任何治療前提供更好的醫護服務去減少痛苦。

**我可以得到更多此項研究的資料嗎？**

你可以聯絡胡永祥博士。他會盡量解答你的問題。

**本研究是得到香港理工大學醫療科技及資訊學系道德委員會批準。如你覺得任何程序侵犯你的個人權益，你可以書面向香港理工大學道德委員會祕書提出投訴及轉交理工大學人力資源部。**

THE HONG KONG
POLYTECHNIC UNIVERSITY
香港理工大學

## *Research Study Consent Form*

Project Title: Role of genetic factors in post-radiotherapy complications in patients with Nasopharyngeal Carcinoma

I, _____ (HKID No._____), hereby consent to take part in the above study.

I confirm that I have read and understood the information sheet for the above study and have had the opportunity to ask questions.

I understand that the data of the study will be kept in a safe place and will only be accessed by the investigators. I also realise that the data will be kept for one more year after the completion of study for producing research reports and publications.

I realise that I can withdraw from the study at any time, and may contact the Secretary of the Human Subjects Ethics Sub-committee of The Hong Kong Polytechnic University with any enquiries or complaints.

| | |
|---|---|
| _____ | _____ |
| Investigator's Signature | Patient's Signature |
| _____ | _____ |
| Investigator's Name | Patient's Name |
| _____ | _____ |
| Date | Date |

THE HONG KONG
POLYTECHNIC UNIVERSITY
香港理工大學

## *II. 研究同意書*

研究題目：遺傳因素對鼻咽癌病人在接受強度調控放射療法或一般放射療法並發症的影響

本人_____(香港身分證號碼:_____)茲同意接受此上述研究。

我已詳細閱讀這份研究資料及同意書，並且已有足夠的時間對這項研究提出詢問。

本人知道此研究之數據將會存放在一安全地方及只會給此研究之研究員使用。本人也明悉研究數據將會在此研究結束後儲存一年作選寫研究報告之用。

本人更明悉，本人有權隨時拒絕接受此研究和向香港理工大學道德委員會祕書提出咨詢或投訴。

| | |
|---|---|
| _____ | _____ |
| 研究員簽署 | 病人簽署 |
| _____ | _____ |
| 研究員姓名 | 病人姓名 |
| _____ | _____ |
| 日期 | 日期 |

# Research Study Information Sheet

**Title of Project:**
Gene expression and lymphocyte viability after radiation as a predictor for individual radiosensitivity for nasopharyngeal carcinoma [GEN-RAD]

**Research Coordinators:**
Ms. Isabella Cheuk Wai Yin
Department of Health Technology and Informatics, The Hong Kong Polytechnic University
Tel: 3400

Ms. Nerissa Lee Chui-mei
Department of Oncology, Princess Margaret Hospital
Tel: 2990

**Aims of the Project:**

The aims of this research study are to establish a correlation of cell-based assays and acute post-RT complications with respect to NPC patients. Effects of genetic variants between patients with and without acute post-RT complications with respect to lymphocyte apoptosis and genes expression levels will be investigated.

**What do volunteers for the study have to do?**

If you volunteer for the study, you will be asked:

1. to sign an informed consent form that states you understand the information presented on this sheet and willing to participate in this study
2. to give some personal information (such as name, age) and information of your medical history. All information, results, and data will be kept confidential, and will only be accessed by the investigators
3. to donate 6 ml blood for DNA analysis and related studies

**Duration of examination**

The blood extraction will take about 5 minutes.

**Any medication involves in the study?**

No

**Is there any discomfort during the blood extraction?**

No. The potential hazards include pain and occasional bruising following venepuncture, but without serious consequences.

**Can a volunteer withdraw from the study?**

Yes, you can stop participating in the study at any time with no penalty.

**Any benefit to the volunteer?**

There is no intended clinical benefit to you from taking part in this study. Your participation will generate useful data for identifying patients with high risk of suffering various severe adverse effects before any treatment and provide better patient care to these patients in the future.

**Can I get more information on the study?**

Yes, contact Ms. Isabella Cheuk and she will try to answer any questions you may have.

**This study was approved by the Ethics Sub-Committee, Department of Health Technology and Informatics, the Hong Kong Polytechnic University. However, if you think there are any procedures that seem to be unethical, please do not hesitate to contact the Secretary of the Human Subjects Ethics Sub-committee of the Hong Kong Polytechnic University in writing c/o Human Resources Office of the University.**

# 研 究 資 料 詳 情 及 同 意 書

研 究 題 目 ：
以 基 因 表 達 和 血 液 中 的 淋 巴 細 胞 作 為 基 礎 預 測 鼻 咽 癌 病 人 在 接 受 強 度 調 控 放 射 療 法 或 一 般 放 射 療 法 並 發 症 的 反 應 [GEN-RAD]

研 究 員 ：
卓 慧 賢 小 姐
香 港 理 工 大 學 醫 療 科 技 及 資 訊 學 系
電 話 ：3400

李 翠 媚 小 姐
瑪 嘉 烈 醫 院 腫 瘤 科
電 話 ：2990

研 究 目 的 ：

此 項 研 究 的 目 的 是 旨 在 探 討 以 基 因 表 達 ， 基 因 變 異 和 血 液 中 的 淋 巴 細 胞 作 為 基 礎 作 為 預 測 鼻 咽 癌 病 人 在 接 受 強 度 調 控 放 射 療 法 或 一 般 放 射 療 法 並 發 症 的 反 應 的 可 能 性 。

自願參加者需要怎樣做？

如你願意參加這項研究，你將會需要：
1. 簽署一張研究同意書以表示你明白本研究資料詳情和願意參加這項研究。
2. 提供一些個人資料，所有資料和研究結果將會保密和只許上列研究員參閱。
3. 接受一次抽血化驗(大約6毫升血液)作為有關你的基因分析及有關的研究。

所需時間
整個抽血過程大概需時5分鐘。

這項研究需要使用藥物嗎？
不需要。

抽血會引起身體不適嗎？
不會，但潛在的危險包括疼痛，靜脈穿刺後可能有瘀傷，但不會造成嚴重後果。

參加者可否中途退出這項研究計劃？
你可以隨時退出這項研究而不會有任何懲罰。

參加者會否得到任何利益?
您並不會因參與研究而得到直接利益。這個研究將有利於研究人員在未來找出高危患者並在作出任何治療前提供更好的醫護服務去減少痛苦。

我可以得到更多此項研究的資料嗎？
你可以聯絡卓慧賢小姐。她會盡量解答你的問題。

本研究是得到香港理工大學醫療科技及資訊學系道德委員會批準。如你覺得任何程序侵犯你的個人權益，你可以書面向香港理工大學道德委員會祕書提出投訴及轉交理工大學人力資源部。

THE HONG KONG
POLYTECHNIC UNIVERSITY
香港理工大學

## *Research Study Consent Form*

Project Title: Gene expression and lymphocyte viability after radiation as a predictor for individual radiosensitivity for nasopharyngeal carcinoma [GEN-RAD]

I, _____ (HKID No._____), hereby consent to take part in the above study.

I confirm that I have read and understood the information sheet for the above study and have had the opportunity to ask questions.

I understand that the data of the study will be kept in a safe place and will only be accessed by the investigators. I also realise that the data will be kept for three more year after the completion of study for producing research reports and publications.

I realise that I can withdraw from the study at any time, and may contact the Secretary of the Human Subjects Ethics Sub-committee of The Hong Kong Polytechnic University with any enquiries or complaints.

| | |
|---|---|
| _____ | _____ |
| Investigator's Signature | Patient's Signature |
| _____ | _____ |
| Investigator's Name | Patient's Name |
| _____ | _____ |
| Date | Date |

## *II. 研究同意書*

研究題目：以基因表達和血液中的淋巴細胞作為基礎預測鼻咽癌病人在接受強度調控放射療法或一般放射療法並發症的反應 [GEN-RAD]

本人 _____(香港身分證號碼:_____) 茲同意接受此上述研究。

我已詳細閱讀這份研究資料及同意書，並且已有足夠的時間對這項研究提出詢問。

本人知道此研究之數據將會存放在一安全地方及只會給此研究之研究員使用。本人也明悉研究數據將會在此研究結束後儲存一年作選寫研究報告之用。

本人更明悉，本人有權隨時拒絕接受此研究和向香港理工大學道德委員會祕書提出咨詢或投訴。

| | |
|---|---|
| _____ | _____ |
| 研究員簽署 | 病人簽署 |
| _____ | _____ |
| 研究員姓名 | 病人姓名 |
| _____ | _____ |
| 日期 | 日期 |

# Bibliography


Alsner, J., Andreassen, C. N. and Overgaard, J. (2008), 'Genetic markers for prediction of normal tissue toxicity after radiotherapy', *Semin Radiat Oncol* **18**(2), 126–135.

Andreassen, C. N. and Alsner, J. (2009), 'Genetic variants and normal tissue toxicity after radiotherapy: a systematic review', *Radiother Oncol* **92**(3), 299–309.

Andreassen, C. N., Alsner, J., Overgaard, M. and Overgaard, J. (2003), 'Prediction of normal tissue radiosensitivity from polymorphisms in candidate genes.', *Radiother Oncol* **69**(2), 127.

Andreassen, C. N., Alsner, J., Overgaard, M., Sørensen, F. B. and Overgaard, J. (2006a), 'Risk of radiation-induced subcutaneous fibrosis in relation to single nucleotide polymorphisms in TGFB1, SOD2, XRCC1, XRCC3, APEXand ATMndash; a study based on DNA from formalin fixed paraffin embedded tissue samples', *Int J Radiat Biol* **82**(8), 577–586.

Andreassen, C. N., Barnett, G. C., Langendijk, J. A., Alsner, J., De Ruysscher, D., Krause, M., Bentzen, S. M., Haviland, J. S., Griffin, C., Poortmans, P. and Yarnold, J. R. (2012b), 'Conducting radiogenomic research–do not forget careful consideration of the clinical data.', *Radiother Oncol* **105**(3), 337–340.

Andreassen, C. N., Dikomey, E., Parliament, M. and West, C. M. L. (2012a), 'Will SNPs be useful predictors of normal tissue radiosensitivity in the future?', *Radiother Oncol* **105**(3), 283–288.

Andreassen, C. N., Overgaard, J., Alsner, J., Overgaard, M., Herskind, C., Cesaretti, J. A., Atencio, D. P., Green, S., Formenti, S. C., Stock, R. G. and Rosenstein, B. S. (2006b), 'ATM sequence variants and risk of radiation-induced subcutaneous fibrosis after postmastectomy radiotherapy', *Int J Radiat Oncol Biol Phys* **64**(3), 776–783.

Azria, D., Betz, M., Bourgier, C., Jeanneret Sozzi, W. and Ozsahin, M. (2012), 'Identifying patients at risk for late radiation-induced toxicity.', *Crit. Rev. Oncol. Hematol.* **84 Suppl 1**, e35–41.

Azria, D., Ozsahin, M., Kramar, A., Peters, S., Atencio, D. P., Crompton, N., Mornex, F., Pelegrin, A., Dubois, J. B., Mirimanoff, R. O. and Rosenstein, B. S. (2008), 'Single Nucleotide Polymorphisms, Apoptosis, and the Development of Severe Late Adverse Effects After Radiotherapy', *Clin Cancer Res* **14**(19), 6284–6288.

Azzam, E. I., de Toledo, S. M., Harris, A. L., Ivanov, V., Zhou, H., Amundson, S. A., Lieberman, H. B. and Hei, T. K. (2013), The Ionizing Radiation-Induced Bystander Effect: Evidence, Mechanism, and Significance, *in* 'Pathobiology of Cancer Regimen-Related Toxicities', Springer, pp. 35–61.

Barnett, G. C., Coles, C. E., Elliott, R. M., Baynes, C., Luccarini, C., Conroy, D., Wilkinson, J. S., Tyrer, J., Misra, V., Platte, R., Gulliford, S. L., Sydes, M. R., Hall, E., Bentzen, S. M., Dearnaley, D. P., Burnet, N. G., Pharoah, P. D. P., Dunning, A. M. and West, C. M. L. (2012a), 'Independent validation of genes and polymorphisms reported to be associated with radiation toxicity: a prospective analysis study.', *Lancet Oncol.* **13**(1), 65–77.

Barnett, G. C., Elliott, R. M., Alsner, J., Andreassen, C. N., Abdelhay, O., Burnet, N. G., Chang-Claude, J., Coles, C. E., Gutiérrez-Enríquez, S., Fuentes-Raspall, M. J., Alonso-Muñoz, M. C., Kerns, S., Raabe, A., Symonds, R. P., Seibold, P., Talbot, C. J., Wenz, F., Wilkinson, J., Yarnold, J., Dunning, A. M., Rosenstein, B. S., West, C. M. L. and Bentzen, S. M. (2012b), 'Individual patient data meta-analysis shows no association between the SNP rs1800469 in TGFB and late radiotherapy toxicity', *Radiother Oncol* **105**(3), 289–295.

Barnett, G. C., West, C. M. L., Dunning, A. M., Elliott, R. M., Coles, C. E., Pharoah, P. D. P. and Burnet, N. G. (2009), 'Normal tissue reactions to radiotherapy: towards tailoring treatment dose by genotype', *Nat Rev Cancer* **9**(2), 134–142.

Barrett, J. C., Fry, B., Maller, J. and Daly, M. J. (2005), 'Haploview: analysis and visualization of LD and haplotype maps', *Bioinformatics* **21**(2), 263–265.

Bartsch, H., Dally, H., Popanda, O., Risch, A. and Schmezer, P. (2007), 'Genetic risk profiles for cancer susceptibility and therapy response.', *Recent Results Cancer Res.* **174**, 19–36.

Bassing, C. H., Chua, K. F., Sekiguchi, J., Suh, H., Whitlow, S. R., Fleming, J. C., Monroe, B. C., Ciccone, D. N., Yan, C., Vlasakova, K., Livingston, D. M., Ferguson, D. O., Scully, R. and Alt, F. W. (2002), 'Increased ionizing radiation sensitivity and genomic instability in the absence of histone H2AX.', *Proc. Natl. Acad. Sci. U.S.A.* **99**(12), 8173–8178.

Becker-Catania, S. G., Chen, G., Hwang, M. J., Wang, Z., Sun, X., Sanal, O., Bernatowska-Matuszkiewicz, E., Chessa, L., Lee, E. Y. and Gatti, R. A. (2000), 'Ataxia-telangiectasia: phenotype/genotype studies of ATM protein expression, mutations, and radiosensitivity', *Mol Genet Metab* **70**(2), 122–133.

Bei, J.-X., Li, Y., Jia, W.-H., Feng, B.-J., Zhou, G., Chen, L.-Z., Feng, Q.-S., Low, H.-Q., Zhang, H., He, F., Tai, E. S., Kang, T., Liu, E. T., Liu, J. and Zeng, Y.-X. (2010), 'A genome-wide association study of nasopharyngeal carcinoma identifies three new susceptibility loci.', *Nat Genet* **42**(7), 599–603.

Bentzen, S. M. (2006), 'Preventing or reducing late side effects of radiation therapy: radiobiology meets molecular pathology', *Nat Rev Cancer* **6**(9), 702–713.

Bentzen, S. M., Constine, L. S., Deasy, J. O., Eisbruch, A., Jackson, A., Marks, L. B., Ten Haken, R. K. and Yorke, E. D. (2010), 'Quantitative Analyses of Normal Tissue Effects in the Clinic (QUANTEC): an introduction to the scientific issues.', *Int J Radiat Oncol Biol Phys* **76**(3 Suppl), S3–9.

Berman, N. G. and Parker, R. A. (2002), 'Meta-analysis: neither quick nor easy.', *BMC Med Res Methodol* **2**, 10.

Bordon, E., Henríquez-Hernández, L. A., Lara, P. C., Pinar, B., Fontes, F., Rodriguez-Gallego, C. and Lloret, M. (2009), 'Prediction of clinical toxicity in localized cervical carcinoma by radio-induced apoptosis study in peripheral blood lymphocytes (PBLs).', *Radiat Oncol* **4**, 58.

Bordon, E., Henríquez-Hernández, L. A., Lara, P. C., Ruíz, A., Pinar, B., Rodriguez-Gallego, C. and Lloret, M. (2010), 'Prediction of clinical toxicity in locally advanced head and neck cancer patients by radio-induced apoptosis in peripheral blood lymphocytes (PBLs)', *Radiat Oncol* **5**(1), 4.

Borgmann, K., Röper, B., El-Awady, R., Brackrock, S., Bigalke, M., Dörk, T., Alberti, W., Dikomey, E. and Dahm-Daphi, J. (2002), 'Indicators of late normal tissue response after radiotherapy for head and neck cancer: fibroblasts, lymphocytes, genetics, DNA repair, and chromosome aberrations', *Radiother Oncol* **64**(2), 141–152.

Bryant, P. E., Gray, L., Riches, A. C., Steel, C. M., Finnon, P., Howe, O., Kesterton, I., Vral, A., Curwen, G. B. and Smart, V. (2002), 'Technical report. The G2 chromosomal radiosensitivity assay', *Int J Radiat Biol* **78**(9), 863–866.

Chan, A. T. C. (2010), 'Nasopharyngeal carcinoma', *Ann Oncol* **21**(Supplement 7), vii308–vii312.

Chan, A. T. C., Teo, P. M. L. and Johnson, P. J. (2002), 'Nasopharyngeal carcinoma', *Ann Oncol* **13**(7), 1007–1015.

Chang-Claude, J., Ambrosone, C. B., Lilla, C., Kropp, S., Helmbold, I., von Fournier, D., Haase, W., Sautter-Bihl, M.-L., Wenz, F., Schmezer, P. and Popanda, O. (2009), 'Genetic polymorphisms in DNA repair and damage response genes and late normal tissue complications of radiotherapy for breast cancer.', *Br J Cancer* **100**(10), 1680–1686.

Chang, E. T. and Adami, H. O. (2006), 'The Enigmatic Epidemiology of Nasopharyngeal Carcinoma', *Cancer Epidemiol Biomarkers Prev* **15**(10), 1765–1777.

Chau, R. M., Teo, P. M., Choi, P. H., Cheung, K. y. and Lee, W. Y. (2001), 'Three-dimensional dosimetric evaluation of a conventional radiotherapy technique for treatment of nasopharyngeal carcinoma.', *Radiother Oncol* **58**(2), 143–153.

Chaudhry, M. A. (2008), 'Biomarkers for human radiation exposure', *J Biomed Sci* **15**(5), 557–563.

Cookson, W., Liang, L., Abecasis, G., Moffatt, M. and Lathrop, M. (2009), 'Mapping complex disease traits with global gene expression.', *Nat Rev Genet* **10**(3), 184–194.

Cornetta, T., Festa, F., Testa, A. and Cozzi, R. (2006), 'DNA damage repair and genetic polymorphisms: Assessment of individual sensitivity and repair capacity', *Int J Radiat Oncol Biol Phys* **66**(2), 537–545.

Cox, J., Stetz, J. and Pajak, T. (1995), 'Toxicity criteria of the radiation therapy oncology group (RTOG) and the European organization for research and treatment of cancer (EORTC)', *Int J Radiat Oncol Biol Phys* **31**(5), 1341–1346.

Cram, L. (2002), 'Flow cytometry, an overview', *Methods Cell Sci.* **24**(1), 1–9.

Crompton, N. E., Miralbell, R., Rutz, H. P., Ersoy, F., Sanal, O., Wellmann, D., Bieri, S., Coucke, P. A., Emery, G. C., Shi, Y. Q., Blattmann, H. and Ozsahin, M. (1999), 'Altered apoptotic profiles in irradiated patients with increased toxicity', *Int J Radiat Oncol Biol Phys* **45**(3), 707–714.

de Muro, M. A. (2008), Probe Design, Production, and Applications, *in* G. J. S. Jenkins, ed., 'Molecular biomethods handbook', Springer, pp. 1–13.

Djuzenova, C. S., Mühl, B., Fehn, M., Oppitz, U., Müller, B. and Flentje, M. (2006), 'Radiosensitivity in breast cancer assessed by the Comet and micronucleus assays.', *Br J Cancer* **94**(8), 1194–1203.

Duthie, S., Pirie, L., Jenkinson, A. and Narayanan, S. (2002), 'Cryopreserved versus freshly isolated lymphocytes in human biomonitoring: endogenous and induced DNA damage, antioxidant status and repair capability', *Mutagenesis* **17**(3), 211–214.

Eisenberg-Lerner, A., Bialik, S., Simon, H.-U. and Kimchi, A. (2009), 'Life and death partners: apoptosis, autophagy and the cross-talk between them.', *Cell Death Differ* **16**(7), 966–975.

Falvo, E., Strigari, L., Citro, G., Giordano, C., Arcangeli, S., Soriani, A., D'Alessio, D., Muti, P., Blandino, G., Sperduti, I. and Pinnarò, P. (2011), 'Dose and polymorphic genes xrcc1, xrcc3, gst play a role in the risk of developing erythema in breast cancer patients following single shot partial breast irradiation after conservative surgery', *BMC Cancer* **11**(1), 291.

Fang, F.-M., Chien, C.-Y., Tsai, W.-L., Chen, H.-C., Hsu, H.-C., Lui, C.-C., Huang, T.-L. and Huang, H.-Y. (2008), 'Quality of Life and Survival Outcome for Patients With Nasopharyngeal Carcinoma Receiving Three-Dimensional Conformal Radiotherapy vs. Intensity-Modulated Radiotherapy—A Longitudinal Study', *Int J Radiat Oncol Biol Phys* **72**(2), 356–364.

Fang, F. M., Tsai, W. L., Go, S. F., Ho, M. W., Wu, J. M., Wang, C. J., Su, C. Y., Chen, W. C. and Huang, E. Y. (2001), 'Implications of quantitative tumor and nodal regression rates for nasopharyngeal carcinomas after 45 Gy of radiotherapy.', *Int J Radiat Oncol Biol Phys* **50**(4), 961–969.

Fang, F.-M., Tsai, W.-L., Lee, T.-F., Liao, K.-C., Chen, H.-C. and Hsu, H.-C. (2010), 'Multivariate analysis of quality of life outcome for nasopharyngeal carcinoma patients after treatment', *Radiother Oncol* **97**(2), 263–269.

Faulhaber, O. and Bristow, R. (2005), *Basis of cell kill following clinical radiotherapy*, Springer, chapter 13, pp. 293–320.

Finnon, P., Kabacik, S., MacKay, A., Raffy, C., A'Hern, R., Owen, R., Badie, C., Yarnold, J. and Bouffler, S. (2012), 'Correlation of in vitro lymphocyte radiosensitivity and gene expression with late normal tissue reactions following curative radiotherapy for breast cancer', *Radiother Oncol* **105**(3), 329–336.

Gatti, R. A. (2001), 'The inherited basis of human radiosensitivity.', *Acta oncologica (Stockholm, Sweden)* **40**(6), 702.

Ghazali, N., Shaw, R. J., Rogers, S. N. and Risk, J. M. (2012), 'Genomic determinants of normal tissue toxicity after radiotherapy for head and neck malignancy: A systematic review', *Oral Oncol* **48**(11), 1090–1100.

Green, H., Ross, G., Peacock, J., Owen, R., Yarnold, J. and Houlston, R. (2002), 'Variation in the manganese superoxide dismutase gene (SOD2) is not a major cause of radiotherapy complications in breast cancer patients', *Radiother Oncol* **63**(2), 213–216.

Greve, B., Bölling, T., Amler, S., Rössler, U., Gomolka, M., Mayer, C., Popanda, O., Dreffke, K., Rickinger, A., Fritz, E., Eckardt-Schupp, F., Sauerland, C., Braselmann, H., Sauter, W., Illig, T., Riesenbeck, D., Könemann, S., Willich, N., Mörtl, S., Eich, H. T. and Schmezer, P. (2012), 'Evaluation of Different Biomarkers to Predict Individual Radiosensitivity in an Inter-Laboratory Comparison–Lessons for Future Studies', *PLoS ONE* **7**(10), e47185.

Greve, B., Dreffke, K., Rickinger, A., Könemann, S., Fritz, E., Eckardt-Schupp, F., Amler, S., Sauerland, C., Braselmann, H., Sauter, W., Illig, T., Schmezer, P., Gomolka, M., Willich, N. and Bölling, T. (2009), 'Multicentric investigation of ionising radiation-induced cell death as a predictive parameter of individual radiosensitivity', *Apoptosis* **14**(2), 226–235.

Han, G., Bian, L., Li, F., Cotrim, A., Wang, D., Lu, J., Deng, Y., Bird, G., Sowers, A., Mitchell, J. B., Gutkind, J. S., Zhao, R., Raben, D., ten Dijke, P., Refaeli, Y., Zhang, Q. and Wang, X.-J. (2013), 'Preventive and therapeutic effects of Smad7 on radiation-induced oral mucositis.', *Nat. Med.* **19**(4), 421–428.

Hawley, T. S. and Hawley, R. G. (2004), *Flow Cytometry Protocols*, Springer.

Henríquez-Hernández, L. A., Bordon, E., Pinar, B., Lloret, M., Rodriguez-Gallego, C. and Lara, P. C. (2012), 'Prediction of normal tissue toxicity as part of the individualized treatment with radiotherapy in oncology patients.', *Surg Oncol* **21**(3), 201–206.

Henríquez-Hernández, L. A., Carmona-Vigo, R., Pinar, B., Bordon, E., Lloret, M., Núñez, M. I., Rodriguez-Gallego, C. and Lara, P. C. (2011), 'Combined low initial DNA damage and high radiation-induced apoptosis confers clinical resistance to long-term toxicity in breast cancer patients treated with high-dose radiotherapy.', *Radiat Oncol* **6**, 60.

Henríquez-Hernández, L. A., Lara, P., Pinar, B., Bordon, E., Gallego, C., Bilbao, C., Pérez, L. and Morales, A. (2009), 'Constitutive gene expression profile segregates toxicity in locally advanced breast cancer patients treated with high-dose hyperfractionated radical radiotherapy', *Radiat Oncol* **4**(1), 17.

Higgins, J. P. T. and Green, S. (2011), *Cochrane Handbook for Systematic Reviews of Interventions*, The Cochrane Collaboration.

Hirschhorn, J. N. and Daly, M. J. (2005), 'Genome-wide association studies for common diseases and complex traits.', *Nat Rev Genet* **6**(2), 95–108.

Ho, A. Y., Atencio, D. P., Peters, S., Stock, R. G., Formenti, S. C., Cesaretti, J. A., Green, S., Haffty, B., Drumea, K., Leitzin, L., Kuten, A., Azria, D., Ozsahin, M., Overgaard, J., Andreassen, C. N., Trop, C. S., Park, J. and Rosenstein, B. S. (2006), 'Genetic Predictors of Adverse Radiotherapy Effects: The Gene-PARE project', *Int J Radiat Oncol Biol Phys* **65**(3), 646–655.

*Hong Kong Cancer Stat 2010* (2012), Hong Kong Cancer Registry, Hospital Authority.

Huang, X., Halicka, H. D., Traganos, F., Tanaka, T., Kurose, A. and Darzynkiewicz, Z. (2005), 'Cytometric assessment of DNA damage in relation to cell cycle phase and apoptosis.', *Cell Prolif.* **38**(4), 223–243.

Huber, R., Braselmann, H., Geinitz, H., Jaehnert, I., Baumgartner, A., Thamm, R., Figel, M., Molls, M. and Zitzelsberger, H. (2011), 'Chromosomal radiosensitivity and acute radiation side effects after radiotherapy in tumour patients - a follow-up study', *Radiat Oncol* **6**(1), 32.

Hunt, M. and Burman, C. (2003), *Treatment planning considerations using IMRT*, Medical Physics Publishing, chapter 13, pp. 103–121.

Hunt, M., Zelefsky, M., Wolden, S., Chui, C., LoSasso, T., Rosenzweig, K., Chong, L., Spirou, S., Fromme, L. and Lumley, M. (2001), 'Treatment planning and delivery of intensity-modulated radiation therapy for primary nasopharynx cancer', *Int J Radiat Oncol Biol Phys* **49**(3), 623–632.

Iannuzzi, C. M., Atencio, D. P., Green, S., Stock, R. G. and Rosenstein, B. S. (2002), 'ATM mutations in female breast cancer patients predict for an increase in radiation-induced late effects', *Int J Radiat Oncol Biol Phys* **52**(3), 606–613.

Jeggo, P. and Lavin, M. F. (2009), 'Cellular radiosensitivity: How much better do we understand it?', *Int J Radiat Biol* **85**(12), 1061–1081.

Jenkins, G. J. S. (2008), Restriction Enzymes, *in* J. M. Walker and R. Rapley, eds, 'Molecular biomethods handbook', Springer, pp. 17–27.

Jioner, M. and van der Kogel, A. J. (2009), *Basic clinical radiobiology*, Hodder Arnold.

Jones, P. A. (2012), 'Functions of DNA methylation: islands, start sites, gene bodies and beyond', *Nat Rev Genet* **13**(7), 484–492.

Kam, M. K. M., Chau, R. M. C., Suen, J., Choi, P. H. K. and Teo, P. M. L. (2003), 'Intensity-modulated radiotherapy in nasopharyngeal carcinoma: dosimetric advantage over conventional plans and feasibility of dose escalation', *Int J Radiat Oncol Biol Phys* **56**(1), 145–157.

Kam, M. K. M., Leung, S.-F., Zee, B., Chau, R. M. C., Suen, J. J. S., Mo, F., Lai, M., Ho, R., Cheung, K.-y., Yu, B. K. H., Chiu, S. K. W., Choi, P. H. K., Teo, P. M. L., Kwan, W.-h. and Chan, A. T. C. (2007), 'Prospective randomized study of intensity-modulated radiotherapy on salivary gland function in early-stage nasopharyngeal carcinoma patients.', *J Clin Oncol* **25**(31), 4873–4879.

Kam, M. K. M., Teo, P. M. L., Chau, R. M. C., Cheung, K. y., Choi, P. H. K., Kwan, W. h., Leung, S. F., Zee, B. and Chan, A. T. C. (2004), 'Treatment of nasopharyngeal carcinoma with intensity-modulated radiotherapy: The Hong Kong experience', *Int J Radiat Oncol Biol Phys* **60**(5), 1440–1450.

Kerns, S. L., Ostrer, H., Stock, R., Li, W., Moore, J., Pearlman, A., Campbell, C., Shao, Y., Stone, N., Kusnetz, L. and Rosenstein, B. S. (2010), 'Genome-Wide Association Study to Identify Single Nucleotide Polymorphisms (SNPs) Associated With the Development of Erectile Dysfunction in African-American Men After Radiotherapy for Prostate Cancer', *Int J Radiat Oncol Biol Phys* **78**(5), 1292–1300.

Kerns, S. L., Stock, R., Stone, N., Buckstein, M., Shao, Y., Campbell, C., Rath, L., De Ruysscher, D., Lammering, G., Hixson, R., Cesaretti, J., Terk, M., Ostrer, H. and Rosenstein, B. S. (2013), 'A 2-Stage Genome-Wide Association Study to Identify Single Nucleotide Polymorphisms Associated With Development of

Erectile Dysfunction Following Radiation Therapy for Prostate Cancer', *Int J Radiat Oncol Biol Phys* **85**(1), e21–e28.

Kiang, J., Garrison, B. and Gorbunov, N. (2010), 'Radiation combined injury: DNA damage, apoptosis, and autophagy', *Adapt Med* **2**, 1–10.

Kundu, S., Aulchenko, Y. S., Duijn, C. M. and Janssens, A. C. J. W. (2011), 'PredictABEL: an R package for the assessment of risk prediction models', *Eur J Epidemiol* **26**(4), 261–264.

Kuwahara, Y., Oikawa, T., Ochiai, Y., Roudkenar, M. H., Fukumoto, M., Shimura, T., Ohtake, Y., Ohkubo, Y., Mori, S., Uchiyama, Y. and Fukumoto, M. (2011), 'Enhancement of autophagy is a potential modality for tumors refractory to radiotherapy', *Cell Death Dis* **2**(6), e177–11.

Kwong, D. L. W., Pow, E. H. N., Sham, J. S. T., McMillan, A. S., Leung, L. H. T., Leung, W. K., Chua, D. T. T., Cheng, A. C. K., Wu, P. M. and Au, G. K. H. (2004a), 'Intensity-modulated radiotherapy for early-stage nasopharyngeal carcinoma: a prospective study on disease control and preservation of salivary function.', *Cancer* **101**(7), 1584–1593.

Kwong, D. L. W., Sham, J. S. T., Au, G. K. H., Chua, D. T. T., Kwong, P. W. K., Cheng, A. C. K., Wu, P. M., Law, M. W. M., Kwok, C. C. H., Yau, C. C., Wan, K. Y., Chan, R. T. T. and Choy, D. D. K. (2004b), 'Concurrent and adjuvant chemotherapy for nasopharyngeal carcinoma: a factorial study.', *J Clin Oncol* **22**(13), 2643–2653.

Lavin, M. F., Scott, S., Gueven, N., Kozlov, S., Peng, C. and Chen, P. (2004), 'Functional consequences of sequence alterations in the ATM gene', *DNA Repair* **3**(8-9), 1197–1205.

Lee, A. W., Law, S. C., Ng, S. H., Chan, D. K., Poon, Y. F., Foo, W., Tung, S. Y., Cheung, F. K. and Ho, J. H. (1992), 'Retrospective analysis of nasopharyngeal carcinoma treated during 1976–1985: late complications following megavoltage irradiation', *Br J Radiol* **65**(778), 918–928.

Lee, A. W. M., Lau, W. H., Tung, S. Y., Chua, D. T. T., Chappell, R., Xu, L., Siu, L., Sze, W. M., Leung, T. W., Sham, J. S. T., Ngan, R. K. C., Law, S. C. K., Yau, T. K., Au, J. S. K., O'Sullivan, B., Pang, E. S. Y., O, S. K., Au, G. K. H., Lau, J. T. and Hong Kong Nasopharyngeal Cancer Study Group (2005), 'Preliminary results of a randomized study on therapeutic gain by concurrent chemotherapy for regionally-advanced nasopharyngeal carcinoma: NPC-9901 Trial by the Hong Kong Nasopharyngeal Cancer Study Group.', *J Clin Oncol* **23**(28), 6966–6975.

Lee, A. W. M., Ng, W. T., Chan, Y. H., Sze, H., Chan, C. and Lam, T. H. (2012), 'The battle against nasopharyngeal cancer.', *Radiother Oncol* **104**(3), 272–278.

Lee, A. W. M., Tung, S. Y., Chua, D. T. T., Ngan, R. K. C., Chappell, R., Tung, R., Siu, L., Ng, W. T., Sze, W. K., Au, G. K. H., Law, S. C. K., O'Sullivan, B., Yau, T. K., Leung, T. W., Au, J. S. K., Sze, W. M., Choi, C. W., Fung, K. K., Lau, J. T. and Lau, W. H. (2010), 'Randomized Trial of Radiotherapy Plus Concurrent-Adjuvant Chemotherapy vs Radiotherapy Alone for Regionally Advanced Nasopharyngeal Carcinoma', *J Natl Cancer Inst* **102**(15), 1188–1198.

Lewis, C. (2002), 'Genetic association studies: design, analysis and interpretation', *Brief Bioinform* **3**(2), 146–153.

Lewis, C. M. and Knight, J. (2012), 'Introduction to genetic association studies.', *Cold Spring Harbor Protoc* **2012**(3), 297–306.

Lewis, R. (2009), *Human genetics: Concepts and application*, 9th edn, Mcgraw Hill.

Li, H., You, Y., Lin, C., Zheng, M., Hong, C., Chen, J., Li, D., Au, W. W. and Chen, Z. (2013), 'XRCC1 codon 399Gln polymorphism is associated with radiotherapy-induced acute dermatitis and mucositis in nasopharyngeal carcinoma patients', *Radiat Oncol* **8**(1), 1–1.

Little, J., Higgins, J. P. T., Ioannidis, J. P. A., Moher, D., Gagnon, F., von Elm, E., Khoury, M. J., Cohen, B., Davey-Smith, G., Grimshaw, J., Scheet, P., Gwinn, M., Williamson, R. E., Zou, G. Y., Hutchings, K., Johnson, C. Y., Tait, V., Wiens, M., Golding, J., van Duijn, C., McLaughlin, J., Paterson, A., Wells, G., Fortier, I., Freedman, M., Zecevic, M., King, R., Infante-Rivard, C., Stewart, A. and Birkett, N. (2009), 'STrengthening the REporting of Genetic Association studies (STREGA)–an extension of the STROBE statement.', *Eur. J. Clin. Invest.* **39**(4), 247–266.

Logan, R. M. (2009), 'Advances in understanding of toxicities of treatment for head and neck cancer', *Oral Oncol* **45**(10), 844–848.

Loo, D. T. (2002), 'TUNEL assay. An overview of techniques.', *Methods Mol. Biol.* **203**, 21–30.

López, E., Guerrero, R., Núñez, M. I., del Moral, R., Villalobos, M., Martínez-Galán, J., Valenzuela, M. T., Muñoz-Gámez, J. A., Oliver, F. J., Martín-Oliva, D. and Ruiz de Almodóvar, J. M. (2005), 'Early and late skin reactions to radiotherapy for breast cancer and their correlation with radiation-induced DNA damage in lymphocytes.', *Breast Cancer Res.* **7**(5), R690–8.

Lorimore, S. A., Coates, P. J. and Wright, E. G. (2003), 'Radiation-induced genomic instability and bystander effects: inter-related nontargeted effects of exposure to ionizing radiation', *Oncogene* **22**(45), 7058–7069.

Mariano Ruiz de Almodóvar, J., Guirado, D., Isabel Núŋez, M., López, E., Guerrero, R., Teresa Valenzuela, M., Villalobos, M. and del Moral, R. (2002), 'Individualisation of radiotherapy in breast cancer patients: possible usefulness of a

DNA damage assay to measure normal cell radiosensitivity', *Radiother Oncol* **62**(3), 327–333.

Martin, M., Lefaix, J. and Delanian, S. (2000), 'TGF-1 and radiation fibrosis: A master switch and a specific therapeutic target?', *Int J Radiat Oncol Biol Phys* **47**(2), 277–290.

Martinez, M. M., Reif, R. D. and Pappas, D. (2010), 'Detection of apoptosis: A review of conventional and novel techniques', *Anal. Methods* **2**(8), 996.

Mayer, C., Popanda, O., Greve, B., Fritz, E., Illig, T., Eckardt-Schupp, F., Gomolka, M., Benner, A. and Schmezer, P. (2011), 'A radiation-induced gene expression signature as a tool to predict acute radiotherapy-induced adverse side effects.', *Cancer Lett* **302**(1), 20–28.

McCarthy, M. I., Abecasis, G. R., Cardon, L. R., Goldstein, D. B., Little, J., Ioannidis, J. P. A. and Hirschhorn, J. N. (2008), 'Genome-wide association studies for complex traits: consensus, uncertainty and challenges', *Nat Rev Genet* **9**(5), 356–369.

McPherson, M. and Møller, S. (2007), *PCR*, Taylor & Francis.

Moher, D., Liberati, A., Tetzlaff, J., Altman, D. G. and PRISMA Group (2009), 'Preferred reporting items for systematic reviews and meta-analyses: the PRISMA statement.'.

Montgomery, J., Wittwer, C. T., Palais, R. and Zhou, L. (2007), 'Simultaneous mutation scanning and genotyping by high-resolution DNA melting analysis', *Nat Protoc* **2**(1), 59–66.

Moretti, L., Attia, A., Kim, K. W. and Lu, B. (2007), 'Crosstalk between Bak/Bax and mTOR signaling regulates radiation-induced autophagy.', *Autophagy* **3**(2), 142–144.

Moullan, N., Cox, D. G., Angèle, S., Romestaing, P., Gerard, J. P. and Hall, J. (2003), 'Polymorphisms in the DNA repair gene XRCC1, breast cancer risk, and response to radiotherapy', *Cancer Epidemiol Biomarkers Prev* **12**(11), 1168–1174.

Munafò, M. R. and Flint, J. (2004), 'Meta-analysis of genetic association studies.', *Trends Genet.* **20**(9), 439–444.

Nakaoka, H. and Inoue, I. (2009), 'Meta-analysis of genetic association studies: methodologies, between-study heterogeneity and winner's curse.', *J Hum Genet* **54**(11), 615–623.

Ng, C. C., Yew, P. Y., Puah, S. M., Krishnan, G., Yap, L. F., Teo, S. H., Lim, P. V. H., Govindaraju, S., Ratnavelu, K., Sam, C. K., Takahashi, A., Kubo, M., Kamatani, N., Nakamura, Y. and Mushiroda, T. (2009), 'A genome-wide

association study identifies ITGA9 conferring risk of nasopharyngeal carcinoma', *J Hum Genet* **54**(7), 392–397.

Ng, W. T., Choi, C. W., Lee, M. C. H., Law, L. Y., Yau, T. K. and Lee, A. W. M. (2010), 'Outcomes of nasopharyngeal carcinoma screening for high risk family members in Hong Kong.', *Familial Cancer* **9**(2), 221–228.

Ng, W. T., Lee, M. C. H., Hung, W. M., Choi, C. W., Lee, K. C., Chan, O. S. H. and Lee, A. W. M. (2011), 'Clinical outcomes and patterns of failure after intensity-modulated radiotherapy for nasopharyngeal carcinoma.', *Int J Radiat Oncol Biol Phys* **79**(2), 420–428.

Nicholls, J. M., Agathanggelou, A., Fung, K., Xiangguo, Z. and Niedobitek, G. (1997), 'The association of squamous cell carcinomas of the nasopharynx with Epstein–Barr virus shows geographical variation reminiscent of Burkitt's lymphoma', *J. Pathol.* **183**(2), 164–168.

Núñez, M., Guerrero, M., López, E., Del Moral, M., Valenzuela, M., Siles, E., Villalobos, M., Pedraza, V., Peacock, J. and De Almodóvar, J. (1998), 'DNA damage and prediction of radiation response in lymphocytes and epidermal skin human cells', *Int. J. Cancer* **76**(3), 354–361.

Olive, P. L. and Banáth, J. P. (2006), 'The comet assay: a method to measure DNA damage in individual cells', *Nat Protoc* **1**(1), 23–29.

Ozsahin, M., Crompton, N. E. A., Gourgou, S., Kramar, A., Li, L., Shi, Y., Sozzi, W. J., Zouhair, A., Mirimanoff, R. O. and Azria, D. (2005), 'CD4 and CD8 T-lymphocyte apoptosis can predict radiation-induced late toxicity: a prospective study in 399 patients', *Clin Cancer Res* **11**(20), 7426–7433.

Page, G., George, V., Go, R., Page, P. and Allison, D. (2003), '"Are we there yet?": Deciding when one has demonstrated specific genetic causation in complex diseases and quantitative traits', *Am J Hum Genet* **73**(4), 711–719.

Pettersson, E., Lundeberg, J. and Ahmadian, A. (2009a), 'Generations of sequencing technologies.', *Genomics* **93**(2), 105–111.

Pettersson, F. H., Anderson, C. A., Clarke, G. M., Barrett, J. C., Cardon, L. R., Morris, A. P. and Zondervan, K. T. (2009b), 'Marker selection for genetic case–control association studies', *Nat Protoc* **4**(5), 743–752.

Pinar, B., Henríquez-Hernández, L. A., Lara, P. C., Bordon, E., Rodriguez-Gallego, C., Lloret, M., Nuñez, M. and De Almodovar, M. (2010), 'Radiation induced apoptosis and initial DNA damage are inversely related in locally advanced breast cancer patients', *Radiat Oncol* **5**(1), 85.

Pogribny, I., Raiche, J., Slovack, M. and Kovalchuk, O. (2004), 'Dose-dependence, sex- and tissue-specificity, and persistence of radiation-induced genomic DNA methylation changes', *Biochem Biophys Res Commun* **320**(4), 1253–1261.

Popanda, O., Ebbeler, R., Twardella, D., Helmbold, I., Gotzes, F., Schmezer, P., Thielmann, H. W., von Fournier, D., Haase, W., Sautter-Bihl, M. L., Wenz, F., Bartsch, H. and Chang-Claude, J. (2003), 'Radiation-induced DNA damage and repair in lymphocytes from breast cancer patients and their correlation with acute skin reactions to radiotherapy', *Int J Radiat Oncol Biol Phys* **55**(5), 1216–1225.

Popanda, O., Marquardt, J. U., Chang-Claude, J. and Schmezer, P. (2009), 'Genetic variation in normal tissue toxicity induced by ionizing radiation', *Mutat Res* **667**(1-2), 58–69.

Pratesi, N., Mangoni, M., Mancini, I., Paiar, F., Simi, L., Livi, L., Cassani, S., Buglione, M., Grisanti, S., Almici, C., Polli, C., Saieva, C., Magrini, S. M., Biti, G., Pazzagli, M. and Orlando, C. (2011), 'Association between single nucleotide polymorphisms in the XRCC1 and RAD51 genes and clinical radiosensitivity in head and neck cancer', *Radiother Oncol* **99**(3), 356–361.

Price, E. A., Bourne, S. L., Radbourne, R., Lawton, P. A., Lamerdin, J., Thompson, L. H. and Arrand, J. E. (1997), 'Rare microsatellite polymorphisms in the DNA repair genes XRCC1, XRCC3 and XRCC5 associated with cancer in patients of varying radiosensitivity.', *Somat. Cell Mol. Genet.* **23**(4), 237–247.

Rasmussen, B. H. (2012), Chapter 18, *in* S. Magdeldin, ed., 'Gel Electrophoresis – Principles and Basics', InTech, pp. 315–334.

Rødningen, O. K., Børresen-Dale, A.-L., Alsner, J., Hastie, T. and Overgaard, J. (2008), 'Radiation-induced gene expression in human subcutaneous fibroblasts is predictive of radiation-induced fibrosis', *Radiother Oncol* **86**(3), 314–320.

Sanger, F., Nicklen, S. and Coulson, A. R. (1977), 'DNA sequencing with chain-terminating inhibitors', *Proc. Natl. Acad. Sci. U.S.A.* **74**(12), 5463–5467.

Schnarr, K., Boreham, D., Sathya, J., Julian, J. and Dayes, I. (2009), 'Radiation-induced lymphocyte apoptosis to predict radiation therapy late toxicity in prostate cancer patients', *Int J Radiat Oncol Biol Phys* **74**(5), 1424–1430.

Sciubba, J. J. and Goldenberg, D. (2006), 'Oral complications of radiotherapy', *Lancet Oncol.* **7**(2), 175–183.

Shendure, J. and Ji, H. (2008), 'Next-generation DNA sequencing.', *Nat. Biotechnol.* **26**(10), 1135–1145.

Smirnov, D. A., Morley, M., Shin, E., Spielman, R. S. and Cheung, V. G. (2009), 'Genetic analysis of radiation-induced changes in human gene expression', *Nature* **459**(7246), 587–591.

Sonis, S. (2007), 'Pathobiology of oral mucositis: novel insights and opportunities', *J Support Oncol* **5**(9 Suppl 4), 3–11.

Sonis, S., Haddad, R., Posner, M., Watkins, B., Fey, E., Morgan, T. V., Mookanamparambil, L. and Ramoni, M. (2007), 'Gene expression changes in peripheral blood cells provide insight into the biological mechanisms associated with regimen-related toxicities in patients being treated for head and neck cancers', *Oral Oncol* **43**(3), 289–300.

Sonis, S. T. (2004), 'The pathobiology of mucositis', *Nat Rev Cancer* **4**(4), 277–284.

Sonis, S. T. (2009), 'Mucositis: The impact, biology and therapeutic opportunities of oral mucositis.', *Oral Oncol* **45**(12), 1015–1020.

Sterpone, S., Cornetta, T., Padua, L., Mastellone, V., Giammarino, D., Testa, A., Tirindelli, D., Cozzi, R. and Donato, V. (2010), 'DNA repair capacity and acute radiotherapy adverse effects in Italian breast cancer patients', *Mutat Res* **684**(1-2), 43–48.

Strasser, H., Grabenbauer, G. G., Sprung, C. N., Sauer, R. and Distel, L. V. R. (2007), 'DNA Double-Strand Break Induction and Repair in Irradiated Lymphoblastoid, Fibroblast Cell Lines and White Blood Cells from ATM, NBS and Radiosensitive Patients', *Strahlenther Onkol* **183**(8), 447–453.

Suga, T., Ishikawa, A., Kohda, M., Otsuka, Y., Yamada, S., Yamamoto, N., Shibamoto, Y., Ogawa, Y., Nomura, K., Sho, K., Omura, M., Sekiguchi, K., Kikuchi, Y., Michikawa, Y., Noda, S., Sagara, M., Ohashi, J., Yoshinaga, S., Mizoe, J., Tsujii, H., Iwakawa, M. and Imai, T. (2007), 'Haplotype-Based Analysis of Genes Associated With Risk of Adverse Skin Reactions After Radiotherapy in Breast Cancer Patients', *Int J Radiat Oncol Biol Phys* **69**(3), 685–693.

Svensson, J. P., Stalpers, L. J. A., Esveldt-van Lange, R. E. E., Franken, N. A. P., Haveman, J., Klein, B., Turesson, I., Vrieling, H. and Giphart-Gassler, M. (2006), 'Analysis of gene expression using gene sets discriminates cancer patients with and without late radiation toxicity', *PLoS Med* **3**(10), e422.

Tabor, H. K., Risch, N. J. and Myers, R. M. (2002), 'Candidate-gene approaches for studying complex genetic traits: practical considerations.', *Nat Rev Genet* **3**(5), 391–397.

Talbot, C. J., Tanteles, G. A., Barnett, G. C., Burnet, N. G., Chang-Claude, J., Coles, C. E., Davidson, S., Dunning, A. M., Mills, J., Murray, R. J. S., Popanda, O., Seibold, P., West, C. M. L., Yarnold, J. R. and Symonds, R. P. (2012), 'A replicated association between polymorphisms near TNF and risk for adverse reactions to radiotherapy.', *Br J Cancer* **107**(4), 748–753.

Tan, X.-L., Popanda, O., Ambrosone, C. B., Kropp, S., Helmbold, I., Fournier, D., Haase, W., Sautter-Bihl, M. L., Wenz, F., Schmezer, P. and Chang-Claude, J. (2005), 'Association between TP53 and p21 genetic polymorphisms and acute side effects of radiotherapy in breast cancer patients', *Breast Cancer Res Treat* **97**(3), 255–262.

Teo, P. M. L., Ma, B. B. Y. and Chan, A. T. C. (2004), 'Radiotherapy for nasopharyngeal carcinoma—transition from two-dimensional to three-dimensional methods', *Radiother Oncol* **73**(2), 163–172.

Thompson, L. H., Brookman, K. W., Jones, N. J., Allen, S. A. and Carrano, A. V. (1990), 'Molecular cloning of the human XRCC1 gene, which corrects defective DNA strand break repair and sister chromatid exchange.', *Mol Cell Biol.* **10**(12), 6160–6171.

Tuan, J. K. L., Ha, T. C., Ong, W. S., Siow, T. R., Tham, I. W. K., Yap, S. P., Tan, T. W. K., Chua, E. T., Fong, K. W. and Wee, J. T. S. (2012), 'Late toxicities after conventional radiation therapy alone for nasopharyngeal carcinoma', *Radiother Oncol* pp. 1–7.

Turesson, I., Nyman, J., Holmberg, E. and Odén, A. (1996), 'Prognostic factors for acute and late skin reactions in radiotheraphy patients', *Int J Radiat Oncol Biol Phys* **36**(5), 1065–1075.

Wagner, J. M. and Karnitz, L. M. (2009), 'Cisplatin-induced DNA damage activates replication checkpoint signaling components that differentially affect tumor cell survival.', *Mol. Pharmacol.* **76**(1), 208–214.

Walker, E., Hernandez, A. V. and Kattan, M. W. (2008), 'Meta-analysis: Its strengths and limitations', *Cleve Clin J Med* **75**(6), 431–439.

Wall, J. D. and Pritchard, J. K. (2003), 'Haplotype blocks and linkage disequilibrium in the human genome', *Nat Rev Genet* **4**(8), 587–597.

Wang, W.-d., Chen, Z.-t., Li, D.-z., Cao, Z.-h., Pu, P., Fu, S.-z., Chen, J., Sun, S.-l. and Chen, X.-p. (2005a), 'Detecting Normal Cell Radiosensitivity via Assay of DNA Damage in Lymphocytes for Individualizing Radiotherapy in Head and Neck Cancer Patients', *Oncology* **69**(3), 208–213.

Wang, W. Y. S., Barratt, B. J., Clayton, D. G. and Todd, J. A. (2005b), 'Genome-wide association studies: theoretical and practical concerns.', *Nat Rev Genet* **6**(2), 109–118.

Watanabe, M., Hitomi, M., van der Wee, K., Rothenberg, F., Fisher, S. A., Zucker, R., Svoboda, K. K. H., Goldsmith, E. C., Heiskanen, K. M. and Nieminen, A.-L. (2002), 'The pros and cons of apoptosis assays for use in the study of cells, tissues, and organs.', *Microsc. Microanal.* **8**(5), 375–391.

Wei, W. I. and Sham, J. S. T. (2005), 'Nasopharyngeal carcinoma.', *Lancet* **365**(9476), 2041–2054.

Wells, M. and MacBride, S. (2003), Radiation skin reactions, *in* S. Faithfull and M. Wells, eds, 'Supportive care in radiotherapy', Churchill Livingstone, pp. 135–159.

West, C. M. L., Dunning, A. M. and Rosenstein, B. S. (2012), 'Genome-wide association studies and prediction of normal tissue toxicity.', *Semin Radiat Oncol* **22**(2), 91–99.

West, C., Rosenstein, B. S., Alsner, J., Azria, D., Barnett, G., Begg, A., Bentzen, S., Burnet, N., Chang-Claude, J., Chuang, E., Coles, C., De Ruyck, K., De Ruysscher, D., Dunning, A., Elliott, R., Fachal, L., Hall, J., Haustermans, K., Herskind, C., Hoelscher, T., Imai, T., Iwakawa, M., Jones, D., Kulich, C., EQUAL-ESTRO, Langendijk, J.-H., O'Neils, P., Ozsahin, M., Parliament, M., Polański, A., Rosenstein, B., Seminara, D., Symonds, P., Talbot, C., Thierens, H., Vega, A., West, C. and Yarnold, J. (2010), 'Establishment of a Radiogenomics Consortium.', *Int J Radiat Oncol Biol Phys* **76**(5), 1295–1296.

Westbury, C. B. and Yarnold, J. R. (2012), 'Radiation fibrosis – current clinical and therapeutic perspectives.', *Clin Oncol (R Coll Radiol)* **24**(10), 657–672.

Wilkins, R. C., Kutzner, B. C., Truong, M., Sanchez-Dardon, J. and McLean, J. R. N. (2002a), 'Analysis of radiation-induced apoptosis in human lymphocytes: Flow cytometry using Annexin V and propidium iodide versus the neutral comet assay', *Cytometry* **48**(1), 14–19.

Wilkins, R. C., Wilkinson, D., Maharaj, H. P., Bellier, P. V., Cybulski, M. B. and McLean, J. R. N. (2002b), 'Differential apoptotic response to ionizing radiation in subpopulations of human white blood cells.', *Mutat Res* **513**(1-2), 27–36.

Wirawan, E., Berghe, T. V., Lippens, S., Agostinis, P. and Vandenabeele, P. (2012), 'Autophagy: for better or for worse', *Cell Res* **22**(1), 43–61.

Wittke-Thompson, J., Pluzhnikov, A. and Cox, N. (2005), 'Rational inferences about departures from Hardy-Weinberg equilibrium', *Am J Hum Genet* **76**(6), 967–986.

Wlodkowic, D., Telford, W., Skommer, J. and Darzynkiewicz, Z. (2011), 'Apoptosis and beyond: cytometry in studies of programmed cell death.', *Methods Cell Biol.* **103**, 55–98.

Wong, V. W. C., Szeto, Y. T., Collins, A. R. and Benzie, I. F. (2004), 'THE COMET ASSAY: a biomonitoring tool for nutraceutical research', *Curr Topics Nutraceutical Res* pp. 1–14.

Wray, N. R., Yang, J., Hayes, B. J., Price, A. L., Goddard, M. E. and Visscher, P. M. (2013), 'Pitfalls of predicting complex traits from SNPs.', *Nat Rev Genet* **14**(7), 507–515.

Wynn, T. A. (2008), 'Cellular and molecular mechanisms of fibrosis.', *J. Pathol.* **214**(2), 199–210.

Zhou, L., Xia, J., Li, H., Dai, J. and Hu, Y. (2010), 'Association of XRCC1Variants with Acute Skin Reaction After Radiotherapy in Breast Cancer Patients', *Cancer Biother Radiopharm* **25**(6), 681–685.

Zondervan, K. T. and Cardon, L. R. (2007), 'Designing candidate gene and genome-wide case-control association studies.', *Nat Protoc* **2**(10), 2492–2501.

Zschenker, O., Raabe, A., Boeckelmann, I. K., Borstelmann, S., Szymczak, S., Wellek, S., Rades, D., Hoeller, U., Ziegler, A., Dikomey, E. and Borgmann, K. (2010), 'Association of single nucleotide polymorphisms in ATM, GSTP1, SOD2, TGFB1, XPD and XRCC1 with clinical and cellular radiosensitivity', *Radiother Oncol* .